Geometrical and Exact Unification of Spacetime, Gravity and Quanta

The Theory of the Dynamics of Volume
is Derived from Physical Principles

This text has also been published in the form of a printed book and is available in book trading companies or book stores since July 2023.
author: Hans-Otto Carmesin
title: Geometrical and Exact Unification of Spacetime, Gravity and Quanta
ISBN: 978-3-96831-042-8
ISSN: 2629 - 1525

Please cite this text as follows:
Carmesin, Hans-Otto (July 2023): Geometrical and Exact Unification of Spacetime, Gravity and Quanta. Verlag Dr. Köster, Berlin.

Berlin: Verlag Dr. Köster

Book Series: Universe: Unified from Microcosm to Macrocosm, Volume 10

Hans-Otto Carmesin

August 15, 2023

b

How are relativity, gravity and quantum physics unified?
Our solution is geometrical: the dynamics of volume.
Our solution fulfills the following criteria:
We completely use elements of reality.
Our solution is derived exactly from physical principles.
We use no hypothesis or fit.
We achieve precise accordance with observation.
We provide precise predictions.
Relativity including gravity implies the dynamics of volume. The dynamics of volume provides the

- transmission of gravitational interaction
- curvature of spacetime
- expansion of space
- solution of the flatness problem
- mapping to Ricci flow
- Schrödinger equation
- correct postulates of quantum physics
- universality of quantization
- second quantization by elements of reality
- exact dynamics and explanation of nonlocality
- full causality in spacetime
- explanation of Einstein's principle of locality
- exact explanation of quantum paradoxes
- explanation of a measurement process by elements of reality
- dynamics of the measurement process
- explanation of zero-point energy by elements of reality
- formation of matter by phase transitions
- observed density of dark energy
- explanation of dark energy by elements of reality
- observed Hubble - tension
- observable value of H_0 as a function of the redshift (front cover)
- era of 'cosmic inflation'
- evolution of dark energy during 'cosmic inflation'
- dynamics and explanation of fundamental interactions
- interpretation of quanta by dynamics of volume
- cosmological parameters
- derivation of quantum gravity by elements of reality

In this book we derive all findings in a systematic, clear and smooth manner. We summarize our results by many definitions, propositions and theorems. We are classes from grade 10 or higher, courses, research clubs, enthusiasts, observers, experimentalists, mathematicians, natural scientists, researchers etc.

Physics Archive, Physik Archive, Verlag Dr. Köster, Berlin

PD Dr. Hans-Otto Carmesin (July 2023): Geometrical and Exact Unification of Spacetime, Gravity and Quanta; ISBN 978-3-96831-042-8

PD Dr. Hans-Otto Carmesin (December 2022): Unification of Spacetime, Gravity and Quanta; ISBN 978-3-96831-036-7

PD Dr. Hans-Otto Carmesin (March 16 2022): The Electroweak Interaction Explained by and Derived from Gravity and Relativity; ISBN 978-3-96831-032-9

PD Dr. Hans-Otto Carmesin (February 11 2022): Quantum Physics Explained by Gravity and Relativity; ISBN 978-3-96831-028-2

PD Dr. Hans-Otto Carmesin (October 2021). The Elementary Charge Explained by Quantum Gravity; lSBN 978-3-86831-023-7

Prof. Dr. Peter Möller (2021): Warum es Leben im Universum gibt; ISBN 978-3-96831-019-0

PD Dr. Hans-Otto Carmesin (August 2021): Cosmological and Elementary Particles Explained by Quantum Gravity; lSBN 978-3-96831-018-3

PD Dr. Hans-Otto Carmesin (March 2021): Quanta of Spacetime Explain Observations, Dark Energy, Graviton and Nonlocality; lSBN 978-3-96831-008-4

PD Dr. Hans-Otto Carmesin (September 2020): The Universe Developing from Zero-Point Energy - Discovered by Making Photos, Experiments and Calculations; ISBN 978-3-89574-993-3

PD Dr. Hans-Otto Carmesin (March 2020): Wir entdecken die Geschichte des Universums mit eigenen Fotos und Experimenten; lSBN 978-3-89574-973-5

Prof. Dr. Peter Möller (2020): Corona - Zahlen richtig verstehen; ISBN 978-3-96831-005-3

Dr. Gerold O. Schellstede (2020): Über nichtlineare Effekte in den Elektrodynamiken der Plebanskiklasse; ISBN S78-3-89574-968-1

PD Dr. Hans-Otto Carmesin (2019): Die Grundschwingungen des Universums - The Cosmic Unification; ISBN 978-3-89574-961-2

Prof. Dr. Peter Möller (2019): Geheimnisse des Universums - Relativitätstheorie, Quantenmechanik und schwarze Löcher; ISBN 978-3-89574-959-9

PD Dr. Hans-Otto Carmesin (November 2018): Entstehung der Raumzeit durch Quantengravitätion - Theory for the Emergence of Space, Dark Matter, Dark Energy and Space-Time; ISBN 978-3-89574-951-3 d

PD Dr. Hans-Otto Carmesin (July 2018): Entstehung dunkler Energie durch Quantengravitation - Universal Model for Dynamics of Space, Dark Matter and Dark Energy; ISBN 978-3-89574-944-5

PD Dr. Hans-Otto Carmesin (May 2018): Entstehung dunkler Materie durch Gravitation - Model for the Dynamics of Space and the Emergence of Dark Matter; ISBN 978-3-89574-939-1

PD Dr. Hans-Otto Carmesin (2017): Vom Big Bang bis heute mit Gravitation - Model for the Dynamics of Space; ISBN 978-3-89574-899-8

Geometrical and Exact Unification of Spacetime, Gravity and Quanta

The Theory of the Dynamics of Volume
is Derived from Physical Principles

This text has also been published in the form of a printed book and is available in book trading companies or book stores since July 2023.
author: Hans-Otto Carmesin
title: Geometrical and Exact Unification of Spacetime, Gravity and Quanta
ISBN: 978-3-96831-042-8
ISSN: 2629 - 1525

Please cite this text as follows:
Carmesin, Hans-Otto (July 2023): Geometrical and Exact Unification of Spacetime, Gravity and Quanta. Verlag Dr. Köster, Berlin.

Book Series: Universe: Unified from Microcosm to Macrocosm, Volume 10
bibliographic data are available at http://dnb.dnb.de

Hans-Otto Carmesin

August 15, 2023

Contents

1 **Introduction** 1

I Semiclassical Spacetime and Gravity 3

2 **Basic Principles** 5
- 2.1 How can you find the theory? . . . 5
- 2.2 Equivalence principle, EP . . . 6
- 2.3 Special relativity, SR . . . 7
- 2.4 Radial structure of gravity near a mass . . . 13
- 2.5 Law of energy conservation . . . 14
- 2.6 Measures of observable distance . . . 16
- 2.7 Objects of interaction . . . 26
- 2.8 Gravity near a mass, GG . . . 28
- 2.9 Dynamic volume, DV . . . 34
- 2.10 Spacetime quadruple, SQ . . . 36

3 **Universal Position Factor** 37
- 3.1 Position factor $\varepsilon_E(R)$ . . . 37
- 3.2 Derivation of the Schwarzschild metric . . . 41
- 3.3 Universality of the position factor . . . 43

4 **Universal Quantization** 47
- 4.1 Possible minimal portion . . . 48
- 4.2 Universality of the quantization ratio . . . 49

5 **Classical Expansion of Space** 57
- 5.1 Expansion of space . . . 57
- 5.2 Derivation of the FLE . . . 58
- 5.3 A solution of the flatness problem . . . 62
- 5.4 Second solution of the flatness problem . . . 63

6 Energy Density of the Gravitational Field G^* 71
6.1 Absolute value of $\rho_{gr.\ f.}$ 71
6.2 Free fall of M 73

II Theory of Dynamic Volume 77

7 Caused Additional Volume 79
7.1 A mass causes curvature of spacetime 79
7.2 A mass causes additional volume 83
7.3 ε_L provides a gravitational potential 89

8 Propagation of Additional Volume 93
8.1 Relative additional volume 94
8.2 Plane waves 99
8.3 Invariant and generalized dynamics 103

9 Local Formation of Volume 109
9.1 Normalized LFV 110
9.2 Formation of ε_L near a mass M 116
9.3 Invariant and generalized LFV 119

10 Geometry of the Change of Volume 121
10.1 Volume tensor 122
10.2 Non-diagonal elements 124
10.3 Rates for LFV and GFV 128
10.4 No measurement of absolute position 129

11 Formation and Propagation of Volume 131
11.1 Linear superposition 131
11.2 Energy and momentum 135

12 Global Formation of Volume 139
12.1 Globally formed volume 139
12.2 LFV can cause GFV 140

III Fundamental Dynamics of Quanta 147

13 Stabilization of Quanta 149

14 Derivation of Quantum Postulates **153**
14.1 Time evolution . . . 153
14.2 Hilbert space . . . 160
14.3 Observables and operators . . . 162
14.4 Outcomes of measurements . . . 165
14.5 Energy of a wave packet of a RGW . . . 167
14.6 Probabilistic outcomes . . . 179
14.7 Mixed states . . . 190
14.8 Angular momentum and spin . . . 194
14.9 Identical particles . . . 194
14.10 Entanglement . . . 196

15 Consequences of Quantum Postulates **201**
15.1 Phenomena . . . 201
15.2 Theories . . . 202

16 On Bell's theorem **203**
16.1 On Bell's inequality . . . 203
16.2 Experimental test of Bell's inequality . . . 206
16.3 Explanation by the dynamics of volume . . . 210

17 Mapping theorem **215**

18 Interpretation **221**
18.1 Role of paradoxes . . . 221
18.2 Delayed choice experiment . . . 221
18.3 DV overcomes Copenhagen interpretation . . . 226

IV Basic Dynamics of Spacetime & Gravity **227**

19 Derivation of Dark Energy **229**
19.1 Nature of density of volume . . . 229
19.2 u_{vol} in a universe of volume . . . 230
19.3 u_{vol} at another time . . . 242

20 Dark Energy in a Homogeneous Universe **245**
20.1 Spatial averages in cosmology . . . 245
20.2 Formation and propagation of volume . . . 247

21 Dark Energy by Heterogeneity **249**
21.1 Physics of the observed discrepancy . . . 249
21.2 Time dependence of H_0 . . . 251

21.3 Derivation of the ideal value of H_0 251
21.4 Parameter measured with a probe 253

22 Dark Energy at 'Cosmic Inflation' 269
22.1 Incompleteness of GR 269
22.2 Gravity at higher dimension 272
22.3 Phase transitions in the early universe 276
22.4 Quanta of dark energy 283

23 Derivation of GR 293
23.1 Curvature of spacetime is included in the SQ 293
23.2 Semiclassical limit via path integrals 294
23.3 Semiclassical limit at stationary action 294
23.4 Most simple action 295

24 Discussion 297
24.1 Achieved key results 297
24.2 Fulfilled criteria 302
24.3 Relations among theories 304

25 Appendix 311
25.1 Mathematical methods 311
25.2 Methods of physics 312
25.3 Universal constants 315
25.4 Glossary on volume 316
25.5 Natural units 317
25.6 Glossary 318

Chapter 1

Introduction

We humans improve our understanding of nature. In particular, we describe space so that we can navigate and organize telecommunication, Hoskin (1997).

For instance, Maxwell (1865) developed a very successful theory including electromagnetic waves. For it, he proposed an **aether** in which these waves propagate.

However, Einstein (1905) realized that a propagation of electromagnetic waves is better described in **spacetime**. Hereby, Einstein (1915) proposed a very successful theory describing curvature and expansion of spacetime since the Big Bang.

Moreover, de Broglie (1925) and Schrödinger (1926b) postulated a very successful theory for the propagation of **abstract wave functions** describing matter and physical objects in general: a theory of quantum physics. However, Einstein et al. (1935) realized that quantum physics is **nonlocal**, see also Bell (1964), Aspect et al. (1982), Hensen et al. (2015),Rosenfeld et al. (2017), Handsteiner et al. (2017). Thereby, Einstein (1948) proposed his **principle of locality**: No unmediated effect should be faster than the velocity of light c.

Furthermore, Perlmutter et al. (1998), Riess et al. (2000), Smoot (2007) discovered that space has an energy density, the **dark energy**. However, very different concepts of 'vacuum' have been proposed in the very successful theory of elementary particles: For instance, an 'electromagnetic vacuum', see Zeldovich (1968), Cugnon (2012), and a 'vacuum expectation value', see (Pich, 2007, section 4.2), (Zyla et al., 2020, section 11.2), have been introduced.

Additionally, the Hubble constant describing the rate of expansion of spacetime since the Big Bang exhibits an observed **Hubble tension**, see e. g. Riess et al. (2022).

In addition, Guth (1981) proposed a very rapid increase of space in an early era of 'cosmic inflation'.

Altogether, in present-day physics, we find various very successful theories that provide quite different answers about the nature of space. However, we live in one world. So there should be a unified theory. Indeed, a unified theory has always been preferred, see e. g. Styrman (2019). For it, we derive a geometrical and exact **theory of the dynamics of volume** in nature, including the formation of volume. We derive that theory from fundamental principles of physics, Fig (12.3). We do not propose any hypothesis or execute any fit. Hereby, we achieve precise accordance with observation, within the inaccuracy of measurement. Using that dynamics of volume, we achieve detailed answers to the following questions in a unified manner:

How are the proposed curvature and expansion of space derived and explained? How are the postulates of quantum physics derived? How is the space explained, in which electromagnetic waves propagate? What is a wave function? How is the propagation of nonlocal wave functions explained? How is nonlocality derived and explained on the basis of the dynamics of the volume? How is the observed dark energy explained and derived? How is the observed Hubble tension explained and derived, see the front cover and Fig. (21.3)? How is the 'cosmic inflation' derived and explained? How do the dynamics of the volume resolve the paradoxes of quantum physics?

How can you find the theory? For it, see section (2.1).

Part I

Semiclassical Spacetime and Gravity

Chapter 2

Basic Principles

2.1 How can you find the theory?

Most systematically, you start with chapter (2), in order to **comprehend the whole theory**, see Fig. (12.3).

The **key to the unification is the volume** and its dynamics. For it, the reality (DEF 15) of the additional volume is derived in section (2.6) and chapter (7). Thereby, the basics of the dynamics of the volume in chapter (7) can be derived with help of the Schwarzschild (1916) metric, SM, or with help of the Einstein (1915) field equation, EFE, or with help of the Ricci flow, Hamilton (1982), see mapping theorem in chapter (17).

Though the basics of the dynamics of the volume can be derived with help of general relativity (via the SM or EFE or Ricci flow), the dynamics of the volume provide results far beyond the present-day theory of general relativity, Hobson et al. (2006), Straumann (2013), Bartelmann (2019): For instance, quantum theory and the energy density of dark energy are derived and explained.

Moreover, our result is far beyond the usual theories of quantum gravity, Kiefer (2003), Kiefer and Sandhöfer (2008), (Schulz, 2020, chapter 2): Usual theories of quantum gravity use quantum physics, a hypothetical quantization procedure and relativity and gravity. In contrast, we derive and explain quantum physics on the basis of general relativity and gravity. Of course, as a consequence, our theory includes quantum gravity, without using any quantization procedure, or any hypothesis at all. Next, we summarize the used fundamental principles of physics.

2.2 Equivalence principle, EP

In this section, we summarize the experimentally confirmed Einstein equivalence principle, see e. g. Einstein (1915), Will (2014), Carmesin (2022d):

Definition 1 Einstein equivalence principle

The Einstein equivalence principle, EEP, includes the following statements:

(1) The weak equivalence principle, WEP, states that the gravitational force F_G is proportional to the mass m, or $\vec{F}_G = m \cdot \vec{G}^*$, see e. g. (Will, 2014, section 2.1). According to the action principle, $\vec{F} = m \cdot \vec{a}$, we derive the following statement: A probe mass m that is freely falling in a gravitational field $\vec{G}^*$ has an acceleration $\vec{a}$ equal to that field:

$$\vec{G}^* = \vec{a} \tag{2.1}$$

(2) The outcome of any local non-gravitational experiment is independent of the velocity of the freely falling reference frame in which it is performed.

(3) The outcome of any local non-gravitational experiment is independent of where and when in the universe it is performed.

(4) Lorentz invariance is included, see e. g. (Will, 2014, section 2.1), so SR is included (see section 2.3).

2.3 Special relativity, SR

In this section, we summarize essential results of special relativity, SR, see e. g. Einstein (1905), Landau and Lifschitz (1971), Moore (2013), Newell et al. (2018), Carmesin (1996), Carmesin (2020b):

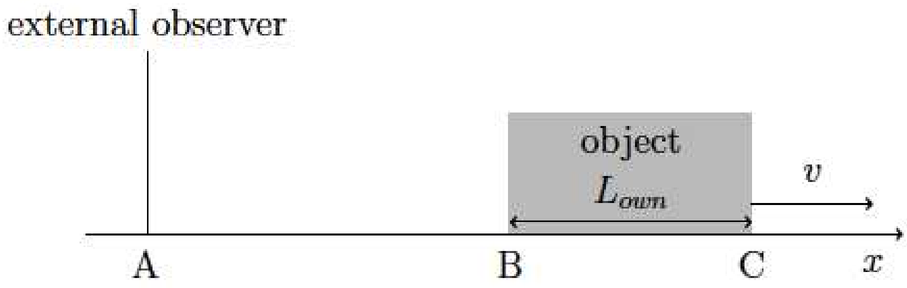

Figure 2.1: The length L of the object is measured with help of the light-travel distance d_{LT}. For it, a light signal is used that travels from B to C and back to C. The time dt_{own} of propagation of that signal in the own frame provides the own length $dL_{own} = c \cdot dt_{own}/2$. The time dt_{ext} of propagation of that signal in the external frame provides the external length $dL_{ext} = c \cdot dt_{ext}/2$. In order to measure the light-travel time from B to C and back to B, the external observer can measure the light-travel time from A to C and back to A and subtract the light-travel time from A to B and back to A.

Corollary 1 Special relativity

In each inertial frame, the following holds:

(1) The velocity of light or electromagnetic waves has the same value, Maxwell (1865), Zyla et al. (2020), Carmesin (2006):

$$c = 299\,792\,458\,\frac{\mathrm{m}}{\mathrm{s}} \tag{2.2}$$

(2) If an object moves at a velocity $v < c$ relative to an external inertial frame, and if a time t_{own} elapses between two events in the own frame of the object, then the time t_{ext} or t_{rel} elapses between these two events in the external inertial frame as follows, see e. g. (Landau and Lifschitz, 1971, Eq. 3.1):

$$\begin{aligned} t_{ext} = t_{rel} &= \gamma \cdot t_{own} \\ \text{with the Lorentz factor } \gamma &= \frac{1}{\sqrt{1 - v^2/c^2}} \end{aligned} \tag{2.3}$$

That relation is called time dilation, see e. g. (Einstein, 1905, § 2) or (Hobson et al., 2006, section 1.7).

(3) If an object moves at a velocity $v = |\vec{v}|$ *relative to an inertial frame, and if the object has a mass* m_{own} *in its own frame, then the object exhibits the own energy* E_{own} *in its own frame as follows, see e. g. (Landau and Lifschitz, 1971, Eq. 9.5):*

$$E_{own} = m_{own} \cdot c^2 \tag{2.4}$$

Moreover, the object exhibits the relativistic energy E_{rel} *or* E_{ext} *in the external inertial frame as follows, see e. g. (Landau and Lifschitz, 1971, Eq. 9.4):*

$$E_{rel} = \gamma \cdot E_{own} \tag{2.5}$$

(4) If an object moves at a velocity v *relative to an external inertial frame, and if the object has a mass* m_{own} *in its own frame, then the object exhibits the relativistic momentum* p_{ext} *and the energy* E_{ext} *in the external inertial frame as follows, see e. g. (Landau and Lifschitz, 1971, Eqs. 9.1, 9.6, 9.7):*

$$p_{ext} = m_{own} \cdot v \cdot \gamma = m_{own} \cdot \frac{v}{\sqrt{1 - v^2/c^2}} \tag{2.6}$$

$$E_{ext} = \sqrt{m_{own}^2 c^4 + p_{ext}^2 c^2} \tag{2.7}$$

(5) If an object moves at a velocity $v < c$ *relative to an external inertial frame, and if the object has a length* L_{own} *in the own frame, and if that length is measured with help of the light-travel distance in the external frame, then the following results are obtained, see e. g. see e. g. Einstein (1905); Landau and Lifschitz (1971) or Fig. (2.1):*

In the own frame, the following time dt_{own} elapses during the propagation of the light from B to C and back to B, see e. g. Condon and Mathews (2018):

$$dt_{own} = \frac{2}{c} \cdot L_{own} \tag{2.8}$$

In the external frame, the following time dt_{ext} elapses during the propagation of the light from B to C and back to B, see e. g. (Einstein, 1905, § 2):

$$dt_{ext,\,\mathrm{B\,to\,C}} = \frac{L_{ext}}{c-v}, \text{ external time from B to C} \tag{2.9}$$

$$dt_{ext,\,\mathrm{C\,to\,B}} = \frac{L_{ext}}{c+v}, \text{ external time from C to B} \tag{2.10}$$

$$dt_{ext} = dt_{ext,\,\mathrm{B\,to\,C}} + dt_{ext,\,\mathrm{C\,to\,B}} \text{ or} \tag{2.11}$$

$$dt_{ext} = \frac{L_{ext}}{c-v} + \frac{L_{ext}}{c+v} = \frac{2}{c}\frac{L_{ext}}{\sqrt{1-\frac{v^2}{c^2}}^{2}} \text{ or} \tag{2.12}$$

$$dt_{ext}\sqrt{1-\frac{v^2}{c^2}} = \frac{2}{c}\frac{L_{ext}}{\sqrt{1-\frac{v^2}{c^2}}} \tag{2.13}$$

Time dilation (Eq. 2.3) is involved in the measurement of the light-travel distance. Accordingly $dt_{ext}\sqrt{1-\frac{c^2}{v^2}} = dt_{own}$ and $dt_{own} = \frac{2}{c} \cdot L_{own}$ are used:

$$dt_{own} = \frac{2}{c}\frac{L_{ext}}{\sqrt{1-\frac{v^2}{c^2}}} = \frac{2}{c} \cdot L_{own} \text{ or} \tag{2.14}$$

$$L_{ext} = L_{own} \cdot \sqrt{1-\frac{v^2}{c^2}} \tag{2.15}$$

That relation is called length contraction, see e. g. (Einstein, 1905, § 2) or (Hobson et al., 2006, section 1.7).

(5) As the length contraction can be derived from time dilation, space and time form a combined system, spacetime. In order

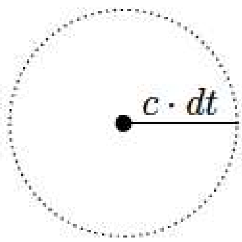

Figure 2.2: A lamp (black) emitted a light flash (dotted). During a time dt, the flash reached the radius $c \cdot dt$. Its square is equal to $dx^2 + dy^2 + dz^2 = c^2 \cdot dt^2$.

to describe that system in a coherent manner, Einstein (1905) used the concept of a light flash, see Fig. (2.2). If a lamp emits a light flash, then its radius reaches the radius $c \cdot dt$ during a time dt. Thus, the positions of the flash as a function of the time dt are described by the following relation:

$$ds^2 = -c^2 \cdot dt^2 + dx^2 + dy^2 + dz^2 = 0 \qquad (2.16)$$

Thereby, ds is called line element, see e. g. (Hobson et al., 2006, section 1.9). That equation holds for each system or frame that moves at a constant velocity v relative to the lamp. If the lamp moves at a constant velocity v relative to a rest frame in the direction of the x-axis, then the line element in the rest frame includes the time dilation and length contraction as a function of the Lorentz factor $\gamma(v)$ follows:

$$ds^2 = -c^2 \cdot dt^2/\gamma^2 + dx^2 \cdot \gamma^2 + dy^2 + dz^2 = 0 \quad (2.17)$$

This line element describes a metric, called Minkowski metric.

Corollary 2 Properties of special relativity

(1a) The invariance of the velocity of light has been observed. For instance, light emitted by binary stars at different velocities has been observed, see e. g. de Sitter (1913), Carmesin (2006), Carmesin (2022d).

Figure 2.3: An observer in an external frame can measure the length L_{own} of the stone with a yardstick. For it, the observer moves the yardstick to the stone and into the frame of the stone. Then the length $L_{own} \approx 177\,\mathrm{mm}$ can be measured.

(1b) The invariance of the velocity of light can be obtained with help of a thought experiment, additionally, see (Carmesin, 2022d, section 7.8).

(2) Time dilation has been observed. For instance, atomic clocks at satellites have been compared with atomic clocks at Earth Ashby (2002).

(3) Relativistic energy has been observed. According to (Einstein, 1907, title), relativistic energy represents inertia. That inertia has been observed, see e. g. Kaufmann (1901, 1906); Bucherer (1908).

(4) The equivalence of mass and energy has been observed. For instance, the positron has been observed, Anderson (1933), and the annihilation of the positron and the electron has been observed, see e. g. Zyla et al. (2020); Workman et al. (2022).

(5a) If a length parallel to the velocity $\vec{v}$ of a moving object is measured with the light-travel distance d_{LT}, then the time dilation is involved, and then the length contraction can be observed, see corollary (1) and (Einstein, 1905, § 2).

(5b) Accordingly, three-dimensional space and one-dimensional time are combined to a four-dimensional spacetime Einstein (1905); Landau and Lifschitz (1971).

(5c) In particular, there is no length contraction orthogonal to the velocity $\vec{v}$.

(5d) Einstein (1911b) explained the possible reality of the length of an object with two examples: If an object has its own length L_{own}, and if an external observer moves his yardstick into the objects frame, then the observer measures the own length L_{own} of the object, without length contraction. The reason is that the measurement takes place in the own frame of the object. This is illustrated in Fig. (2.1).

However, an external observer not moving with the object of an own length L_{own} can in principle measure the length contraction. Here, we elaborated such a measurement, see Fig. (2.1) or corollary (1).

(6) For instance, Laue (1912) as well as Debs and Redhead (1996) propose solutions of the twin paradox. Here we discuss a version of that paradox, whereby the time dilation can be measured with help of a usual satellite and spacecraft, see e. g. Ashby (2002):

One twin travels in a satellite at a constant velocity v at a circular Earth orbit with a radius R, whereby the orbit passes a point above the north pole. The other twin is at a spacecraft at the same radius R and constantly above the north pole (Fig. 2.4).

Geometrically, each twin can say that he is at rest and that the other moves on a circular orbit - that is the essence of the paradox. However, physically, the orbits are not equivalent:

Both twins are in the same gravitational field. An acceleration-sensor of the twin in the satellite shows the result zero, as a consequence of his circular motion at the velocity v. Thus, during one orbit, his age increases by the own periodic time T_{own}. In contrast, an acceleration-sensor of the twin at the spacecraft shows $9.81 m/s^2$, as he does not move at a circular orbit. So, *his age increases by the external time* $T_{ext} = \frac{T_{own}}{\sqrt{1-v^2/c^2}}$.

Note that a paradox is an apparent cognitive conflict, the solution of which provides a deeper insight.

(7a) Most physical systems consist of parts that move relative to each other, similarly as the external observer and the moving object discussed in SR. Such composed physical systems are described by SR. For instance, an atomic clock is a composed system, as an atom consists of the nucleus and at least one electron. Accordingly, SR holds for composed systems in a **universal manner**.

(7b) If the parts of a composed system move at velocities smaller than c, then the addition of velocities in SR can be applied, see e. g. Einstein (1905); Landau and Lifschitz (1971); Carmesin (1996); Moore (2013).

(8) Einstein argued ((Einstein, 1907, p. 381)), that a propagation of a signal faster than light is not compatible with special relativity. We use this result for the case of natural three-dimensional volume. More general physical systems have been derived with help of phase transitions, see e. g. Carmesin (2021b, 2019b, 2017, 2018b).

2.4 Radial structure of gravity near a mass

In this section, we introduce the first basic principle of gravity. For it, we introduce the principle of gravity in the surroundings of a mass M. On that basis, we will derive more general situations including gravity later.

2.4.1 Radial structure near a mass M

In the vicinity of a mass M, according to symmetry, the following holds: If a hand lead is in a frame that does not rotate and

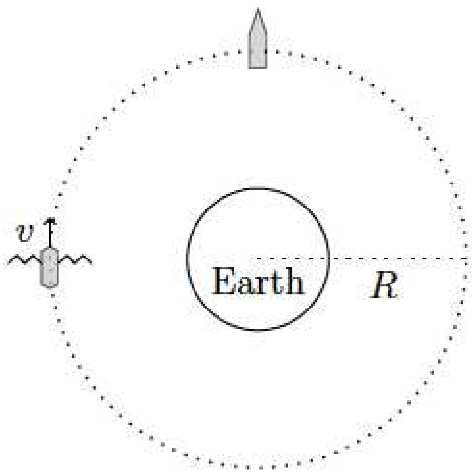

Figure 2.4: Twin paradox: One twin travels in the satellite at a velocity v, the other twin waits in the spacecraft at a constant position above the north pole.

that is at a constant distance to M, then the hand lead points towards M, see Fig. (2.5).

Using two such hand leads, a gravitational parallax distance d_{GP} can be measured as shown in Fig. (2.8).

2.5 Law of energy conservation

If a system is stationary, then the system is symmetric with respect to translation in time, and then the energy of the system is conserved, see Noether (1918). In parts I, II and III of the present book, and in most cases in part IV of this book, we analyze stationary systems only. Thus the basic principle of energy conservation holds.

According to the energy time uncertainty relation, see e. g. Heisenberg (1927); Kumar (2018); Ballentine (1998); Scheck (2013), and corresponding to possible zero-point energies, the basic law of energy conservation is slightly modified.

In this sense, we summarize the law of energy conservation, see e. g. Mayer (1842), Landau and Lifschitz (1973), Tryon (1973), Carmesin (2018b, 2019b, 2020b):

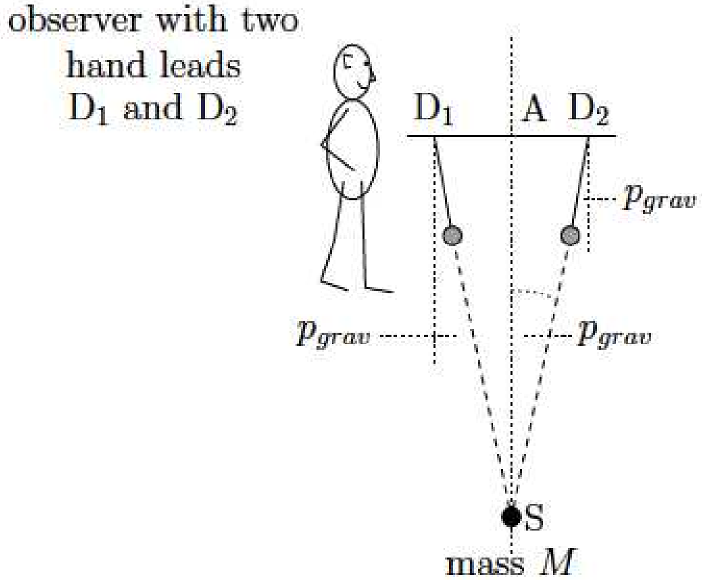

Figure 2.5: In the isotropic surroundings of a mass M, the radial structure of gravity can be measured by using two hand leads. These can be arranged so that equal angles of gravitational parallax p_{grav} are measured.

Corollary 3 Law of energy conservation

If a process of energy transformation or energy transport takes place in a closed subsystem, and if that process is completely described within a desired frame[1]*, then the following holds:*

(1) The amount of energy available for transport or transformation of energy within the chosen frame does not change.

(2) Hereby, a zero-point energy is not available for transport or transformation of energy, as the corresponding oscillation, the zero-point oscillation, is already at its lowest energy state[2]*.*

[1] The frame is not changed during the analysis of the process, of course.

[2] If the size of a system changes, then the number of ZPOs of that system can change, see e. g. (Ballentine, 1998, section 19.3), (Sakurai and Napolitano, 1994, p. 476-480). The ZPE of a ZPO is not available, see e. g. Mehra and Rechenberg (1999), Fornasini and Grisenti (2015), Lamb and Retherford (1947), (Landau and Lifschitz, 1965, § 3), (Kumar, 2018, p. 65), (Ballentine, 1998, section 19.3), (Sakurai and Napolitano, 1994, p. 476-480), (Scheck, 2013, p. 25).

(3) The law of energy conservation may exhibit a standard deviation according to the energy time uncertainty relation, see e. g. Heisenberg (1927); Kumar (2018); Ballentine (1998); Scheck (2013).

2.6 Measures of observable distance

If a physical quantity can be measured, then it is part of **physical reality**, see definition (15). A distance measure is an essential basis for a metric space, see e. g. (Hilbert, 1903, § 5), (Lee, 1997, p. 91). For instance, we travel and communicate in the space described by the light-travel distance d_{LT}.

In this section, we provide that basis by introducing procedures for the measurement of a distance between an observer and an object, see e. g. Fig. (2.6). Each such procedure of measurement provides a **measure of observable distance**.

2.6.1 Insights from measures of observable distance

In general, there are various methods for the measurement of a physical quantity. For instance, if you want to measure a mass at Earth, then you can use a beam balance or a spring balance. However, you may obtain wrong values at the Moon, as the beam balance really measures mass, whereas the spring balance basically measures force. The difference of both measures can provide insights about the relation of mass and force.

Similarly, the difference of two measures of observable distance can provide insights about the dynamics of volume.

2.6.2 Light-travel distance

In this section, we describe how an observer can apply an optical source, in order to measure the **light-travel distance**, $d_{LT}(A, B)$ between two locations A and B, see Fig. (2.6).

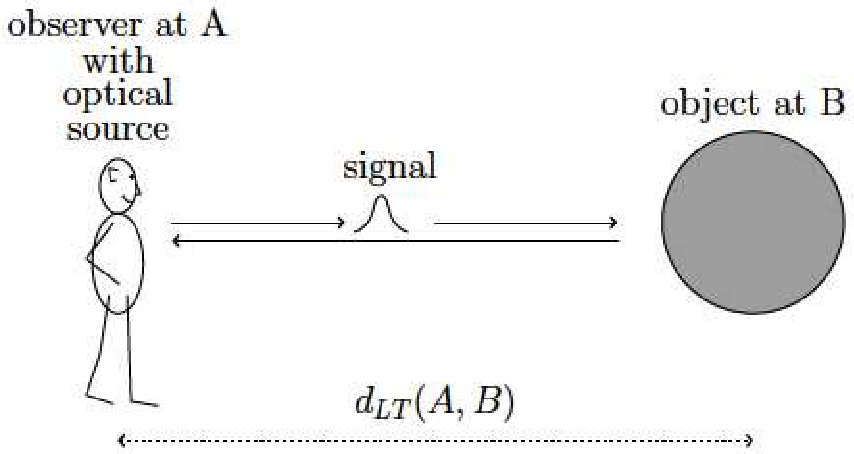

Figure 2.6: Measurement of the time of flight t_{of} and of the corresponding light-travel distance d_{LT} between an observer and an object, Condon and Mathews (2018).

Definition 2 Light-travel distance

The light-travel distance between locations A and B is defined by the following procedure:

(1) The observer at A emits a signal of his optical source towards the object, whereby the observer starts a clock.

(2) The object at B reflects the signal.

(3) The observer detects the reflected signal, whereby the observer stops the clock.

(4) The time interval between emission and detection of the signal is called **time of flight**, t_{of}.

(5) The **light-travel distance** *is as follows:*

$$d_{LT}(A, B) = \frac{t_{of} \cdot c}{2} \tag{2.18}$$

$$\text{with time of flight } t_{of} \text{ and velocity of light } c \tag{2.19}$$

2.6.3 Optical parallax distance

Even very large distances must be measured by local devices. For it, the concept of the parallax is appropriate. In this section, we describe how an observer can apply two local optical detectors, in order to measure even a large distance. The corresponding distance is called **optical parallax distance**, d_{OP}, see Fig. (2.7).

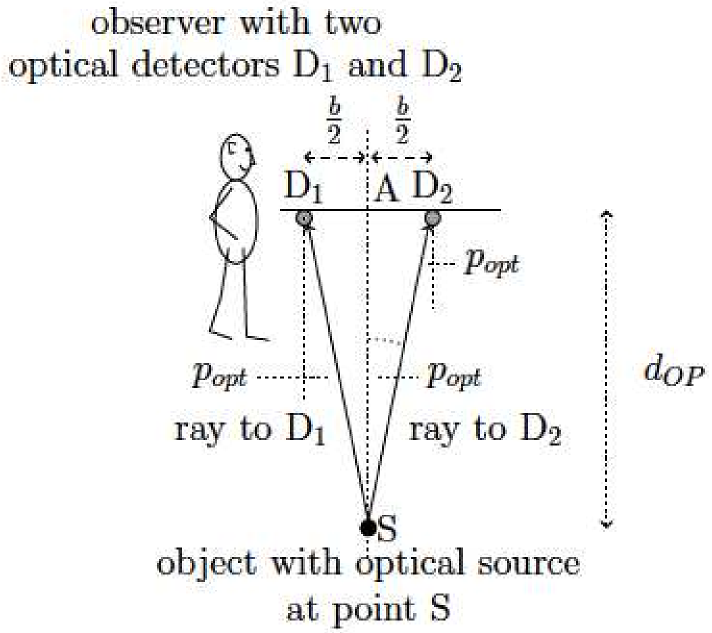

Figure 2.7: Measurement of the optical angle of parallax p_{opt} and of the corresponding optical parallax distance d_{OP} between an observer and an object. Hereby, D_1, D_2 and S form an isosceles triangle D_1D_2S, with the baseline D_1D_2, having the center A.

Definition 3 Optical parallax distance

The optical parallax distance between an observer and an object is defined by the following procedure, for an illustration see Fig. (2.7):

(1) The object emits optical rays.

(2) The observer detects a ray propagating from the object to his first detector D_1 and a ray propagating from the object to his second detector D_2. Hereby, the distance between these detectors is named b. Moreover, the detectors are placed so that these detectors D_1 and D_2 and the object are the corners of an

isosceles triangle. For it, the detectors are placed so that the observer measures the same **optical angle of parallax** p_{opt} *at both detectors.*

(3) The observer calculates the **optical parallax distance** $d_{par,opt}$ *according to the following equations:*

$$\text{triangle } SD_2A, \text{ is rectangular with } \tan(p_{opt}) = \frac{b/2}{d_{OP}} \tag{2.20}$$

$$\text{thus, } d_{OP} = \frac{b/2}{\tan(p_{opt})} \tag{2.21}$$

$$\text{with optical parallax } p_{opt} \tag{2.22}$$

In cosmology, the optical parallax distance is generalized to the angular diameter distance, Condon and Mathews (2018).

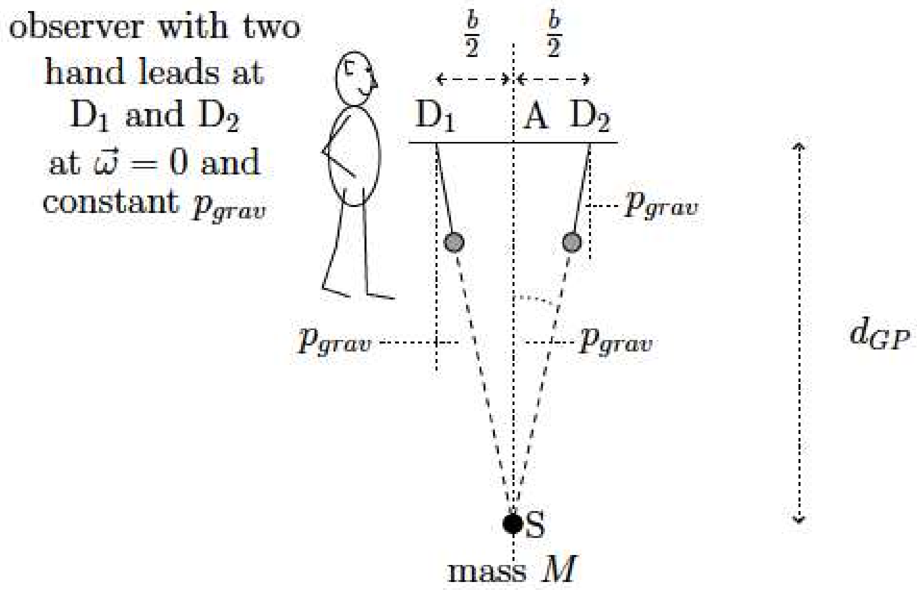

Figure 2.8: Measurement of the angle of gravitational parallax p_{grav} and of the corresponding gravitational parallax distance d_{GP} between an observer and an object. Hereby, D_1, D_2 and S form an isosceles triangle D_1D_2S, with the baseline D_1D_2, having the center A.

2.6.4 Gravitational parallax distance

In this section, we describe how an observer can apply two hand leads, in order to measure the distance of an object. The corresponding distance is called **gravitational parallax distance**, d_{GP}, see Fig. (2.8).

Definition 4 Gravitational parallax distance

The gravitational parallax distance between an observer and an object is defined by the following procedure, for an illustration see Fig. (2.8):

(1) The observer places two hand leads D_1 and D_2 at a distance b. Hereby, the hand leads are placed so that D_1 and D_2 and the object are the corners of an isosceles triangle. For it, the hand leads are placed so that the observer measures the same **angle of gravitational parallax** *p_{grav} at both detectors. The center of the baseline D_1D_2 is named A. Hereby, the observer has zero rotational velocity, $\vec{\omega} = 0$, and a constant gravitational angle of parallax.*

(2a) Thereby, the observer places his laboratory in such a manner that two conditions are obeyed.

(2b) The gravitational parallax distance d_{GP} does not change as a function of time. For it, the observer can use a closed loop control.

(2c) The angular velocity is zero. For it, the observer can use a gyroscope and a closed loop control.

$$d_{GP} = constant \quad \text{and} \quad (\omega_1, \omega_2, \omega_3) = (0, 0, 0) \qquad (2.23)$$

(2d) Thus, the observer has constant polar coordinates $R = d_{GP}$ and θ and ϕ relative to the mass M.

(2e) Thence, the observer has a fixed position relative to the mass M.

(3) The observer calculates the **gravitational parallax distance** d_{GP} *according to the following equations:*

$$\text{triangle } SD_2A, \text{ is rectangular} \tag{2.24}$$

$$\text{with } \tan(p_{grav}) = \frac{b/2}{d_{GP}} \tag{2.25}$$

$$\text{thus, } d_{GP} = \frac{b/2}{\tan(p_{grav})} \tag{2.26}$$

$$\text{with gravitational parallax } p_{grav} \tag{2.27}$$

(4) A frame with the properties in (1) and (2a-e) is named d_{GP} *frame.*

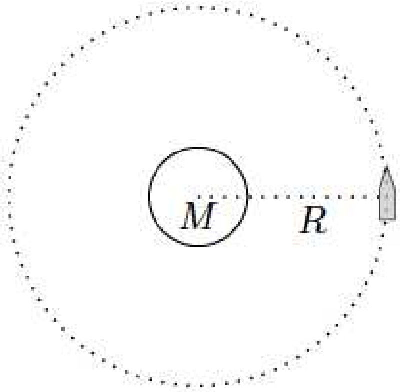

Figure 2.9: If a spacecraft is in a circular orbit around a mass M and in the isotropic vicinity of M, and if the spacecraft measures the circumference U of the orbit, the circumferential radial coordinate is $R_{circumferential} = \frac{U}{2\pi}$.

2.6.4.1 Circumferential radial coordinate

A circumference C of a circle with the mass M at its center and the corresponding *circumferential radial coordinate* (Moore, 2013, Eq. 9.5)

$$R = \frac{C}{2\pi} = R_{circumferential} \tag{2.28}$$

can be measured as follows. A spacecraft can travel in an orbit around M, whereby the distance to the mass M is constant in the isotropic vicinity of M. The circumference C of the orbit can be measured as follows. A large number N of such spacecrafts travel at the same orbit at the same speed and in an equidistant manner. Two neighboring spacecrafts measure the distance d from each other. That distance is not influenced by gravity, as the straight line between the two spacecrafts is horizontal. The circumference is the product of N and d:

$$C = N \cdot d \tag{2.29}$$

The circumferential radial coordinate is a part of physical reality, as it can be measured, Einstein et al. (1935). Moreover, that coordinate is a distance between M and the spacecraft. In general, the circumferential distance R is different from the light-travel distance d_{LT} between M and the spacecraft. The circumferential radial coordinate R and the gravitational parallax distance between the spacecraft and the mass M are equal, as both measure the distance in the limit M to zero:

$$d_{GP,\, M \text{ to observer}} = R_{circumferential} = \lim_{M \to 0} d_{LT,\, M \text{ to observer}} \tag{2.30}$$

2.6.4.2 Measurable map of non-curved space

In this section, we show how the gravitational parallax distance d_{GP} provides a measurable map of non-curved or flat space.

(1) We show the following: For each object in the vicinity of M, the gravitational parallax distances d_{GP} to M are equal to the distance of the non-curved or flat space.

The d_{GP}-distance is measured by the triangle in Fig. (2.8). That triangle has the sum of interior angles equal to π. It is shown next:

The angle $\angle D_1AS$ is equal to $\pi/2$, as the observer provides an isosceles triangle.

$\angle SD_1A$ is smaller than $\pi/2$ by a difference p_{grav}. So, $\angle SD_1A$ is equal to $\pi/2 - p_{grav}$.

As gravity has radial symmetry (section 2.4), two sides of the triangle intersect at M or S. So, $\angle ASD_1$ is equal to p_{grav}.

Thus, the sum of the above three interior angles is π.

As the used triangle in Fig. (2.8) has the sum of interior angles equal to π, it is in accordance with non-curved space, see e. g. (Lee, 1997, Angle-Sum Theorem, p. 166).

As the used triangle in Fig. (2.8) is in accordance with non-curved space, it provides the distance of the non-curved space.

(2) We show that for each object, the polar coordinates of the non-curved space are provided.

The radial coordinate is provided according to item (1).

The angular coordinates can be measured similarly as the angles of parallax in Fig. (2.8).

(3) As the polar coordinates of the non-curved space are provided for each object, a measurable map of non-curved or flat space is provided. For an illustration see Fig. (2.10).

We summarize our finding, see illustrations in Figs. (2.11, 2.10).

Theorem 1 d_{GP} provides flat measured space

(1) The procedure of measurement of the gravitational parallax distance d_{GP} in DEF (4) provides a distinction between gravity and acceleration.

(2) In the surroundings of a mass M, the gravitational parallax distance d_{GP} can be measured without ambiguity.

(3) Based on that measured distance d_{GP}, the corresponding measured space is not curved, but flat. Accordingly, a gravitational parallax distance d_{GP} is equal to the corresponding light-travel distance $d_{LT,M\to 0}$ in the limit M to zero. Hereby and in general, two distances between two events A and B that take

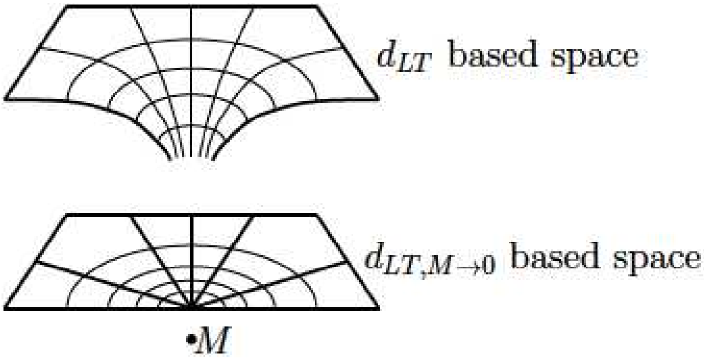

Figure 2.10: Two maps: In this illustration, three-dimensional space is represented by a two-dimensional manifold, similarly as in (Stephani, 1980, Fig. 10.1) or (Hobson et al., 2006, Fig. 11.7 or Fig. 11.10 upper panel or Fig. 13.1), whereby a mass M is at the origin. The light-travel distance d_{LT} is a measurable physical distance. With it, the d_{LT} based map is formed. That map is curved, see e. g. (Stephani, 1980, Fig. 10.1). The gravitational parallax distance $d_{GP} = d_{LT,M\to 0}$ is a measurable physical distance. With it, the d_{GP} based map is formed. That map is not curved. As most measurements are based on light, the d_{LT} based map is the mostly used map. Moreover, the d_{GP} based map can be regarded as the limit of M to zero of the d_{LT} based map. Note: You can use a map instead of a globe of Earth, without thinking Earth would be flat. Similarly, we travel or use telecommunication in the curved space described by the upper map.

place at the same time are named corresponding distances.

$$d_{GP}(A,B) = \lim_{M\to 0} d_{LT}(A,B) =: d_{LT,M\to 0}(A,B) \tag{2.31}$$

(4) The measured distance d_{GP} and the corresponding measured space are part of physical reality, according to DEF (15).

(5) In contrast, in general, the space that is based on the light-travel distance d_{LT} is curved. That space is usually considered as the physical space, as distances in space are usually measured on the basis of light.

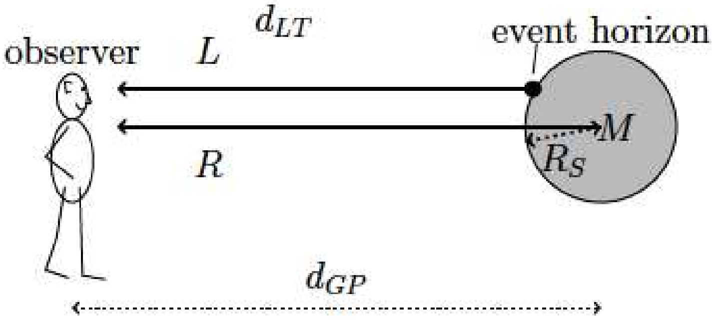

Figure 2.11: Two observations provide physical reality: Observation using light provides the light based space structure ending at the event horizon, see e. g. (Stephani, 1980, Fig. 10.1). Observation using gravity provides the gravity based spatial structure.

2.6.5 Two space structures

In this section, we summarize the two space structures, for an illustration see Figs. (2.11, 2.10).

Corollary 4 Two physical spatial structures

Physical reality provides two space structures as follows:

(1) Physical reality provides a gravity based spatial structure by the following polar coordinates[3]*:*

$$(d_{GP}, \theta, \phi) = \text{ gravity based space structure} \tag{2.32}$$

(2) Physical reality provides a light based space structure by the following coordinates[4]*:*

$$(d_{GP} \cdot \sqrt{g_{RR}(R)}, \theta, \phi) = \text{ light based space structure,} \tag{2.33}$$

$$\text{with an elongation factor } \sqrt{g_{RR}(R)}, \tag{2.34}$$

$$\text{whereby } g_{RR}(R) \text{ is a function of } R \tag{2.35}$$

[3]For polar coordinates in three dimensional flat space, see e. g. (Hobson et al., 2006, p. 35).

[4]This space structure represents the spatial part of the Schwarzschild metric, see e. g. Schwarzschild (1916), (Landau and Lifschitz, 1971, Eq. 97.14) (Hobson et al., 2006, Eq. 9.12).

(3) The gravity based spatial structure represents a flat space, whereas the light based space structure represents a curved space, that is part of a curved spacetime.

(4) The light based space structure is the usual space structure, as most measurements are obtained with help of light, electromagnetic radiation or particles. Within natural space, all such objects propagate through the light based space structure at a velocity $v \leq c$.

2.7 Objects of interaction

In this section, we summarize the physics of objects of interaction. Such objects of interaction are used in the three fundamental interactions, electromagnetic interaction, weak interaction and strong interaction, see e. g. Zyla et al. (2020), Griffiths (2008). Hereby, the corresponding objects of interaction are the (virtual) photons, the Z - and W - bosons and the gluons. These objects of interaction propagate in space.

In the case of gravity, the d_{GP} distance provides a non-curved map. We can use that map in order to **describe** the objects of interaction of gravity. We will **investigate** the propagation of the objects of interaction in part (II). Next, we summarize the properties of objects of interaction described in a non-curved space.

2.7.1 Properties of objects of interaction

In this section, we summarize the properties of objects of interaction described in a non-curved space. For it, we analyze the principle of the transfer of a fundamental interaction as follows, see Fig. (2.12):

A fundamental interaction or force is transferred by objects of interaction, so that the following holds, e. g. Zyla et al. (2020).

As a principle, a **source** Q of the interaction emits an amount

Δq of objects of interaction per time Δt proportional to Q. So the corresponding **current** I_q is as follows:

$$\frac{\Delta q}{\Delta t} = I_q \propto Q \tag{2.36}$$

As a consequence, in an isotropic region around Q, the current I_q flows in an isotropic manner. Thus, at a distance R from Q, the corresponding **current density** j_q is as follows:

$$j_q = \frac{I_q}{4\pi R^2} \propto \frac{Q}{R^2} \tag{2.37}$$

As another part of the principle, a probing particle with a source Q_{probe} has a cross section $A_{Q_{probe}} \propto Q_{probe}$, so that the amount $\Delta q_{transferred}$ of objects of interaction transferred to Q_{probe} per time $\frac{\Delta q_{transferred}}{\Delta t}$ is proportional to $j_q \cdot A_{Q_{probe}}$:

$$\frac{\Delta q_{transferred}}{\Delta t} \propto j_q \cdot A_{Q_{probe}} \propto j_q \cdot Q_{probe} \tag{2.38}$$

Here, we insert the relation for the current density in Eq. (2.37):

$$\frac{\Delta q_{transferred}}{\Delta t} \propto \frac{Q \cdot Q_{probe}}{R^2} \tag{2.39}$$

As a part of the principle, an amount $\Delta q_{transferred}$ causes a momentum transfer $\Delta p_{transferred}$ proportional to $\Delta q_{transferred}$:

$$\Delta q_{transferred} \propto \Delta p_{transferred}, \tag{2.40}$$

According to Newton's action principle (second axiom, Newton (1687)), the probing particle Q_{probe} experiences a force F_q, which is equal to the momentum transferred per time:

$$|F_q| = \frac{\Delta p_{transferred}}{\Delta t} \tag{2.41}$$

Here, we use the relations for the transferred objects of interaction in Eqs. (2.40, 2.39):

$$|F_q| = \frac{\Delta p_{transferred}}{\Delta t} \propto \frac{\Delta q_{transferred}}{\Delta t} \propto \frac{Q \cdot Q_{probe}}{R^2} \tag{2.42}$$

We summarize in the form of a definition:

Definition 5 Principle of transfer of interaction

A fundamental force is transferred by objects of interaction. Thereby, without screening, the following holds in three - dimensional space, see e. g. Zyla et al. (2020).

(1) A source Q emits an amount Δq of objects of interaction per time Δt proportional to Q. So, the corresponding **current** *is as follows:*

$$\frac{\Delta q}{\Delta t} = I_q \propto Q \tag{2.43}$$

(2) An amount $\Delta q_{transferred}$ of objects of interaction transferred to a probing particle Q_{probe} causes a momentum transfer, named $\Delta p_{transferred}$, that is proportional to $\Delta q_{transferred}$:

$$\Delta q_{transferred} \propto \Delta p_{transferred}, \tag{2.44}$$

(3) If a probing particle has a source Q_{probe}, and if it is at a distance R from Q, and if it has a cross section $A_{Q_{probe}}$, then the amount $\Delta q_{transferred}$ of objects of interaction transferred to Q_{probe} per time Δt is as follows: The ratio $\frac{\Delta q_{transferred}}{\Delta t}$ is proportional to the product $j_q \cdot A_{Q_{probe}}$ of the **current density***, the current I_q per area A; $j_q = I_q/A$ and the cross section $A_{Q_{probe}}$:*

$$\frac{\Delta q_{transferred}}{\Delta t} \propto j_q \cdot A_{Q_{probe}} \propto j_q \cdot Q_{probe} \propto \frac{Q \cdot Q_{probe}}{R^2} \tag{2.45}$$

(4) A corresponding force $|\vec{F}_q|$ is as follows:

$$|\vec{F}_q| = \frac{\Delta p_{transferred}}{\Delta t} \propto \frac{Q \cdot Q_{probe}}{R^2} \tag{2.46}$$

2.8 Gravity near a mass, GG

In this section, we introduce the second basic principle of gravity. For it, we use the gravitational parallax distance d_{GP} and

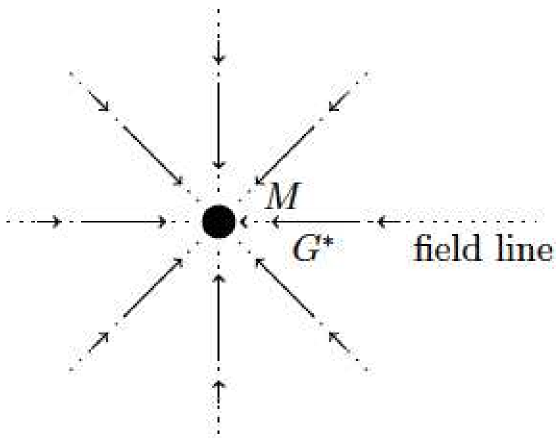

Figure 2.12: Mass M with field lines (dotted) and vectors (solid) of the gravitational field G^*. The gravitational field is proportional to a corresponding outwards flowing current density j_p, see definition (5).

the objects of interaction. As a consequence, there will be a $1/R^2$ law. Accordingly, we name that gravity generalized Gaussian gravity, GG, as Gaussian gravity exhibits the same law. The present gravity is more general, as it provides curvature of space, in addition, see e. g. Carmesin (2021d).

For it, we apply the definition (5) to the case of gravity. Hereby, the source Q is the considered mass M, the probing particle Q_{probe} is a probe mass m_{probe}, and the distance R is the gravitational parallax distance d_{GP}. Thus, the gravitational force is as follows[5]

$$|F_G| \propto \frac{M \cdot m_{probe}}{d_{GP}^2} \tag{2.47}$$

Hereby, the proportionality factor is the universal constant of gravitation (Zyla et al., 2020, table 1.1):

$$G = 6.674\,30(15) \cdot 10^{-11} \, \frac{\mathrm{m}^3}{\mathrm{kg} \cdot \mathrm{s}^2} \tag{2.48}$$

[5]Note that the proportionality in Eq. (2.47) is in accordance with the analysis of gravity by Gauss (1840).

Thus, the corresponding force is as follows:

$$\vec{F}_G = \frac{G \cdot M \cdot m_{probe}}{d_{GP}^2} \cdot \vec{e}_{downwards\ unit\ vector} \tag{2.49}$$

By definition, the gravitational force divided by the probe mass is the gravitational field:

$$\vec{G^*} = \frac{\vec{F}_G}{m_{probe}} \tag{2.50}$$

As a consequence, the gravitational field is as follows:

$$\vec{G^*} = \frac{G \cdot M}{R^2} \cdot \vec{e}_{downwards\ unit\ vector} \quad \text{with} \quad R = d_{GP} \tag{2.51}$$

We summarize our results:

Theorem 2 Law of inverse squared distance

For a fundamental force that is transferred by objects of interaction according to definition (5), the following holds:

(1) If a source Q and a probing object Q_{probe} are at a distance $R = d_{GP}$, and if no screening takes place, then the force of interaction $|F_q|$ between Q and Q_{probe} is proportional to the inverse squared distance as follows:

$$|F_q| \propto \frac{Q \cdot Q_{probe}}{R^2} \tag{2.52}$$

(2) In particular, if a mass M and a probe mass m_{probe} are at a distance $R = d_{GP}$, then the gravitational force of interaction $\vec{F}_G$ between M and m_{probe} is as follows:

$$\vec{F}_G = \frac{G \cdot M \cdot m_{probe}}{R^2} \cdot \vec{e}_{downwards\ unit\ vector} \tag{2.53}$$

(3) Thus, the corresponding gravitational field is as follows:

$$\vec{G^*} = \frac{G \cdot M}{R^2} \cdot \vec{e}_{downwards\ unit\ vector} \tag{2.54}$$

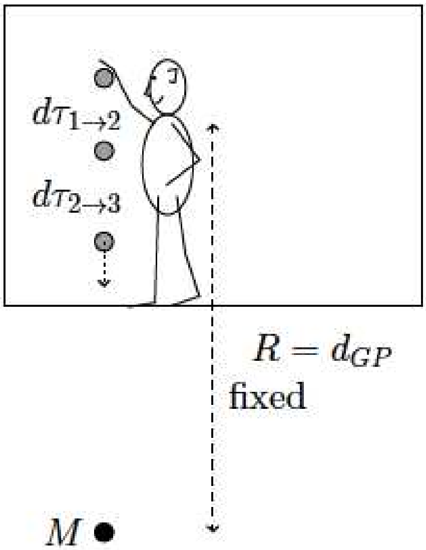

Figure 2.13: Two dimensional scheme of an observer localized at a constant gravitational parallax distance $R = d_{GP}$ and at zero angular velocity $\vec{\omega} = \vec{0}$. He measures the height $h(\tau)$ of a falling ball as a function of time τ and evaluates the gravitational acceleration $a = h''(\tau)$.

2.8.1 Consequence: measurement of a mass M

In this section, we describe how an observer can measure a distant mass or dynamic mass M.

Definition 6 Measurement of a distant mass M

An observer can measure the mass or dynamic mass M of a distant object by the following procedure, for an illustration see Fig. (2.13):

(1) The observer measures the gravitational parallax distance d_{GP}, see definition (4).

(2) The observer places his laboratory in such a manner that two conditions are obeyed:

(2a) The gravitational parallax distance d_{GP} does not change as a function of time.

(2b) The angular velocity is zero. For it, the observer can use a gyroscope.

$$d_{GP} = constant \quad \text{and} \quad (\omega_1, \omega_2, \omega_3) = (0,0,0) \tag{2.55}$$

(2c) Thus, the observer has constant polar coordinates $R = d_{GP}$ and θ and ϕ relative to the mass M.

(2d) Thence, the observer has a fixed position relative to the mass M.

(3) The observer measures the acceleration a of a ball that is freely falling in his laboratory. For it, the observer can apply the following steps:

(3a) The observer starts the falling of a ball.

(3b) The observer measures the height $h(\tau)$ of the ball as a function of time τ.

(3c) The observer evaluates the second derivative of the measured function $h(\tau)$ and identifies it with the acceleration a:

$$\left|\frac{\partial^2 h}{\partial \tau^2}\right| = |a| \tag{2.56}$$

$$\vec{a} = |a| \cdot \vec{e}_{downwards\ unit\ vector} \tag{2.57}$$

(4) The observer determines the gravitational field $\vec{G}^*$ by using the principle of equivalence of the acceleration $\vec{a}$ and the gravitational field $\vec{G}^*$:

$$\vec{G}^* = \vec{a} \tag{2.58}$$

(5) The observer applies the term for the gravitational field $\vec{G}^*$, and solves it for the mass M:

$$|\vec{G}^*| = \frac{G \cdot M}{R^2}, \quad \text{thus} \tag{2.59}$$

$$M = \frac{|\vec{G}^*| \cdot R^2}{G}, \quad \text{with} \quad R = d_{GP} \quad \text{We summarize:} \tag{2.60}$$

Corollary 5 Observer at an isotropic vicinity of M

An observer in an isotropic vicinity of a mass M can observe the following physical quantities, that are part of physical reality:

(1) The observer can measure the polar coordinates (Eq. 2.32):

$$(d_{GP}, \theta, \phi) = \text{ gravity based space structure} \tag{2.61}$$

(2) The observer can measure the acceleration and the gravitational field (Eq. 2.58):

$$\vec{G}^* = \vec{a} \tag{2.62}$$

(3) The observer can measure the mass M (Eq. 2.33):

$$M = \frac{|\vec{G}^*| \cdot R^2}{G}, \quad \text{with} \quad R = d_{GP} \tag{2.63}$$

(4) The observer can confirm the gravitational field $|G^*|$ as a function of the gravitational parallax distance $R = d_{GP}$ (Eq. 2.59):

$$|\vec{G}^*(R)| = \frac{G \cdot M}{R^2}, \quad \text{with} \quad R = d_{GP} \tag{2.64}$$

Corollary 6 Observed effective mass M_{eff}

If an observer searches for a mass according to DEF (6), then the following holds:

(1) If the observer measures a nonzero angle p_{grav}, he/she can interpret the result in terms of a mass M or an effective mass M_{eff}. In both cases, the observer can derive a distance R or an effective distance R_{eff} as well as a gravitational field $\vec{G}^*$.

(2) If the observer measures a zero angle p_{grav}, he/she can interpret the result as follows: There is no measurable mass M or effective mass M_{eff}. Accordingly, there is neither a measurable finite distance R or R_{eff} to a mass or effective mass, nor a measurable nonzero gravitational field $\vec{G}^*$. So the gravitational field is zero within the accuracy of the measurement.

2.9 Dynamic volume, DV

Idea: A possible accelerated expansion of the universe is described by a **cosmological constant** Λ. It has been introduced in a hypothetic manner by Einstein (1917).

Zeldovich (1968) suggested a *density of the cosmological constant* ρ_Λ with $\Omega_\Lambda = \frac{\rho_\Lambda}{\rho_{cr.}} = \frac{\Lambda c^2}{3H^2}$ (Eq. VII.2). Hereby, $\rho_{cr.0}$ is the present-day value of the critical density. Thereby, the global curvature of space is zero at the critical density, C. (5), Hobson et al. (2006). For the density ρ_Λ, Zeldovich (1968) proposed a 'density of a classical vacuum' $\rho_\Lambda = \rho_{\text{classical vacuum, Zeldovich}} \approx 2 \cdot 10^{-26} \frac{\text{kg}}{\text{m}^3}$ [Eq. VII.1]. Similarly, the density ρ_Λ has been named *density of vacuum* $\rho_{vac} = \frac{\Lambda c^2}{8\pi G}$, see (Hobson et al., 2006, Eq2. 8.22, 15.1, 15.5):

$$\rho_{vac} = \rho_\Lambda = \rho_0 - \rho_{m,0} - \rho_{r,0} = \frac{3H_0^2}{8\pi G} = \rho_{cr.0} \tag{2.65}$$

Hereby, H_0 is the Hubble constant, $\rho_{m,0}$ is the present-day value of the density of matter, and $\rho_{r,0}$ is the present-day value of the density of radiation, C. (5), Hobson et al. (2006). The densities in Eq. (2.65) are basic constituents of the ΛCDM model of cosmology, Planck-Collaboration (2020), Kosowsky et al. (2002), Zyla et al. (2020).

2.9.1 Evidence for a density ρ_Λ

Perlmutter Perlmutter et al. (1998), Riess et al. (2000) and Smoot (2007) discovered the accelerated expansion of the universe.

In the framework of general relativity, that accelerated expansion is explained with a nonzero value of the cosmological constant Λ or of the corresponding density ρ_Λ or energy density $u_\Lambda = \rho_\Lambda \cdot c^2$. The corresponding energy $\delta E_\Lambda = u_\Lambda \cdot \delta V$ has been named *dark energy*, Huterer and Turner (1998). We mark it by the subscript DE. The observed value is as follows, see e. g. Planck-Collaboration (2020):

$$\rho_{DE} = u_{DE}/c^2 \approx 5 \cdot 10^{-27}\,\frac{\mathrm{kg}}{\mathrm{m}^3} \tag{2.66}$$

Thus, the accelerated expansion is basically described by the cosmological constant Λ. However, within general relativity, that constant has not been derived, so the observed value cannot be tested or falsified Popper (1974).

Carmesin (2021d) overcame that impossibility of falsification by deriving Λ, ρ_Λ and u_Λ from first principles (see also e. g. Carmesin (2018c), Carmesin (2018b), Carmesin (2019b), Carmesin (2021b), Carmesin (2021a), Carmesin (2023a)).

2.9.2 H_0 tension

Discovery of the H_0 tension: Riess et al. (2022) discovered that observed values of the Hubble constant H_0 can exhibit differences at a high level of confidence of five σ.

In the framework of the ΛCDM model of cosmology, the densities ρ_{DE}, ρ_Λ and ρ_{vac} could be determined from the observed value H_0, according to Eq. (2.65). However, the observed values of H_0 exhibit differences at the 5σ confidence level, Riess et al. (2022). So, the following question arises: **How can the concept of dark energy be improved by principles of physics?**

2.9.3 Properties of the dynamic volume

In this section, we present a scheme of our fundamental dynamics of volume and its density. That dynamics of volume is elaborated in part (II) and applied in parts (III, IV):

There is only **one volume** in nature, and it has only **one density of volume** $\rho_{vol} = \Omega_{vol} \cdot \rho_{cr.0}$. Hereby, $\Omega_{vol} = \rho_{vol}/\rho_{cr.0}$ is the density parameter of volume.

(1) Volume is usually measured on the basis of the light travel distance d_{LT}, C. (2, 7, 17).

(2) The density of three-dimensional volume, ρ_{vol}, is determined by the quanta of volume in C. (22, 20): $\Omega_{vol} = 2/3$, in precise accordance with observation.

(3) Heterogeneity causes an additional summand in Eq. (2.65). That summand is equivalent to a density. Accordingly, that summand is called $\rho_{het,equi}$. With it, the density ρ_Λ is the function $f_\Lambda(\rho_{vol} + \rho_{het,equi})$ in Eq. (25.2).

$$\rho_\Lambda = f_\Lambda(\rho_{vol} + \rho_{het,equi}) \tag{2.67}$$

Thus, the dark energy has two components, the density of three-dimensional volume and the equivalent density of heterogeneity, in precise accordance with observation.

In earlier publications, I did not always distinguish ρ_{vol} and $\rho_{het,equi}$. Correspondingly, I often described the density ρ_Λ.

(4) Items (1-3) indicate that volume exhibits a dynamics, so we call it vacuum dynamics. And we call the volume the dynamic volume, DV.

2.10 Spacetime quadruple, SQ

The set of the four basic physical principles, special relativity, SR, equivalence principle, EP, generalized Gaussian gravity, GG, and the physical reality of the dynamic volume, DV, is named as follows: **spacetime quadruple, SQ**.

Chapter 3

Universal Position Factor

Idea: If a mass m_0 is in the isotropic vicinity of a field generating mass M, then M causes a constant physical situation in its vicinity. Thus, the Noether (1918) theorem implies that the law of energy conservation can be applied. If m_0 starts at zero velocity, then it starts with the energy $E = E_0 = m_0c^2$. If the mass is at free fall, then its velocity v increases, and its distance R from M decreases. Thereby, v causes an increase of the energy by the Lorentz factor $\gamma(v)$. However, that factor is compensated by a position factor $\varepsilon_E(R)$, as the energy is conserved. Thus, it should be possible to derive the position factor from the Lorentz factor.

3.1 Position factor $\varepsilon_E(R)$

In this section, we derive the energy function $E(R, v)$ of a probe mass m_0[1] that is at free fall towards a field generating mass M.

3.1.1 Freely falling mass m_0

In this section, we derive the **energy function** $E(R, v)$ of a mass m_0 that is falling in the field of a mass M, and that starts at the radial distance $d_{GP} = R \to \infty$ and at the velocity $v =$

[1] Of course, an object with nonzero rest mass has velocity below c, see e. g. Moore (2013).

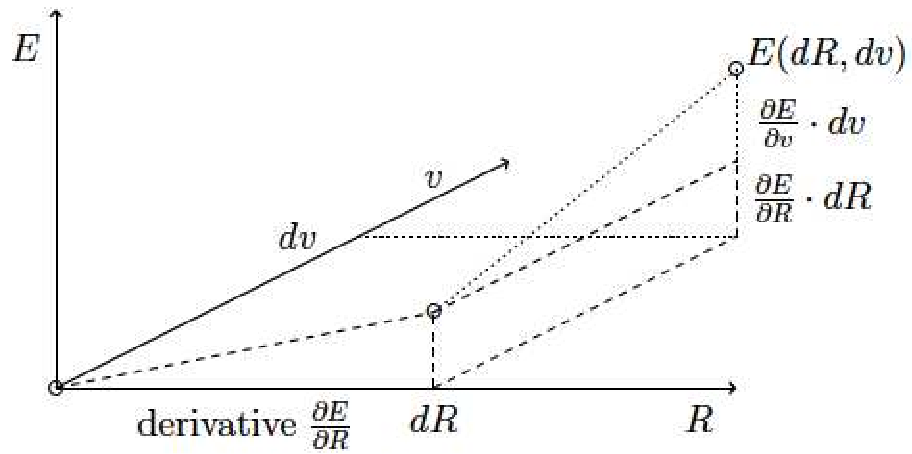

Figure 3.1: Change dE of $E(R, v)$ (∘): The two slope triangles result in the changes $\frac{\partial E}{\partial v} \cdot dv$ and $\frac{\partial E}{\partial R} \cdot dR$. The total change $dE = E(R + dR, v + dv) - E(R, v)$ is the sum $dE = \frac{\partial E}{\partial v} \cdot dv + \frac{\partial E}{\partial R} \cdot dR$.

0. Thereby, the velocity v and the radial coordinate R are measured relative to the mass M, and the own mass or rest mass[2] are denoted by $m_{own} = m_0$. Solutions with more general initial conditions are elaborated in (Carmesin (2020b)).

For it, we apply the **principle of energy conservation**, see section (2.5). In particular, we apply the **relativistic energy** derived in SR, see section (2.3).

$$E(v) = m_0 \cdot c^2 \cdot \gamma(v) \quad \text{in SR and with} \quad \gamma(v) = \frac{1}{\sqrt{1 - v^2/c^2}} \tag{3.1}$$

As m_0 is falling, the velocity v increases and R decreases. Hence, the energy would increase by the factor $\gamma(v)$, according to Eq. (3.1). Correspondingly, the energy decreases by a **position factor** $\varepsilon_E(R) = 1/\gamma(v)$, so that the energy is conserved. Thus, we derive:

$$E = m_0 \cdot c^2 \cdot \gamma(v) \cdot \varepsilon_E(R) \quad \text{with} \quad \gamma(v) = 1/\varepsilon_E(R) \tag{3.2}$$

The functional term of $\varepsilon_E(R)$ must be determined. We consider

[2]Note that we do not use the concept of a relativistic mass in this book.

the change dE of the energy, which clearly depends on R and v (Fig. 3.1). Accordingly, we derive:

$$dE = \frac{\partial E}{\partial R} dR + \frac{\partial E}{\partial v} dv \tag{3.3}$$

From this equation, we obtain a differential equation, DEQ, for $\varepsilon_E(R)$. According to the principle of energy conservation, dE is zero. The partial derivative regarding v is $\frac{\partial E}{\partial v} = E \cdot \gamma^2 \cdot v / c^2$, while the partial derivative with respect to R is $\frac{\partial E}{\partial R} = E \cdot \varepsilon'_E / \varepsilon_E$ with $\varepsilon'_E = \frac{\partial \varepsilon_E}{\partial R}$. Thus, we derive:

$$0 = E \cdot \frac{\varepsilon'_E}{\varepsilon_E} \cdot dR + E \cdot \gamma^2 \cdot \frac{v}{c^2} \cdot dv \tag{3.4}$$

We divide by E and $d\tau$, and we use $v = \frac{dR}{d\tau}$ as well as $a = \frac{dv}{d\tau}$, see Fig. (2.13). We also resolve for ε'_E. Thence, we obtain:

$$\varepsilon'_E = -\frac{\varepsilon_E \cdot \gamma^2}{c^2} \cdot a \tag{3.5}$$

We use $\gamma(v) = 1/\varepsilon_E(R)$ (Eq. 3.2). We utilize the equivalence principle $a = |G^*|$, see section (2.2). Additionally, we apply Eq. (2.64). So, we derive:

$$\varepsilon'_E = \frac{1}{\varepsilon_E \cdot c^2} \cdot \frac{G \cdot M}{R^2} \tag{3.6}$$

We use the well known term $R_S = \frac{2G \cdot M}{c^2}$ for the **Schwarzschild radius**. So, we derive the following DEQ for $\varepsilon_E(R)$:

$$\boxed{\varepsilon'_E = \frac{1}{\varepsilon_E} \cdot \frac{R_S}{2R^2}} \tag{3.7}$$

Solution of the DEQ for ε_E: For the case of a constant mass M, we solve the DEQ for ε_E with the following Ansatz:

$$\boxed{\varepsilon_E(R) = \sqrt{1 - \frac{R_S}{R}}} \tag{3.8}$$

The derivative corresponds to the DEQ (3.7). Thus, Eq. (3.8) is a solution. We use the two factors $\varepsilon_E(R)$ and $\gamma(v)$ in Eqs. (3.2, 3.8, 3.1)). So, we derive a term for the **invariant** energy depending on R and v:

$$\boxed{E(R,v) = m_0 \cdot c^2 \cdot \frac{\sqrt{1-\frac{R_S}{R}}}{\sqrt{1-v^2/c^2}}} \tag{3.9}$$

This term generally represents the functional dependence of the energy on R and v. Landau and Lifschitz (1981) obtain the same result (page 299), this confirms our derivation. We summarize:

Proposition 1 Energy in an isotropic vicinity of a mass: *In the constant isotropic vicinity of a* **field generating mass or dynamic mass** *M, and at a circumferential radial coordinate R (or at a gravitational parallax distance R), a* **probe mass** *m_0 has the following properties:*

(1) The energy of the mass m_0 can be directly analyzed.

(2) M generates a radial gravitational **field** *with the value $G^* = |\vec{G}^*| = \frac{GM}{R^2}$.*

(3) A local observer at R can **locally observe** *the body's radial velocity $v(R) = \frac{\partial R}{\partial \tau}$ and its radial coordinate $R = d_{GP}$, see section (2.6) and Fig. (2.13).*

(4) If the probe mass falls freely in the field of M, and if $v = 0$ at $R \to \infty$, then the **energy function** *$E(R,v)$ of m_0 is described by Eq. (3.9):*

$$E(R,v) = m_0 \cdot c^2 \cdot \frac{\sqrt{1-\frac{R_S}{R}}}{\sqrt{1-v^2/c^2}} = m_0 \cdot c^2 \cdot \gamma(v) \cdot \varepsilon_E(R) \tag{3.10}$$

(5) In particular, that energy function $E(R,v)$ of m_0 represents an **invariant** *of the motion in the frame in which M is at rest*

and at the origin. The reason is that the law of energy conservation holds in that frame, as the vicinity of M is constant, so that the Noether (1918) theorem can be applied:

$$1 = \gamma(v) \cdot \varepsilon_E(R) \tag{3.11}$$

3.2 Derivation of the Schwarzschild metric

Idea: If the mass m_0 is at free fall towards the field generating mass M, then it has a velocity v relative to M at a distance R from M. As a consequence of the velocity v, in the frame of M, the mass m_0 could be described by the Minkowski metric[3], see Eq. (2.17):

$$ds^2 = \frac{-c^2 \cdot dt^2}{\gamma^2(v)} + dx^2 \cdot \gamma^2(v) + dy^2 + dz^2 = 0 \tag{3.12}$$

If we transform the Lorentz factor $\gamma(v)$ to the position factor $\varepsilon_E(R)$, then we obtain a metric as a function of R. That metric is elaborated in this section.

We consider the mass m_0 at free fall in the isotropic vicinity of the field generating mass M. For our analysis, we use the rest frame of M. At a distance R from M, the mass m_0 has a velocity v. As a consequence of the velocity v alone, the mass m_0 would be described by the following line element (Eq. 2.17):

$$ds^2(v) = \frac{-c^2 \cdot dt^2}{\gamma^2(v)} + dx^2 \cdot \gamma^2(v) + dy^2 + dz^2 \tag{3.13}$$

We transform it to a function of the distance R alone. For it, we use the relation of energy conservation $1 = \gamma(v) \cdot \varepsilon_E(R)$:

$$ds^2(R) = -c^2 dt^2 \cdot \varepsilon_E^2(R) + \frac{dx^2}{\varepsilon_E^2(R)} + dy^2 + dz^2 \tag{3.14}$$

[3]Remind that we mark increments of time and radius by dt and dR in a d_{GP}-map, while we mark increments of time and radius by $d\tau$ and dL in a d_{LT}-map. Hereby, we use both maps as tools only. For instance, you can represent Earth with a terrestrial globe or with maps in an atlas. Of course, if you use a map in an atlas, you do presumably still think that Earth is nearly a ball or ellipsoid or geoid.

If the mass m_0 is at free fall until it reaches the distance R from M, and if the velocity is slowed down to zero at R, then the above line element describes the system correctly, as the metric depends on R only in that case.

Usually, spherical polar coordinates are used. In that case, the above line element is expressed as follows:

$$ds^2 = -c^2 dt^2 \varepsilon_E^2(R) + \frac{dR^2}{\varepsilon_E^2(R)} + R^2 d\vartheta^2 + R^2 \sin^2 \vartheta d\varphi^2 \quad (3.15)$$

This metric described by the above line element is called Schwarzschild metric, SM, see Schwarzschild (1916) or e. g. Straumann (2013), Carmesin (1996), Hobson et al. (2006), see also Carmesin (2022d). Hereby, the time increment dt is reduced by the position factor $\varepsilon_E(R)$. This phenomenon is called gravitational time dilation. Moreover, the radial length increment dR is increased by the inverse position factor $1/\varepsilon_E(R)$. So there occurs a gravitational increase of length. We summarize our findings:

Theorem 3 Derivation of the Schwarzschild metric

(1) In an isotropic vicinity of a mass M, the gravitational field of the mass M and the gravitational parallax distance $R = d_{GP}$ can be measured.

(2) On the basis of the gravitational parallax distance $R = d_{GP}$, the polar coordinates (R, θ, ϕ) can be introduced.

(3) On the basis of the position factor $\varepsilon_E(R)$, the metric tensor $g_{ik}(R, \theta, \phi)$ can be derived. The resulting metric tensor describes the Schwarzschild metric:

$$g_{ik}(R,\theta) = \begin{pmatrix} 1-\frac{R_S}{R} & 0 & 0 & 0 \\ 0 & \frac{1}{1-\frac{R_S}{R}} & 0 & 0 \\ 0 & 0 & R^2 & 0 \\ 0 & 0 & 0 & R^2 \sin^2 \vartheta \end{pmatrix} \quad (3.16)$$

$$\text{with } \eta_{ik} = \begin{pmatrix} -1 & 0 & 0 & 0 \\ 0 & 1 & 0 & 0 \\ 0 & 0 & 1 & 0 \\ 0 & 0 & 0 & 1 \end{pmatrix} \text{ and} \tag{3.17}$$

$$ds^2 = \sum_{i=0}^{3} \sum_{k=0}^{3} g_{ik} \cdot \eta_{ik} \cdot dx_i \cdot dx_k \text{ or} \tag{3.18}$$

$$ds^2 = -c^2 dt^2 \varepsilon_E^2(R) + \frac{dR^2}{\varepsilon_E^2(R)} + R^2 d\vartheta^2 + R^2 \sin^2 \vartheta d\varphi^2 \tag{3.19}$$

(4) In particular, a time interval dt in a flat gravitational parallax space is transformed to a d_{LT}-time $d\tau$ in a curved light-travel time space:

$$d\tau = dt \cdot \sqrt{1 - R_S/R} \tag{3.20}$$

Similarly, radial intervals between two locations A and B are related as follows:

$$dL = dL(A, B) = \frac{dR(A, B)}{\sqrt{1 - R_S/R}} = \frac{dR}{\sqrt{1 - R_S/R}} \tag{3.21}$$

3.3 Universality of the position factor

Question: In the isotropic vicinity of a mass M, each probe mass m_0 has the energy function $E(R, v) = m_0 \cdot c^2 \cdot \gamma(v) \cdot \varepsilon_E(R)$, with the same position factor $\varepsilon_E(R)$ for each probe mass. Does a monochromatic light signal or any other object have the same position factor?

Definition 7 Energy available for transformation

If an object is at a circumferential radial coordinate or gravitational parallax distance R from a field generating mass M, then the following can be defined:

(1) If R is near the limit to infinity, then we call the radius R_∞:

$$R_\infty \approx \lim_{R \to \infty} R \text{ or} \tag{3.22}$$

$$\frac{1}{R_\infty} << 1 \tag{3.23}$$

The value of a physical quantity q *at* R_∞ *is called* q_∞*:*

$$q_\infty = q(R_\infty) \tag{3.24}$$

(2) If an object, called object$_b$*, starts a free fall at* R_∞ *with the energy* E_∞*, then the object has the same energy at* R*:*

$$E(R) = E_\infty \tag{3.25}$$

Thereby, $E(R)$ *consists of a factor* $E_{av,b}(R)$ *that is available for a transformation of energy at* R *and of a position factor* $\varepsilon_{E,b}(R)$ *of object*$_b$ *that is inherent to the position of that object:*

$$E(R) = E_{av,b}(R) \cdot \varepsilon_{E,b}(R) \text{ or} \tag{3.26}$$

$$\varepsilon_{E,b}(R) = \frac{E(R)}{E_{av,b}(R)} \tag{3.27}$$

Hereby, $E_{av,b}(R)$ *is called* **available energy** *of the object. It can be measured at* R *with help of a transformation of that energy. For instance, a signal of monochromatic light can be absorbed at* R *by a black body, whereby that signal is transformed into thermal energy. In this manner, the available energy is basically defined by such a measurement at* R*.*

(3) If an object$_b$ *starts a free fall at* R_∞ *with the energy* E_∞*, then the available energy* $E_{av}(R)$ *is a product of* E_∞ *and a factor* $\gamma_b(R)$*:*

$$\gamma_b(R) = \frac{E_{av,b}(R)}{E_\infty} \tag{3.28}$$

Hereby, $\gamma_b(R)$ *describes the increase of internal energy during free fall, and* $\gamma_b(R)$ *is called* **internal energy factor.**

In order to show the universality of the position factor, we show the position factor $\varepsilon_{E,b}(R)$ of *object*$_b$ is equal to the position factor $\varepsilon_E(R)$. Remind that $\varepsilon_E(R)$ is the inverse of the Lorentz factor.

For it, we consider a sequence of changes of the energy $E_\infty = m_0c^2$ of a probe mass, whereby energy conservation holds at each change:

Theorem 4 Universality of the position factor

If a probe mass m_0 and an object$_b$ are at circumferential radial coordinates or gravitational parallax distances R from a field generating mass M and in the isotropic vicinity of M, then the following holds:

(1) If the probe mass m_0 is at $v = 0$ at R_∞, then m_0 has its energy:

$$E_\infty = m_0c^2 \tag{3.29}$$

(2) In a first change, the probe mass m_0 in part (1) is transformed to an object$_b$. Thus, object$_b$ has the energy E_∞ in Eq. (3.29):

$$E_b(R_\infty) = E_\infty = m_0c^2 \tag{3.30}$$

(3) In a second change, the object$_b$ in part (2) falls freely from R_∞ to R. Thus, the energy E_b in Eq. (3.30) is factorized as follows, see Eq. (3.26):

$$E_b(R) = E_\infty = E_{av,b}(R) \cdot \varepsilon_{E,b}(R) \tag{3.31}$$

(4) In a third change, a copy of the probe mass m_0 in part (1) falls freely from R_∞ to R. Thus, the energy E_∞ in Eq. (3.29) is factorized as follows, see Eq. (3.26):

$$E_\infty = E_{av}(R) \cdot \varepsilon_E(R) \tag{3.32}$$

Remind that the position factor is equal to the inverse Lorentz factor, as m_0 is a mass.

(5) In a fourth change, object$_b$ at R in part (3) is transformed to a mass at R. Thus, the available energy $E_{av,b}(R)$ of the object

is transformed to the available energy $E_{av}(R)$ of a mass that has the same energy and that experienced the same free fall. As the available energy $E_{av,b}(R)$ is transformed into the available energy $E_{av}(R)$, the two available energies are equal:

$$E_{av}(R) = E_{av,b}(R) \tag{3.33}$$

(6) As each of the changes in parts (2-5) conserves the energy of the object, The resulting energies in Eqs. (3.31) and (3.32) are equal:

$$E_{av}(R) \cdot \varepsilon_E(R) = E_{av,b}(R) \cdot \varepsilon_{E,b}(R) \tag{3.34}$$

According to part (5), the available energies in the above Eq. are equal:

$$E_{av}(R) \cdot \varepsilon_E(R) = E_{av}(R) \cdot \varepsilon_{E,b}(R) \tag{3.35}$$

As the available energies in the above Eq. cancel out, the position factors in the above Eq. are equal:

$$\varepsilon_E(R) = \varepsilon_{E,b}(R) \tag{3.36}$$

(7) As object$_b$ is an arbitrary object in space, all objects in space have the same position factor $\varepsilon_E(R)$ as a function of R. Thus, the position factor is universal.

Proof: The proof is provided by the transformations described within the above theorem.

In the next section, we show that the universality of the position factor has far reaching consequences for the fact of quantization and for the universality of the quantization constant.

Chapter 4

Universal Quantization

Idea: A signal of monochromatic light can be described in two ways:
as a wave with a circular frequency ω
and as a portion E of energy with the momentum $p = E/c$.
Thus, even at the classical level, there is a wave - particle duality, and we can try to derive a universal quantization therefrom.

In this chapter, we show the following: If portions of a physical quantity propagate at the group velocity, see e. g. (Scheck, 2013, section 1.3.1) or (Kumar, 2018, sections 3.2 and 5.2), $\frac{d\omega}{dk} = v_g = c$ in a direction $\vec{e}_j$, and if they have a corresponding wave vector component $k_j = k$ as well as a circular frequency ω, then the portions are quantized in an emergent manner[1].

In SR, such a portion has an energy dE and a corresponding momentum component $dp_j = p = |\vec{p}|$, so that the following holds, (Landau and Lifschitz, 1971, Eq. 9.6):

$$\frac{dE}{dp} = c \text{ or } \frac{dE}{dp_j} = c \text{ in direction of the unit vector } \vec{e}_j \quad (4.1)$$

Thereby, the ratio of the circular frequency $d\omega$ and the corresponding component of a wave vector dk_j is as follows, (Landau and Lifschitz, 1971, Eq. 48.4):

[1] The results of this chapter have been derived in similar contexts in Carmesin (2022d), Carmesin (2022a).

$$\frac{d\omega}{dk} = c \text{ or } \quad \frac{d\omega}{dk_j} = c \text{ in direction of } \vec{e}_j \tag{4.2}$$

So, the above fractions are equal:

$$\frac{d\omega}{dk} = \frac{dE}{dp} = c \text{ or } \quad \frac{d\omega}{dk_j} = \frac{dE}{dp_j} = c \text{ in direction of } \vec{e}_j \tag{4.3}$$

As $d\omega$ is nonzero, we can derive the following relation:

$$\frac{dp}{dk} = \frac{dE}{d\omega} \text{ or } \quad \frac{dp_j}{dk_j} = \frac{dE}{d\omega} \text{ in direction of } \vec{e}_j \tag{4.4}$$

4.1 Possible minimal portion

In this section, we analyze a possible minimal measurable portion of energy $dE = E_{min,\omega_1}$ that may occur at a circular frequency ω_1. Hereby, $\omega = \omega(\vec{k})$ is a function of the wave vector. At propagation towards $\vec{e} = \vec{e}_j$, $\omega = \omega(k)$ is a function of the absolute value k of the wave vector. Thereby, the elongation of the wave is concentrated around a central value k_1, and ω_1 is the value of the circular frequency at that value k_1, $\omega_1 = \omega(k_1)$, see e. g. (Scheck, 2013, 1.3.1).

The corresponding portion of momentum is $dp = p_{j,min,\omega_1} = E_{min,\omega_1}/c$. So, the above relations, see Eqs. (4.1, 4.2, 4.3, 4.4), can be derived for the minimal values in a similar manner. Thus, the relation corresponding to Eq. (4.4) is obtained:

$$\frac{p_{min,\omega_1}}{k_1} = \frac{E_{min,\omega_1}}{\omega_1} \text{ or } \quad \frac{p_{j,min,\omega_1}}{dk_{j,1}} = \frac{E_{min,\omega_1}}{\omega_1} \text{ for } \vec{e} = \vec{e}_j \tag{4.5}$$

The two fractions represent the same ratio $K(\omega)$.

$$\frac{p_{min,\omega_1}}{k_1} = \frac{E_{min,\omega_1}}{\omega_1} = K(\omega_1) \text{ or}$$
$$\frac{p_{j,min,\omega_1}}{k_{j,1}} = \frac{E_{min,\omega_1}}{\omega_1} = K(\omega_1) \text{ for } \vec{e} = \vec{e}_j \tag{4.6}$$

As the ratio $K(\omega_1)$ has the same form as in the quantization of light, see e. g. Griffiths (1994) or Kumar (2018), we call it quantization ratio.

4.2 Universality of the quantization ratio

Question: Do different circular frequencies ω_1 and ω_2 have the same quantization ratios $K(\omega_1)$ and $K(\omega_2)$?

For it, we consider two minimal portions with circular frequencies ω_1 and ω_2:

Theorem 5 Universal quantization

We analyze two minimal portions in section (4.1) that propagate at $v = c$ with two different circular frequencies. Thereby, we call the smaller circular frequency ω_1 and the larger circular frequency ω_2. The corresponding quantization factors are called $K(\omega_1)$ and $K(\omega_2)$.

(1) The locations are not restricted, at which the minimal portions in section (4.1) propagate. Thus, we can analyze these portions in an isotropic vicinity of a field generating mass M. Thereby, we can choose circumferential radial coordinates or gravitational parallax distances R of the portions as desired.

(2) We analyze the minimal portion with circular frequency ω_1 at the radius $R = R_\infty$ (DEF 7). According to Eq. (4.6), that portion has the following energy:

$$E_{min,\omega_1} = K(\omega_1) \cdot \omega_1 \text{ for } R_\infty \tag{4.7}$$

(3) According to THM (3), increments of time at R_∞ and at R are related as follows:

$$\frac{dt(R)}{dt_\infty} = \varepsilon_E(R) \tag{4.8}$$

In particular, such time increments can be periodic times T of radiation. This is possible, as in each frame, the time between *the same two maxima of the elongation is the periodic time:*

$$\frac{T(R)}{T_\infty} = \varepsilon_E(R) \tag{4.9}$$

According to the definition of the circular frequency $\omega = 2\pi/T$, *the position factor is the following ratio of the circular frequencies:*

$$\varepsilon_E(R) = \frac{\omega_1}{\omega_2} \text{ or} \tag{4.10}$$

$$\sqrt{1-\frac{R_S}{R}} = \varepsilon_E(R) = \frac{\omega_1}{\omega_2} = \frac{\omega_\infty}{\omega(R)} \tag{4.11}$$

(4) As the vicinity of M is constant, the Noether (1918) theorem is applicable, so that energy is conserved. Thus, the energy E_{min,ω_1} *at the start of the free fall in part (2) is equal to the energy at R in part (3), see THM (4):*

$$E_{min,\omega_1} = K(\omega_1)\cdot\omega_1 = E_{av}(R)\cdot\varepsilon_E(R) \tag{4.12}$$

Thus, the available energy is the ratio of the energy $K(\omega_1)\cdot\omega_1$ *at* R_∞ *and the position factor at R:*

$$E_{av}(R) = \frac{K(\omega_1)\cdot\omega_1}{\varepsilon_E(R)} = \frac{E_\infty}{\varepsilon_E(R)} \tag{4.13}$$

(5) The available energy $E_{av}(R)$ *is defined by its measurement, see DEF (7). Similarly, the circular frequency* ω_2 *is measured at R. For instance, the wavelength* λ *of light is measured with a spectrometer, and it can be transformed by* $\omega = 2\pi\cdot\frac{c}{\lambda}$. *Thus, the minimal energy* E_{min,ω_2} *is measured at R. Hence, the minimal energy* E_{min,ω_2} *and the available energy at R are equal:*

$$E_{min,\omega_2} = K(\omega_2)\cdot\omega_2 = E_{av}(R) \tag{4.14}$$

We apply the available energy in Eq. (4.13) to the energy E_{min,ω_2} at R in Eq. (4.14):

$$E_{min,\omega_2} = K(\omega_2) \cdot \omega_2 = \frac{K(\omega_1) \cdot \omega_1}{\varepsilon_E(R)} \tag{4.15}$$

We apply the position factor in Eq. (4.11) to the energy E_{min,ω_2} at R in Eq. (4.15):

$$E_{min,\omega_2} = K(\omega_2) \cdot \omega_2 = \frac{K(\omega_1) \cdot \omega_1}{\frac{\omega_1}{\omega_2}} = K(\omega_1) \cdot \omega_2 \tag{4.16}$$

We divide the energy in the above Eq. (4.16) by ω_2:

$$K(\omega_2) = K(\omega_1) \tag{4.17}$$

Thus, we showed that the quantization factors do not depend on the circular frequency ω. According to Eq. (4.2), that quantization ratio $K(\omega)$ does not depend on the wave number. Thence, the quantization ratio $K(\omega)$ is a universal constant.

(6) Thereby, the value of the universal quantization ratio $K(\omega)$ has been measured, and $2\pi \cdot K(\omega)$ takes the following value:

$$2\pi \cdot K(\omega) = 6.626\,070\,15 \cdot 10^{-34}\,\mathrm{Js} \tag{4.18}$$

(7) The universal quantization ratio $K(\omega)$ is named reduced Planck constant $\hbar$, whereby $2\pi \cdot \hbar$ is named Planck constant h:

$$K(\omega) = \hbar = \frac{h}{2\pi} \tag{4.19}$$

As a convention, the value of the Planck constant in Eq. (4.18) is defined to be an exact value, see e. g. Newell et al. (2018) or Workman et al. (2022).

(8) The transformation from a gravitational parallax distance dR and a corresponding time dt to the values dL and $d\tau$ in

curved spacetime, is provided by the Schwarzschild metric in chapter (3).

(9) We show that the universality of quantization holds in an even more general investigation: In the Schwarzschild metric, the field generating or curvature generating mass M is clearly distinguished from the probe mass m_0. More generally, the probe mass m_0 does influence the available energy of the field generating mass M. When the available energy of M causes the curvature, then R_S is influenced by m_0 and by the distance R. Accordingly, the position factor is a function of these quantities, $\varepsilon_{E,\,\text{more general}} = \sqrt{1 - \frac{R_S(M,m_0,R)}{R}}$. In such a case, Eq. (4.10) can still be applied, whereby the term in Eq. (4.11) becomes more complicated. However, the derivation can still be applied. In general, the quantization ratio is universal, whenever the time dilation is expressed by a factor, $\frac{T(R)}{T_\infty} = \varepsilon_{E,\,\text{more general}}(R) = \frac{\omega_\infty}{\omega(R)}$ $= \frac{\omega_1}{\omega_2}$. This should be the case, whenever the time is a scalar quantity, not a vector or tensor, for instance. This is a very general condition. In particular, this relation is more general than the framework of the Einstein field equation, see e. g. Einstein (1915), Hilbert (1915). The relation shows the following:

Nature is quantized.

The constant of quantization is universal.

The Einstein field equation is a semiclassical approximation Carmesin (2022f), Carmesin (2023b).

(10) We show that the universality of quantization holds at higher dimension. Note that higher dimension has been observed, see Lohse et al. (2018) or Zilberberg et al. (2018).

If a change of the dimension from a dimension D_1 to a lower dimension D_2 causes an increase of a wavelength λ_{vol,D_1} of volume to the wavelength λ_{vol,D_2} according to a dimensional dis-

tance enlargement factor $Z_{D_1 \to D_2}$ *as follows*

$$\lambda_{vol,D_2} = \lambda_{vol,D_1} \cdot Z_{D_1 \to D_2}, \tag{4.20}$$

then the following holds:

(10a) The waves of volume are quantized, as they propagate with $v = c$. *Thereby, there occurs a constant of quantization:*

$$E_{min,\omega_{vol,D_1}} \;=\; K(\omega_{vol,D_1}) \cdot \omega_{vol,D_1} \tag{4.21}$$

(10b) The corresponding circular frequencies change as follows:

$$\frac{\omega_{vol,D_1}}{\omega_{vol,D_2}} = Z_{D_1 \to D_2} \tag{4.22}$$

(10c) At the dimensional transition, the available energy (of the quantum) at D_1, $E_{min,\omega_{vol,D_1}}$ *is reduced by the increase of the wavelength to the following available energy at* D_2*:*

$$E_{av}(D_2) = \frac{E_{min,\omega_{vol,D_1}}}{Z_{D_1 \to D_2}} = \frac{K(\omega_{vol,D_1}) \cdot \omega_{vol,D_1}}{Z_{D_1 \to D_2}} \tag{4.23}$$

(10d) Similarly as in part (5), the available energy at D_2 *is equal to the minimal energy of the quantum:*

$$E_{av}(D_2) = K(\omega_{vol,D_2}) \cdot \omega_{vol,D_2} = E_{min,\omega_{vol,D_2}} \tag{4.24}$$

(10e) As a consequence of the energies in Eqs. (4.22, 4.23, 4.24), the constants of quantization are equal:

$$K(\omega_{vol,D_2}) \cdot \omega_{vol,D_2} = \frac{K(\omega_{vol,D_1}) \cdot \omega_{vol,D_1}}{Z_{D_1 \to D_2}} = K(\omega_{vol,D_1}) \cdot \omega_{vol,D_2} \tag{4.25}$$

$$\text{or } K(\omega_{vol,D_2}) = K(\omega_{vol,D_1}) \tag{4.26}$$

(11) In principle, the quantization constant $K(\omega_{vol,D_1})$ *of the volume could be different from the quantization constant* $K(\omega_1)$ *of radiation. However, if a minimal portion of energy of volume*

is at its zero-point oscillation at a wavelength λ, and if a minimal portion of energy of radiation is at its zero-point oscillation at the same wavelength λ, then the wave functions are geometrically equal. Accordingly, they should have the same zero-point energy, ZPE:

$$K(\omega_1) \cdot \frac{\pi \cdot c}{\lambda} = ZPE_{radiation} = ZPE_{vol} = K(\omega_{vol,D_1}) \cdot \frac{\pi \cdot c}{\lambda} \tag{4.27}$$

$$\text{or } K(\omega_1) = K(\omega_{vol,D_1}) \tag{4.28}$$

Correspondingly, the same constant of quantization occurs for an object at different circular frequencies and for different types of objects.

(12) The circular frequency $\omega(k)$ as a function of the wave number k is obtained by integration:

$$\omega(k) = \omega_0 + \int_0^k \frac{d\omega}{dk_3} dk_3 \tag{4.29}$$

$$\text{with } \omega_0 = \omega(k = 0) \tag{4.30}$$

Hereby, the derivative $\frac{d\omega}{dk_3}$ is equal to the group velocity $v_g = c$. So we obtain:

$$\omega(k) = \omega_0 + c \cdot k \tag{4.31}$$

As a consequence, the **phase velocity** *v_p, see e. g. (Kumar, 2018, Eq. 3.2.8), is as follows:*

$$v_p = \frac{\omega(k)}{k} = \frac{\omega_0}{k} + c = \frac{\omega_0}{k} + v_g \tag{4.32}$$

Thus, the phase velocity v_p can differ from the group velocity v_g, see e. g. (Kumar, 2018, section 5.2 or p. 191). For instance, such a difference $v_p \neq v_g$ occurs in the Cherenkov radiation, see e. g. (Landau and Lifschitz, 1963, section 115). Another example is provided by de Broglie (1925) in his theory of matter waves: These exhibit phase velocities v_p larger than the velocity *of light and larger than the group velocity* v_g, $v_p > c > v_g$ *(see Eqs. 1.2.3, 1.2.6).*

In the case of nonzero ω_0, *and in the limit of zero momentum* $p = \hbar k$ *or infinite wavelength* λ, *the phase velocity* v_p *tends to infinity:*

$$\lim_{p \to 0} v_p = \lim_{k \to 0} v_p = \lim_{\lambda \to \infty} v_p = \infty \tag{4.33}$$

As the light horizon is finite, that limit is almost, but not fully, achieved in a causal system in spacetime.

For instance, in electromagnetic waves, the phase velocity in vacuum is c, *so* ω_0 *is zero. However, in chapter (8), we will derive various phase velocities, corresponding to nonzero* ω_0, *in the dynamics of volume.*

Example: An example for such a minimal portion is the photon. Pound and Rebka (1960) have confirmed the gravitational redshift of the photon experimentally, we analyzed that redshift above theoretically.

Altogether, SR together with the curvature of spacetime described by the position factor cause the quantization of waves propagating at $v = c$, we name it emergent quantization.

Chapter 5

Classical Expansion of Space

Idea: The kinetic gas theory shows how the dynamics of local molecules provides the equation of state of the global ideal gas. Similarly, the Schwarzschild metric of a local mass should provide the global dynamics of space.

Accordingly, in this section, we unify the classical local dynamics of the position factor and the classical global expansion of space. For it, we derive the **Friedmann Lemaître equation, FLE** from the position factor.

5.1 Expansion of space

Einstein (1917) analyzed a possible expansion of the space. Slipher (1915) discovered the redshift of distant galaxies, Wirtz (1922) analyzed empirical evidence for the expansion of space, and Hubble (1929) obtained a convincing empirical basis for that expansion of space. That expansion is usually described by a **uniform scaling**.

Models of that expansion of space since the Big Bang typically apply the cosmological principle: isotropy and homogeneity of space, including its content, see e. g. Karttunen et al. (1996). Accordingly, we model space by a homogeneous ball with a density ρ, see Fig. (5.1). So, we derive the DEQ for the time evolution of the radius of such a homogeneous ball.

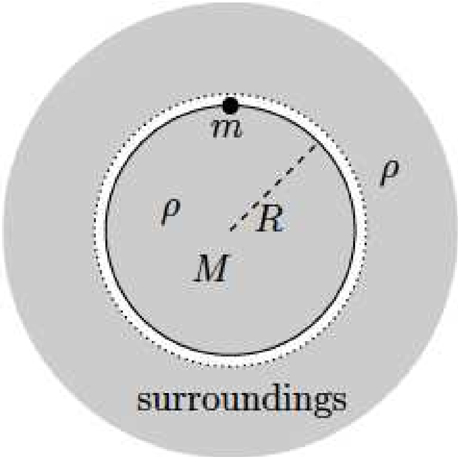

Figure 5.1: Ball with mass M and radius R embedded in a homogeneous surrounding and exhibited to a probe mass m or m_0.

5.2 Derivation of the FLE

In this section, we derive the Friedmann Lemaître equation, Friedmann (1922) and Lemaitre (1927). The DEQ describes the expansion of space since the Big Bang. For it, we apply the position factor.

5.2.1 DEQ of uniform scaling: derivation

The surroundings of the ball do not generate a field $\vec{G}^*$ in the embedded sphere (section 25.2.1). A homogeneous sphere with a mass M generates a field in its vicinity that is equal to the field generated by the mass M in the center of the ball (Gauss (1840)). So the position factor applies (Eq. 3.9), and thus the energy of a probe mass with the condition $(R|v) = (R|\dot{R}) = (\infty|0)$ at some time is as follows (other conditions are analyzed in Carmesin (2020b)):

$$E(R, v) = m_0 \cdot c^2 \cdot \gamma(v) \cdot \varepsilon_E(R) = E_0 \text{ alias } E_{ref} \tag{5.1}$$

Thereby, the factors are as follows:

$$\gamma(v) = \frac{1}{\sqrt{1 - v^2/c^2}} \;\; ; \;\; \varepsilon_E(R) = \sqrt{1 - \frac{R_S}{R}} \;\; \text{and} \;\; m_0 \cdot c^2 = E_0 \tag{5.2}$$

The Eq. (5.1) represents a DEQ, as it contains v, which in turn represents a derivative. This DEQ describes the dynamics of the probe mass. Next, we **transform** this DEQ, in order to obtain a transformed DEQ, still describing the dynamics of m and $R(t)$.

5.2.2 Structured energy function

In this section, we derive a **structured energy function.** This may be interpreted as a result of a mathematical transformation of the DEQ, or it may be interpreted physically in addition:

The structured energy function might be interpreted as a normalized **excess energy** (Carmesin (2020b)) as follows:

In SR, the difference of the square E^2 of the energy and of the square of the own energy $m_0^2 \cdot c^4 = E_0^2$ represents the square of the kinetic energy $p^2 \cdot c^2$. By construction, it represents the square of the excess energy that the mass m has compared to its own mass m_0.

According to the position factor, that excess energy contains the kinetic energy and, additionally, a gravitational energy in the field.

Correspondingly, we derive the excess energy as follows: We take the square of Eq. (5.1), and we subtract the squared own energy $m_0^2 c^4$ (so we obtain the square of the generalized excess energy):

$$E(R, v)^2 - m_0^2 c^4 = m_0^2 \cdot c^4 \cdot (\varepsilon_E(R)^2 \cdot \gamma(v)^2 - 1) \tag{5.3}$$

The model of the uniform scaling of space does not apply an object moving or propagating through space, accordingly, in that model there is no factor γ^2. Correspondingly, in order to transform the local physics of the probe mass to the global physics of the uniform scaling of space, we divide by γ^2 (Eq. 5.1):

$$\frac{E(R,v)^2 - m_0^2 c^4}{\gamma^2} = m_0^2 \cdot c^4 \cdot \left(\varepsilon_E(R)^2 - \gamma(v)^{-2}\right) \tag{5.4}$$

In order to simplify, we insert the factors $\varepsilon_E(R)$ and $\gamma(v)$:

$$\boxed{\frac{E(R,v)^2 - m_0^2 c^4}{\gamma^2} = m_0^2 c^4 \cdot \left(\frac{v^2}{c^2} - \frac{R_S}{R}\right)} \tag{5.5}$$

Conventional form: In this paragraph, we derive a conventional energy function with a conventional kinetic and potential energy term. For it, we divide by $2m_0c^2$. So, we derive:

$$\frac{E(R,v)^2 - m_0^2 c^4}{2\gamma^2 m_0 c^2} = m_0 \cdot c^2 \cdot \left(\frac{v^2}{c^2} - \frac{R_S}{R}\right) \cdot \frac{1}{2} \tag{5.6}$$

We apply the Schwarzschild radius $R_S = \frac{2GM}{c^2}$: So, the result is a conventional structured energy function. We denote that energy function by a bar, $\bar{E}(R,v)$. Thus, we derive $\bar{E}(R,v)$:

$$\boxed{\frac{E(R,v)^2 - E_0^2}{2\gamma^2 E_0} =: \bar{E}(R,v) = \frac{m_0 \cdot v^2}{2} - \frac{G \cdot M \cdot m_0}{R}} \tag{5.7}$$

Form with the Hubble parameter: In this part, we transform the DEQ (5.5) further, so that we obtain a term for the **Hubble parameter**:

$$H = \frac{\dot{R}}{R} \text{ and } R \neq 0 \tag{5.8}$$

For it, we multiply Eq. (5.5) with $\frac{1}{m_0^2 \cdot c^4} \cdot \frac{c^2}{R^2}$, and we use the density $\rho = \frac{M}{R^3 \cdot 4\pi/3}$. So, we derive:

$$\frac{E(R,\dot{R})^2 - m_0^2 c^4}{m_0^2 \cdot c^4 \gamma^2} \cdot \frac{c^2}{R^2} = \frac{\dot{R}^2}{R^2} - \frac{8\pi G \cdot \rho}{3} \tag{5.9}$$

We identify the scaled squared energy $-\frac{E(R,\dot{r})^2-m_0^2c^4}{m_0^2\cdot c^4\gamma^2}$, or the scaled energy term $-\frac{2\bar{E}(R,\dot{R})}{m_0\cdot c^2}$, with the **curvature parameter** k (Friedmann (1922), Lemaitre (1927), Stephani (1980)), Carmesin (2021d), Carmesin (2021a)). We identify $\frac{\dot{R}^2}{R^2}$ with the squared Hubble parameter H^2, and we solve for H^2. So, we derive the **Friedmann Lemaître equation, FLE** (Friedmann (1922) and Lemaitre (1927)), the DEQ for the homogeneous system:

$$\boxed{H^2 = \frac{8\pi G\cdot\rho}{3} - k\cdot\frac{c^2}{R^2}} \tag{5.10}$$

In the above Eq. the curvature parameter is $-\frac{2}{m_0c^2}$ multiplied by the structured energy term:

$$k = -\frac{2}{m_0c^2}\cdot\bar{E}(R,\dot{R}) = -\frac{2}{m_0c^2}\cdot\frac{E(R,\dot{R})^2-E_0^2}{2\gamma^2E_0} \tag{5.11}$$

Hereby, the energy $E(R,\dot{R})$ takes the value E_0 at R to infinity. Thus, for R to infinity, the structured energy function $\bar{E}(R,\dot{R})$ is zero. Hence, $\bar{E}(R,\dot{R})$ is zero during the whole time evolution of the system, as the law of energy conservation holds. Thence, the curvature parameter is zero, as a result of the dynamics, $k_{theo}=0$.

That theoretical result $k_{theo}=0$ is confirmed by observations (Collaboration (2020), Bennett et al. (2013)). As the curvature parameter k is zero, space is globally flat. We summarize our derivation:

Theorem 6 FLE derived from the position factor

The expansion of the universe has the following properties, see (Carmesin, 2021d, THM 3).

(1) In classical GR, it is described by a **uniform scaling** *with a scale factor* $R(t)$ *Fig. (5.1).*

(2) In classical GR, the time evolution of the scale factor $R(t)$ is described by the FLE:

$$H^2 = \left(\frac{\dot{R}}{R}\right)^2 = \frac{8\pi G \cdot \rho}{3} - k \cdot \frac{c^2}{R^2} \tag{5.12}$$

(3) The FLE of that uniform scaling can be derived from the time evolution of a **microscopic probe mass** *m as follows:*

(3a) At a density ρ, there is a homogeneous ball of the universe with the same density and generating a field $\vec{G}^*$, and m is at the surface of that ball (Fig. 5.1).

(3b) The time evolution of the location of m is derived in the d_{GP} frame and from the position factor, see the DEQ (5.1), and the transformed DEQ (5.7) is derived from the position factor.

(4) Thereby, these above two DEQs use a **structured energy function** *$\bar{E}(R, \dot{R})$ with $\bar{E}(R, \dot{R}) = 0 = k =$ invariant:*

$$\boxed{-k := \frac{2\bar{E}(R, \dot{R})}{m_0 \cdot c^2} \text{ with } \bar{E}(R, \dot{R}) = \frac{m_0 \dot{R}^2}{2} - \frac{GMm_0}{R}} \tag{5.13}$$

(5) That **structured energy function** *of m_0 is defined as follows, whereby it is proportional to E_0 and to a normalized energy $E_{norm} = \frac{E}{E_0}$:*

$$\boxed{\frac{E(R, \dot{R})^2 - E_0^2}{2\gamma^2 E_0} =: \bar{E}(R, \dot{R}) = E_0 \cdot \left(\frac{\dot{R}^2}{2c^2} - \frac{G \cdot M}{R \cdot c^2}\right)} \tag{5.14}$$

5.3 A solution of the flatness problem

If a law in physics is particular for each type of atom, molecule, matter or energy, then that law is not universal. Conversely, a law in physics that holds for each type of matter or energy is universal.

In this chapter, for the ideal case of a homogeneous universe, we used the local dynamics of the position factor, in order to derive the global flatness of the formed space. This derived global flatness is universal, as it does not depend on the composition of the objects contained in space.

5.4 Second solution of the flatness problem

In the above solution of the flatness problem, we use energy conservation. In our second solution, we do not use energy conservation. Of course, we do not state energy conservation would be violated, but we do not apply energy conservation. In principle, one might think that energy could be lost at a redshift of radiation, if one does not consider a corresponding gravitational potential, for instance.

5.4.1 Notations in cosmology

In this section, we summarize notations. In cosmology, dynamically essential densities are denoted as follows, see e. g. Hobson et al. (2006) or Carmesin (2019b) or (Carmesin et al., 2020, pp 296-301).

Essential densities in cosmology: The essential densities in cosmology are the density of matter ρ_m, of radiation ρ_r and of the cosmological constant ρ_Λ, see Einstein (1917), (Hobson et al., 2006, p. 389, Eq. 15.5), Karttunen et al. (1996), or the glossary:

$$\rho = \rho_m + \rho_r + \rho_\Lambda \tag{5.15}$$

In the case of the density of matter, heterogeneity is essential, see e. g. Peebles (1973), Kravtsov and Borgani (2012), Carmesin (2021d), Haude et al. (2022).

Time evolution: In the time evolution, present-day values are marked by the subscript zero. For instance, the present-day value of the Hubble parameter is the Hubble constant $H_0 = H(t_0)$. The inverse of the Hubble constant is called Hubble time, at a good approximation, see Hobson et al. (2006) or Carmesin (2019b), it is the age of the universe:

$$t_{H_0} = 1/H_0 \tag{5.16}$$

During the Hubble time, light traveled the light-travel distance $c \cdot t_{H_0}$, it is called Hubble radius:

$$R_{H_0} = c \cdot t_{H_0} = c/H_0 \tag{5.17}$$

The density of flat space is called critical density, we derive with the FLE:

$$H^2 = 8\pi G/3\rho_{cr} \text{ and } H_0^2 = 8\pi G/3\rho_{cr.0} \tag{5.18}$$

$$\text{or } \rho_{cr.0} = \frac{3H_0^2}{8\pi G} \tag{5.19}$$

The present-day curvature parameter is expressed with a density:

$$\rho_k = -\rho_{cr}\frac{c^2}{H^2R^2}k \text{ or } \Omega_k = -\frac{c^2}{H^2R^2}k \tag{5.20}$$

Density parameters: The ratio of a density and the critical density is called density parameter:

$$\rho_j/\rho_{cr} = \Omega_j \text{ and } \rho_{j,0}/\rho_{cr.0} = \Omega_{j,0} \text{ with } j \in \{r, m, \Lambda, k\} \tag{5.21}$$

Einstein (1917) introduced the cosmological constant Λ. Accordingly, the corresponding density is a constant:

$$\rho_\Lambda(t) = \rho_{\Lambda,0} \tag{5.22}$$

As the volume is proportional to the third power of the radius $R^3(t)$, and as matter does not change as a consequence of expansion, the density of matter is proportional to $R^{-3}(t)$:

$$\rho_m(t) = \rho_{m,0} \cdot (R/R_{H_0})^{-3} = \rho_{m,0}/a^3 \tag{5.23}$$

Hereby, we introduce the scaled radius and the redshift $z = \Delta\lambda/\lambda$:

$$a(t) = R(t)/R_{H_0} = 1/(z+1) \tag{5.24}$$

As the volume is proportional to the third power of the radius $R^3(t)$, and as the energy or dynamical density of radiation changes as a consequence of expansion by the redshift proportional to $R^{-1}(t)$, the density of radiation is proportional to $R^{-4}(t)$:

$$\rho_r(t) = \rho_{r,0} \cdot (R/R_{H_0})^{-4} = \rho_{m,0}/a^4 \tag{5.25}$$

Using the above definitions, we express the density in terms of the density parameters as follows:

$$\rho(a) = \rho_{cr.0}(\Omega_\Lambda + \Omega_{k,0}a^{-2} + \Omega_{m,0}a^{-3} + \Omega_{r,0}a^{-4}) \tag{5.26}$$

And the dynamics in the FLE are as follows:

$$H^2 = H_0^2(\Omega_\Lambda + \Omega_{k,0}a^{-2} + \Omega_{m,0}a^{-3} + \Omega_{r,0}a^{-4}) \tag{5.27}$$

Hereby, the sum of the density parameters is one:

$$1 = \Omega_\Lambda + \Omega_{k,0} + \Omega_{m,0} + \Omega_{r,0} \tag{5.28}$$

The Planck-Collaboration (2020) measured the following parameters, see the TT-mode in table 2, the abstract as well as Carmesin (2019b) for an evaluation of $\Omega_{r,0}$:

$$\Omega_\Lambda = 0,679 \pm 0.013 \tag{5.29}$$

$$\Omega_{m,0} = 0.321 \pm 0.013 \tag{5.30}$$

$$\Omega_{k,0} = 0.001 \pm 0.002 \tag{5.31}$$

$$\Omega_{r,0} = 9.265 \cdot 10^{-5} \cdot (1 \pm 0.031) \tag{5.32}$$

$$H_0 = 66.88 \pm 0.92 \frac{\text{km}}{\text{s} \cdot \text{Mpc}} \tag{5.33}$$

Summarizing notation The proportionality of a density ρ_j can be characterized as follows:

$$\rho_j \propto R^{-3\cdot(1+w_j)} \text{ with}$$

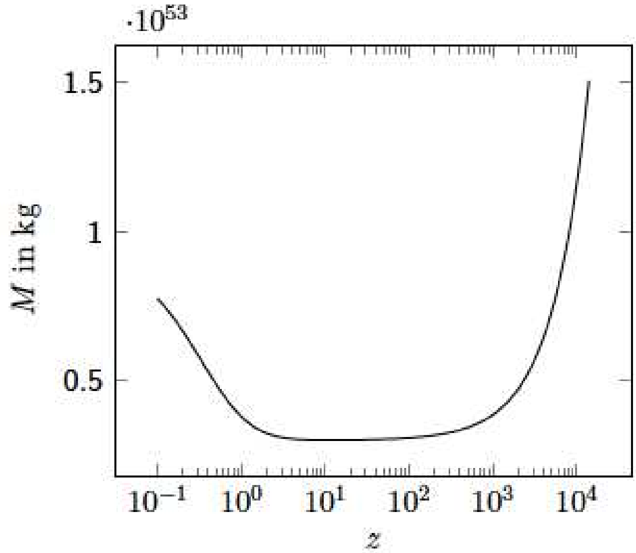

Figure 5.2: Mass or dynamical mass M in the ball with present-day radius R_{H_0} as a function of the redshift z. Thereby, the density $\rho(z)$ in Eq. (5.26, 5.24) is a function of the redshift z, see Eqs. (5.35, 5.36).

$$w_j = \begin{cases} 1/3 & \text{for } j = r \\ 0 & \text{for } j = m \\ -1/3 & \text{for } j = k \\ -1 & \text{for } j = \Lambda \end{cases} \tag{5.34}$$

5.4.2 Time evolution of M

As the only possibility for a nonzero curvature parameter is a time evolution of the field generating mass M, we analyze that time evolution. For instance, we consider a ball with the present-day radius equal to the Hubble radius. At a scaled radius $a(t)$, that ball had the radius $a(t)$. Thus, that ball had the following mass or dynamical mass, with the density in Eq. (5.26), the critical density and the parameters (see section 5.4.1):

$$M(a) = \rho(a) \cdot 4\pi/3 \cdot a^3 \cdot R_{H_0}^3 \text{ or} \tag{5.35}$$
$$M(z) = \rho(z) \cdot 4\pi/3 \cdot 1/(1+z)^3 \cdot R_{H_0}^3 \tag{5.36}$$

That mass or dynamical mass M as a function of the redshift is shown in Fig. (5.2). That function exhibits a local minimum. Thus, that (dynamical) mass M is constant at the local minimum z_{const}, so that the density parameter of curvature is zero at that redshift:

$$\Omega_k = \frac{-c^2}{H^2 R^2} \cdot k \text{ and } \Omega_k(z_{const}) = 0 \tag{5.37}$$

That result implies that the curvature is zero also at smaller redshifts $z \leq z_{const}$, or at later times $t \geq t_{const}$, see next two sections.

5.4.3 Time derivative of Ω_k

In this section, we derive the time derivative of Ω_k. It has also been provided in (Hobson et al., 2006, Eq. 15.48).

We apply the time derivative to the FLE:

$$\frac{2\dot{R}\ddot{R}}{R^2} - \frac{2\dot{R}^3}{R^3} = \frac{8\pi G}{3} \sum_{j=r,m,k,\Lambda} \frac{\rho_{crit.,0}\Omega_{j,0}}{a^{3(1+w_j)}} \frac{\dot{a}}{a}(-3(1+w_j)) \tag{5.38}$$

We identify $a^{-1}\dot{a}$ with H and $\rho_{crit.,0} \cdot \Omega_{j,0} \cdot a^{-3(1+w_j)}$ with ρ_j, we use $H = \frac{\dot{R}}{R}$, and we multiply by $\frac{1}{2H^3}$:

$$\begin{aligned} \frac{\ddot{R}R}{\dot{R}^2} - 1 &= -\frac{4\pi G}{3H^2} \cdot \sum_{j=r,m,k,\Lambda} \rho_j \cdot 3(1+w_j) \text{ or} \\ \frac{\ddot{R}R}{\dot{R}^2} &= -\frac{4\pi G}{3H^2} \cdot \sum_{j=r,m,k,\Lambda} \rho_j \cdot (1+3w_j) \end{aligned} \tag{5.39}$$

We apply the time derivative to $\rho_j = \rho_{crit.,0} \cdot \Omega_{j,0} \cdot a^{-3(1+w_j)}$:

$$\dot{\rho}_j = -3(1+w_j)H\rho_j \tag{5.40}$$

We apply the time derivative to $\Omega_j = \frac{8\pi G}{3H^2}\rho_i$:

$$\dot{\Omega}_j = \frac{8\pi G}{3H^2} \cdot \left(\dot{\rho}_j - \frac{2\dot{H}}{H}\rho_j\right) \tag{5.41}$$

We combine the above two equations:

$$\dot{\Omega}_j = -\Omega_j H \cdot \left(3(1+w_j) + \frac{2\dot{H}}{H^2}\right) \quad (5.42)$$

We apply $\frac{2\dot{H}}{H^2} = \frac{2\ddot{R}R}{\dot{R}^2} - 2$ to the above equation:

$$\dot{\Omega}_j = \Omega_j H \cdot \left(-3 - 3w_j - \frac{2\ddot{R}R}{\dot{R}^2} + 2\right) \quad (5.43)$$

We use Eq. (5.39):

$$\dot{\Omega}_j = \Omega_j H \cdot \left(-1 - 3w_j + \frac{8\pi G}{3H^2} \cdot \sum_{j=r,m,k,\Lambda} \rho_j \cdot (1+3w_j)\right) \quad \text{or}$$

$$\dot{\Omega}_j = \Omega_j H \cdot \left(-1 - 3w_j + \sum_{j=r,m,k,\Lambda} \Omega_j \cdot (1+3w_j)\right) \quad \text{or}$$

$$\dot{\Omega}_j = \Omega_j H \cdot (-1 - 3w_j + \Omega_m + 2\Omega_r - 2\Omega_\Lambda) \quad (5.44)$$

In particular, we apply the case $j = k$ to the above equation.

$$\dot{\Omega}_k = \Omega_k H \cdot (\Omega_m + 2\Omega_r - 2\Omega_\Lambda) \quad (5.45)$$

5.4.4 Time evolution of Ω_k

We apply the method of the analysis of the curvature parameter k and of the density parameter Ω_k as a function of the radius r of the ball. Firstly, at very small R or in the very early universe, the radiation was blue-shifted compared to the present-day primordial radiation, for details see Carmesin (2021a). In principle, that could have caused an increased field generating mass or dynamic mass M in the ball in Fig. (5.1). In principle, that could have caused a large positive curvature, as proposed by (Hobson et al., 2006, p. 417) or by Guth (1981). This could be the case even if that effect was made smaller by the era of 'cosmic inflation', see e. g. Guth (1981), Carmesin (2019b). We will show that such possible values of curvature in the early universe are not essential for the curvature in the present-day universe:

Secondly, the curvature is zero at z_{const} or at the time t_{const}. Thirdly, the density parameter Ω_k in Eq. (5.37) is a function of time. With it and the FLE, the time derivative of that density parameter can be derived, see section (5.4.3):

$$\dot{\Omega}_k = \Omega_k[H \cdot (\Omega_m + 2\Omega_r - 2\Omega_\Lambda)] \tag{5.46}$$

As the term in the rectangular bracket does not become infinite at redshifts z_{const} or at the time t_{const}, that bracket is limited by its maximum and by its minimum:

$$[H \cdot (\Omega_m + 2\Omega_r - 2\Omega_\Lambda)] \leq B_{max} \tag{5.47}$$

$$[H \cdot (\Omega_m + 2\Omega_r - 2\Omega_\Lambda)] \geq B_{min} \tag{5.48}$$

With it, we derive an upper limit $\Omega_{k,upper}$ and a lower limit $\Omega_{k,lower}$ of the density parameter as follows:

$$\Omega_{k,lower} \leq \Omega_k \leq \Omega_{k,upper} \tag{5.49}$$

$$\Omega_{k,upper}/dt = \Omega_{k,upper} \cdot B_{max} \tag{5.50}$$

$$\Omega_{k,lower}/dt = \Omega_{k,lower} \cdot B_{max} \tag{5.51}$$

The solutions are exponential functions with the initial value $\Omega_k(z_{const})$:

$$\Omega_{k,upper} = \Omega_k(z_{const}) \cdot e^{B_{max} \cdot (t - t_{const})} = 0 \tag{5.52}$$

$$\Omega_{k,lower} = \Omega_k(z_{const}) \cdot e^{B_{min} \cdot (t - t_{const})} = 0 \tag{5.53}$$

As both functions are zero, and as the density parameter is limited by these limiting solutions, the density parameter is zero at times t_{const} or at redshifts z_{const}:

$$\Omega_k = 0 \text{ for } t \geq t_{const} \text{ or } z \leq z_{const} \tag{5.54}$$

Altogether, we derived that the curvature is zero at the present-day universe. Thus, we derived a second solution of the flatness problem. We summarize our finding, see also Carmesin (2021d):

Theorem 7 Unification of micro- and macrodynamics

(1) The classical expansion of the universe since the Big Bang has been derived in the d_{GP} frame from the local dynamics of space described by the position factor, see (Carmesin, 2021d, THM 3). For it, a homogeneous density has been modeled, according to the cosmological principle, see e. g. Einstein (1917), Friedmann (1922), Lemaitre (1927), Karttunen et al. (1996).

(2) Thereby, it has been shown that the curvature parameter is zero, independent of the composition of objects in space. So, the flatness problem has been solved in a universal manner.

(3) Moreover, the derivation shows that the d_{GP} frame is compatible with the FLE.

(4) In a second solution of the flatness problem, see section (5.4), the flatness is derived on the basis of cosmological parameters, of a minimum of the mass or dynamic mass M in a prototypical ball of the universe (Fig. 5.2) and of the time derivative of the density parameter of curvature Ω_k.

(5) Altogether, a first unification has been derived: the unification of the classical local dynamics in GR with the classical global dynamics in GR.

Chapter 6

Energy Density of the Gravitational Field G^*

Idea: If a probe mass changes its position in a gravitational field, then the change ΔE of energy of the probe mass can be determined. If that motion causes a change $\Delta\vec{G}^*$ of the field, then the change ΔE might be used in order to derive the energy of the changed field $\Delta\vec{G}^*$.

Accordingly, in this chapter, we apply the law of energy conservation, in order to derive the energy density $u_{gr.f}$ and the density $\rho_{gr.f} = u_{gr.f}/c^2$ of the gravitational field $\vec{G}^*$.

6.1 Absolute value of $\rho_{gr.\ f.}$

In this section, we derive the absolute value $|\rho_{gr.\ f.}|$ of the energy density $\rho_{gr.\ f.}$ of the gravitational field $|G^*(R)| = |G^*(d_{GP})|$. For it, we analyze the energy ΔE_M that is necessary in order to lift a mass M in a shell with a radius R to a shell with a radius $R + \Delta R$, see Fig. (6.1). Thereby, the mass is lifted as follows: Differential parts dM are lifted, while the part M_{rest} is still at R. Moreover, the velocity of M remains approximately zero. So, a part dM is lifted at the following gravitational field of the part M_{rest}, see theorem (2):

$$|\vec{G}^*_{of\ M_{rest}}(R)| = \frac{G \cdot M_{rest}}{R^2} \tag{6.1}$$

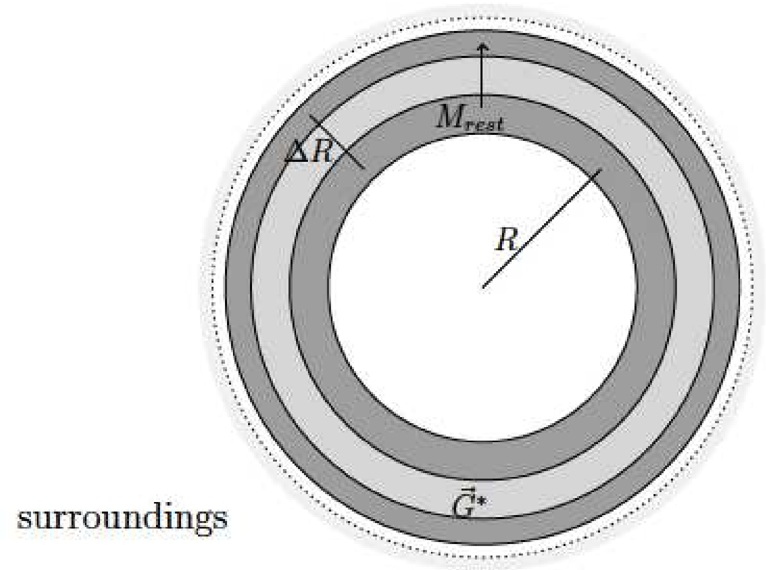

Figure 6.1: A mass M (dark grey) in a shell at a radius R is lifted to a radius $R+\Delta R$ as follows: Differential parts dM are lifted, while the rest M_{rest} is still at R. Thereby the field G^* (medium grey) in the shell with radius R and thickness ΔR becomes zero, when the whole mass is at $R+\Delta R$ (see Fig. 6.2).

So, the field $|G^*_{of\ M_{rest}}|$ is proportional to the part M_{rest} (Fig. 6.2). If a mass dM is lifted, and if the mass M_{rest} is still at R, then dM experiences the following force, see theorem (2): $|\vec{F}_G| = |\vec{G}^*_{of\ M_{rest}}(R)| \cdot dM$. Thus, the following energy $dE = |\vec{F}_G| \cdot \Delta R$ is required:

$$dE = |\vec{G}^*_{of\ M_{rest}}(R)| \cdot dM \cdot \Delta R = \frac{G \cdot M_{rest}}{R^2} \cdot dM_{lifted} \cdot \Delta R \quad (6.2)$$

We derive the full change in gravitational energy ΔE_M by integrating the above Eq.:

$$\Delta E_M = \int_0^E dE' \quad (6.3)$$

We apply Eq. (6.2):

$$\Delta E_M = \int_0^M \frac{G \cdot M_{rest}}{R^2} dM_{lifted} \cdot \Delta R \quad (6.4)$$

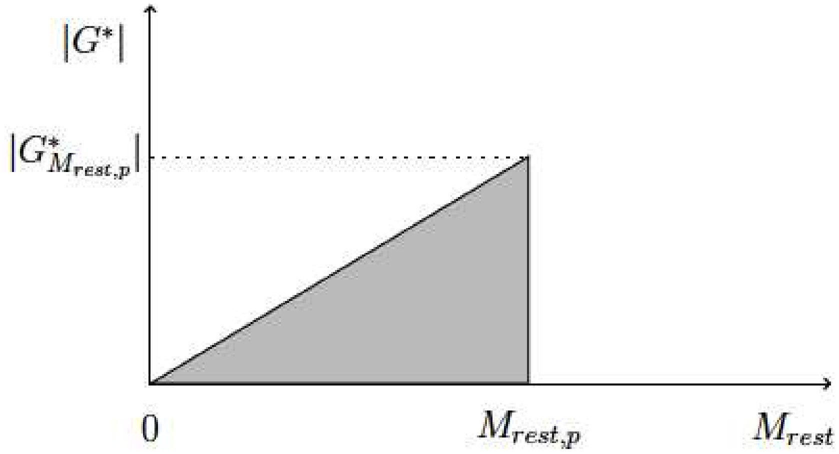

Figure 6.2: The field $|G^*|$ is shown as a function of the mass M_{rest}, that is still at the shell with the radius R. A particular value $M_{rest,p}$ is marked.

We substitute the change dM_{lifted} of the lifted mass to the change dM_{rest} of the rest mass. As the rest mass M_{rest} is decreased by dM_{lifted}, we obtain $dM_{lifted} = -dM_{rest}$. At the lower bound of the integral, M_{rest} has the value M of the complete mass that is lifted. And at the upper bound of the integral, M_{rest} has the value zero, as the whole mass has been lifted. Altogether, the substitution yields:

$$\Delta E_M = -\int_M^0 \frac{G \cdot M_{rest}}{R^2} dM_{rest} \cdot \Delta R \qquad (6.5)$$

We evaluate the integral:

$$\Delta E_M = \frac{G \cdot M^2 \cdot \Delta R}{2R^2} \qquad (6.6)$$

6.2 Free fall of M

In order to identify the energy density of the gravitational field, we analyze the inverse process:

Initially, the mass M is distributed isotropically at $R + \Delta R$. Then the mass M falls freely towards R. Thereby, the following holds:

Firstly, the potential energy E_{pot} is decreased by the value ΔE_M in Eq. (6.6):

$$\Delta E_{pot} = -\Delta E_M = -\frac{G \cdot M^2 \cdot \Delta R}{2R^2} \tag{6.7}$$

Secondly, the energy $E(M)$ of M does not change, according to the law of energy conservation.

Thirdly, the mass M does not change, as $M = E(M)/c^2$.

Fourthly, the internal energy E_{intern} of M is equal to ΔE_M in Eq. (6.6), as the energy of M does not change:

$$\Delta E_{internal} = \Delta E_M = \frac{G \cdot M^2 \cdot \Delta R}{2R^2} \tag{6.8}$$

Fifthly, the potential energy E_{pot} is located outside M. At a radial coordinate larger than $R + \Delta R$, there is no change, as M is not changed. At a radial coordinate smaller than R, there is no change, as there is no field. Thus, the change occurred in the shell at radial coordinate between R and $R + \Delta R$. Moreover, in that shell, there emerged the gravitational field according to theorem (2). Accordingly, we derive the energy density in that shell, and we identify that energy density by the energy density of the gravitational field $u_{gr.f}$.

The above analysis holds for an observer, who interprets M as a sum of rest masses, e. g. of elementary particles[1].

Absolute value $|u_{gr.f}|$ of the energy density $u_{gr.f}$ of the field: The field $|G^*|$ is in the shell with radius R and thickness ΔR (see Fig. 6.1). The corresponding volume is $\Delta V = 4\pi \cdot R^2 \cdot \Delta R$. So, we derive the energy density by dividing the energy ΔE_M by the volume ΔV. So, we get:

$$|u_{gr.f}| = \frac{\Delta E_M}{\Delta V} = \frac{G \cdot M^2 \cdot \Delta R}{2R^2 \cdot 4\pi \cdot R^2 \cdot \Delta R} \tag{6.9}$$

[1]If the observer assigns the change of energy via the position factor ε_E to the mass M, then the same energy can hardly be assigned a second time to the field.

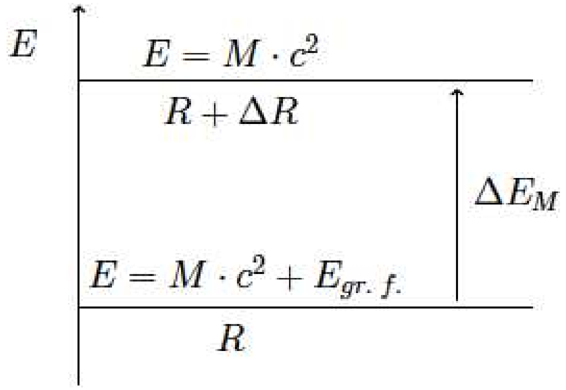

Figure 6.3: The energy of the mass is shown at the initial radius R and at the final radius $R + \Delta R$.

We simplify the above term, we expand by G, and we apply the field $|G^*| = \frac{G \cdot M}{R^2}$, see theorem (2). So, we derive:

$$\boxed{|u_{gr.f}| = \frac{\vec{G}^{*2}}{8\pi \cdot G} = |\rho_{gr.\ f.}| \cdot c^2} \tag{6.10}$$

Hereby, $\rho_{gr.\ f.}$ is the mass density corresponding to the energy density of the gravitational field according to the equivalence of mass and energy.

6.2.1 Sign of $u_{gr.f}$

As the potential energy has a negative sign, the energy density $u_{gr.\ f.}$ of the gravitational field has a negative sign as well. Note that the negative sign of the energy density $u_{gr.\ f.}$ is a direct consequence of the fact that gravity is attractive. Moreover, that negative sign does not cause any difficulty in the following, see also Carmesin (2021d):

Theorem 8 Energy density of the gravitational field

(1) The gravitational energy is inherent to modifications of space such as curvature or additionally formed volume or a gravitational field.

(2) A gravitational field $\vec{G}^*$ has the energy density $u_{f,par,grav}$ as follows:

$$u_{f,par,grav} = \rho_{gr.\ f.} \cdot c^2 = -\frac{\vec{G}^{*2}}{8\pi \cdot G} \quad \text{or}$$
$$|u_{f,par,grav}| = |\rho_{gr.\ f.}| \cdot c^2 = \frac{\vec{G}^{*2}}{8\pi \cdot G} \tag{6.11}$$

(3) In an isotropic vicinity of a field generating mass M and at a distance $R = d_{GP}$ from the mass M, a gravitational field $G^*(R)$ occurs as follows, see theorem (2):

$$|\vec{G}^*| = \frac{G \cdot M}{R^2} \tag{6.12}$$

Part II

Theory of Dynamic Volume

Chapter 7

Caused Additional Volume

In this chapter, we show that a nonzero mass or dynamic mass M with an *isotropic vicinity* of M causes additional volume and a corresponding additional dark energy or energy of the volume.

7.1 A mass causes curvature of spacetime

Idea: We compare the *isotropic vicinity* of a *nonzero mass* M with the same vicinity in the *zero mass limit*. Thereby, we realize that the mass M causes curvature of spacetime according to the Schwarzschild metric. This comparison is illustrated in Fig. (7.1).

Theorem 9 A mass causes curvature of spacetime.

If a mass or dynamic mass M is in an empty environment, and if M is neither accelerated nor rotating nor charged, then the following holds:

(1) The vicinity of M is isotropic.

(2) The vicinity of M is characterized by the **Schwarzschild metric** *in THM (3):*

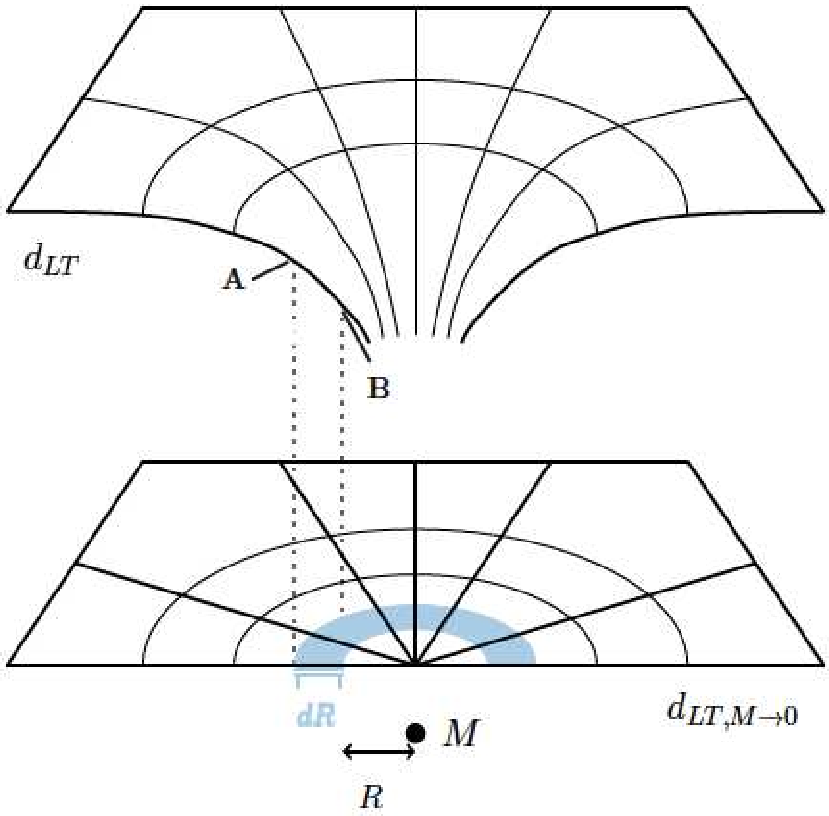

Figure 7.1: Two maps: A mass M causes nonzero curvature in its vicinity, illustrated by the upper map. In the zero mass limit, that curvature vanishes, illustrated by the lower map.

$$\text{in} \quad \text{polar coordinates :} \tag{7.1}$$

$$g_{ik,SM}(R,\vartheta) = \begin{pmatrix} \varepsilon_E^2 & 0 & 0 & 0 \\ 0 & \varepsilon_E^{-2} & 0 & 0 \\ 0 & 0 & R^2 & 0 \\ 0 & 0 & 0 & R^2 \sin^2\vartheta \end{pmatrix} \tag{7.2}$$

$$\text{with} \quad R_S = \frac{2G \cdot M}{c^2} \tag{7.3}$$

$$\text{and} \quad \varepsilon_E(R) = \sqrt{1 - \frac{R_S}{R}} \tag{7.4}$$

Hereby, the **Schwarzschild radius** *R_S is used as an abbreviation, and $\varepsilon_E(R)$ is the* **position factor**.

(3) In the **zero mass limit**, *the isotropic vicinity of M is characterized by the metric of flat space:*

$$
\begin{aligned}
& \text{in} \quad \text{polar coordinates:} & (7.5)\\
g_{ik,flat}(R,\vartheta) &= \lim_{M\to 0} g_{ik,SM}(R,\vartheta) & (7.6)\\
g_{ik,flat}(R,\vartheta) &= \begin{pmatrix} 1 & 0 & 0 & 0 \\ 0 & 1 & 0 & 0 \\ 0 & 0 & R^2 & 0 \\ 0 & 0 & 0 & R^2\cdot\sin^2\vartheta \end{pmatrix} & (7.7)
\end{aligned}
$$

The metric of flat space has zero curvature.

(4) A nonzero value of the mass or dynamic M causes a nonzero curvature of spacetime according to the Schwarzschild metric.

Proof

(1) As M does not rotate, it does not cause any anisotropic drag, see e. g. Kerr (1963). As M is not charged, it does not cause any conceivable anisotropic interaction, see e. g. Workman et al. (2022). As the vicinity of M is empty, there is no external anisotropic effect. Altogether, the vicinity of M is isotropic.

(2) As M and its vicinity are isotropic, that vicinity is characterized by the Schwarzschild metric, see Schwarzschild (1916) or THM (3).

(3) In the zero mass limit, the Schwarzschild radius is zero:

$$\lim_{M\to 0} R_S = \lim_{M\to 0} \frac{2G\cdot M}{c^2} = 0 \tag{7.8}$$

As a consequence, the position factor is one:

$$\lim_{M\to 0} \varepsilon_E(R) = \lim_{M\to 0} \sqrt{1-\frac{R_S}{R}} = 1 \tag{7.9}$$

Consequently, the zero mass limit of the Schwarzschild metric is the metric of flat space:

$$\lim_{M \to 0} g_{ik,SM} \tag{7.10}$$

$$= \lim_{M \to 0} \begin{pmatrix} \varepsilon_E^2 & 0 & 0 & 0 \\ 0 & \varepsilon_E^{-2} & 0 & 0 \\ 0 & 0 & R^2 & 0 \\ 0 & 0 & 0 & R^2 \sin^2 \vartheta \end{pmatrix} \tag{7.11}$$

$$= \begin{pmatrix} 1 & 0 & 0 & 0 \\ 0 & 1 & 0 & 0 \\ 0 & 0 & R^2 & 0 \\ 0 & 0 & 0 & R^2 \cdot \sin^2 \vartheta \end{pmatrix} \tag{7.12}$$

$$= g_{ik,flat}(R, \vartheta) \tag{7.13}$$

Flat space has *zero curvature*.

(4) In the isotropic vicinity of M, a nonzero value of M causes a nonzero value of the Schwarzschild radius:

$$M > 0 \to R_S = \frac{2G \cdot M}{c^2} > 0 \tag{7.14}$$

A nonzero value of the Schwarzschild radius causes a value of the position factor smaller than one:

$$R_S > 0 \to \varepsilon_E(R) = \sqrt{1 - \frac{R_S}{R}} < 1 \tag{7.15}$$

A value of the position factor smaller than one causes a curvature of spacetime according to the Schwarzschild metric. In that case, the Schwarzschild metric differs from the metric of flat space. Thus, the Schwarzschild metric has *nonzero curvature*, in this case.

As a consequence of the transitivity of implications, a nonzero value of M causes a nonzero curvature of spacetime according to the Schwarzschild metric.

Altogether, this proves all parts of the theorem.

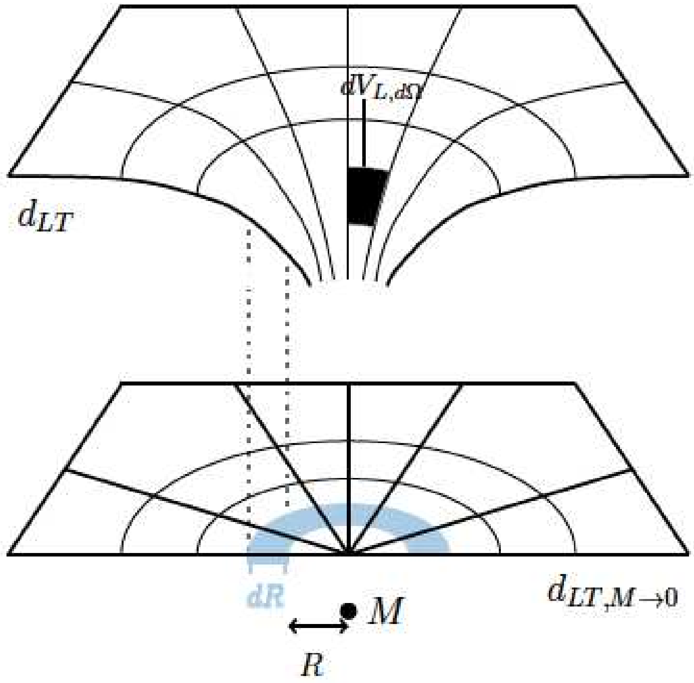

Figure 7.2: Incremental volume $dV_{L,d\Omega} = d\Omega \cdot R^2 \cdot dL$ at the solid angle $d\Omega = d\vartheta \cdot \sin^2\vartheta \cdot d\varphi$ (black). The upper grey shell has the solid angle $d\Omega = 4\pi$ and the volume $dV_L = 4\pi \cdot R^2 \cdot dL$. The incremental volume $dV_{L,d\Omega}$ is in that upper grey shell.

7.2 A mass causes additional volume

Idea: We compare a shell S_M in the *isotropic vicinity* of a *nonzero mass* M with the corresponding shell $S_{M\to 0}$ in *zero mass limit*. Thereby, we realize that the shell S_M has a larger volume than the shell $S_{M\to 0}$, as a consequence of curvature. Accordingly, the mass M causes *additional volume* δV.

That additional volume δV has the corresponding *dark energy* $\delta E_{vol} = \delta V \cdot u_{vol}$, see e. g. Huterer and Turner (1998); Planck-Collaboration (2020); Workman et al. (2022). This comparison is illustrated in Fig. (7.1).

Theorem 10 A mass causes additional volume.

If a mass or dynamic mass M is in an empty environment, and if M is neither accelerated nor rotating nor charged, and if two *locations A and B have the same angular coordinates and an incremental distance $d_{LT}(A,B)$, then the following holds (Fig. (7.1):*

(1) A nonzero M causes nonzero curvature of spacetime according to the **Schwarzschild metric, SM** *with a radial coordinate R.*

(2) An observer Alice at a location A can in principle observe her radial coordinate R_A. An observer Bob at a location B can in principle observe his radial coordinate R_B. Alice and Bob can in principle observe their mutual light-travel distance $d_{LT}(A,B) =: dL$, and they can evaluate their mutual radial distance $dR(A,B) = R_A - R_B =: dR$. Hereby, we abbreviate $dR(A,B)$ by dR and $d_{LT}(A,B)$ by dL.

(3) The increment dL is larger than the increment dR. The difference δR is caused by the mass M and has the following amount:

$$\delta R \;=\; dL - dR = dR \cdot \left(\frac{1}{\varepsilon_E} - 1 \right) \tag{7.16}$$

(4) The shell S_M with the center at M, the radius R and the thickness dL (Fig. 7.1) has the following volume dV_L:

$$dV_L \;=\; 4\pi \cdot R^2 \cdot dL \tag{7.17}$$

In the shell, the solid angle

$$d\Omega = d\vartheta \cdot \sin^2 \vartheta \cdot d\varphi \tag{7.18}$$

is equal to 4π. In a solid angle $d\Omega$, the corresponding part $dV_{L,d\Omega}$ of the volume dV_L is as follows (Fig. 7.2):

$$dV_{L,d\Omega} \;=\; d\Omega \cdot R^2 \cdot dL \tag{7.19}$$

(5) The shell $S_{M\to 0}$ with the center at M, the radius R and the thickness dR (Fig. 7.1) has the following volume dV_R:

$$dV_R \;=\; 4\pi \cdot R^2 \cdot dR \tag{7.20}$$

In a solid angle $d\Omega$, the corresponding part $dV_{R,d\Omega}$ of the volume dV_R is as follows:

$$dV_{R,d\Omega} = d\Omega \cdot R^2 \cdot dR \tag{7.21}$$

(6) The shell S_M has a larger volume than the shell $S_{M\to 0}$. The difference δV is caused by the mass M and has the following amount:

$$\delta V := dV_L - dV_R \tag{7.22}$$
$$= 4\pi \cdot R^2 \cdot \delta R \text{ or} \tag{7.23}$$
$$\delta V = 4\pi \cdot R^2 \cdot dR \cdot \left(\frac{1}{\varepsilon_E} - 1\right) \tag{7.24}$$

The corresponding relations in a solid angle $d\Omega$ are as follows:

$$\delta V_{d\Omega} := dV_{L,d\Omega} - dV_{R,d\Omega} \tag{7.25}$$
$$= d\Omega \cdot R^2 \cdot \delta R \text{ or} \tag{7.26}$$
$$\delta V_{d\Omega} = d\Omega \cdot R^2 \cdot dR \cdot \left(\frac{1}{\varepsilon_E} - 1\right) \tag{7.27}$$

The differences δV and $\delta V_{d\Omega}$ are called **additional volumes**. *The corresponding minuends dV_L and $dV_{L,d\Omega}$ are named* **complete volume**. *The subtrahend dV_R is called* **reference volume**.

(7) The additional volume δV has the following **additional dark energy***:*

$$\delta E_{vol} = \delta V \cdot u_{vol} \tag{7.28}$$

Thereby, u_{vol} is the energy density of dark energy. That energy density is alternatively and usually named dynamic density of dark energy $\rho_{vol} := u_{vol}/c^2$, see e. g. Planck-Collaboration (2020); Workman et al. (2022); Hobson et al. (2006).

(8) An additional volume δV or $\delta V_{d\Omega}$ divided by the corresponding complete volume is called **relative additional volume** ε_L,

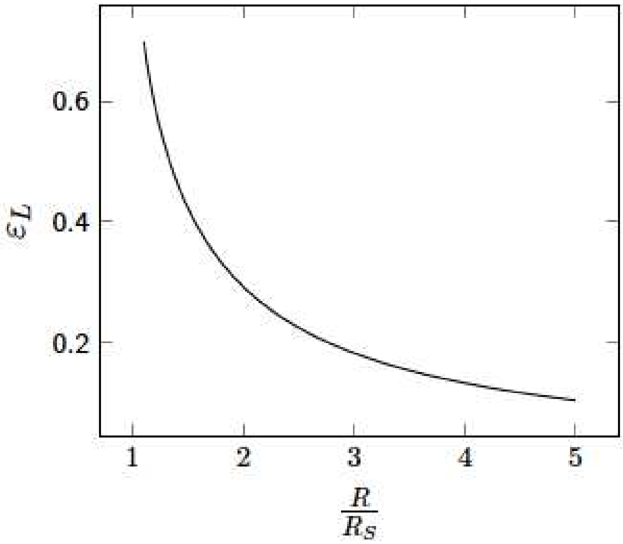

Figure 7.3: Relative additional volume ε_L.

and it can be calculated as follows (Fig. 7.3):

$$\varepsilon_L := \frac{\delta V}{dV_L} = \frac{\delta V_{d\Omega}}{dV_{L,d\Omega}} \quad \text{and} \tag{7.29}$$

$$\varepsilon_L = 1 - \varepsilon_E \tag{7.30}$$

Proof

(1) The Schwarzschild metric is a function of the radial coordinate R, see theorem (9) or Schwarzschild (1916); Hobson et al. (2006).

(2) Alice and Bob can measure their radial coordinates R_A and R_B based on the light-travel distance. For it, they can measure the circumferential radial coordinate $R_{circumferential} = \frac{U}{2\pi}$, see section (2.6.4.1). Alternatively, Alice and Bob can measure their radial coordinates with help of the gravitational parallax distance, see section (2.6.4).

The radial coordinates provide the corresponding radial difference $dR = R_A - R_B$.

Alice and Bob can measure their mutual distance dL by measuring the light-travel distance.

(3) A nonzero mass M causes a position factor smaller 1, see theorem (9). The Schwarzschild metric can be expressed by a line element ds as follows, see e. g. (Landau and Lifschitz, 1971, Eq. 82.1):

$$ds^2 = -c^2 dt^2 \varepsilon_E^2 + dR^2/\varepsilon_E^2 + R^2 d\vartheta^2 + R^2 \cdot \sin^2\vartheta \cdot d\varphi^2 \quad (7.31)$$

If the increments dt, $d\vartheta$ and $d\varphi$ are zero, then the incremental length dL is equal to the line element ds, see e. g. Landau and Lifschitz (1971):

$$ds = dL = dR \cdot \frac{1}{\varepsilon_E} \quad (7.32)$$

The above relation implies Eq. (7.16). Thus, a mass or dynamic mass M causes the additional increment δR according to Eq. (7.16).

(4) The volume of the shell is the product of the area A of the surface of the shell multiplied by the thickness dL, as the thickness is incremental. As there is no change of length in the angular directions of ϑ and φ, the circumference has the length $2\pi \cdot R$ and the area A of the surface is equal to $A = 4\pi R^2$. Thence, we derive $dV_L = 4\pi R^2 dL$. Similarly, we derive $dV_{L,d\Omega} = d\Omega R^2 dL$.

(5) The volume of the shell is the product of the area $A = 4\pi R^2$ of the surface of the shell multiplied by the thickness dR, as the thickness is incremental. Thus, we obtain $dV_R = 4\pi R^2 dR$. Similarly, we derive $dV_{R,d\Omega} = d\Omega R^2 dR$.

(6) The difference $\delta V = dV_L - dV_R$ is derived by inserting Eqs. (7.16, 7.20, 7.17). Similarly, we derive $\delta V_{d\Omega} = dV_{L,d\Omega} - dV_{R,d\Omega}$.

(7) The additional energy δE_{vol} is derived by multiplication of the additional volume δV with the corresponding energy density u_{vol}. So we derive $\delta E_{vol} = \delta V \cdot u_{vol}$.

(8) In the *relative additional volume* $\varepsilon_L = \frac{\delta V}{dV_L}$, the definition of

additional volume δV (Eq. 7.22) provides ε_L as a function of dR/dL:

$$\varepsilon_L = 1 - \frac{dV_R}{dV_L} = 1 - \frac{dR}{dL} \tag{7.33}$$

Similarly, we derive:

$$\varepsilon_L = 1 - \frac{dV_{R,d\Omega}}{dV_{L,d\Omega}} = 1 - \frac{dR}{dL} \tag{7.34}$$

The ratio dR/dL is equal to the position factor ε_E (Eq. 7.32). Thus, ε_L as a function of that factor:

$$\varepsilon_L = 1 - \varepsilon_E \tag{7.35}$$

Altogether, this proves all parts of the theorem.

Corollary 7 Additional volume

(1) Alice and Bob can observe their radii R_A and R_B. For instance, they can observe the circumferential radial coordinate $R_{circumferential} = \frac{U}{2\pi}$, see section (2.6.4.1). Or they can observe the gravitational parallax distance d_{GP}, see section (2.6.4).

(2) Thus, Alice and Bob can observe the increments dR and dL. With it, they can observe the additional volume δV. As a consequence, the additional volume δV is an element of physical reality. With it, relative additional volume ε_L is an element of physical reality.

(3) Moreover, the energy density of volume u_{vol} can be observed. So it is an element of physical reality as well.

(4) As a consequence of items (2) and (3), the additional energy $\delta E_{vol} = u_{vol} \cdot \delta V$ can be observed. Thus, it is an element of physical reality too.

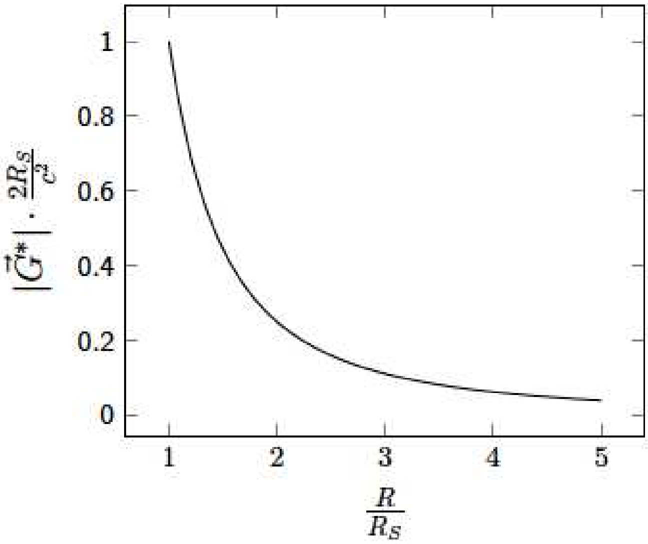

Figure 7.4: Absolute value of the gravitational field $|\vec{G}^*| \cdot \frac{2R_S}{c^2}$.

7.3 ε_L provides a gravitational potential

Idea: The relative additional volume $\varepsilon_L = 1 - \varepsilon_E(R)$ is an element of physical reality (corollary 7). Moreover, ε_L is a scalar, and it decreases monotonously, when the distance to M increases. So, ε_L might be proportional to a gravitational potential.

This possibility is analyzed next. Thereby, the precise details of an exact gravitational potential are derived.

Theorem 11 An exact gravitational potential

If a mass or dynamic mass M is in an empty environment, and if M is neither accelerated nor rotating nor charged, then the following holds:

(1) At each radius $R > R_S$, an observer can measure the following gravitational field $\vec{G}^*$ as a function of R, see section (2.6.4) and (Moore, 2013, Eq. 9.9) (Fig. 7.4):

$$|\vec{G}^*| = \frac{G \cdot M}{R^2} = \frac{c^2}{2R_S} \cdot \left(\frac{R_S}{R}\right)^2 \tag{7.36}$$

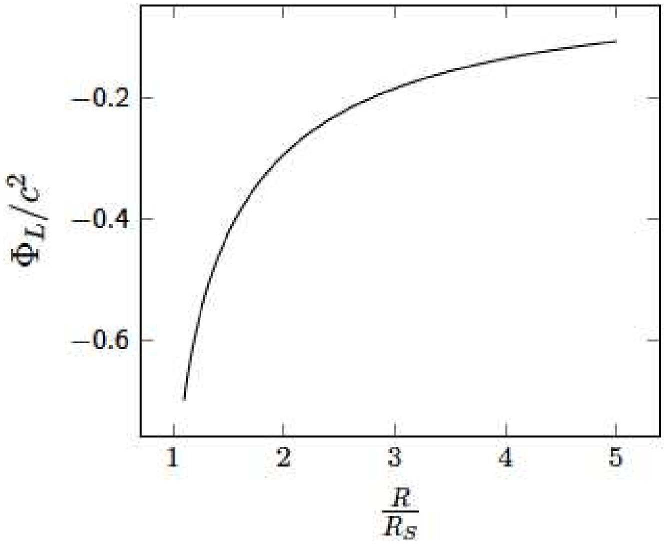

Figure 7.5: Gravitational potential Φ_L/c^2, according to the derivative with respect to the light-travel distance dL.

The field is antiparallel to the radial unit vector $\vec{e}_L$ (Fig. 7.6):

$$\vec{G}^* = -\frac{G \cdot M}{R^2} \cdot \vec{e}_L \tag{7.37}$$

(2) At each location with $R \geq R_S$, the gravitational potential $\Phi_L(\vec{R})$ is equal to the relative additional volume multiplied by $-c^2$, see Fig. (7.5),

$$\Phi_L \; := \; -c^2 \varepsilon_L \tag{7.38}$$

and the field is the gradient of the potential:

$$\vec{G}^* \; = \; -\frac{\partial}{\partial L}\Phi_L \cdot \vec{e}_L, \text{ thence,} \tag{7.39}$$

$$\vec{G}^* \; = \; -grad_L \Phi_L \text{ or with } \vec{\partial}_L := grad_L \tag{7.40}$$

$$\vec{G}^* \; = \; -\vec{\partial}_L \Phi_L \tag{7.41}$$

Proof

(1) The gravitational field as a function of R is provided in THM (2).

(2) In order to confirm the potential

$$\Phi_L = -c^2\varepsilon_L, \tag{7.42}$$

we apply the derivative, and we use $\varepsilon_L = 1 - \varepsilon_E$:

$$-\frac{\partial}{\partial L}\Phi_L = -c^2\frac{\partial}{\partial L}(1 - \varepsilon_E(R)) \tag{7.43}$$

We apply the chain rule, and we use $\varepsilon_E = \sqrt{1 - \frac{R_S}{R}}$:

$$-\frac{\partial}{\partial L}\Phi_L = -c^2 \underbrace{\frac{\partial R}{\partial L}}_{\varepsilon_E} \frac{\partial}{\partial R}\left(1 - \sqrt{1 - \frac{R_S}{R}}\right) \tag{7.44}$$

We evaluate the derivative:

$$-\frac{\partial}{\partial L}\Phi_L = -c^2\varepsilon_E\frac{1}{2\varepsilon_E}\frac{-R_S}{R^2} \tag{7.45}$$

We use the Schwarzschild radius $R_S = \frac{2GM}{c^2}$, and we identify the field (Eq. 7.37):

$$-\frac{\partial}{\partial L}\Phi_L = c^2\frac{1}{2}\frac{2GM}{c^2R^2} = \frac{GM}{R^2} = |\vec{G}^*| \tag{7.46}$$

Altogether, this proves all parts of the theorem.

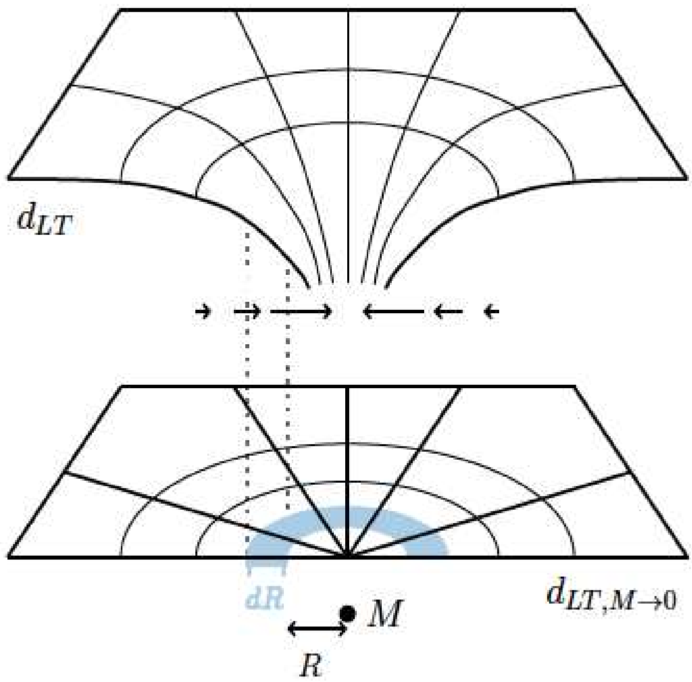

Figure 7.6: Vectors of the gravitational field.

Chapter 8

Propagation of Additional Volume

In this chapter, we analyze the propagation of dynamic volume in the vicinity of a mass M. In particular, we derive the differential equation, DEQ, for relative additional volume. Moreover, we analyze plane wave solutions of that DEQ. Furthermore, we generalize that propagation so that the DEQ does not depend on the mass M.

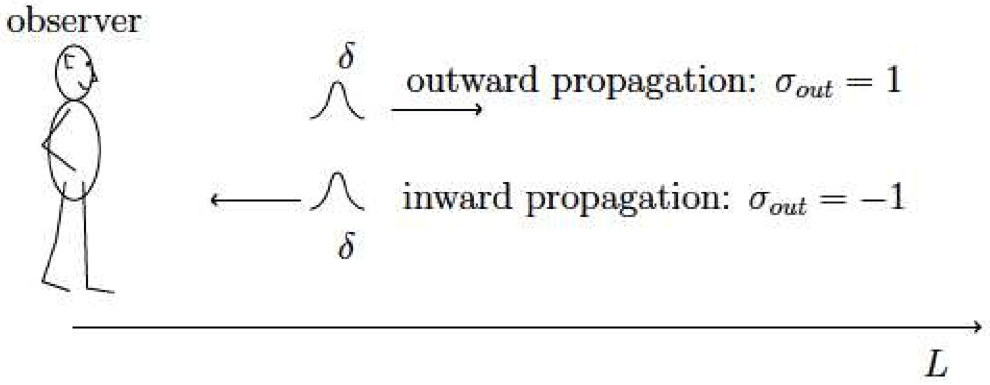

Figure 8.1: If a portion δ increases its light-travel distance to an observer, then the portion propagates outwards. In that case, a corresponding sign function has the value one, $\sigma_{out} = 1$. If that distance decreases, then the sign function has the value minus one, $\sigma_{out} = -1$.

Definition 8 Unidirectional propagation

(1) If at each location $\vec{R}$, a propagation takes place in exactly one direction, then the propagation is called **unidirectional propagation**. *For instance, the radial propagation in the vicinity of a mass M is unidirectional.*

(2) The radial direction has the direction vector $\vec{e}_L$.

(3) If a portion δ increases its light-travel distance to an observer, then the portion propagates outwards, see Fig. (8.1).

(4) If a portion δ decreases its light-travel distance to an observer, then the portion propagates inwards.

(5) For a portion δ propagating relative to an observer, we define a sign function σ_{out} as follows:

If δ propagates outwards, then $\sigma_{out} = 1$.

If δ propagates inwards, then $\sigma_{out} = -1$.

Otherwise, the value is $\sigma_{out} = 0$.

8.1 Relative additional volume

Idea: A **portion** of relative additional volume has zero rest mass. Accordingly, such a portion should propagate at the velocity of light, as derived below. We investigate that propagation in this section.

Theorem 12 Propagation of relative additional volume

If a mass or dynamic mass M is in an empty environment, and if M is neither accelerated nor rotating nor charged, then the following holds:

(1) Within natural volume, for a **portion** *of relative additional volume, the group velocity v_g is equal to the velocity of light $v_g = c$.*

(2) A portion of relative additional volume propagates parallel or antiparallel to the radial direction vector $\vec{e}_L$.

(3a) A **portion** *of relative additional volume propagates as follows, see (Figs. 8.1 and 8.2) and DEF (8):*

$$L(\tau_0 + \tau) = L(\tau_0) + c \cdot \tau \cdot \sigma_{out}, \text{ thus,} \tag{8.1}$$
$$\frac{\partial L}{\partial \tau} = c \cdot \sigma_{out}, \text{ with } d\tau = dt \cdot \varepsilon_E \tag{8.2}$$

(4a) The unidirectional propagation of a **portion** *of relative additional volume is driven by the gravitational potential as follows:*

$$\frac{\partial}{\partial L}\Phi_L = -c^2 \underbrace{\frac{\partial \tau}{\partial L}}_{\sigma_{out}/c} \cdot \frac{\partial}{\partial \tau}\varepsilon_L, \text{ implied DEQ :} \tag{8.3}$$
$$\frac{\partial}{\partial L}\Phi_L = -c \cdot \sigma_{out} \cdot \frac{\partial}{\partial \tau}\varepsilon_L, \text{ or} \tag{8.4}$$
$$|\vec{G}^*| = |c \cdot \frac{\partial}{\partial \tau}\varepsilon_L|, \tag{8.5}$$
$$\text{with radial direction } \vec{e}_L \text{ of propagation} \tag{8.6}$$

(3b) In parts (3a) and (4a), we treated portions of relative additional volume. In parts (3b) and (4b), correspondingly, we treated phases of relative additional volume.
A **phase** *of a harmonic wave of relative additional volume propagates as follows, see (Figs. 8.1 and 8.2) and DEF (8):*

$$L(\tau_0 + \tau) = L(\tau_0) + v_p \cdot \tau \cdot \sigma_{out}, \text{ thus,} \tag{8.7}$$
$$\frac{\partial L}{\partial \tau} = v_p \cdot \sigma_{out}, \text{ with } d\tau = dt \cdot \varepsilon_E \tag{8.8}$$

(4b) In the unidirectional propagation of relative additional volume, the propagation of the **phase** *of a harmonic wave is driven by the gravitational potential and characterized by the phase velocity v_p as follows (see THM 5, part 12). In general, v_p is a*

function of the wave number $|\vec{k}|$ as follows:

$$\frac{\partial}{\partial L}\Phi_L = -c^2 \underbrace{\frac{\partial \tau}{\partial L}}_{\sigma_{out}/v_p} \cdot \frac{\partial}{\partial \tau}\varepsilon_L, \text{ implied DEQ :} \quad (8.9)$$

$$\frac{\partial}{\partial L}\Phi_L = -\frac{c}{v_p} \cdot c \cdot \sigma_{out} \cdot \frac{\partial}{\partial \tau}\varepsilon_L, \text{ or} \quad (8.10)$$

$$|\vec{G}^*| = \left|\frac{c}{v_p} \cdot c \cdot \frac{\partial}{\partial \tau}\varepsilon_L\right|, \quad (8.11)$$

$$\left|\frac{1}{c}\frac{v_p}{c} \cdot \vec{G}^*\right| = \left|\frac{\partial}{\partial \tau}\varepsilon_L\right|, \quad (8.12)$$

$$\text{with radial direction } \vec{e}_L \text{ of propagation} \quad (8.13)$$

The gradient of the potential $\frac{\partial}{\partial L}\Phi_L$ or the field $|\vec{G}^*|$ can cause a high phase velocity v_p. Such high v_p can occur especially at large wavelengths, see THM (5, part (12)).

Correspondingly, the potential and the field can cause a high rate of relative additional volume $\dot{\varepsilon}_L$. Hereby that rate is increased by the factor $\frac{v_p}{c}$. Accordingly, there can be a sufficient rate of relative additional volume $\dot{\varepsilon}_L$ for a high phase velocity, by which the relative additional volume ε_L can propagate.

Using the DEQ (8.10) and the potential $\Phi_L = -c^2 \cdot \varepsilon_L$, we derive the DEQ of relative additional volume:

$$\boxed{v_p \cdot \frac{\partial}{\partial L}\varepsilon_L = \sigma_{out} \cdot \frac{\partial}{\partial \tau}\varepsilon_L} \quad (8.14)$$

That DEQ is fully geometric in spacetime. Correspondingly, that DEQ does not depend on any physical constant such as G, c or h. Accordingly, the phase velocity v_p of a harmonic wave of volume is not limited.

Proof

(1) A portion of volume can transform at a phase transition to a mass, according to the Higgs (1964) mechanism, see Carmesin

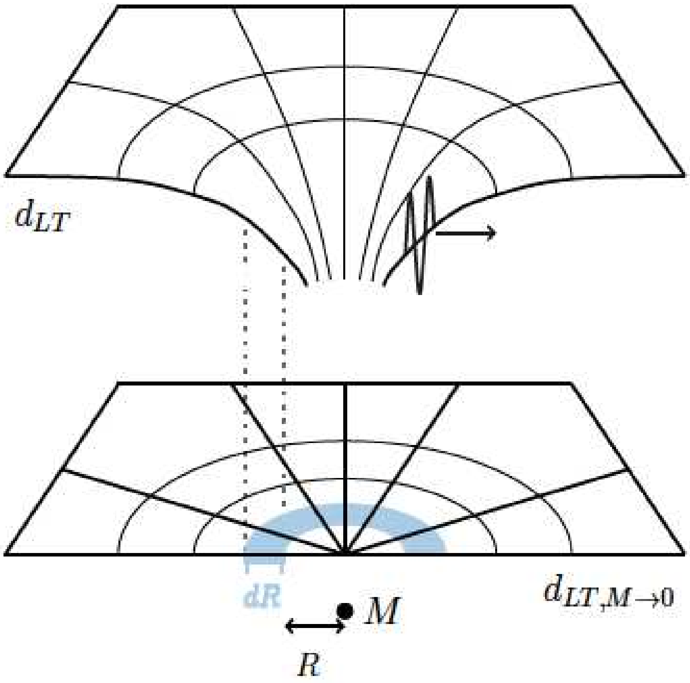

Figure 8.2: Propagation of additional volume (black waveform).

(2021a) for an explicit analysis thereof. Such a phase transition is the only mechanism, by which a portion of volume can achieve a nonzero rest energy E_0. Thus, each portion of natural three-dimensional volume has zero rest energy $E_0 = 0$.

In SR, the following energy relation holds:

$$E^2 = E_0^2 \cdot \frac{1}{1 - v^2/c^2} \tag{8.15}$$

We solve for v^2/c^2:

$$1 - \frac{E_0^2}{E^2} = \frac{v^2}{c^2} \tag{8.16}$$

If a portion of volume would have a rest energy, then an observer could in principle measure his position relative to that portion (as positions can in principle be determined relative to an object with rest energy). However, no position relative to a portion of natural volume can be measured in SR. Thus, a portion of such volume has no rest energy E_0. As the rest energy E_0 is zero, each portion of natural three-dimensional additional volume has the velocity $v = c$ within natural three-dimensional volume, see Eq. (8.16).

(2) A portion of additional volume propagates parallel or antiparallel to the radial direction. As a portion of additional volume propagates at the velocity $v = c$, see part (1), the light-travel distance $L(\tau_0)$ increases by $c \cdot \sigma_{out} \cdot \tau$, during a time τ. Thus the propagation is described by Eq. (8.1).

(3a) We use the potential (Eq. 7.38), and we apply the derivative:

$$\frac{\partial}{\partial L}\Phi_L = -c^2 \frac{\partial}{\partial L}\varepsilon_L \tag{8.17}$$

we apply the chain rule:

$$\frac{\partial}{\partial L}\Phi_L = -c^2 \underbrace{\frac{\partial \tau}{\partial L}}_{\sigma_{out}/c} \frac{\partial}{\partial \tau}\varepsilon_L \tag{8.18}$$

Altogether, this proves all parts of the theorem. Thereby, the parts (3b) and (4b) are shown in a similarly to parts (3a) and (4a).

Corollary 8 Interpretation of phase velocity of volume

(1) In a monochromatic harmonic electromagnetic wave in volume (or vacuum), the energy density propagates at the phase velocity, see e. g. (Landau and Lifschitz, 1971, section 31). According to SR, energy does not propagate faster than c. Correspondingly, the phase velocity of classical light in volume (or vacuum) is limited by $c = \frac{1}{\sqrt{\varepsilon_0 \cdot \mu_0}}$*, with* $\mu_0 = 4\pi \cdot 10^{-7}\,\frac{\mathrm{N}}{\mathrm{A}^2}$*. In the quantum theory of the electromagnetic field, the quantum properties are added to the properties of classical electromagnetic waves, see e. g. (Ballentine, 1998, section 19), (Landau and Lifschitz, 1982, chapter I).*

(2) In contrast, a possible harmonic rate gravity wave of volume (C. 8) has zero energy density u and momentum density $u/c = p/V$ (C. 6, 11). Accordingly, the phase velocity v_p of volume is not limited by the velocity c of light in volume (or vacuum).

8.2 Plane waves

Idea: The gradient of the potential represents a driving force for the relative additional volume, see THM (12, part 3) and Fig. (8.3). Thus, the DEQ of unidirectional propagation of relative additional volume (Eq. 8.5) might have solutions representing plane waves. We investigate that possibility in this section.

Theorem 13 Plane waves of relative additional volume

If a mass or dynamic mass M is in an empty environment, and if M is neither accelerated nor rotating nor charged, then the following holds:

(1) The following plane waves are solutions of the DEQ $\frac{\partial}{\partial L}\Phi_L = -c \cdot \sigma_{out} \cdot \frac{\partial}{\partial \tau}\varepsilon_L$ (Eq. 8.4) of relative additional volume (Fig. 8.2):

$$\varepsilon_{L,\omega} = \hat{\varepsilon}_{L,\omega} \cdot \exp(i \cdot \omega \cdot \tau - i \cdot k \cdot L) \text{ and} \tag{8.19}$$

$$\Phi_{L,\omega} = \hat{\Phi}_{L,\omega} \cdot \exp(i \cdot \omega \cdot \tau - i \cdot k \cdot L), \text{ with} \tag{8.20}$$

$$\text{direction } \vec{e}_L \text{ of unidirectional propagation} \tag{8.21}$$

$$\sigma_{out} = 1 \tag{8.22}$$

(2) Inserting these waves into the DEQ yields the following relations:

The amplitudes are summarized as follows:

$$\hat{\Phi}_{L,\omega} = c^2 \cdot \hat{\varepsilon}_{L,\omega} \tag{8.23}$$

These plane waves are summarized as follows:

$$\Phi_{L,\omega} = c^2 \cdot \varepsilon_{L,\omega} \tag{8.24}$$

The DEQ of these plane waves propagating outwards are summarized as follows:

$$-c\frac{\partial}{\partial L}\varepsilon_{L,\omega} = \frac{\partial}{\partial \tau}\varepsilon_{L,\omega} \tag{8.25}$$

(3) All finite, discrete infinite or continuously infinite sufficiently converging linear combinations are also solutions of the DEQ in part (2). Thus, even non-periodic solutions are included. Accordingly, the only particular property of these solutions is the propagation in the positive direction of the unit vector $\vec{e}_L$*:.*

$$-c\frac{\partial}{\partial L}\varepsilon_L = \frac{\partial}{\partial \tau}\varepsilon_L, \text{ or} \tag{8.26}$$
$$-\frac{\partial}{\partial L}\Phi_L = c\cdot\frac{\partial}{\partial \tau}\varepsilon_L, \text{ with} \tag{8.27}$$
$$\text{direction vector } \vec{e}_L \text{ of propagation} \tag{8.28}$$

In vector notation and in operator notation of the derivatives, the DEQ is as follows:

$$-c|\cdot\vec{\partial}_L\varepsilon_L| = \partial_\tau\varepsilon_L, \text{ or} \tag{8.29}$$
$$-|\vec{\partial}_L\Phi_L| = c\cdot\partial_\tau\varepsilon_L \text{ with} \tag{8.30}$$
$$\varepsilon_L = \varepsilon_L(\tau,\vec{L}) \text{ and } \Phi_L = \Phi_L(\tau,\vec{L}) \tag{8.31}$$

Waves of additional volume, as well as waves of volume in general, have been called **rate gravity waves, RGW**, *see e. g. Carmesin (2021d,a, 2022d,a).*

Proof

(1) We insert the proposed solutions in Eq. (8.20) into the DEQ (Eq. 8.4) $\frac{\partial}{\partial L}\Phi_L = -c\cdot\sigma_{out}\cdot\frac{\partial}{\partial\tau}\varepsilon_L$ of relative additional volume:

$$\frac{\partial}{\partial \tau}\varepsilon_{L,\omega} = i\omega\cdot\hat{\varepsilon}_{L,\omega}\cdot\exp(i\cdot\omega\cdot\tau - i\cdot k\cdot L) \text{ and} \tag{8.32}$$
$$\frac{\partial}{\partial L}\Phi_{L,\omega} = -i\cdot k\cdot\hat{\Phi}_{L,\omega}\cdot\exp(i\cdot\omega\cdot\tau - i\cdot k\cdot L) \tag{8.33}$$

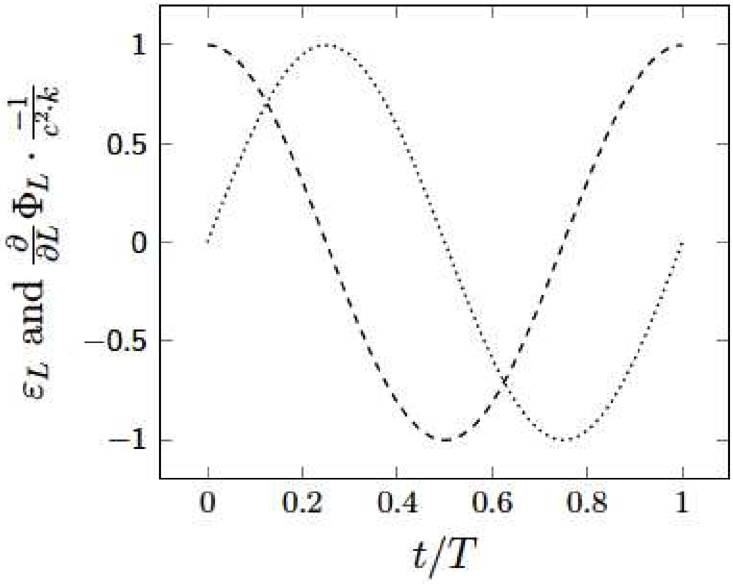

Figure 8.3: Plane wave of relative additional volume ε_L (dotted) and scaled gradient of gravitational potential $\frac{\partial}{\partial L}\Phi_L \cdot \frac{-1}{c^2 \cdot k}$ (dashed). The scaled gradient of the potential is the driving force for the relative additional volume.

So we derive:

$$-c \cdot i \cdot \omega \cdot \hat{\varepsilon}_{L,\omega} \cdot \exp(i \cdot \omega \cdot \tau - i \cdot k \cdot L) \quad (8.34)$$

$$= -i \cdot k \cdot \hat{\Phi}_{L,\omega} \cdot \exp(i \cdot \omega \cdot \tau - i \cdot k \cdot L) \quad (8.35)$$

The above Eq. implies:

$$c \cdot \omega \cdot \hat{\varepsilon}_{L,\omega} = k \cdot \hat{\Phi}_{L,\omega} \quad (8.36)$$

With it, the relation $c = \frac{\omega}{k}$ implies:

$$c^2 \cdot \hat{\varepsilon}_{L,\omega} = \hat{\Phi}_{L,\omega} \quad (8.37)$$

(2) We insert Eq. (8.37) into Eq. (8.20), and we compare with Eq. (8.19). So we derive the relation:

$$c^2 \cdot \varepsilon_{L,\omega} = \Phi_{L,\omega} \quad (8.38)$$

We insert Eq. (8.38) into the DEQ (Eq. 8.5). So we derive the DEQ in (8.25).

(3) Part (3) is a consequence of the Fourier transform, Teschl (2014) or Ballentine (1998) or Sakurai and Napolitano (1994).

Altogether, this proves all parts of the theorem.

Corollary 9 Wave packets

(1) A propagating portion can be described as a wave packet. For instance, at a propagation in a direction $\vec{k}$, a one-dimensional analysis is appropriate: A wave packet can be described as a linear combination of wave vectors, (Scheck, 2013, section 1.3.1):

$$\varepsilon_L(t,x) = \hat{\varepsilon}_L \int_{-\infty}^{\infty} \frac{dk}{\sqrt{2\pi}} \tilde{\varepsilon}_L(k) \exp(i\omega t - ikx) \tag{8.39}$$

A wave packet has a central wave number k_0. With it, a wave number k can be expressed as follows:

$$k \cdot x = k_0 \cdot x + (k - k_0) \cdot x \tag{8.40}$$

As the circular frequency ω is a function of the wave number k, it can be described relative to $\omega(k_0) = \omega_0$:

$$\omega(k) \doteq \omega_0 + \frac{\partial \omega}{\partial k}|_{k_0} \cdot (k - k_0) \tag{8.41}$$

With it, the wave in Eq. is as follows:

$$\varepsilon_L(t,x) = \hat{\varepsilon}_L \exp(i\omega_0 t - ik_0 x) \cdot \tag{8.42}$$

$$\cdot \int_{-\infty}^{\infty} \frac{dk}{\sqrt{2\pi}} \tilde{\varepsilon}_L(k) \exp\left(i \frac{\partial \omega}{\partial k}|_{k_0} \cdot (k - k_0)t - i(k - k_0)x \right) \tag{8.43}$$

In the large bracket, $i(k - k_0)$ is factorized:

$$\varepsilon_L(t,x) = \hat{\varepsilon}_L \exp(i\omega_0 t - ik_0 x) \cdot \tag{8.44}$$

$$\cdot \int_{-\infty}^{\infty} \frac{dk}{\sqrt{2\pi}} \tilde{\varepsilon}_L(k) \exp\left(i(k - k_0) \left[\frac{\partial \omega}{\partial k}|_{k_0} \cdot t - x \right] \right) \tag{8.45}$$

The integral represents the envelope of the packet. It takes its maximum, if the integrand does not oscillate, as oscillation diminishes the integral. Thus, the rectangular bracket is zero at *the maximum. Hence, the derivative represents the velocity v_g of the wave packet:*

$$\text{maximum at } \left[\frac{\partial \omega}{\partial k}|_{k_0} \cdot t - x\right] = 0 \quad (8.46)$$

$$\frac{\partial \omega}{\partial k}|_{k_0} \cdot t = x = v_g \cdot t \quad (8.47)$$

(2) A wave packet of volume propagates at $v = c$, according to SR.

(3) In a harmonic wave of volume, the phase cannot be used for a determination of an absolute position. Accordingly, SR does not pose a restriction to the phase velocity of a harmonic wave of volume.

8.3 Invariant and generalized dynamics

Idea: Equation (8.5) provides the rate of change of relative additional volume $\frac{\partial}{\partial \tau}\varepsilon_L$ as a function of the gravitational field $\vec{G}^*$. That field can be measured (chapter 2) in a manner independent of a mass. For it, an effective mass is used (chapter 2). Thus, Eq. (8.5) generalizes the dynamics of $\frac{\partial}{\partial \tau}\varepsilon_L$ so that no mass is necessary.

Moreover, we analyze a possible Lorentz invariance of the dynamics described by that equation (8.5). For it, we provide definitions and a summarizing corollary first.

Definition 9 Four-vector and four-scalar

(1) The **rate gravity vector, RGV**$_L$*, a four-vector, is the following combination of the rate $\frac{\partial}{\partial \tau}\varepsilon_L$ and of the gravitational field $\vec{G}^*$:*

$$RGV_L = \begin{pmatrix} c\frac{\partial}{\partial\tau}\varepsilon_L \\ G_x^* \\ G_y^* \\ G_z^* \end{pmatrix} \tag{8.48}$$

(2) In a relativistic scalar product of two four-vectors, we apply the following common sign convention, see e. g. Moore (2013); Straumann (2013):

$$(\eta_{ik}) = \begin{pmatrix} -1 & 0 & 0 & 0 \\ 0 & 1 & 0 & 0 \\ 0 & 0 & 1 & 0 \\ 0 & 0 & 0 & 1 \end{pmatrix} \tag{8.49}$$

With it, the relativistic scalar product of two four-vectors $\vec{a} = \begin{pmatrix} a_0 \\ a_1 \\ a_2 \\ a_3 \end{pmatrix}$ *and* $\vec{b} = \begin{pmatrix} b_0 \\ b_1 \\ b_2 \\ b_3 \end{pmatrix}$ *is as follows, see e. g. (Landau and Lifschitz, 1971, § 6) or Moore (2013); Straumann (2013):*

$$(\vec{a}|\vec{b}) = \sum_{i=0}^{3}\sum_{k=0}^{3} a_i \cdot \eta_{ik} \cdot b_k \tag{8.50}$$

(3) The **rate gravity scalar, $\mathbf{RGS}_L$** *is the relativistic scalar product of the rate gravity four-vector RGV_L with itself.*

(4) The **slope four-vector, $\mathbf{SFV}_L$** *expresses the field in the RGV_L by the potential, see e. g. (Carmesin, 2021d, section 5.2.1):*

$$SFV_L = \begin{pmatrix} c\frac{\partial}{\partial\tau}\varepsilon_L \\ -\frac{\partial}{\partial L_1}\Phi_L \\ -\frac{\partial}{\partial L_2}\Phi_L \\ -\frac{\partial}{\partial L_3}\Phi_L \end{pmatrix} \tag{8.51}$$

(5) The **slope four-scalar, $\mathbf{SFS}_L$** *is the relativistic scalar product of the slope four-vector SFV_L with itself.*

Corollary 10 Four-vectors

(1) A scalar product in four-dimensional spacetime is invariant with respect to any rotation of the four-dimensional coordinate system, including Lorentz transformations, see e. g. (Landau and Lifschitz, 1971, § 6) or Carmesin (1996).

(2) A four-scalar is called a Lorentz invariant or a Lorentz scalar.

Theorem 14 Invariant and generalized dynamics

In natural volume and at an effective mass or mass, the following holds:

(1a) The dynamic equation (8.5) of relative additional volume implies the rate gravity scalar:

$$0 = -c^2 \cdot \left(\frac{\partial}{\partial \tau} \varepsilon_L \right)^2 + (G_x^*)^2 + (G_y^*)^2 + (G_z^*)^2 = RGS_L \quad (8.52)$$

The above equation is an implied dynamic equation of relative additional volume.

(1b) In the implied dynamic equation (8.52) of relative additional volume, the information about the sign σ_{out} is lost.

(1c) The implied dynamic equation (8.52) of relative additional volume is invariant with respect to Lorentz transformations.

(1d) The rate gravity scalar RGS_L is a function of the field and of the relative additional volume ε_L. Thus, the implied dynamic equation of relative additional volume is generalized so that the implied dynamics does neither depend on the mass M nor on the radius R.

(2) If the gravitational field in the RGV_L is expressed by derivatives of the potential, then the slope four-vector SFV_L is obtained:

$$SFV_L = \begin{pmatrix} c\frac{\partial}{\partial\tau}\varepsilon_L \\ -\frac{\partial}{\partial L_1}\Phi_L \\ -\frac{\partial}{\partial L_2}\Phi_L \\ -\frac{\partial}{\partial L_3}\Phi_L \end{pmatrix} = \begin{pmatrix} c\frac{\partial}{\partial\tau}\varepsilon_L \\ G_x^* \\ G_y^* \\ G_z^* \end{pmatrix} = RGV_L \qquad (8.53)$$

(3a) The scalar product of the SFV_L with itself provides the implied dynamic equation (8.52) as a function of the potential or of the slope four-scalar, SFS_L:

$$0 \;=\; SFS_L = -c^2 \cdot \left(\frac{\partial}{\partial\tau}\varepsilon_L\right)^2 + \sum_{j=1}^{j=3}\left(\frac{\partial}{\partial L_j}\Phi_L\right)^2 \quad (8.54)$$

(3b) In the implied dynamic equation (8.54) of relative additional volume, the information about the sign σ_{out} is lost.

(3c) The implied dynamic equation (8.54) of relative additional volume is invariant with respect to Lorentz transformations.

(3d) The SFS_L is a function of the potential Φ_L and of relative additional volume ε_L. Thus, the implied dynamic equation (8.54) of relative additional volume is generalized so that the implied dynamics does neither depend on the mass M nor on the radius R.

Proof

(1a) The square of the dynamic equation (8.5) is as follows:

$$(\vec{G}^*)^2 \;=\; c^2 \cdot \left(\frac{\partial}{\partial\tau}\varepsilon_L\right)^2 \qquad (8.55)$$

Subtraction of $c^2 \cdot \left(\frac{\partial}{\partial\tau}\varepsilon_L\right)^2$ implies:

$$0 \;=\; -c^2 \cdot \left(\frac{\partial}{\partial\tau}\varepsilon_L\right)^2 + (\vec{G}^*)^2 \qquad (8.56)$$

The coordinate representation of $(\vec{G^*})^2$ implies the required equation (8.52).

(1b) The square in Eq. (8.55) implies the loss of information about the square.

(1c) The RGS_L in Eq. (8.52) is the scalar product of the RGV_L with itself, see DEF (9). Thus, it is invariant with respect to Lorentz transformations, see corollary (10).

(1d) The generalization is founded in part (1d) of the theorem.

(2) The equality of the four-vectors is founded in part (1d) of the theorem.

(3a-d) The equality of the four-vectors is founded in part (1d) of the theorem.

Altogether, all parts of the theorem are derived.

Corollary 11 Generalization with respect to mass

At a location without any mass or dynamic mass in its vicinity, a possible gravitational field can be measured with help of an effective mass (chapter 2). With that field, the dynamics of ε_L can be derived via Eq. (8.52) or (8.4) or (8.5 and 8.6). So the dynamics do neither depend on a mass M nor on the distance R to a mass.

Corollary 12 Invariant dynamics

(1) An observer can distinguish a portion propagating outwards ($\sigma_{out} = 1$) from a portion propagating inwards ($\sigma_{out} = -1$), see Fig. (8.1). As a consequence, the DEQ of the propagation of relative additional volume depends on that sign function σ_{out}, see Eq. (8.4): $\frac{\partial}{\partial L}\Phi_L = -c \cdot \sigma_{out} \cdot \frac{\partial}{\partial \tau}\varepsilon_L$.

(2) The corresponding Lorentz invariant dynamics is achieved by application of the square to that DEQ. So the sign function becomes irrelevant, and the information about the sign is lost.

Chapter 9

Local Formation of Volume

Idea: A portion δV or $\delta V_{d\Omega}$ of additional volume near a mass M propagates outwards, see chapter (8) and Fig. (9.1). If that portion increases during that propagation, then there occurs locally **formed volume, LFV**, within that portion. Moreover, the dynamics at a mass or dynamic mass can be generalized to the dynamics at an effective mass (section 8.3). In this chapter, we investigate such possible LFV.

The LFV is described by two essential and different quantities:

Firstly, the time derivative $\partial_\tau \varepsilon_L = \dot{\varepsilon}_L$ of the relative additional volume ε_L is essential for gravity, curvature of spacetime and quantum physics.

Secondly, a **normalized rate** $\underline{\dot{\varepsilon}_L}$ (DEF 10) is normalized similar to the normalization of the derivative $\dot{R}$ of scale factor R in the Hubble rate $H = \frac{\dot{R}}{R}$ (compare with Hobson et al. (2006), Carmesin (2019b), chapter 12). Accordingly, the normalized rate is essential in the description of the expansion of space since the Big Bang.

Of course, we compare the normalized LFV with the rate of the relative additional volume $\dot{\varepsilon}_L$.

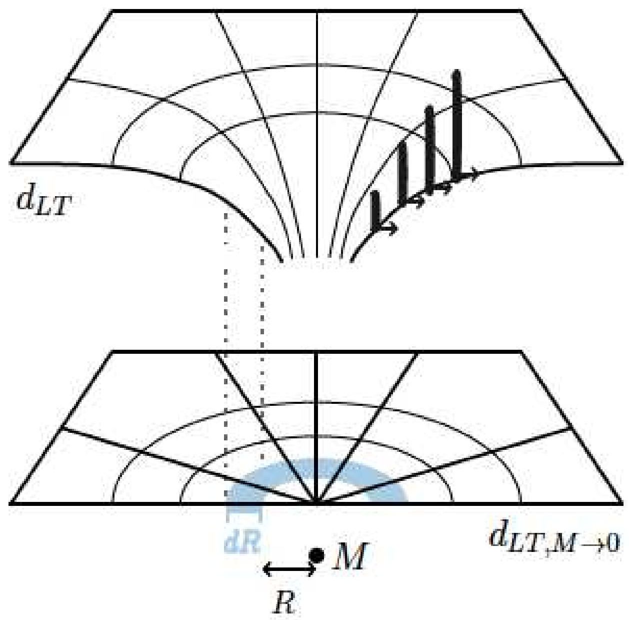

Figure 9.1: A portion of additional volume δV propagates outwards. Thereby, the portion increases. Thus, locally formed volume, LFV, occurs within that portion of additional volume.

9.1 Normalized LFV

Idea: If a portion δV or $\delta V_{d\Omega}$ of additional volume increases by an amount $\underline{\delta} V$ or $\underline{\delta} V_{d\Omega}$ during its propagation through a complete volume dV_L or $dV_{L,d\Omega}$, then this increase can be observed in that complete volume. Accordingly, the amount of LFV is normalized by the corresponding complete volume.

In this section, we investigate such normalized LFV. For it, we define useful concepts first:

Definition 10 Normalized locally formed volume

(1a) The process of propagation of a portion δV or $\delta V_{d\Omega}$ of additional volume (Fig. 9.1) exhibits the following physical quantities:

(1b) The propagation has a **time of propagation** $\underline{\delta}\tau$.

(1c) Propagation has a **distance of propagation** $\underline{\delta} L = c \cdot \underline{\delta}\tau$.

(1d) The propagation takes place in a **complete volume of propagation** dV_L *or* $dV_{L,d\Omega}$.

(1e) The propagation exhibits a **formed volume** $\underline{\delta}V$ *or* $\underline{\delta}V_{d\Omega}$.

(2) The increase $\underline{\delta}V_{d\Omega}$ *per time* $\underline{\delta}\tau$ *is the* **rate of LFV** *in a solid angle of a shell* $\frac{\underline{\delta}V_{d\Omega}}{\underline{\delta}\tau}$.

$$rate_{LFV} = \frac{\underline{\delta}V_{d\Omega}}{\underline{\delta}\tau} \text{ at } dV_{L,d\Omega} \tag{9.1}$$

The whole shell is included as a special case with $d\Omega = 4\pi$.

(3) The rate of LFV normalized by the corresponding complete volume is the **normalized rate of LFV***:*

$$\underline{\dot{\varepsilon}}_L = \frac{\underline{\delta}V_{d\Omega}/\underline{\delta}\tau}{dV_{L,d\Omega}} \text{ at } dV_{L,d\Omega} \tag{9.2}$$

(4a) In the vicinity of a mass or dynamic mass or dynamic mass M*, the Schwarzschild radius* $R_S = \frac{2GM}{c^2}$ *is an appropriate unit of length.*

(4b) Correspondingly, for relatively large distances $\frac{R_S}{R} << 1$*, a* **far distance approximation, FDA***, is applicable. Hereby, a* $k-th$ *order is proportional to the* $k-th$ *power* $\left(\frac{R_S}{R}\right)^k$ *of* $\frac{R_S}{R}$.

(5) The rate multiplied by $\frac{1}{c \cdot dR}$ *forms a* **characteristic function of LFV** f_L *as a function of* $\frac{R}{R_S}$*:*

$$f_L\left(\frac{R}{R_S}\right) = \frac{\partial}{\partial\tau}\delta V \cdot \frac{1}{c \cdot dR} \tag{9.3}$$

That function provides the sign (and a scaled amount) of the rate of change of additional volume.

Theorem 15 Law of unidirectional formation of volume

If a mass or dynamic mass M *is in an empty environment, and if* M *is neither accelerated nor rotating nor charged, then the following holds:*

(1) At a distance $R = d_{GP}$ from M, the rate of LFV is as follows:

$$rate_{LFV} = \frac{\delta V_{d\Omega}}{\underline{\delta}\tau} = c \cdot dR \cdot f_L\left(\frac{R}{R_S}\right) \quad \text{with} \tag{9.4}$$

$$f_L\left(\frac{R}{R_S}\right) = \frac{2 \cdot dV_L}{R \cdot dR} \cdot \left(\varepsilon_E - \varepsilon_E^2 - \frac{1}{4\varepsilon_E \cdot \frac{R}{R_S}}\right) \quad \text{or} \tag{9.5}$$

$$f_L\left(\frac{R}{R_S}\right) = 8\pi \cdot R \cdot \left(1 - \varepsilon_E - \frac{1}{4\varepsilon_E^2 \cdot \frac{R}{R_S}}\right) \tag{9.6}$$

(2) Hereby, volume forms in radial direction in a unidirectional manner.

(2a) The function $f_L\left(\frac{R}{R_S}\right)$ is illustrated in Fig. (9.2).

(2b) The function $f_L\left(\frac{R}{R_S}\right)$ has a zero at $\frac{R}{R_S} = 1.659\,194$.

(2c) In the very near vicinity of the Schwarzschild radius, at $\frac{R}{R_S} < 1.659\,194$, volume is annihilated locally.

(2d) Outside that very near vicinity of the Schwarzschild radius at $\frac{R}{R_S} > 1.659\,194$, volume is formed locally.

(3a) At a distance $R = d_{GP}$ from M and at leading order in the FDA, the normalized rate of LFV is as follows:

$$\dot{\underline{\varepsilon}}_L(R) = |\vec{G}^*|(R) \cdot \frac{1}{c} \tag{9.7}$$

(3b) The rate of LFV corresponding to part (3a) is as follows:

$$rate_{LFV} = \frac{dV_L}{c}\frac{G \cdot M}{R^2} = \frac{4\pi \cdot dL \cdot G \cdot M}{c} \tag{9.8}$$

At leading order in the FDA, the rate of LFV is constant.

Proof: (1) We analyze the rate in Eq. (9.1):

$$rate_{LFV} = \frac{\delta V_{d\Omega}}{\underline{\delta}\tau} \quad \text{at} \quad dV_{L,d\Omega} \tag{9.9}$$

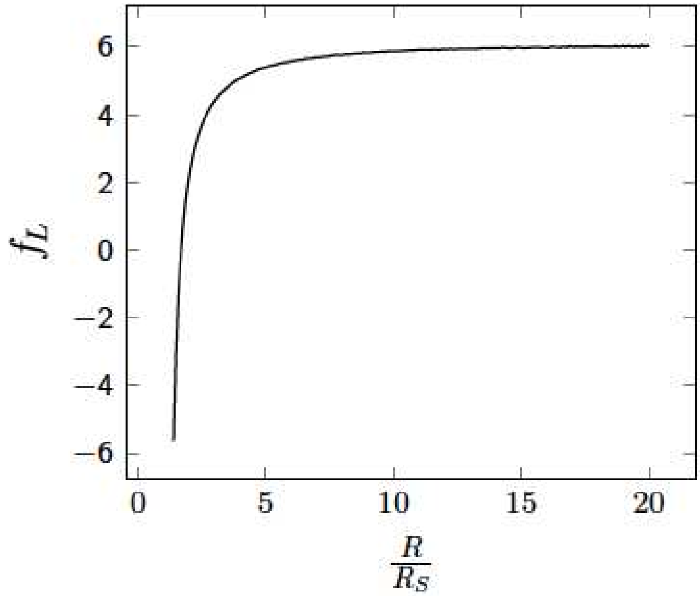

Figure 9.2: Characteristic function of LFV: At $\frac{R}{R_S} > 1.6952$, volume is formed locally. At $\frac{R}{R_S} < 1.6951$, in that vicinity of the Schwarzschild radius, volume is locally annihilated.

The increase of δV is described by the difference:

$$rate_{LFV} = \frac{\delta V_{d\Omega}(\tau_0 + \underline{\delta}\tau) - \delta V_{d\Omega}(\tau_0)}{\underline{\delta}\tau} \tag{9.10}$$

As the time of propagation $\underline{\delta}\tau$ is incremental, we can express the difference at linear order in $\underline{\delta}\tau$:

$$rate_{LFV} = \frac{\delta V_{d\Omega}(\tau_0) + \frac{\partial}{\partial \tau}\delta V_{d\Omega} \cdot \underline{\delta}\tau - \delta V_{d\Omega}(\tau_0)}{\underline{\delta}\tau} = \frac{\partial V_{d\Omega}}{\partial \tau} \tag{9.11}$$

We analyze the time derivative with help of the chain rule:

$$rate_{LFV} = \frac{\partial}{\partial \tau}\delta V_{d\Omega} = \underbrace{\frac{\partial L}{\partial \tau}}_{c} \cdot \frac{\partial}{\partial L}\delta V_{d\Omega} \tag{9.12}$$

We apply the chain rule again:

$$rate_{LFV} = c \cdot \underbrace{\frac{\partial R}{\partial L}}_{\varepsilon_E} \cdot \frac{\partial}{\partial R}\delta V_{d\Omega} \tag{9.13}$$

We use THM (10):

$$rate_{LFV} = c \cdot \varepsilon_E \frac{\partial}{\partial R}\left(4\pi R^2 dR\left(\frac{1}{\varepsilon_E} - 1\right)\right) \text{ or} \quad (9.14)$$

$$rate_{LFV} = c \cdot \varepsilon_E \cdot 4\pi \cdot dR \frac{\partial}{\partial R}\left(R^2\left(\frac{1}{\varepsilon_E} - 1\right)\right) \quad (9.15)$$

We evaluate the derivative:

$$rate_{LFV} = c \cdot \varepsilon_E \cdot 4\pi \cdot dR \cdot \quad (9.16)$$

$$\left(2R\left(\frac{1}{\varepsilon_E} - 1\right) + R^2 \frac{1}{-2\varepsilon_E^3} \frac{R_S}{R^2}\right) \text{ or} \quad (9.17)$$

$$rate_{LFV} = c \cdot dR \cdot f_L\left(\frac{R}{R_S}\right) \text{ with} \quad (9.18)$$

$$f_L\left(\frac{R}{R_S}\right) = 8\pi \cdot R \cdot \left(1 - \varepsilon_E - \frac{1}{4\varepsilon_E^2 \cdot \frac{R}{R_S}}\right) \quad (9.19)$$

With it, $dV_L = 4\pi R^2 dL = 4\pi R^2 dR/\varepsilon_E$ implies the following form of the characteristic function of LFV:

$$f_L\left(\frac{R}{R_S}\right) = \frac{2 \cdot dV_L}{R \cdot dR} \cdot \left(\varepsilon_E - \varepsilon_E^2 - \frac{1}{4\varepsilon_E \cdot \frac{R}{R_S}}\right) \quad (9.20)$$

(2a) The characteristic function of LFV is plotted in Fig. (9.2).

(2b) The zero $\frac{R}{R_S} = 1.659\,194$ of the characteristic function of LFV has been evaluated numerically.

(2c) The characteristic function of LFV provides the sign of the normalized rate of formation of LFV. At $\frac{R}{R_S} < 1.659\,194$, that sign is negative, so that volume is annihilated.

(2d) At $\frac{R}{R_S} > 1.659\,194$, that sign is positive, so LFV is formed.

(3a) We apply the characteristic function of LFV (Eq. 9.5) to the rate (Eq. 9.4):

$$rate_{LFV} = c \cdot \frac{2 \cdot dV_L}{R} \cdot \left(\varepsilon_E - \varepsilon_E^2 - \frac{1}{4\varepsilon_E \cdot \frac{R}{R_S}}\right) \quad (9.21)$$

In order to derive the normalized rate (DEF 10), we divide by the complete volume dV_L. Additionally, we factorize the position factor ε_E:

$$\dot{\underline{\varepsilon}}_L = c \cdot \frac{2}{R} \cdot \varepsilon_E \cdot \left(1 - \varepsilon_E - \frac{1}{4\varepsilon_E^2 \cdot \frac{R}{R_S}}\right) \tag{9.22}$$

At leading order in the FDA, the above square ε_E^2 is one, as that square is multiplied by $\frac{R}{R_S}$. Moreover, at leading order in the FDA, the position factor is as follows $\varepsilon_E = \sqrt{1 - \frac{R_S}{R}} \doteq 1 - \frac{R_S}{2R}$. So the normalized rate is as follows:

$$\dot{\underline{\varepsilon}}_L = c \cdot \frac{2}{R} \cdot \varepsilon_E \cdot \left(1 - 1 + \frac{R_S}{2R} - \frac{1}{4}\frac{R_S}{R}\right) \text{ or} \tag{9.23}$$

$$\dot{\underline{\varepsilon}}_L = c \cdot \frac{2}{R} \cdot \varepsilon_E \cdot \frac{1}{4} \cdot \frac{R_S}{R} \tag{9.24}$$

At leading order in the FDA, the above position factor ε_E is one, as that factor is multiplied by $\frac{R}{R_S}$:

$$\dot{\underline{\varepsilon}}_L = c \cdot \frac{1}{2} \cdot \frac{R_S}{R^2} \tag{9.25}$$

The definition of the Schwarzschild radius $R_S = \frac{2GM}{c^2}$ implies the following:

$$\dot{\underline{\varepsilon}}_L = \frac{1}{c} \cdot \frac{G \cdot M}{R^2} \tag{9.26}$$

We identify the field, in order to derive Eq. (9.7):

$$\dot{\underline{\varepsilon}}_L = \frac{1}{c} \cdot |\vec{G}^*| \tag{9.27}$$

We multiply Eq. (9.26) by the complete volume dV_L, in order to derive Eq. (9.8).

Altogether, this proves all parts of the theorem.

Corollary 13 Local formation of volume by a field

(1) At the leading order in the FDA, the normalized rate of LFV in Eq. (9.7) is caused by a mass M:

$$\dot{\varepsilon}_L(R) = |\vec{G}^*|(R) \cdot \frac{1}{c} \tag{9.28}$$

Moreover, at a radius R, that LFV is caused by the gravitational field $\vec{G}^*$ at that radius. Thus, the formation of volume is completely local.

(2) Furthermore, the gravitational field $\vec{G}^*$ is formed by the gradient of the additional volume that did already form, see THM (11). Thus, the gravitational field $\vec{G}^*$ and the additional volume cause each other. This constitutes a situation of positive feedback.

(3) Indeed, the positive feedback in part (2) causes a diverging amount of additional volume, as the same amount of volume of LFV forms in each shell, see Eq. (15). That infinite amount of volume is the same volume that causes the expansion of space since the Big Bang, see THM (6). Thus, the locally formed volume LFV explains the **globally formed volume, GFV**.

(4) In fact, the diverging amount of LFV does not cause any problem, as it explains the GFV that causes the expansion of space. In particular, the diverging amount of LFV does not require any renormalization. In contrast, some theories of quantum gravity require a renormalization, or they are even not renormalizable, see e. g. Prinz (2022).

9.2 Formation of ε_L near a mass M

Idea: In the vicinity of a mass, portions of additional volume δV exhibit a radial pattern of propagation, see Fig. (9.1). Thereby, there could occur a nonzero rate of formation of the corresponding portions of relative additional volume ε_L. That possibility is analyzed in this section.

Theorem 16 LFV of ε_L

If a mass or dynamic mass M is in an empty environment, and if M is neither accelerated nor rotating nor charged, then the following holds:

(1) If a portion of relative additional volume propagates during a time $\underline{\delta}\tau$ a distance $\underline{\delta}L = c \cdot \underline{\delta}\tau$, then the **rate of relative additional volume**

$$rate_{\varepsilon_L} = \frac{\underline{\delta}\varepsilon_L}{\underline{\delta}\tau} : = \frac{\varepsilon_L(\tau_0 + \underline{\delta}\tau) - \varepsilon_L(\tau_0)}{\underline{\delta}\tau} \tag{9.29}$$

is as follows:

$$\frac{\underline{\delta}\varepsilon_L}{\underline{\delta}\tau} = \frac{\partial}{\partial\tau}\varepsilon_L(R) = \dot{\varepsilon}_L(R) \tag{9.30}$$

(2) At a distance $R = d_{GP}$ from M, the rate of change of a portion of relative additional volume is as follows:

$$\boxed{\frac{\underline{\delta}\varepsilon_L}{\underline{\delta}\tau} = \frac{\partial}{\partial\tau}\varepsilon_L(R) = -\frac{1}{c}\frac{G \cdot M}{R^2} = -\frac{1}{c}|\vec{G}^*|(R)} \tag{9.31}$$

Proof

(1) We analyze the rate in Eq. (9.29):

$$\frac{\underline{\delta}\varepsilon_L}{\underline{\delta}\tau} = \frac{\varepsilon_L(\tau_0 + \underline{\delta}\tau) - \varepsilon_L(\tau_0)}{\underline{\delta}\tau} \tag{9.32}$$

As the time of propagation $\underline{\delta}\tau$ is incremental, we can express the difference at linear order in $\underline{\delta}\tau$:

$$\frac{\underline{\delta}\varepsilon_L}{\underline{\delta}\tau} = \frac{\varepsilon_L(\tau_0) + \frac{\partial}{\partial\tau}\varepsilon_L \cdot \underline{\delta}\tau - \varepsilon_L(\tau_0)}{\underline{\delta}\tau} \tag{9.33}$$

Evaluation of the above term yields the following:

$$\frac{\underline{\delta}\varepsilon_L}{\underline{\delta}\tau} = \frac{\partial}{\partial\tau}\varepsilon_L \text{ in the limit } \underline{\delta}\tau \to 0 \tag{9.34}$$

(2) We analyze the time derivative with help of the chain rule:

$$\frac{\partial}{\partial \tau}\varepsilon_L(R) = \underbrace{\frac{\partial L}{\partial \tau}}_{c} \cdot \frac{\partial}{\partial L}\varepsilon_L(R) \tag{9.35}$$

We apply the chain rule again:

$$\frac{\partial}{\partial \tau}\varepsilon_L(R) = c \cdot \underbrace{\frac{\partial R}{\partial L}}_{\varepsilon_E} \cdot \frac{\partial}{\partial R}\underbrace{\varepsilon_L}_{1-\varepsilon_E} \tag{9.36}$$

We evaluate the derivative:

$$\frac{\partial}{\partial \tau}\varepsilon_L = c \cdot \varepsilon_E \cdot \frac{\partial}{\partial R}\left(1 - \sqrt{1 - \frac{R_S}{R}}\right) \quad \text{or} \tag{9.37}$$

$$\frac{\partial}{\partial \tau}\varepsilon_L = c \cdot \varepsilon_E \cdot \frac{1}{2\sqrt{1 - \frac{R_S}{R}}} \cdot \frac{-R_S}{R^2} \quad \text{or} \tag{9.38}$$

$$\frac{\partial}{\partial \tau}\varepsilon_L = c \cdot \frac{-2GM}{2R^2c^2} = \frac{-1}{c} \cdot \frac{GM}{R^2} = -\frac{|\vec{G}^*|(R)}{c} \tag{9.39}$$

Using part (1), we derive the rate:

$$\frac{\underline{\delta}\varepsilon_L}{\underline{\delta}\tau}(R) = -\frac{|\vec{G}^*|(R)}{c} \tag{9.40}$$

Altogether, this proves all parts of the theorem.

Corollary 14 Rate of relative additional volume

(1) In the FDA, $rate_{\varepsilon_L} = -\frac{|\vec{G}^*|}{c}$ is equal to minus one multiplied by the normalized rate of LFV, $\dot{\underline{\varepsilon}}_L = \frac{|\vec{G}^*|}{c}$. Thus, the squares of these rates are equal:

$$\boxed{\left(\dot{\underline{\varepsilon}}_L(R)\right)^2 = \left(\dot{\varepsilon}_L(R)\right)^2} \tag{9.41}$$

(2) In the FDA, the $rate_{\varepsilon_L}$ of relative additional volume is the difference of the normalized rate of LFV, $\dot{\underline{\varepsilon}}_L$, and an effective

rate of the complete volume $rate_{dV_{L,d\Omega}}$:

$$\frac{\delta\underline{\varepsilon}_L}{\delta\underline{\tau}} = \frac{\partial}{\partial\tau}\frac{\delta V_{d\Omega}}{dV_{L,d\Omega}} \tag{9.42}$$

Evaluation of the derivative yields:

$$\frac{\delta\underline{\varepsilon}_L}{\delta\underline{\tau}} = \dot{\underline{\varepsilon}}_L - \underbrace{\varepsilon_L \cdot \frac{\frac{\partial}{\partial\tau} dV_{L,d\Omega}}{dV_{L,d\Omega}}}_{=:rate_{dV_{L,d\Omega}}} \tag{9.43}$$

We apply Eqs. (9.40 and 9.7):

$$\underbrace{\frac{\delta\underline{\varepsilon}_L}{\delta\underline{\tau}}}_{-|\vec{G}^*|/c} = \underbrace{\dot{\underline{\varepsilon}}_L}_{|\vec{G}^*|/c} - \underbrace{rate_{dV_{L,d\Omega}}}_{\text{see below}} \tag{9.44}$$

As a consequence, the $rate_{dV_{L,d\Omega}}$ *is equal to* $2|\vec{G}^*|/c$.

(3) In the present radial propagation of additional volume, $\frac{\delta\underline{\varepsilon}_L}{\delta\underline{\tau}}$ *is negative, as the change of the volume* $dV_{L,d\Omega}$ *in the denominator is larger than the increase of* $\delta V_{d\Omega}$ *in the numerator. In contrast, in* $\dot{\underline{\varepsilon}}_L$*, the denominator is normalized and constant.*

9.3 Invariant and generalized LFV

Idea: The equation (9.40) of LFV of relative additional volume, $\frac{\delta\underline{\varepsilon}_L}{\delta\underline{\tau}} = -\frac{|\vec{G}^*|}{c}$ as well as the rate of LFV in Eq. (9.7), $\dot{\underline{\varepsilon}}_L = |\vec{G}^*| \cdot \frac{1}{c}$ can be transformed to a Lorentz scalar. Moreover, both rates are generalized, as they do no longer depend on M. In contrast, the rates depend on the field $\vec{G}^*$ only.

Theorem 17 Invariant and generalized LFV

In natural volume, the following holds:

(1a) The dynamic equation (9.40) of the LFV of relative additional volume implies the following rate gravity scalar of LFV of ε_L:

$$0 = -c^2 \cdot \left(\frac{\delta \varepsilon_L}{\underline{\delta \tau}} \right)^2 + (G_x^*)^2 + (G_y^*)^2 + (G_z^*)^2 = RGS_{\varepsilon_L} \quad (9.45)$$

The above equation is an implied dynamic equation of the LFV of relative additional volume.

(1b) In the implied dynamic equation (9.45), the information about the sign is lost.

(1c) The implied dynamic equation (9.45) is invariant with respect to Lorentz transformations.

(1d) The rate gravity scalar RGS_{ε_L} *is a function of the field and of the relative additional volume* ε_L*. Thus, the implied dynamic equation is generalized so that the implied dynamics does neither depend on the mass* M *nor on the radius* R*.*

(2a) The dynamic equation (9.7) of the LFV implies the following rate gravity scalar of LFV:

$$0 \doteq -c^2 \cdot (\underline{\dot{\varepsilon}_L})^2 + (G_x^*)^2 + (G_y^*)^2 + (G_z^*)^2 = RGS_{\underline{\dot{\varepsilon}_L}} \quad (9.46)$$

The above equation is an implied dynamic equation of the LFV.

(2b) In the implied dynamic equation (9.46), the information about the sign is lost.

(2c) The implied dynamic equation (9.46) is invariant with respect to Lorentz transformations.

(2d) The rate gravity scalar RGS_{LFV} *is a function of the field and of the additional volume* $\delta V_{d\Omega}$*. Thus, the implied dynamic equation is generalized so that the implied dynamics does neither depend on the mass* M *nor on the radius* R*.*

Proof: The proof is analogous to that of THM (14).

Chapter 10

Geometry of the Change of Volume

Idea of change of a cube: The locally formed volume, LFV, in THM (15) is formed in a unidirectional manner. The expansion of space takes place in an isotropic manner, THM (7).

In this section, we describe isotropic, unidirectional as well as anisotropic changes of volume in a systematic manner. Geometrically, we analyze changes of a cube in Fig. (12.1). Hereby, we mark the edges of the cube by dr_j, while we mark the changed edges by dr'_j, and we denote the differences by $\delta r_j = dr'_j - dr_j$. Algebraically, we describe changes of volume with tensors.

Idea of tensors: If a mass or an effective mass can be measured at a region, then the two maps in Fig. (7.1) can be drawn. Thus, gravity causes **incremental changes** of a volume dV.

Similarly, deformations in a solid body represent an incremental change. These changes are described by the *strain tensor*, see e. g. (Sommerfeld, 1978, Eq. 12) or (Landau and Lifschitz, 1975, Eq. 1.5). Thereby, the strain tensor is symmetric. Accordingly, we use the strain tensor as well as the corresponding antisymmetric tensor, in order to describe additional volume, the formation of volume and changes of volume.

Organization: Firstly, we analyze additional volume, see sections (10.1, 10.2). Secondly, we investigate LFV as shown in

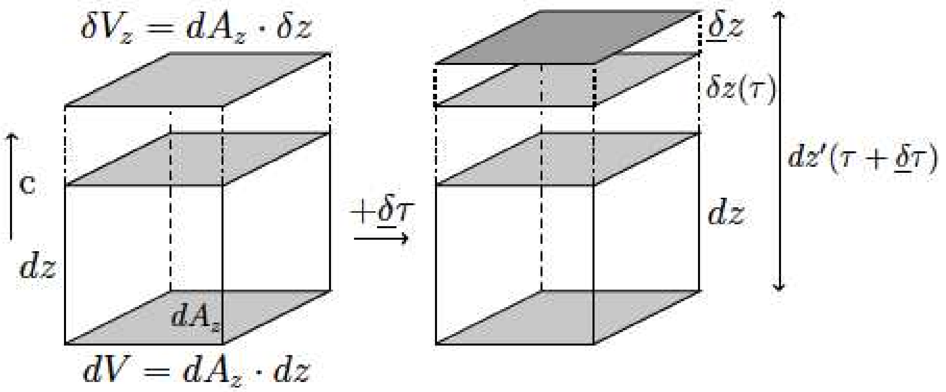

Figure 10.1: Unidirectional formation of volume: Additional volume propagates in z-direction at $v = c$. There is additional volume δV_z. Thereby, during a time $\underline{\delta}t$, a portion of volume $\underline{\delta}V_z = \underline{\delta}z \cdot dA_z$ forms.

Fig. (10.1). Thereby, the additional or formed volume is separated into three Cartesian components, see Figs. (12.1, 10.1). Hereby, we describe higher order terms of increments dr_j as well as δr_j by the factor $(1 + \mathcal{O}(dr_j))$.

10.1 Volume tensor

For instance, additional volume in the z-direction is described in terms of increments (see e. g. the calculus of Leibniz (1684) or differential forms Flanders (1989)) as follows: Basically, we consider the cubic volume dV with a height dz and a surface dA_z orthogonal to dz in Fig. (12.1):

$$dV = dA_z \cdot dz \tag{10.1}$$

The upper surface dA_z is shifted by an increment δz. Hereby, the increment δz is a function of z. In linear order in dz, the increment δz is as follows:

$$\delta z = \frac{\partial dz'}{\partial z} \cdot dz \cdot (1 + \mathcal{O}(dz)) \tag{10.2}$$

Hereby, the partial derivative is an element of a tensor, called **volume - tensor**. It is similar to the strain tensor, see (Sommerfeld, 1978, Eq. 11) or (Landau and Lifschitz, 1975, Eq. 1.8). The diagonal element in direction z is named ε_{zz}:

$$\varepsilon_{zz} = \frac{\partial dz'}{\partial z} = \frac{\partial \delta z}{\partial z} = \frac{\delta z}{dz'} \cdot (1 + \mathcal{O}(dz)) \tag{10.3}$$

Hereby, dz' and $\delta z = dz' - dz$ are regarded as differentiable functions of z. Thus, the corresponding **additional volume** is as follows:

$$\delta V_z = dA_z \cdot \delta z = dA_z \cdot dz \cdot \varepsilon_{zz} \cdot (1 + \mathcal{O}(dz)) \tag{10.4}$$

$$= dV \cdot \varepsilon_{zz} \cdot (1 + \mathcal{O}(dz)) \tag{10.5}$$

By definition, the **unidirectional normalized additional volume** in direction z is the additional volume δV_z divided by the complete volume $dV_L = dA_z \cdot dz'$:

$$\frac{\delta V_z}{dV_L} = \frac{dA_z \cdot \delta z}{dA_z \cdot dz'} = \frac{\delta z}{dz'} = \varepsilon_{zz} \cdot (1 + \mathcal{O}(dz)) \text{ with} \tag{10.6}$$

$$dz' = dz + \delta z \tag{10.7}$$

In the present case of the expansion of space since the Big Bang, the unidirectional normalized additional volume of the other two Cartesian directions occurs in addition:

$$\frac{\delta V_x}{dV_L} = \frac{dA_x \cdot \delta x}{dA_x \cdot dx'} = \frac{\delta x}{dx'} = \varepsilon_{xx} \cdot (1 + \mathcal{O}(dx)) \text{ with} \tag{10.8}$$

$$dx' = dx + \delta x \text{ and } \varepsilon_{xx} = \frac{\partial dx'}{\partial x} = \frac{\partial \delta x}{\partial x} \tag{10.9}$$

$$\frac{\delta V_y}{dV_L} = \frac{dA_y \cdot \delta y}{dA_y \cdot dy'} = \frac{\delta y}{dy'} = \varepsilon_{yy} \cdot (1 + \mathcal{O}(dy)) \text{ with} \tag{10.10}$$

$$dy' = dy + \delta y \text{ and } \varepsilon_{yy} = \frac{\partial dy'}{\partial y} = \frac{\partial \delta y}{\partial y} \tag{10.11}$$

We call the sum of the above three components **poly - directional relative additional volume** $\frac{\delta V}{dV_L}$:

$$\dot{\varepsilon}_{L,poly} = \frac{\delta V}{dV_L} = \Sigma_{j=1}^{3} \frac{\delta V_j}{dV_L} = \Sigma_{j=1}^{3}\, \varepsilon_{jj} \cdot (1 + \mathcal{O}(dr_j)) \tag{10.12}$$

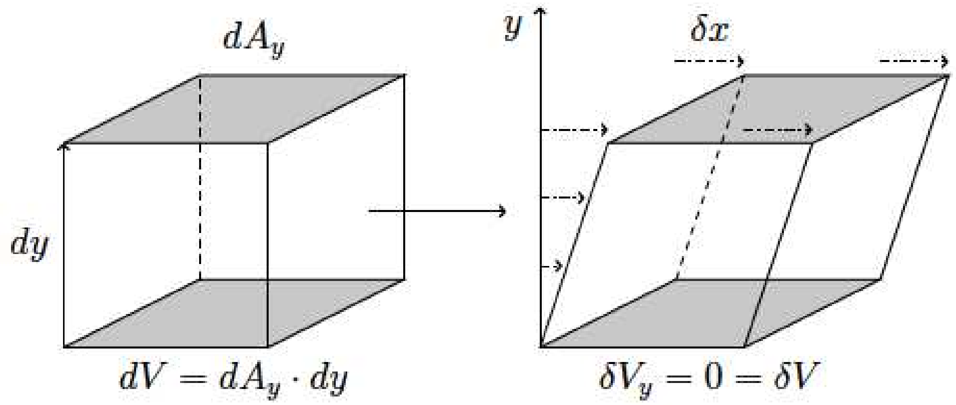

Figure 10.2: Change of a cube. At the height dy, the cross section dA_y is shifted by $\delta x(dy)$, with $\delta x(dy) = \varepsilon_{xy} \cdot dy$. As the height dy can be at any coordinate y, the above relation is generalized as follows: $\delta x(y) = \varepsilon_{xy} \cdot y$.

Thereby, the three summands could be equal. In that case, we call it **isotropic relative additional volume** $\frac{\delta V}{dV_L}$:

$$\dot{\varepsilon}_{L,iso} = \frac{\delta V}{dV_L} = \Sigma_{j=1}^{3} \frac{\delta V_j}{dV_L} = \Sigma_{j=1}^{3} \varepsilon_{jj} \cdot (1 + \mathcal{O}(dr_j)) \text{ if} \tag{10.13}$$

$$\frac{\delta V_1}{dV_L} = \frac{\delta V_2}{dV_L} = \frac{\delta V_3}{dV_L} \tag{10.14}$$

10.2 Non-diagonal elements

Idea: In order to understand the exceptional role of diagonal elements for the formation of additional volume, we analyze non-diagonal elements.

For it, we consider non-diagonal elements ε_{ij} of the volume - tensor, with $i \neq j$. For instance, at each height dy, the cross section dA_y is shifted by an increment δx, see Fig. (10.2). Thereby, the increment is the product of dy and a factor ε_{xy}:

$$\delta x = \varepsilon_{xy} \cdot dy \cdot (1 + \mathcal{O}(dy)) \text{ with} \tag{10.15}$$

$$\varepsilon_{xy} = \frac{\partial \delta x}{\partial y} = \frac{\delta x}{dy} \cdot (1 + \mathcal{O}(dy)) \tag{10.16}$$

As the increment dy can be chosen equal to the coordinate y in Fig. (10.2), there occurs a corresponding shift at each y:

$$\delta x(y) \quad = \quad \varepsilon_{xy} \cdot y \cdot (1 + \mathcal{O}(dy)) \tag{10.17}$$

Thus, the element ε_{xy} represents a shear of the volume dV. A shear of a cube does not change the volume, see Fig. (10.2). Similarly, the volume of a solid body is changed by diagonal elements of the strain tensor only, see (Sommerfeld, 1978, Eqs. 11, 18, 20) or (Landau and Lifschitz, 1975, Eq. 1.6).

Linear change of a cube: The changes of an incremental cube at linear order in dr_j are described by the diagonal and non-diagonal elements of the volume - tensor. These are described in a uniform manner as follows:

$$\varepsilon_{ij} = \frac{\partial \delta r_i}{\partial r_j} = \frac{\delta r_i}{dr'_j} \cdot (1 + \mathcal{O}(dr_j)) \tag{10.18}$$

With it, the incremental change of volume is described as follows:

$$\delta r_i = \sum_j \varepsilon_{ij} \cdot dr'_j \cdot (1 + \mathcal{O}(dr_j)) \tag{10.19}$$

For instance, non-diagonal elements of the volume - tensor occur in a gravitational wave, see e. g. Einstein (1916), Landau and Lifschitz (1971), Abbott (2016) or Carmesin (2021d). We summarize our findings:

Definition 11 volume - tensor

If an observable cube experiences an observable change, then the amount of volume in that cube changes correspondingly. That change is described by a volume - tensor as follows, see Fig. (12.1). Firstly, Cartesian coordinates r_j parallel to the edges of the cube with length dr_j are used, without loss of generality.

(1) If an edge dr_j of the cube changes to a length dr'_j, then change of length is as follows:

$$\delta r_j = dr'_j - dr_j = \frac{\partial \delta r_j}{\partial r_j} \cdot dr_j \cdot (1 + \mathcal{O}(dr_j)) \quad (10.20)$$

Thereby, δr_j is regarded as a differentiable function of r_j, and the corresponding element of the volume - tensor is as follows:

$$\varepsilon_{jj} = \frac{\partial dr'_j}{\partial r_j} = \frac{\partial \delta r_j}{\partial r_j} = \frac{\delta r_j}{dr_j} \cdot (1 + \mathcal{O}(dr_j)) \quad (10.21)$$

(2) If dA_j is the surface of the cube orthogonal to the edge dr_j, then the change δr_j provides the following **unidirectional additional volume***:*

$$\delta V_j = \delta r_j \cdot dA_j \quad (10.22)$$

That change of volume divided by the complete volume $dV_L = dr'_j \cdot dA_j$ is called **unidirectional normalized additional volume** *in direction r_j:*

$$\frac{\delta V_j}{dV_L} = \frac{\delta r_j \cdot dA_j}{dr'_j \cdot dA_j} = \frac{\delta r_j}{dr'_j} \quad (10.23)$$

(3) If the cube changes in an isotropic manner, then three Cartesian changes of length δr_j are equal, and the **isotropic additional volume** *δV is the sum of the three unidirectional additional volumes in part (2):*

$$\delta V = \sum_{j=1}^{3} \delta V_j \quad (10.24)$$

The ratio of δV and the complete volume $dV_L = \sum_j dr'_j \cdot dA_j$ is the **isotropic normalized additional volume***:*

$$\varepsilon_V := \frac{\delta V}{dV_L} = \frac{\delta V}{\sum_j dr'_j \cdot dA_j} \text{ if } dr'_i/dr_i = dr'_j/dr_j \quad (10.25)$$

(4) The elements of the **volume - tensor** *are derivatives:*

$$\varepsilon_{ij} = \frac{\partial \delta r_i}{\partial r_j} \tag{10.26}$$

An **incremental change** δr_i *is described as follows:*

$$\delta r_i = \sum_j \varepsilon_{ij} \cdot dr_j \tag{10.27}$$

Proposition 2 volume - tensor

(1) If a mass or effective mass can be observed, then the elements of the volume - tensor can be measured by evaluating corresponding differences between observed gravitational parallax distance d_{GP} *and light-travel distances* d_{LT}.

(2) At leading order, the unidirectional normalized additional volume is equal to the corresponding diagonal element of the volume - tensor:

$$\frac{\delta V_j}{dV_L} = \varepsilon_{jj} \cdot (1 + \mathcal{O}(dr_j)) = \frac{\delta r_j \cdot dA_j}{dr'_j \cdot dA_j} = \frac{\delta r_j}{dr'_j} \tag{10.28}$$

(3) At leading order, the isotropic normalized additional volume is the sum of the diagonal elements of the three equal diagonal elements of the volume - tensor:

$$\varepsilon_V = \sum_{j=1}^{3} \varepsilon_{jj} \cdot (1 + \mathcal{O}(dr_j)) = 3\varepsilon_{11}(1 + \mathcal{O}(dr_j)) \tag{10.29}$$

(4) A non-diagonal element of the volume - tensor ε_{ij} *with* $i \neq j$ *does* **not cause any difference of the volume.**

10.3 Rates for LFV and GFV

In this section, we apply the time derivative to Eq. (10.29):

$$\begin{aligned}
\partial_t \varepsilon_V &= \sum_{j=1}^{3} \partial_t \varepsilon_{jj} \cdot (1 + \mathcal{O}(dr_j)) \text{ or} && (10.30)\\
\dot{\varepsilon}_V &= \sum_{j=1}^{3} \dot{\varepsilon}_{jj} \cdot (1 + \mathcal{O}(dr_j)) \text{ or} && (10.31)\\
\dot{\varepsilon}_V &= 3 \cdot \dot{\varepsilon}_{11} \cdot (1 + \mathcal{O}(dr_j)) \text{ with} && (10.32)\\
\dot{\varepsilon}_V &= \partial_t \varepsilon_V \text{ and } \dot{\varepsilon}_{jj} = \partial_t \varepsilon_{jj} && (10.33)
\end{aligned}$$

We summarize our findings (Fig. 12.1):

Definition 12 Rates of formation of volume

(1) The time derivative of the isotropic normalized additional volume ε_V is called **rate of isotropic normalized additional volume***:*

$$\dot{\varepsilon}_V = \partial_t \varepsilon_V \qquad (10.34)$$

(2) The time derivative of the unidirectional normalized additional volume ε_{jj} is called **rate of unidirectional normalized additional volume***:*

$$\dot{\varepsilon}_{jj} = \partial_t \varepsilon_{jj} \qquad (10.35)$$

Proposition 3 Rates of formation of volume

(1) The rate of isotropic normalized additional volume is the sum of the rates of unidirectional normalized additional volume as follows:

$$\dot{\varepsilon}_V = \sum_{j=1}^{3} \dot{\varepsilon}_{jj} \cdot (1 + \mathcal{O}(dr_j)) \qquad (10.36)$$

In the limit dr_j to zero, the above relation becomes exact:

$$\dot{\varepsilon}_V = \Sigma_{j=1}^{3} \dot{\varepsilon}_{jj}, \quad \text{in the limit } dr_j \to 0 \tag{10.37}$$

(2) If a perspective of an observer is included, then each rate $\dot{\varepsilon}_{jj}$ of unidirectional normalized additional volume is multiplied by a corresponding factors $\sigma_{out,j}$. In that case, the above relations have the following form:

$$\dot{\varepsilon}_V = \sum_{j=1}^{3} \dot{\varepsilon}_{jj} \cdot \sigma_{out,j} \cdot (1 + \mathcal{O}(dr_j)) \tag{10.38}$$

$$\dot{\varepsilon}_V = \Sigma_{j=1}^{3} \dot{\varepsilon}_{jj} \cdot \sigma_{out,j}, \quad \text{in the limit } dr_j \to 0 \tag{10.39}$$

10.4 No measurement of absolute position

Idea: According to experience and to SR, it is not possible to measure an absolute position relative to space. This fact has the following consequence for LFV:

Proposition 4 No position relative to space

If a portion of homogeneous volume δV causes a portion of formed volume $\underline{\delta}V$, then the following holds:

(1) The location of δV cannot be measured.

(2) The portion of formed volume $\underline{\delta}V$ does not take part in a physical process, that could provide a measurement of the location of δV.

(3) The portion of formed volume $\underline{\delta}V$ does not take part in a physical process, that could provide a measurement of a locus (Hart (1912)) of δV.

Chapter 11

Formation and Propagation of Volume

11.1 Linear superposition

Idea: The time evolution of relative additional volume is described by the derivative $\frac{\partial}{\partial\tau}\varepsilon_L$. In principle, that derivative can have two different contributions:

Firstly, in the propagation of relative additional volume, the term $\frac{\partial}{\partial\tau}\varepsilon_L$ has a contribution, see the DEQ (8.4):

$$\frac{\partial}{\partial\tau}\varepsilon_L(R) = -\frac{\sigma_{out}}{c}\cdot\frac{\partial}{\partial L}\Phi_L \tag{11.1}$$

Secondly, a mass M or an effective mass M_{eff} give rise to LFV which provides a contribution to the term $\frac{\partial}{\partial\tau}\varepsilon_L$, see Eq. (9.31):

$$\frac{\underline{\delta\varepsilon_L}}{\underline{\delta\tau}} = \frac{\partial}{\partial\tau}\varepsilon_L(R) = -\frac{1}{c}\frac{G\cdot M}{R^2} \tag{11.2}$$

As two volumes can be added, two rates of additional volume can be added. Moreover, two rates of relative additional volume can be added, as the two denominators $dV_{d\Omega}$ are equal, by definition.

In this section, the resulting combined dynamics is analyzed.

Theorem 18 Formation and propagation of volume

In natural volume, the following holds:

(1) A mass or an effective mass or a dynamic mass M give rise to LFV. That LFV can be described by the relative additional volume at a distance R and by the following DEQ:

$$\frac{\underline{\delta}\varepsilon_L}{\underline{\delta}\tau} = \frac{\partial}{\partial\tau}\varepsilon_L(R) = -\frac{1}{c}\frac{G\cdot M}{R^2} = -\frac{1}{c}|G_M^*| \text{ with} \tag{11.3}$$

$$|G_M^*| = \frac{G\cdot M}{R^2} \tag{11.4}$$

(2) In natural volume, relative additional volume can propagate according to the following DEQ, THM (12):

$$\frac{\partial}{\partial\tau}\varepsilon_L(R) = -\frac{\sigma_{out}}{c}\cdot\frac{\partial}{\partial L}\Phi_L \tag{11.5}$$

(3) If both processes take place at the same time, then the combined process is described by the sum of the rates $\frac{\partial}{\partial\tau}\varepsilon_L$ in Eqs. (11.3 and 11.5):

$$\frac{\partial}{\partial\tau}\varepsilon_L = -\frac{\sigma_{out}}{c}\cdot\frac{\partial}{\partial L}\Phi_L - \frac{1}{c}\frac{G\cdot M}{R^2} \tag{11.6}$$

(4a) If both processes take place at the same time, then the combined process is described by the following nonhomogeneous linear DEQ:

$$\boxed{\left(c\cdot\frac{\partial}{\partial\tau} - c^2\cdot\sigma_{out}\cdot\frac{\partial}{\partial L}\right)\varepsilon_L(\tau,\vec{L}) = -|\vec{G}_M^*|(\tau,\vec{L})} \tag{11.7}$$

(4b) The corresponding linear DEQ and its linear differential operator $\hat{L}$ are as follows:

$$\hat{L}\cdot\varepsilon_{L,hom}(\tau,\vec{L}) = 0 \text{ with} \tag{11.8}$$

$$\hat{L} = c\cdot\frac{\partial}{\partial\tau} - c^2\cdot\sigma_{out}\cdot\frac{\partial}{\partial L} \tag{11.9}$$

A solution $\varepsilon_{L,hom}$ of that DEQ describes the **propagation** *of that relative additional volume $\varepsilon_{L,hom}$ in the $(\tau, \vec{L})$ - system of curved spacetime.*

(4c) The nonhomogeneous linear DEQ is described with the same linear differential operator $\hat{L}$:

$$\hat{L} \cdot \varepsilon_{L,nonhom}(\tau, \vec{L}) \;=\; -|\vec{G}^{*}|(\tau, \vec{L}) \tag{11.10}$$

A solution of that DEQ includes the **formation** *of relative additional volume $\varepsilon_{L,nonhom}$ caused by the local field $\vec{G}^{*}$.*

(4d) A general solution is the superposition:

$$\varepsilon_{L,general}(\tau, \vec{L}) \;=\; \varepsilon_{L,nonhom}(\tau, \vec{L}) + \varepsilon_{L,hom}(\tau, \vec{L}) \tag{11.11}$$

That solution describes the **formation and propagation** *of relative additional volume.*

Proof: The proof is provided by the transformations described within the above theorem. Thereby, we use the fact that a general solution of a linear DEQ is the sum of a solution of the nonhomogeneous DEQ and a solution or linear combination of solutions of the homogeneous DEQ (Ross, 2004, THM 11.13).

Corollary 15 Superposition of additional volume

(1) As volume is an additive geometrical quantity, it provides the property of linear superposition.

(2) As volume provides the property of linear superposition, the DEQ of the relative additional volume ε_L is a linear DEQ.

(3) As relative additional volume ε_L is formed by a mass or by an effective mass or by a gravitational field, the DEQ of the relative additional volume is nonhomogeneous and describes the process of formation of ε_L, including the process of **formation of volume** *$\underline{\delta}V/\underline{\delta}t$.*

(4) Correspondingly, the homogeneous DEQ describes the propagation of relative additional volume ε_L in curved spacetime described by the $(\tau, \vec{L})$ - system.

(5) Solutions of the homogeneous and nonhomogeneous DEQ provide linear superposition, as volume is an additive geometrical and physical quantity.

(6) The linearity of the DEQ of relative additional volume ε_L is a necessary condition for an exact and direct derivation of the Schrödinger Eq. from that DEQ.

(7) The linear DEQ of relative additional volume ε_L provides non-linear physical processes. For instance, that DEQ provides curvature of spacetime. Moreover, that DEQ describes propagation in curved spacetime. Furthermore, that DEQ describes processes of positive feedback explaining the diverging amount of formation of volume in the expansion of the universe, see corollary (13).

Corollary 16 Propagation of gravitational interaction

(1) The DEQ of the formation and propagation of relative additional volume ε_L in THM (18) includes the description of the formation and propagation of ε_L.

(2) The relative additional volume ε_L includes the description of the gravitational field and potential, see THM (11).

(3) Parts (1) and (2) show that the relative additional volume ε_L provides the mechanism of the propagation and formation of the gravitational field and potential. Thus, the relative additional volume ε_L provides the exact mechanism of the propagation and formation of the gravitational interaction. In this sense, relative additional volume ε_L provides the exact mechanism of the hypothetical graviton, the boson of the gravitational interaction, see e. g. Blokhintsev and Galperin (1934) or Workman et al. (2022).

Corollary 17 Propagation of curvature of spacetime

(1) The DEQ of relative additional volume ε_L in THM (18) describes the formation and propagation of ε_L.

(2) The relative additional volume ε_L provides the amount of additional volume corresponding to the Schwarzschild metric, as it has been derived from the Schwarzschild metric, see chapter (7).

(3) Parts (1) and (2) show that the relative additional volume ε_L provides the mechanism of the propagation and formation of the curvature of spacetime.

11.2 Energy and momentum

Idea: The propagation and the formation of volume can be expressed in terms of the gravitational field $\vec{G}^*$. With it, both phenomena can be summarized. Moreover, the different perspectives described by the factor σ_{out} can be summarized with help of the square $\sigma_{out}^2 = 1$. Furthermore, the square provides $(\vec{G}^*)^2$, proportional to the energy density, see chapter (6). Altogether, a four-vector of momentum densities of the additional volume can be derived, see e. g. (Landau and Lifschitz, 1971, Eq. 9.13) or (Hobson et al., 2006, section 5.8). It is invariant with respect to Lorentz transformations.

Theorem 19 Energy and momentum

In natural volume, the following holds:

(1) The formation and propagation of volume in the presence of a mass M can be described by the DEQ (11.6) and with help of the gravitational field in terms of the rate gravity scalar RGS_L in Eq. (8.52):

$$\dot{\varepsilon}_L = -\frac{\sigma_{out}}{c} \cdot \frac{\partial}{\partial L}\Phi_L - \frac{1}{c}\frac{G \cdot M}{R^2} \quad \text{or} \tag{11.12}$$

$$\dot{\varepsilon}_L = -\frac{\sigma_{out}}{c}|\vec{G}^*_{propagation}|\vec{e}_L + \frac{\sigma_{out}}{c}|\vec{G}^*_{formation}|\vec{e}_L \text{ or} \quad (11.13)$$

$$\dot{\varepsilon}_L^2 = \frac{(\vec{G}^*)^2}{c^2} \text{ or} \quad (11.14)$$

$$0 = -c^2\dot{\varepsilon}_L^2 + \sum_{j=1}^{3}(\vec{G}^*_j)^2 = RGS_L \text{ with} \quad (11.15)$$

$$\dot{\varepsilon}_L = \frac{\partial}{\partial\tau}\varepsilon_L \quad (11.16)$$

$$\vec{G}^* = \vec{G}^*_{propagation} + \vec{G}^*_{formation} \quad (11.17)$$

(2) With help of the absolute value of the energy density of the field $|u_{f,par,grav}| = \frac{(\vec{G}^*)^2}{8\pi G}$ *(chapter 6), the* RGS_L *in part (1) is transformed as follows:*

$$0 = -c^2\dot{\varepsilon}_L^2 + \sum_{j=1}^{3}(\vec{G}^*_j)^2 = RGS_L \text{ or} \quad (11.18)$$

$$0 = -\frac{c^2}{8\pi G}\dot{\varepsilon}_L^2 + \sum_{j=1}^{3}\frac{(\vec{G}^*_j)^2}{8\pi G} = \frac{RGS_L}{8\pi G} \text{ or} \quad (11.19)$$

$$0 = \frac{c^2}{8\pi G}\dot{\varepsilon}_L^2 - |u_{f,par,grav}| \quad (11.20)$$

As $|u_{f,par,grav}|$ *(*$|u_{grav}|$ *for short) is an energy density, the term* $\frac{c^2}{8\pi G}\dot{\varepsilon}_L^2$ *is an energy density too. As there is no field inherent to that term, it is a kinetic energy density:*

$$u_{kin} = \frac{c^2}{8\pi G}\dot{\varepsilon}_L^2 \quad (11.21)$$

As additional volume propagates at $v = c$*, its momentum density is* $\sum_{j=1}^{3}\frac{p_j}{V} = \frac{p}{V} = u_{kin}/c$*. So Eq. (11.19) takes the following form:*

$$0 = \frac{u_{kin}}{c} - \frac{|u_{grav}|}{c} \text{ or} \tag{11.22}$$

$$0 = \sum_{j=1}^{3} \frac{p_j}{V} - \frac{|u_{grav}|}{c} \text{ with} \tag{11.23}$$

$$u_{kin,jj} = c \cdot \frac{p_j}{V} = \frac{c^2}{8\pi G}\dot{\varepsilon}_{jj}^2 \text{ for } j \in \{1,2,3\} \text{ and} \tag{11.24}$$

$$|u_{grav}| = \sum_{j=1}^{3} \frac{(\vec{G}_j^*)^2}{8\pi G} \tag{11.25}$$

(3) The kinetic energy density is equal to the sum of momentum densities density multiplied by c:

$$u_{kin} = \sum_{j=1}^{3} c \cdot \frac{p_j}{V} \tag{11.26}$$

The kinetic energy density is equal to the sum of diagonal elements of the kinetic tensor:

$$u_{kin} = \sum_{j=1}^{3} u_{kin,jj} \tag{11.27}$$

As the above two sums are equal in general, the summands are equal:

$$u_{kin,jj} = c \cdot \frac{p_j}{V} = \frac{c^2}{8\pi G}\dot{\varepsilon}_{jj}^2 \tag{11.28}$$

The Cartesian components correspond to each other:

$$u_{kin,jj} = c \cdot \frac{p_j}{V} = \frac{(\vec{G}_j^*)^2}{8\pi G} \tag{11.29}$$

(4) The following scalar product of a four-vector is introduced:

$$|u_{grav}| = \sum_{j=1}^{3} \frac{(\vec{G}_j^*)^2}{8\pi G} = c \cdot \frac{p_0}{V} \tag{11.30}$$

As a consequence, we derive:

$$u_{grav}^2 = c^2 \cdot (p_0/V)^2 = \sum_{j=1}^{3} c^2 \cdot (p_j/V)^2 \quad \text{or} \tag{11.31}$$

$$0 = -(p_0/V)^2 + \sum_{j=1}^{3} (p_j/V)^2 \tag{11.32}$$

This is a relativistic scalar product of an energy momentum four-vector, EMV_{kin}, of kinetic energy as follows:

$$EMV_{kin} = \begin{pmatrix} \frac{p_0}{V} \\ \frac{p_1}{V} \\ \frac{p_2}{V} \\ \frac{p_3}{V} \end{pmatrix} \tag{11.33}$$

(5) A corresponding energy momentum tensor T_{kin}^{ij} of the kinetic energy can be formally introduced as follows, see e. g. (Hobson et al., 2006, p. 178) or (Landau and Lifschitz, 1971, p. 33): T_{kin}^{00} is the kinetic energy density u_{kin} in Eqs. (11.27, 11.28). The momentum densities $\frac{p_1}{V}$ multiplied by c are the tensor elements $T_{kin}^{j0} = T_{kin}^{0j}$. The non-diagonal elements are generalized in a continuous manner:

$$T_{kin}^{ik} = \frac{c^2}{8\pi G} \begin{pmatrix} \frac{8\pi G}{c^2} u_{kin} & \dot{\varepsilon}_{11}^2 & \dot{\varepsilon}_{22}^2 & \dot{\varepsilon}_{33}^2 \\ \dot{\varepsilon}_{11}^2 & \dot{\varepsilon}_{11}^2 & \dot{\varepsilon}_{11}\dot{\varepsilon}_{22} & \dot{\varepsilon}_{11}\dot{\varepsilon}_{33} \\ \dot{\varepsilon}_{22}^2 & \dot{\varepsilon}_{11}\dot{\varepsilon}_{22} & \dot{\varepsilon}_{22}^2 & \dot{\varepsilon}_{22}\dot{\varepsilon}_{33} \\ \dot{\varepsilon}_{33}^2 & \dot{\varepsilon}_{33}\dot{\varepsilon}_{11} & \dot{\varepsilon}_{33}\dot{\varepsilon}_{22} & \dot{\varepsilon}_{33}^2 \end{pmatrix} \tag{11.34}$$

The corresponding tensor of the field is as follows (Eq. 11.29):

$$T_{grav}^{ik} = \frac{-1}{8\pi G} \begin{pmatrix} 8\pi G \cdot |u_{grav}| & (\vec{G}_1^*)^2 & (\vec{G}_2^*)^2 & (\vec{G}_3^*)^2 \\ (\vec{G}_1^*)^2 & (\vec{G}_1^*)^2 & \vec{G}_1^*\vec{G}_2^* & \vec{G}_1^*\vec{G}_3^* \\ (\vec{G}_2^*)^2 & \vec{G}_2^*\vec{G}_1^* & (\vec{G}_2^*)^2 & \vec{G}_2^*\vec{G}_3^* \\ (\vec{G}_3^*)^2 & \vec{G}_3^*\vec{G}_1^* & \vec{G}_3^*\vec{G}_2^* & (\vec{G}_3^*)^2 \end{pmatrix} \tag{11.35}$$

Proof: The proof is provided by the explained transformations in the theorem.

Chapter 12

Global Formation of Volume

12.1 Globally formed volume

Idea: In GR, the process of the expansion of space is described by a uniform scaling. It is a transformation of space. However, in reality, space is not transformed. Instead, the amount of volume increases. At what rate does the amount of volume increase?

In this section, we derive the corresponding rate, at which volume V increases during the expansion of the universe since the Big Bang. For it, we express the volume V by the scale factor R:

$$V = \frac{4\pi}{3} R^3 \tag{12.1}$$

Using the chain rule, we obtain the derivative:

$$\dot{V} = 3\dot{R}\frac{V}{R} \tag{12.2}$$

So we derive:

$$\frac{\dot{V}}{V} = 3\frac{\dot{R}}{R} = 3 \cdot H \tag{12.3}$$

In order to use the FLE, we apply the square to Eq. (12.3):

$$\left(\frac{\dot{V}}{V}\right)^2 = 9H^2 \tag{12.4}$$

We insert the FLE, Eq. (5.12) with $k = 0$:

$$\left(\frac{\dot{V}}{V}\right)^2 = 24\pi G \cdot \rho \tag{12.5}$$

We summarize our finding:

Theorem 20 Rate of GFV according to the FLE

If the universe expands according to the FLE, Eq. (5.12), and if the curvature parameter is zero, $k = 0$, then the volume increases at the following normalized rate:

$$\boxed{\frac{\underline{\delta} V/\underline{\delta} t}{dV} := \frac{\dot{V}}{V} = \pm\sqrt{24\pi G \cdot \rho}} \tag{12.6}$$

Hereby, the plus-sign corresponds to the case of the expanding universe, whereas the minus sign describes the scenario of a big crunch, Goodstein (1997).

Thereby, the normalized rate $\frac{\underline{\delta} V/\underline{\delta} t}{dV}$ describes the formation of a volume $\underline{\delta} V$ in a volume dV during a time $\underline{\delta} t$.

12.2 LFV can cause GFV

Idea: Masses or dynamic masses m_i cause unidirectional formation of LFV in their vicinity. In contrast, isotropic formation of GFV is observed in the expansion of space. In this section, we show how the unidirectional LFV caused by many m_i can add up to isotropic GFV.

Theorem 21 LFV causes GFV

In a natural three-dimensional volume, filled with masses or dynamic masses m_i in a homogeneous and isotropic manner, the following holds:

(1) According to THM (18), each local mass or dynamic mass m_i causes unidirectional additional volume in its vicinity. The

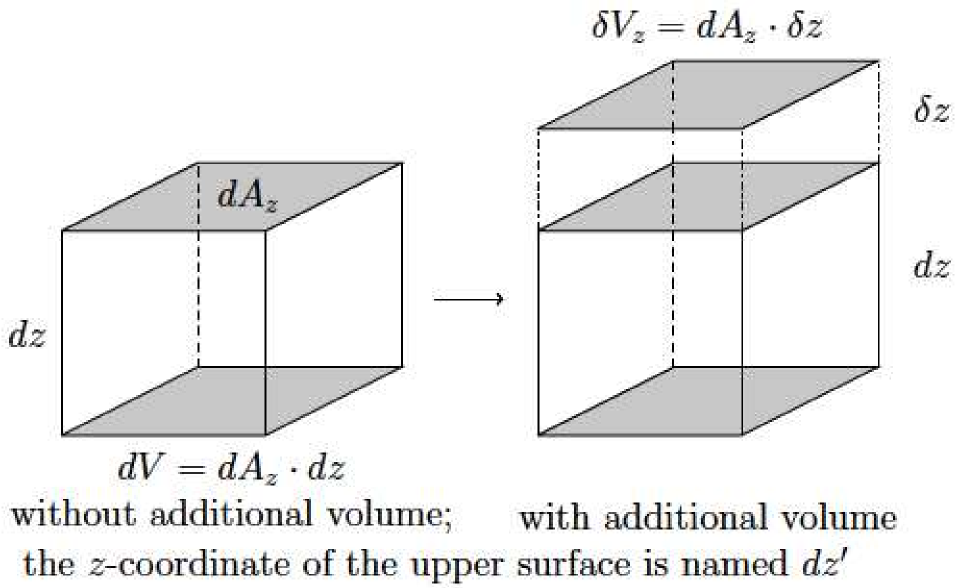

Figure 12.1: Additional volume in the z-direction: A cube with lower and upper surface dA_z is enlarged. Thereby, the upper surface is a portion or increment δz higher than at the left. Hereby, the upper position is at $dz' = dz + \delta z$.

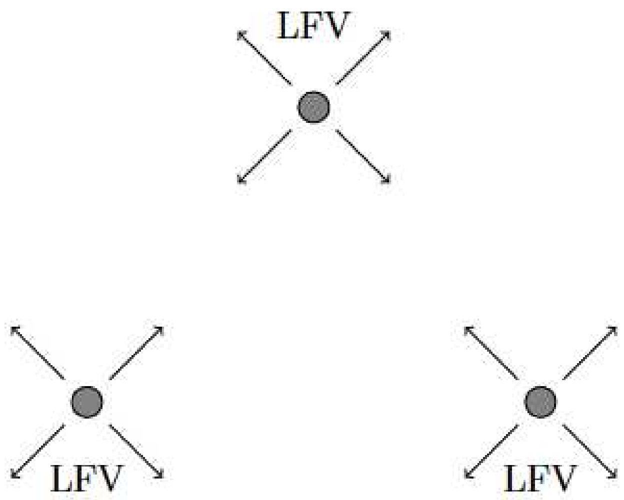

Figure 12.2: Unidirectional LFV at masses or dynamic masses can summarize to isotropic GFV.

volume caused by a mass propagates in a radial direction. That direction is marked by an index q. In particular, $\frac{\partial}{\partial L_q}$ *marks the derivative in that direction,* $\varepsilon_{L,i,qq}$ *marks the tensor element of that direction,* $\vec{e}_q$ *is the unit vector of that direction,* $G^*_{m_i,q}(\tau,\vec{L})$ *is the coordinate of the field of that direction (in an appropriate local coordinate system). That unidirectional additional volume propagates according to the following nonhomogeneous linear DEQ (Eq. 11.7):*

$$\left(c\cdot\frac{\partial}{\partial\tau}-c^2\cdot\sigma_{out,i}\cdot\frac{\partial}{\partial L_q}\right)\varepsilon_{L,i,qq}(\tau,\vec{L})=G^*_{m_i,q}(\tau,\vec{L}) \quad (12.7)$$

(2) As the above DEQ is linear, the rates of N masses m_i *add up:*

$$\sum_{i=1}^{N}\left(c\frac{\partial}{\partial\tau}-c^2\sigma_{out,i}\frac{\partial}{\partial L_q}\right)\varepsilon_{L,i,qq}(\tau,\vec{L})=\sum_{i=1}^{N}G^*_{m_i,q}(\tau,\vec{L}) \quad (12.8)$$

(3) At a location $\vec{L}$ *that has a sufficient distance to the masses* m_i*, the* **fields can compensate** *each other (Fig. 12.2). In that case, the following holds:*

(3a) The dynamics is characterized by the homogeneous DEQ:

$$\sum_{i=1}^{N}\left(c\frac{\partial}{\partial\tau}+c^2\sigma_{out,i}\frac{\partial}{\partial L_q}\right)\varepsilon_{L,i,qq}(\tau,\vec{L})=0 \quad (12.9)$$

$$\sum_{i=1}^{N}c\frac{\partial}{\partial\tau}\varepsilon_{L,i,qq}(\tau,\vec{L})=\sum_{i=1}^{N}c^2\sigma_{out,i}\frac{\partial}{\partial L_q}\varepsilon_{L,i,qq}(\tau,\vec{L}) \quad (12.10)$$

(3b) The volume caused by each mass propagates according to the **homogeneous DEQ***:*

$$c\dot{\varepsilon}_{L,i,qq}(\tau,\vec{L})=c^2\sigma_{out,i}\frac{\partial}{\partial L_q}\varepsilon_{L,i,qq}(\tau,\vec{L}) \quad (12.11)$$

(3c) We **transform** *the unidirectional rate* $\dot{\varepsilon}_{L,i,qq}$ *for the direction* $\vec{e}_q$ *of propagation to the unidirectional rate* $\dot{\varepsilon}_{L,i,jj}$ *of a*

common coordinate system used for all masses m_i. As usual, we derive the transformation with help of an invariant.

[1] For it, we use the **kinetic energy density** *(Eq. 11.21) $c^2\dot{\varepsilon}^2_{L,i,qq} = 8\pi G \cdot u_{kin,i}$:*

$$c^2\dot{\varepsilon}^2_{L,i,qq} = 8\pi G \cdot u_{kin,i} \tag{12.12}$$

[2] We use the kinetic tensor (Eq. 11.28):

$$c^2\dot{\varepsilon}^2_{L,i,qq} = c^2 \cdot \sum_{j=1}^{3} \dot{\varepsilon}^2_{L,i,jj} \tag{12.13}$$

[3] In order to consider all masses, we apply the **average** *with respect to N masses m_i that cause these rates:*

$$\frac{1}{N}\sum_{i=1}^{N} \dot{\varepsilon}^2_{L,i,qq} = \langle\dot{\varepsilon}^2_{L,i,qq}\rangle_i = \sum_{j=1}^{3}\langle\dot{\varepsilon}^2_{L,i,jj}\rangle_i \tag{12.14}$$

[4] As the masses are distributed in an isotropic manner, the averaged tensor elements are equal for each j:

$$\langle\dot{\varepsilon}_{L,i,11}\rangle_i = \langle\dot{\varepsilon}_{L,i,22}\rangle_i = \langle\dot{\varepsilon}_{L,i,33}\rangle_i \tag{12.15}$$

[5] Thus, the above sum $\sum_{j=1}^{3}$ provides the factor three:

$$\langle\dot{\varepsilon}^2_{L,i,qq}\rangle_i = 3\langle\dot{\varepsilon}^2_{L,i,jj}\rangle_i \tag{12.16}$$

[6] As the masses have a homogeneous density ρ_{hom}, the standard deviations $\langle\dot{\varepsilon}^2_{L,i,jj}\rangle_i - \langle\dot{\varepsilon}_{L,i,jj}\rangle_i^2$ and $\langle\dot{\varepsilon}^2_{L,i,qq}\rangle_i - \langle\dot{\varepsilon}_{L,i,qq}\rangle_i^2$ can be neglected in a good approximation:

$$\langle\dot{\varepsilon}_{L,i,qq}\rangle_i^2 = 3\langle\dot{\varepsilon}_{L,i,jj}\rangle_i^2 \quad \text{or} \tag{12.17}$$

$$\langle\dot{\varepsilon}_{L,i,jj}\rangle_i = \langle\dot{\varepsilon}_{L,i,qq}\rangle_i/\sqrt{3} \tag{12.18}$$

[7] We express the rate in terms of the density (Eq. 12.12):

$$\langle \dot{\varepsilon}_{L,i,jj} \rangle_i = \langle \sqrt{8\pi G u_{kin,i}/c^2} \rangle_i / \sqrt{3} \text{ or} \tag{12.19}$$

$$\langle \dot{\varepsilon}_{L,i,jj} \rangle_i = \langle \sqrt{8\pi G \cdot \rho_{kin,i}/3} \rangle_i \tag{12.20}$$

(3d) We apply the transformed unidirectional rate $\langle \dot{\varepsilon}_{L,i,jj} \rangle_i$, in order to derive the isotropic rate $\dot{\varepsilon}_{L,iso}$ by summation (volume is additive). As usual, we derive the transformation with help of an invariant, the kinetic energy density, which is proportional to the squared rate.

[1] For it, we apply the tensor $u_{kin,jj}$:

$$\dot{\varepsilon}_{L,iso} = \sum_{j=1}^{3} \langle \dot{\varepsilon}_{L,i,jj} \rangle_i = \sum_{j=1}^{3} \langle \sqrt{8\pi G \cdot \rho_{kin,i}/3} \rangle_i \tag{12.21}$$

[2] According to isotropy, the sum provides the factor three:

$$\dot{\varepsilon}_{L,iso} = \langle \sqrt{24\pi G \cdot \rho_{kin,i}} \rangle_i \tag{12.22}$$

[3] Corresponding to homogeneity, as before, and in an appropriate approximation, we neglect a standard deviation:

$$\dot{\varepsilon}^2_{L,iso} = \langle \sqrt{24\pi G \cdot \rho_{kin,i}} \rangle_i^2 = \langle \sqrt{24\pi G \cdot \rho_{kin,i}}^2 \rangle_i \text{ or} \tag{12.23}$$

$$\dot{\varepsilon}^2_{L,iso} = = 24\pi G \cdot \langle \rho_{kin,i} \rangle_i^2 \tag{12.24}$$

(3e) In the GFV, the above average $\dot{\varepsilon}^2_{L,iso}$ describes the squared rate $\frac{\dot{V}}{V}$, and the above average $\langle \rho_{kin,i} \rangle_i$ describes the density of the kinetic energy density of the propagating relative additional volume.

(4) Altogether, we showed, that the density of the kinetic energy of the propagating relative additional volume provides the isotropic squared rate $\dot{\varepsilon}^2_{L,iso}$, whereby this density and its rate are in full accordance with the rate of formation of volume of a density in the FLE (THM 20).

Proof: The proof is provided by the explained transformations in the theorem.

Corollary 18 LFV adds up to GFV

(1) At a location $\vec{R}$, globally formed volume, GFV, has been observed independently with help of many probes, see e. g. Planck-Collaboration (2020), Riess et al. (2022), Blakeslee et al. (2021), Philcox et al. (2020). Thereby, GFV is isotropic, and it is usually described by the FLE.

(2) At a location $\vec{R}$, the Schwarzschild metric has been observed independently with help of many probes, see e. g. Pound and Rebka (1960), Will (2014). With it, locally formed volume, LFV, can be evaluated, see chapters (7, 8, 9, 11). Thereby, LFV is unidirectional.

(3) At a location $\vec{R}$, there arrives unidirectional LFV caused by many masses or dynamic masses m_i. Thereby, in general, classical fields are compensated at $\vec{R}$. Accordingly, the LFV propagates corresponding to the DEQ of additional volume, see chapter (8).

(4) At the location $\vec{R}$, the kinetic energy density of LFV caused by these m_i adds up. Moreover, many directions of unidirectional LFV add up to isotropic additional volume. The rate of that sum as a function of its density is equal to the rate as a function of density of the FLE.

(5) Altogether, the rate of GFV is explained in terms of the rate of LFV coming from several m_i.

(6) So, the global dynamics of space is derived from the local dynamics of space at the level of the formation of additional volume.

The derivations in part (II) and in parts (III, IV) are shown in a cognitive map, Fig. (12.3).

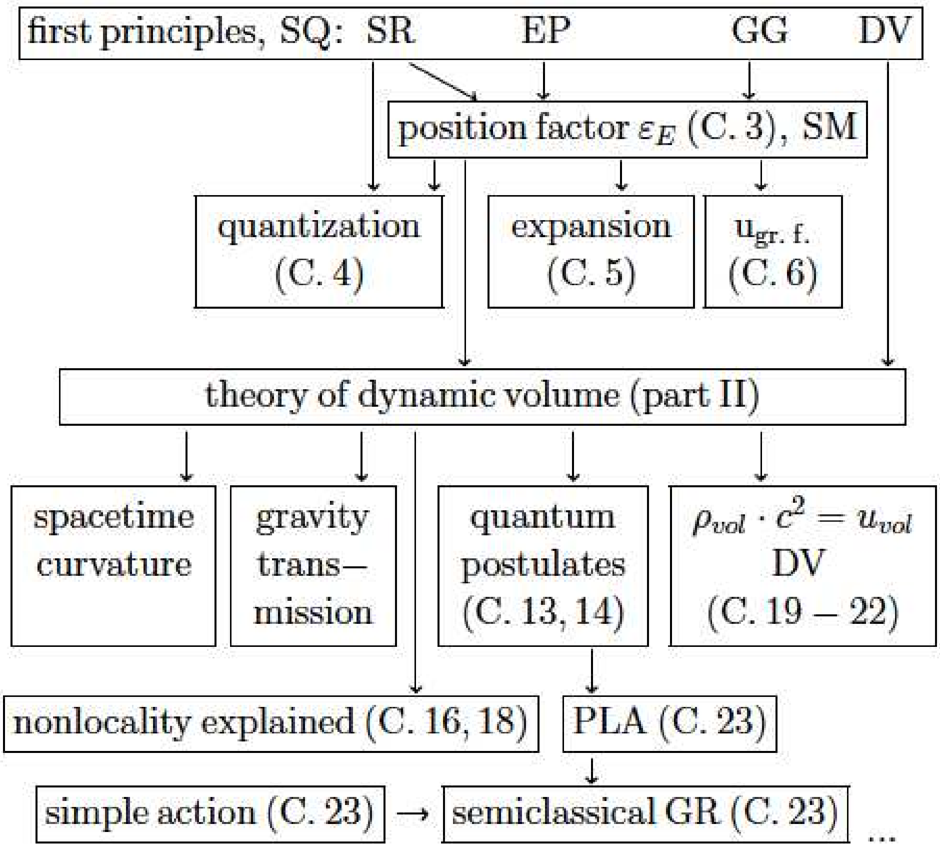

Figure 12.3: **Paths of derivation:** from first principles to the DEQs of volume and beyond. The light-travel distance d_{LT}, the gravitational parallax distance d_{GP} and energy conservation in a stationary system, see Noether (1918), are used. C. 16-22 are beyond usual QP and GR, including the Schwarzschild metric, SM.
SQ: spacetime quadruple
SR: special relativity
EP: equivalence principle
GG: generalized Gaussian gravity
DV: dynamic volume
ε_E: position factor describing energy
$u_{gr.f.}$: energy density of the gravitational field
PLA: principle of least or stationary action
ρ_{vol}: dynamical density of volume.

Part III

Fundamental Dynamics of Quanta

Chapter 13

Stabilization of Quanta

Question: Do the dynamics of volume form the quantum at the smallest possible portion of energy at a given radius?

We analyze the dynamics of a ball with a radius r_b and with a relative additional volume $\varepsilon_{L,b} = \frac{\delta V}{dV_L}$. Consequently, the ball has the volume $V_b = \frac{4\pi}{3} r_b^3$, the complete volume $V_L = \frac{4\pi}{3} r_L^3$ and the surface $A = 4\pi r_L^2$. In the context of $\varepsilon_{L,b}$, the volume V_L is named dV_L, C. (7). Thence, the ball has the following additional volume, see THM (10):

$$\delta V = V_L - V_b = dV_L \cdot \varepsilon_{L,b}, \text{ with } dV_L = V_L \tag{13.1}$$

Accordingly, $\varepsilon_{L,b}$ ranges from 0 towards 1:

$$V_L = \delta V + V_b, \text{ thus, } \delta V \leq V_L \text{ and } \varepsilon_{L,b} \leq 1 \tag{13.2}$$

During a time $\underline{\delta}\tau$, the outer shell with thickness $c \cdot \underline{\delta}\tau$ propagates outwards. Thus, the ball looses the additional volume $\underline{\delta}V_{out}$ in that shell:

$$\underline{\delta}V_{out} = c \cdot \underline{\delta}\tau \cdot A \cdot \varepsilon_{L,b} \tag{13.3}$$

The corresponding rate $\dot{\underline{\varepsilon}}_{L,out}$ is as follows, see THM (10):

$$\dot{\underline{\varepsilon}}_{L,out} = \frac{\underline{\delta}V_{out}}{dV_L \underline{\delta}\tau} = \frac{A \cdot c}{V_L} \varepsilon_{L,b} = \frac{3c}{r_L} \cdot \varepsilon_{L,b}, \text{ with } dV_L = V_L \tag{13.4}$$

During the same time $\underline{\delta}\tau$, the additional volume of the ball exhibits unidirectional formation of volume at the rate $\underline{\dot{\varepsilon}}_{L,jj}$, named $\underline{\dot{\varepsilon}}_{L,formed}$ in this context (THM 18, part 4c):

$$\underline{\delta}V_{formed} = \underline{\dot{\varepsilon}}_{L,formed} \cdot \underline{\delta}\tau \cdot dV_L \tag{13.5}$$

The difference of $\underline{\dot{\varepsilon}}_{L,formed}$ and $\underline{\dot{\varepsilon}}_{L,out}$ is the rate of relative additional volume of the ball:

$$\underline{\dot{\varepsilon}}_{L,b} = \underline{\dot{\varepsilon}}_{L,formed} - \underline{\dot{\varepsilon}}_{L,out} = \underline{\dot{\varepsilon}}_{L,formed} - \frac{3c}{r_L} \cdot \varepsilon_{L,b} \tag{13.6}$$

The sign of the rate $\underline{\dot{\varepsilon}}_{L,b}$ exhibits three cases:
(1) If $\underline{\dot{\varepsilon}}_{L,b} = 0$, then $\varepsilon_{L,b}$ is constant.
(2) If $\underline{\dot{\varepsilon}}_{L,b} < 0$, then $\varepsilon_{L,b}$ decreases. Thus, the subtrahend in the rate in Eq. (13.6) decreases. Consequently, the rate $\underline{\dot{\varepsilon}}_{L,b}$ increases. This process takes place in a local, successive and asymptotic manner (C. 7, 11), until the rate is zero, $\underline{\dot{\varepsilon}}_{L,b} = 0$. As a consequence, case (1) is reached.
(3) If $\underline{\dot{\varepsilon}}_{L,b} > 0$, then $\varepsilon_{L,b}$ increases. Consequently, $\underline{\dot{\varepsilon}}_{L,b}$ decreases, as the subtrahend in the rate in Eq. (13.6) increases. This process takes place in a local, successive and asymptotic manner, until the rate is zero, $\underline{\dot{\varepsilon}}_{L,b} = 0$. Hence, case (1) is reached.

Cases (0-3) show that the dynamics of the rate $\underline{\dot{\varepsilon}}_{L,b}$ converge towards the stable fixed point $\underline{\dot{\varepsilon}}_{L,b} = 0$.

$$\underline{\dot{\varepsilon}}_{L,b} \text{ converges to the stable fixed point } \underline{\dot{\varepsilon}}_{L,b} = 0. \tag{13.7}$$

We analyze the fixed point (Eqs. 13.6, 13.7) of the rate. At that fixed point, the rate of formation is as follows:

$$\underline{\dot{\varepsilon}}_{L,formed} = \underline{\dot{\varepsilon}}_{L,out} = \frac{3c}{r_L} \cdot \varepsilon_{L,b} \tag{13.8}$$

The rate $\underline{\dot{\varepsilon}}_{L,formed}$ represents $u_{kin} = \frac{\dot{\varepsilon}^2_{L,formed} c^2}{8\pi G}$. As $\underline{\dot{\varepsilon}}_{L,formed}$ represents the formation of volume (THM 18, part 4c), $\underline{\dot{\varepsilon}}_{L,formed}$ does not correspond to a potential energy. Thus, the energy E_{fp} of the wave packet is u_{kin} multiplied by V_L:

$$E_{fp} = u_{kin} \cdot V_L = \frac{\dot{\varepsilon}^2_{L,out} c^2}{8\pi G} V_L = \frac{3}{2} \cdot \frac{c}{r_L} \cdot \frac{c^3}{G} r_L^2 \cdot \varepsilon^2_{L,b} > 0 \quad (13.9)$$

We estimate E_{fp}: As we analyze a smallest portion of energy, we obtain the longest possible wavelength λ in the ball (C. 4). It is the circumference $\lambda = 2\pi r_L$. With it, we derive:

$$E_{fp} = \frac{3}{2} \cdot \frac{2\pi c}{\lambda} \cdot \frac{c^3}{G} r_L^2 \cdot \varepsilon^2_{L,b} \quad (13.10)$$

Universal quantization implies (C. 4), that a smallest portion of energy E_{fp} is proportional to the inverse of the wavelength λ. Thus, for each r_L, the factor r_L^2 in Eq. (13.10) must cancel out. This can take place only by the factor $\varepsilon^2_{L,b}$, as other available factors are constants. So, $r_L^2 \cdot \varepsilon^2_{L,b}$ is a constant q_b^2:

$$r_L^2 \cdot \varepsilon^2_{L,b} = q_b^2 \ \text{ or } \ r_L = q_b / \varepsilon_{L,b} \quad (13.11)$$

Thereby, r_L ranges from the Planck length towards the light horizon, $r_L \in [L_P, R_{LH}]$. We use the very good approximation $r_L \in [L_P, \infty[$. Thus, at the largest possible value of $\varepsilon_{L,b}$, at $\varepsilon_{L,b} = 1$ (Eq. 13.2), the radius r_L is equal to L_P:

$$r_L = q_b = L_P, \ \text{ at minimal } \ r_L \ \text{ and at } \ \varepsilon_{L,b} = 1 \quad (13.12)$$

So, r_L is the following function of $\varepsilon_{L,b}$ (Eqs. 13.11, 13.12):

$$r_L = \frac{L_P}{\varepsilon_{L,b}} \ \text{ or } \ \varepsilon_{L,b} = \frac{L_P}{r_L} \quad (13.13)$$

With it and with $\frac{2\pi c}{\lambda} = \omega$, the energy in Eq. (13.10) is:

$$E_{fp} = \frac{3}{2} \cdot \omega \cdot \frac{c^3}{G} \cdot L_P^2 \quad (13.14)$$

Application of the Planck length $L_P = \sqrt{G \cdot \hbar / c^3}$ (see glossary) yields the following energy, see Eq. (13.14):

$$E_{fp} = 3 \cdot \frac{\hbar\omega}{2} \quad (13.15)$$

E_{fp} describes the ZPOs of the ball, in three-dimensional space.

Theorem 22 How the dynamics of volume forms quanta

The dynamics of volume, DV, forms quanta with a radius r_L *and with a relative additional volume* $\varepsilon_{L,b}$ *as follows:*

(1) The rate $\dot{\underline{\varepsilon}}_{L,b}$ *converges to a stable fixed point with* $\dot{\underline{\varepsilon}}_{L,b} = 0$.

(1a) At the fixed point, fp, the rate $\dot{\underline{\varepsilon}}_{L,out}$ *of volume propagating outwards and the rate* $\dot{\underline{\varepsilon}}_{L,formed}$ *of formation are equal:*

$$\dot{\underline{\varepsilon}}_{L,formed} = \dot{\underline{\varepsilon}}_{L,out} = \frac{3c}{r_L} \cdot \varepsilon_{L,b} \tag{13.16}$$

(1b) The rate $\dot{\underline{\varepsilon}}_{L,formed}$ *of formation causes kinetic energy* E_{fp}, *without potential energy (THM 18, part 4c):*

$$E_{fp} = \frac{3}{2} \cdot \frac{c}{r_L} \cdot \frac{c^3}{G} \cdot r_L^2 \cdot \varepsilon_{L,b}^2 \tag{13.17}$$

(1c) At the fixed point and at lowest energy, E_{fp} *is as follows:*

$$E_{fp} = 3 \cdot \frac{\hbar\omega}{2} \text{ with } \omega = \frac{2\pi c}{\lambda} \text{ and } \lambda = 2\pi r_L \tag{13.18}$$

E_{fp} *is the energy of the three ZPOs of the ball in 3D space. That energy is derived formally in section (14.5).*

(2) Altogether, for each radius r_L, *the DV can form the isotropic quantum of lowest energy at that radius. The quantum is a stable fixed point of the dynamics of volume. Depending on initial conditions, other functions* $\dot{\underline{\varepsilon}}_L(t, \vec{R}$ *are possible.*

(3) The DV can form dynamically stable quanta. These generate volume contributing to the expansion of space since the Big Bang (C. 12). The quanta unify microcosm and macrocosm in nature, they are described by the DV, and the DV unifies the theories of spacetime, gravity and quantum physics.

(4) The quantum is a stable fixed point of DV, whereby DV forms as fast in the quantum as DV is lost at the surface region of the quantum.

Chapter 14

Derivation of Quantum Postulates

Idea: As the volume propagates at the velocity of light, it is quantized (chapter 4). Thus, the exact DEQ of formation and propagation of relative volume ε_L in THMs (12, 13, 14 and 18) could be the basis of the DEQ of quanta, the Schrödinger equation, SEQ. Moreover, the full dynamics of volume could provide the postulates of quantum physics.

In this chapter, we derive the postulates of quantum physics[1]. For it, we use the basic principles of the SQ, see chapter (2), and we apply consequences of these basic principles, see Fig. (12.3).

The derived postulates[2] include the five postulates presented by Kumar (2018) as well as the postulate about mixed states in (Ballentine, 1998, p. 46). We begin with the postulate about the time evolution.

14.1 Time evolution

In this section, we derive the postulate about the time evolution, (Kumar, 2018, p. 170):

[1] Earlier derivations, see Carmesin (2022d), Carmesin (2022a), Carmesin (2022f), include the FDA at some points. In this book, we provide an exact derivation.

[2] Hilbert et al. (1928) proposed an early system of postulates, for instance.

Postulate 1 Time evolution

'The time evolution of the state vector is governed by the time-dependent Schrödinger equation, SEQ, see (Schrödinger, 1926b, Eq. (4")):

$$i\hbar\partial_t|\psi\rangle = \hat{H}|\psi\rangle, \tag{14.1}$$

where $\hat{H}$ is the Hamilton operator corresponding to the total energy of the system.'

Hereby, the wave function $|\psi\rangle$ represents a complex valued function. Thus, the complex conjugate function fulfills the DEQ with an opposite sign, see (Schrödinger, 1926b, p. 112 or § 1):

$$-i\hbar\partial_t|\psi\rangle^* = \hat{H}|\psi\rangle^*, \tag{14.2}$$

Thus, in quantum physics, the sign in the SEQ is a convention. Thence, more adequately, the square of the SEQ holds, this corresponds to the Lorentz invariant equation in THM (14).

Derivation: The volume propagates according to the following DEQ, see part (3) in THM (13), for an invariant formulation, see THM (14):

$$\partial_\tau \varepsilon(\tau, \vec{L}) = -\partial_{\vec{L}} \varepsilon(\tau, \vec{L}) \cdot c \tag{14.3}$$

We apply an additional derivative with respect to time τ (in order to additionally derive the later postulate about probabilistic outcomes):

$$\partial_\tau \dot{\varepsilon}(\tau, \vec{L}) = -\partial_{\vec{L}} \dot{\varepsilon}(\tau, \vec{L}) \cdot c \tag{14.4}$$

Hereby, we mark the time derivative with a dot:

$$\partial_\tau \varepsilon(\tau, \vec{L}) = \dot{\varepsilon}(\tau, \vec{L}) \tag{14.5}$$

In order to derive the usual SEQ, we multiply by $i\hbar$ and by a normalization factor t_n:

$$i\hbar\partial_\tau \cdot t_n \cdot \dot{\varepsilon}(\tau, \vec{L}) = -i\hbar\partial_{\vec{L}} \cdot t_n \cdot \dot{\varepsilon}(\tau, \vec{L}) \cdot c \tag{14.6}$$

Hereby, the normalization factor t_n is chosen so that the product $t_n \cdot \dot{\varepsilon}(\tau, \vec{L})$ is normalized, whereby the norm in the corresponding space of the functions $t_n \cdot \dot{\varepsilon}(\tau, \vec{L})$ is used, see e. g. Teschl (2014) or (Kumar, 2018, p. 18). Moreover, in order to derive the traditional form (Kumar, 2018, p. 18) of the SEQ, we name the function $t_n \cdot \dot{\varepsilon}(\tau, \vec{L})$ **wave function** ψ:

$$\psi(\tau, \vec{L}) = t_n \cdot \dot{\varepsilon}(\tau, \vec{L}) \tag{14.7}$$

Hereby, the wave function may be expressed by the **Dirac notation** alternatively (Kumar, 2018, section 4.2):

$$\psi(\tau, \vec{L}) = |\psi\rangle \tag{14.8}$$

14.1.1 Correspondence of operators and observables

If the application of an operator to the wave function provides a physical quantity, then that operator can be used to represent that measurable physical quantity or observable. Such a correspondence of physical quantities and operators is named *correspondence principle*, see e. g. Bohr (1920), (Kumar, 2018, p. 267). For instance, the momentum operator

$$\hat{p} = -i\hbar\partial_{\vec{L}} \tag{14.9}$$

provides the momentum:

$$-i\hbar\partial_{\vec{L}} t_n \exp(-i\omega t + ikL) = \hbar k \cdot t_n \exp(-i\omega t + ikL) \tag{14.10}$$

$$= p \cdot t_n \exp(-i\omega t + ikL) \tag{14.11}$$

According to the usual convention, see e. g. (Kumar, 2018, p. 267), the above plane wave propagates inwards.

With it, the DEQ (14.6) of the propagation of volume takes the following form:

$$i\hbar\partial_\tau \cdot |\psi\rangle = \hat{p} \cdot c \cdot |\psi\rangle \tag{14.12}$$

14.1.2 Propagation of volume at $v = c$

As natural volume propagates at the velocity $v = c$, it has zero rest mass m_0. So it is quantized, see THM (5). Moreover, the energy E is equal to the product of the momentum p and the velocity c of light (Landau and Lifschitz, 1971, Eq. 9.6):

$$E = p \cdot c \tag{14.13}$$

Hereby, the energy E is described by the Hamiltonian H (Kumar, 2018, p. 23):

$$H = p \cdot c \tag{14.14}$$

Accordingly, the Hamilton operator is the momentum operator in Eq. (14.9) multiplied by c:

$$\hat{H} = \hat{p} \cdot c \tag{14.15}$$

So, we derive the following DEQ of the propagation of natural volume:

$$i\hbar\partial_t \cdot |\psi\rangle = \hat{H} \cdot |\psi\rangle \tag{14.16}$$

We identify the above DEQ of the propagation of natural volume with the Schrödinger equation (14.1). So, natural volume propagates according to the Schrödinger equation, SEQ. We summarize our finding:

Theorem 23 Volume and its dynamics imply the SEQ

(1) The natural volume propagates according to the Schrödinger equation, SEQ:

$$\boxed{i\hbar\partial_\tau \cdot |\psi\rangle = \hat{H} \cdot |\psi\rangle} \tag{14.17}$$

(2) The DEQ of the propagation of natural volume implies the postulate (1) about the time evolution of quantum physics, represented by the SEQ.

14.1.3 Derivation: SEQ applicable to matter

Natural volume propagates according to the SEQ, see THM (23). Matter forms from volume via phase transitions, see for instance Higgs (1964), Aad et al. (2012), Carmesin (2021a, 2022e,c, 2019b, 2020b).

Similarly, ice can form from water by a phase transition. Thereby, the same fundamental laws of physics are applicable to water molecules in liquid water, solid water and gaseous water. In general, the same fundamental laws of physics are applicable before, during and after a phase transition, see e. g. van der Waals (1873), Landau (1937), Landau and Lifschitz (1980), Carmesin et al. (1986), Klee et al. (1988), Carmesin et al. (1989), Carmesin (1995).

Accordingly, the SEQ is applicable to volume before, during and after the phase transition to matter. Thus, matter and similarly antimatter propagate according to the SEQ. For instance, the SEQ is applicable to an electron. Hereby, various theories of quantum physics can be derived from the postulates derived here, see chapter (15). We summarize our findings:

Proposition 5 SEQ is applicable to matter:

The SEQ is applicable to matter, as volume generates matter by phase transitions, and as volume propagates according to the SEQ.

14.1.4 Application of the SEQ to matter

In this section, we derive the particular form of time evolution of an object with nonzero rest mass m_0. The group velocity v_g of such an object is slower than the velocity of light, see e. g. Kumar (2018).

Such an object has an energy momentum relation as follows (Landau and Lifschitz, 1971, Eq. 9.6):

$$E^2 = p^2 \cdot c^2 + m_0^2 \cdot c^4 \tag{14.18}$$

In order to obtain the respective Hamilton operator, we apply the square root, we express the energy by the Hamiltonian H (Kumar, 2018, p. 23), and we replace the observables H and p by the respective operators (Kumar, 2018, section 2.7):

$$\hat{H} = \sqrt{\hat{p}^2 \cdot c^2 + m_0^2 \cdot c^4} \tag{14.19}$$

In order to obtain the corresponding SEQ, we apply the particular form of the Hamilton operator to the general form of the SEQ (14.17):

$$\boxed{i\hbar\partial_\tau \cdot |\psi\rangle = \sqrt{\hat{p}^2 \cdot c^2 + m_0^2 \cdot c^4} \cdot |\psi\rangle} \tag{14.20}$$

So, objects with rest mass propagate according to the SEQ.

14.1.5 Time evolution at $pc \ll m_0c^2$

In this section, we analyze the case of an object propagating relatively slow so that the energy of the rest mass m_0c^2 is large compared to the product pc. For it, we apply the Hamiltonian in Eq. (14.19), whereby we factorize m_0c^2:

$$\hat{H} = m_0c^2 \cdot \sqrt{1 + \hat{p}^2/(m_0^2 \cdot c^2)} \tag{14.21}$$

If the fraction in the above Eq. is relatively small compared to one, then a linear approximation is appropriate:

$$\hat{H} = m_0c^2 \cdot \left(1 + \frac{\hat{p}^2}{2m_0^2 \cdot c^2}\right) \tag{14.22}$$

In the above Eq., we evaluate the product:

$$\hat{H} = m_0c^2 + \frac{\hat{p}^2}{2m_0} \tag{14.23}$$

In non-relativistic physics, the energy of the rest mass m_0c^2 is not considered in the Hamiltonian (Landau and Lifschitz, 1965, § 17). So, m_0c^2 is subtracted from the relativistic Hamiltonian:

$$\hat{H}_{non-relativistic} = \hat{H} - m_0c^2 = \frac{\hat{p}^2}{2m_0} \tag{14.24}$$

Thus, the non-relativistic SEQ is derived by inserting the non-relativistic Hamiltonian into the general SEQ (14.17):

$$i\hbar\partial_\tau \cdot |\psi\rangle = \hat{H}_{non-relativistic} \cdot |\psi\rangle \text{ or}$$
$$i\hbar\partial_\tau \cdot |\psi\rangle = \frac{\hat{p}^2}{2m_0} \cdot |\psi\rangle \text{ non}-\text{relativistic SEQ} \qquad (14.25)$$

That form of the SEQ is very popular, Kumar (2018), (Landau and Lifschitz, 1965, § 17), and a non-relativistic form has been suggested by (Schrödinger, 1926b, Eq. 4"). We summarize:

Theorem 24 Volume implies the non-relativistic SEQ

(1) As matter forms from volume by a phase transition, volume and matter propagate according to the SEQ. Similarly, antimatter propagates according to the SEQ.

(2) The relativistic SEQ for objects at $v = c$ (THM 23) implies the SEQ for objects at $v < c$ in items (3, 4, 5, 6). So, also objects with a nonzero rest mass m_0 are described by the SEQ derived here.

(3) Objects of matter or antimatter have nonzero rest mass m_0 and propagate according to the SEQ as follows:

$$i\hbar\partial_\tau \cdot |\psi\rangle = \sqrt{\hat{p}^2 \cdot c^2 + m_0^2 \cdot c^4} \cdot |\psi\rangle \qquad (14.26)$$

(4) In the case of relatively small kinetic energy density, $p \cdot c \ll m_0 \cdot c^2$, the following non-relativistic Hamiltonian is appropriate:

$$\hat{H}_{non-relativistic} = \hat{H} - m_0 c^2 = \frac{\hat{p}^2}{2m_0} \qquad (14.27)$$

With it, the DEQ of the propagation of volume implies the following form of the SEQ:

$$i\hbar\partial_\tau \cdot |\psi\rangle = \frac{\hat{p}^2}{2m_0} \cdot |\psi\rangle \text{ non}-\text{relativistic SEQ} \qquad (14.28)$$

(5) More generally, a potential V_{pot} is added. With it, the DEQ of the propagation of volume implies the following form of the SEQ, which holds for matter:

$$i\hbar\partial_\tau|\psi\rangle = \left(\frac{\hat{p}^2}{2m_0} + V_{pot}\right)|\psi\rangle \quad \text{non-relativistic SEQ} \tag{14.29}$$

(6) Even more generally, an interaction can be included in the SEQ by using the principle of gauge invariance, see e. g. Landau and Lifschitz (1971), Weinberg (1996), Carmesin (2021e), Carmesin (2022e).

(7) The sign in the SEQ is a convention only, (Schrödinger, 1926b, p. 112). Thus, more adequately, the square of the SEQ describes nature. Indeed, that square is basically Lorentz invariant, see THM (14).

(8) The wave function is equal to the rate of formation of volume, multiplied by a normalization factor t_n:

$$\psi(\tau,\vec{L}) = t_n \cdot \dot{\varepsilon}(\tau,\vec{L}) \tag{14.30}$$

More adequately, you can omit the normalization, in order to use the full information about the rate. In QP, that information is not provided, so that the present theory of the dynamic volume includes quantum theory. But quantum theory does not include the present theory of the dynamics of volume.

14.2 Hilbert space

In this section, we derive the following postulate about Hilbert space (Kumar, 2018, p. 168):

Postulate 2 Hilbert space

'The state of a quantum mechanical system, at a given instant of time, is described by a vector $|\Psi(t)\rangle$, in the abstract Hilbert space $\mathcal{H}$ of the system.'

Derivation: Volume and matter propagate according to the SEQ, see theorems (12, 23, 24). So, volume and matter propagate according to a linear DEQ. The time derivative of a solution of that DEQ, $\dot{\varepsilon}(\tau, \vec{L})$, is used as a wave function Ψ, see section (14.1). In the Dirac notation, a wave function Ψ is named a state $|\Psi\rangle$.

Thereby, two wave functions, $\Psi_1(\tau, \vec{L})$ and $\Psi_2(\tau, \vec{L})$, form a scalar product as follows:

$$\langle \Psi_1 | \Psi_2 \rangle = \int d^3L \Psi_1^*(\tau, \vec{L}) \cdot \Psi_2(\tau, \vec{L}) \tag{14.31}$$

Hereby, the superscript $*$ marks the complex conjugate value, this is nowadays usual in quantum physics, see e. g. Griffiths (1994), Ballentine (1998), Scheck (2013), Kumar (2018).

Based on that scalar product, a state $|\Psi\rangle$ is multiplied by a normalization factor t_n so that the following scalar product is equal to one:

$$\langle \Psi \cdot t_n | \Psi \cdot t_n \rangle = \int d^3r \Psi^*(\vec{r}, t) \cdot \Psi(\vec{r}, t) \cdot |t_n|^2 = 1 \tag{14.32}$$

Next, we show that these states form a Hilbert space $\mathcal{H}$:

The states $\Psi(\vec{r}, t)$ form a **complete vector space**, as they are solutions of the linear and homogeneous SEQ, so that they form a linear vector space, and so that they include all linear combinations of states $\Psi(\vec{r}, t)$, including Fourier integrals, for instance. These form a complete Hilbert space $\mathcal{H}$, see e. g. (Teschl, 2014, p. 47) or (Sakurai and Napolitano, 1994, p. 57).

Altogether, the solutions of the DEQ of volume or matter form a Hilbert space $\mathcal{H}$. We summarize our finding.

Theorem 25 Volume implies the Hilbert space of states

(1) As natural volume propagates according to the Schrödinger equation, the states of volume are the solutions of the SEQ, so that they form a Hilbert space $\mathcal{H}$.

(2) As solutions of the DEQ of wave packets of volume or matter at $v < c$ obey the non-relativistic Schrödinger equation, such solutions form a Hilbert space $\mathcal{H}$ as well.

(3) As the rates ε_L of relative additional volume are solutions of the linear DEQ in THMs (38) or (18), these rates form a Hilbert space $\mathcal{H}$ as well.

14.3 Observables and operators

In this section, we derive the following postulate about the relation between observables and operators (Kumar, 2018, p. 169):

Postulate 3 Observables correspond to operators

'A measurable physical quantity A (called an observable or dynamic physical quantity), is represented by a linear and hermitian operator $\hat{A}$ acting in the Hilbert space of state vectors.'

Correspondence principle: We remind the correspondence of operators and physical quantities, see section (14.1.1): **If the application of an operator to the wave function provides a physical quantity, then that operator can be used to represent that physical quantity.** The postulate extends the above correspondence by an additional requirement: To each measurable physical quantity A, there corresponds a hermitian operator $\hat{A}$ acting in the Hilbert space.

Derivation:

(1) As the volume and the states achieved by phase transitions of volume include volume and matter, and as the quantization is universal (THM 5), each physical state is described by the SEQ or by an equation derived from the SEQ.

(2) Consequently, each physical state is a solution of the SEQ.

(3) As a consequence, each physical state is a state vector $|state\rangle$ in the Hilbert space $\mathcal{H}$ of the SEQ.

(4a) Consequently, each **physical function** A is a function $A(|state\rangle)$ of at least one state vector $|state\rangle$.

(4b) At first order, a physical function A is a linear function $\hat{A}|state\rangle$ of at least one state vector $|state\rangle$. That case is covered by the postulate (3). Thus, the present postulate includes the convention that a physical function of first order is a **measurable physical quantity or observable**.

(4bα) Hereby, the linear function is represented by a linear operator $\hat{A}$ acting in the Hilbert space of state vectors.

(4bβ) As each outcome of a measurement is real and member of a discrete or continuous set, the linear operator is a hermitian (or self-adjoint) operator, as such operators provide real eigenvalues that are members of a discrete or continuous set of eigenvalues (Teschl, 2014, THM 3.6 or spectral theorem):

$$\hat{A} = \hat{A}^\dagger \tag{14.33}$$

(4c) At second order, a physical function A is a quadratic function $A(|state\rangle^2)$ of at least one state vector $|state\rangle$. That case is covered by the postulate (14.6) below. It will turn out that the second order gives rise to a variety of probability densities ρ, including mixed states in postulate (6) and entanglement in section (14.10) below.

(4d) At order $n \geq 3$, a physical function A is an $n - th$ power $A(|state\rangle^n)$ of at least one state vector $|state\rangle$. That case is essential in dimensional phase transitions in chapter (22 below.

We summarize our derivation.

Theorem 26 Observables and hermitian operators

Observables and operators are related as follows:

(1) According to section (14.1), the physical states of volume and of matter fulfill the SEQ. Corresponding to universal quantization (THM 5), all physical states fulfill the SEQ.

(2) As a consequence, all physical states are solutions of of the SEQ or of a DEQ derived from the SEQ (chapter 15).

(3) As a consequence, all states form a Hilbert space $\mathcal{H}$.

(4a) Consequently, each **physical function** *A is a function $A(|state\rangle)$ of at least one state vector $|state\rangle$.*

(4b) At first order, a physical funtion A is a linear function $\hat{A}|state\rangle$ of at least one state vector $|state\rangle$. That case is covered by the postulate (3). Thus, the postulate describes a subset of possible physical functions A. The quantities in this subset are called **observables or measurable physical functions**, *as a convention. This does not restrict the generality of the system of postulates, as* **higher order physical functions** *are described by later postulates, see below. Hereby, the linear function is represented by a hermitian (or self-adjoint) linear operator $\hat{A}$ acting in the Hilbert space of state vectors.*

$$\hat{A} = \hat{A}^\dagger \tag{14.34}$$

(4c) At second order, a physical function A is a quadratic function $A(|state\rangle^2)$ of at least one state vector $|state\rangle$. That case describes probabilities, see postulate (14.6), mixed states, see postulate (6) and entanglement, see section (14.10).

(4d) At order $n \geq 3$, a physical function A is an $n-th$ power $A(|state\rangle^n)$ of at least one state vector $|state\rangle$.

(5) Altogether, the above items derive the postulate.

Corollary 19 Observables correspond to operators

According to THM (26), relative additional volume provides many physical functions and observables or measurable physical quantities. Moreover, relative additional volume provides the following properties:

(1) Relative additional volume ε_L propagates at $v = c$. Thus, it is quantized in the universal manner, see THM (5). Hence,

it can be described by the wave function $\Psi = t_n \cdot \dot{\varepsilon}_L$. Thence, quantum physical observables correspond to operators.

(2a) Thereby, relative additional volume ε_L provides the following properties:

(2b) The rate $\dot{\varepsilon}_L$ includes a description of gravity, see THM (17, 9). Thus, the quanta in part (1) include the quantum physical description of gravity.

(2c) The volume and the relative additional volume ε_L should represent the same volume. Thus, the relative additional volume provides curvature of spacetime and its structure as well as propagation, see THMs (1, 9, 12). Thus, the quanta in part (1) constitute the quantization of curvature of spacetime.

(2d) Furthermore, the relative additional volume ε_L provides the expansion of space since the Big Bang, see chapters (7, 9, 11,10, 12). Thus, the quanta in part (1) constitute the quantization of the expansion of space since the Big Bang.

14.4 Outcomes of measurements

In this section, we derive the following postulate about the relation between the possible outcomes of a measurement and the eigenvalues (Kumar, 2018, p. 169):

Postulate 4 Outcomes of measurements are eigenvalues

'The measurement of an observable A in a given state may be represented formally by the action of an operator $\hat{A}$ on the state vector $|\Psi(t)\rangle$. The only possible outcome of such a measurement is one of the eigenvalues, $\{a_j\}, j = 1, 2, 3, \dots,$ of $\hat{A}$.'

Derivation: That postulate has already been derived in section (14.3), see item (4b) in theorem (26).

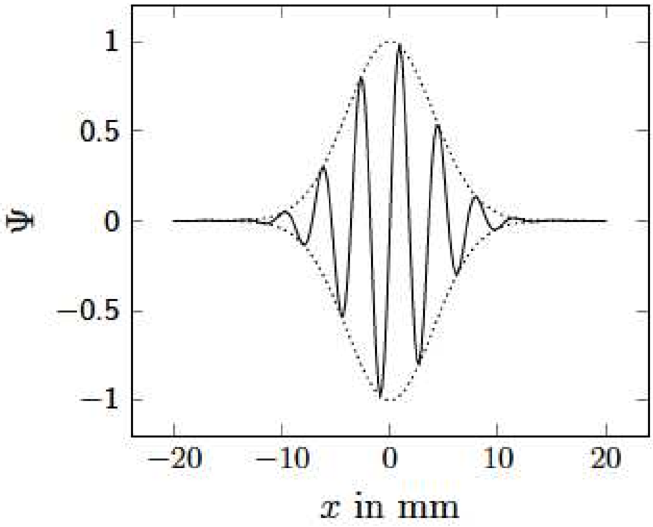

Figure 14.1: Wave packet at $t = 0$: $\Psi(t,x) = \sin(k \cdot x - \omega \cdot t) \cdot \exp(\frac{-x^2}{2 \cdot \sigma^2})$ (solid line). Envelope (dotted). $k = 100/\text{mm}$ and $\sigma = 4\text{mm}$.

14.4.1 On the physical reality of a state

An eigenvalue p_x of the momentum occurs at a corresponding eigenfunction. Such an eigenfunction can be a harmonic wave, for instance. E. g., $\Psi(x,t) = t_n \cdot \sin(k \cdot x - \omega \cdot t)$ is an eigenfunction of the momentum $p_x = \hbar \cdot k$. However, a harmonic function is infinitely extended in the x direction. Such a function is not part of physical reality, as the light horizon presents a limit of observation, see DEF (15).

A realistic state is a wave packet, see e. g. (Kumar, 2018, p. 61). For instance, the wave packet in Fig. (14.1) represents a single wave function and it exhibits several eigenvalues of the momentum. As that wave packet represents a single wave function, it is named a pure state, see e. g. (Ballentine, 1998, section 2.3). A mixture of several wave functions is named mixed state. These are described in section (14.7).

Corollary 20 Spectrum of relative additional volume

(1) Relative additional volume ε_L propagates at $v = c$. Thus,

it is quantized in the universal manner, see THM (5). If the quanta of relative additional volume ε_L propagate in free space, then harmonic waves with a basically continuous spectrum are solutions of the DEQ, see THM (13).

(2) Relative additional volume ε_L cannot be reflected. Thus, it cannot be captured in a resonator. Similarly, it cannot be captured by any interaction. Relative additional volume ε_L always propagates in the available possibly curved space in a free *manner. Waves propagating freely in space have a continuous spectrum.*

(3) Quanta of relative additional volume **have a causal horizon, the light horizon** R_{LH}. *Thus, causally connected waves are limited by R_{LH}. Thus, the waves have a causally open end at R_{LH}. Hence, the wavelengths have an almost continuous spectrum. Based on that limitation by R_{LH}, the density of volume has been derived, see chapter (22).*

(4) Altogether, in natural space, relative additional volume has a causal limitation at the light horizon at astronomically large wavelengths. Thus, the spectrum is almost continuous.

14.5 Energy of a wave packet of a RGW

Question: In chapter (4), we analyzed monochromatic waves. However, a quantum object represents a wave packet, see Fig. (14.1) or COR (9). What energy E_ω has a wave packet of a RGW at a central circular frequency ω_0? In this section, we analyze that question. Thereby, we achieve an especially deep understanding of the zero-point energy.

14.5.1 Modes of a wave packet of a RGW

Idea: A wave packet is a superposition of many modes of various wavelengths. We derive such a superposition by using (Carmesin, 2021d, section 5.6.4):

Superposition of modes in a wave packet:

A wave packet is polychromatic. It can be described as follows:

(1) **Orthonormal basis:** It is convenient to apply normalization factors ν. With these, we use functions, representing plane waves propagating in a direction $\vec{k}$:

$$b_\mu = \nu_b \cdot \exp(i\omega_\mu \cdot \tau) \;\text{ and }\; f_\mu = \nu_f \cdot \exp(-i\vec{k}_\mu \cdot \vec{L}) \quad (14.35)$$

So, we obtain a set of orthonormal basis functions. Hereby, we denote the complex conjugate by a star (for instance, f_μ^* is the complex conjugate of f_μ):

$$\int f_\mu \cdot f_{\mu'}^* \, d^3L = \delta_{\mu,\mu'} \quad (14.36)$$

(2) **Representation by orthonormal basis:** In that basis, an RGW has amplitudes $\hat{\varepsilon}_\mu$ of the monochromatic waves. So we get:

$$\varepsilon_L(\vec{L}, \tau) = \Sigma_\mu \hat{\varepsilon}_\mu \cdot b_\mu(\tau) \cdot f_\mu(\vec{L}) + \varepsilon_{\mu,const.} \quad (14.37)$$

Similarly, the potentials can be expressed with amplitudes $\hat{\phi}_\mu$:

$$\phi_L(\vec{L}, \tau) = \Sigma_\mu \hat{\phi}_\mu \cdot b_\mu(\tau) \cdot f_\mu(\vec{L}) + \phi_{\mu,const.} \quad (14.38)$$

We apply this representation to the energy density in chapters (6, 11). Thereby the squares represent absolute values:

$$u_{RGW}(\varepsilon_L, \phi_L) = \frac{c^2}{8\pi \cdot G} \cdot |\dot{\varepsilon}_L^2| - \frac{|(\partial_{\vec{L}} \phi_L)^2|}{8\pi \cdot G} \quad (14.39)$$

(3) **Polarization:** The RGW can oscillate in various directions represented by the tensors developed in chapter (10). In order to provide relatively short formulas, we include these tensors in the amplitude. So the index μ summarizes the indices of the basis function f_μ, of the polarization q, and of the tensor i and j. So we get:

$$\hat{\varepsilon}_\mu = \hat{\varepsilon}_{\mu,\text{amplitude of } f_\mu} \cdot \hat{\varepsilon}_{q,ij} \quad (14.40)$$

Correspondingly, the indices inherent to μ must be explicated, whenever they become essential.

(4) **Separation of modes μ:** Next, we separate the modes μ inherent to $|\dot{\varepsilon}_L^2|$. For it, we evaluate $|\dot{\varepsilon}_L^2|$ by using Eq. (14.37). Moreover, we replace the absolute values of a square z^2 of a complex number z by the product $z \cdot z^*$:

$$|\dot{\varepsilon}_L^2| = \Sigma_{\mu,\mu'}\hat{\varepsilon}_\mu\hat{\varepsilon}_{\mu'} \cdot \partial_\tau b_\mu \partial_\tau b^*_{\mu'} \cdot f_\mu f^*_{\mu'} = \Sigma_{\mu,\mu'}\omega_\mu\omega_{\mu'}\hat{\varepsilon}_\mu\hat{\varepsilon}_{\mu'} \cdot b_\mu b^*_{\mu'} \cdot f_\mu f^*_{\mu'} \tag{14.41}$$

Analogously we evaluate $|(\partial_{\vec{L}}\phi_L)^2|$:

$$|(\partial_{\vec{L}}\phi_L)^2| = \Sigma_{\mu,\mu'}\hat{\phi}_\mu\hat{\phi}_{\mu'} \cdot b_\mu b^*_{\mu'} \cdot \partial_{\vec{L}} f_\mu \partial_{\vec{L}} f^*_{\mu'} \tag{14.42}$$

We evaluate the derivative, and we apply $\hat{\phi}_\mu = \hat{\varepsilon}_\mu \cdot c^2$ (THM 13):

$$|(\partial_{\vec{L}}\phi_L)^2| = \Sigma_{\mu,\mu'}\vec{k}_\mu\vec{k}_{\mu'}\hat{\varepsilon}_\mu\hat{\varepsilon}_{\mu'} \cdot c^4 \cdot b_\mu b^*_{\mu'} \cdot f_\mu f^*_{\mu'} \tag{14.43}$$

Next, we insert Eqs. (14.42) and (14.43) into Eq. (14.39):

$$u_{RGW}(\varepsilon_L, \phi_L) = \Sigma_{\mu,\mu'}\hat{\varepsilon}_\mu\hat{\varepsilon}_{\mu'} \cdot b_\mu b^*_{\mu'} \cdot f_\mu f^*_{\mu'} \cdot \left(\frac{c^2\omega_\mu\omega_{\mu'}}{8\pi G} - \frac{c^4\vec{k}_\mu\vec{k}_{\mu'}}{8\pi G}\right) \tag{14.44}$$

In order to derive the energy, we integrate over the space:

$$E_{RGW} = \int u_{RGW}\, d^3L \tag{14.45}$$

(5) **Modes ranging up to R_{LH}:** In this part we integrate the modes ranging from zero towards the light horizon. We call the corresponding energy $E_{RGW,LH}$. Thereby, the light horizon is a function of time during the expansion since the Big Bang, and the essential light horizon has been elaborated in (Carmesin (2018c,b, 2019b,a)). We apply that range to Eq. (14.45):

$$E_{RGW,LH} = 4\pi \cdot \int_0^{R_{LH}} L^2 \cdot u_{RGW}\, dL \tag{14.46}$$

We insert Eq. (14.44), and we evaluate the integral (see Eq. 14.36) as well as $\delta_{\mu,\mu'}$. So we get:

$$E_{RGW,LH} = \frac{1}{2} \cdot \Sigma_\mu \hat{\varepsilon}_\mu \hat{\varepsilon}_\mu \cdot b_\mu b_\mu^* \cdot \frac{c^2}{G} \cdot \left(\omega_\mu^2 - c^2 \vec{k}_\mu^2\right) \qquad (14.47)$$

(6) **Generalized coordinates of RGWs $Q_\mu(t)$:** We introduce a **coordinate** Q_μ and its **momentum** P_μ with:

$$\boxed{Q_\mu = \hat{\varepsilon}_\mu \cdot b_\mu \cdot \frac{c}{\sqrt{G}} \text{ and } P_\mu = i\frac{dQ_\mu}{d\tau} \text{ and } P_\mu^* = -i\frac{dQ_\mu^*}{d\tau}} \qquad (14.48)$$

Hereby, we identify P_μ as a generalized momentum of Q_μ: In general, a momentum is a time derivative of a generalized coordinate multiplied by a generalized mass or factor of inertia. In the present case, the generalized factor of inertia is the complex unit i.

We determine derivatives as follows:

$$P_\mu P_\mu^* = \frac{dQ_\mu}{d\tau}\frac{dQ_\mu^*}{d\tau} = \omega_\mu^2 Q_\mu Q_\mu^* \qquad (14.49)$$

Moreover we utilize $\vec{k}_\mu^2 \cdot c^2 = \omega_\mu^2$:

$$P_\mu P_\mu^* = \vec{k}_\mu^2 \cdot c^2 Q_\mu Q_\mu^* \qquad (14.50)$$

We apply Eqs. (14.49) and (14.50) to Eq. (14.47):

$$\boxed{E_{RGW,LH} = \frac{1}{2} \cdot \Sigma_\mu \left(Q_\mu Q_\mu^* \cdot \omega_\mu^2 - P_\mu P_\mu^*\right)} \qquad (14.51)$$

For each mode, this energy is expressed in terms of a four-vector of generalized coordinates Q_μ and momenta $P_{\mu,j}$ with spatial Cartesian momenta $P_\mu P_\mu^* = \Sigma_{j=1}^3 P_{\mu,j} P_{\mu,j}^*$:

$$p_{\mu,i} = \begin{pmatrix} Q_\mu \cdot \omega_\mu \\ P_{\mu,1} \\ P_{\mu,2} \\ P_{\mu,3} \end{pmatrix} \quad \text{With it we get:} \qquad (14.52)$$

$$E_{RGW,LH} = \Sigma_\mu E_{RGW,LH,\mu} \text{ with } (14.53)$$
$$E_{RGW,LH,\mu} = \frac{1}{2} \cdot \Sigma_{j=0}^{j=3} p^*_{\mu,j} \bar{\eta}_{jj} p_{\mu,j} \text{ with } (14.54)$$
$$\bar{\eta}_{00} = 1 \text{ and } \bar{\eta}_{11} = \bar{\eta}_{22} = \bar{\eta}_{33} = -1. \text{ We summarize} : (14.55)$$

Theorem 27 Modes of wave packets of RGWs:

The energy $E_{RGW,LH}$ of a wave packet of a RGW is as follows:

(1) $E_{RGW,LH}$ is a sum of energies of modes:

$$E_{RGW,LH} = \frac{1}{2} \cdot \Sigma_\mu \hat{\varepsilon}_\mu \hat{\varepsilon}_\mu \cdot b_\mu b^*_\mu \cdot \frac{c^2}{G} \cdot \left(\omega^2_\mu - c^2 \vec{k}^2_\mu \right) \qquad (14.56)$$

The above bracket is a relativistic square of the following four-vector:

$$\begin{pmatrix} \omega_\mu \\ k_{\mu,1} \cdot c \\ k_{\mu,2} \cdot c \\ k_{\mu,3} \cdot c \end{pmatrix} \qquad (14.57)$$

Thus, that bracket is a Lorentz scalar and a Lorentz invariant.

(2) The energy $E_{RGW,LH}$ of a wave packet is a sum of energies $E_{RGW,LH,\mu}$ of its modes:

$$E_{RGW,LH} = \Sigma_\mu E_{RGW,LH,\mu} \text{ with} \qquad (14.58)$$
$$E_{RGW,LH,\mu} = \frac{1}{2} \cdot \Sigma_{j=0}^{j=3} p^*_{\mu,j} \bar{\eta}_{jj} p_{\mu,j} \text{ or} \qquad (14.59)$$
$$E_{RGW,LH,\mu} = \frac{1}{2} \cdot \left(Q_\mu Q^*_\mu \cdot \omega^2_\mu - P_\mu P^*_\mu \right) \qquad (14.60)$$

(3) Thereby, for each mode, the energy $E_{RGW,LH,\mu}$ is a square of the following four-vector of a generalized coordinate Q_μ and momenta $P_{\mu,j}$:

$$p_{\mu,i} = \begin{pmatrix} Q_\mu \cdot \omega_\mu \\ P_{\mu,1} \\ P_{\mu,2} \\ P_{\mu,3} \end{pmatrix} \qquad (14.61)$$

Thus, the energy $E_{RGW,LH,\mu}$ of each mode is a Lorentz scalar and a Lorentz invariant.

(4) Hereby, for each mode of the wave packet, the generalized coordinate and momenta are the following functions of the amplitude $\hat{\varepsilon}_\mu$ and of the time evolution b_μ of the mode:

$$Q_\mu = \hat{\varepsilon}_\mu \cdot b_\mu \cdot \frac{c}{\sqrt{G}} \quad \textit{and} \quad P_\mu = i\frac{dQ_\mu}{d\tau} \quad \textit{and} \quad P^*_\mu = -i\frac{dQ^*_\mu}{d\tau} \tag{14.62}$$

Consequently, for each mode, the energy $E_{RGW,LH,\mu}$ includes the amplitude and time evolution of the mode.

14.5.2 Hamilton operator of a mode of a RGW

Idea: A wave packet of a RGW is a superposition of many modes. For each mode, we derive the energy operator or Hamilton operator. For it, we apply the postulates (1, 2, 3, 4), see sections (14.1,14.2,14.3,14.4). Thereby, the Hamilton operator provides the time evolution, see postulate (1).

Energy operator of a mode:

(1) **Hamilton operator of a mode:** Each mode has the following energy, see THM (27):

$$E_{RGW,LH,\mu} = \frac{1}{2} \cdot \left(Q_\mu Q^*_\mu \cdot \omega_\mu^2 - P^*_\mu P_\mu\right) \tag{14.63}$$

According to the postulates (1-4), sections (14.1,14.2,14.3,14.4), we introduce operators for the observables energy $E_{RGW,LH,\mu}$, coordinate $\hat{Q}_\mu$ and momentum $\hat{P}_\mu$. So we get:

$$\hat{H}_\mu = \frac{1}{2} \cdot \left(\hat{Q}_\mu \hat{Q^*}_\mu \cdot \omega_\mu^2 - \hat{P}_\mu \hat{P^*}_\mu\right) \tag{14.64}$$

According to the postulates (1-4), sections (14.1,14.2,14.3,14.4), each generalized coordinate and momentum have the following commutator, see e. g. (Heisenberg (1927) or (Ballentine, 1998, p. 78 or sections 3.3 and 3.4) or (Grawert, 1977, p. 37)):

$$\hat{Q}_\mu \hat{P}_{\mu'} - \hat{P}_{\mu'} \hat{Q}_\mu = [\hat{Q}_\mu, \hat{P}_{\mu'}] = i \cdot \hbar \cdot \delta_{\mu,\mu'} \tag{14.65}$$

This relation can be derived as follows:

$$\begin{aligned}
[\hat{Q}_k, \hat{P}_j]\Psi &= (\hat{Q}_k\hat{P}_j - \hat{P}_j\hat{Q}_k)\Psi \\
[\hat{Q}_k, \hat{P}_j]\Psi &= Q_k\frac{\hbar}{i}\partial_j\Psi - \frac{\hbar}{i}\partial_j(Q_k\Psi) \\
[\hat{Q}_k, \hat{P}_j]\Psi &= -\frac{\hbar}{i}\delta_{k,j} = i\hbar \cdot \delta_{k,j} \qquad (14.66)
\end{aligned}$$

(2) **Linear transformation:** In order to derive ladder operators, see for instance (Ballentine, 1998, p. 152), we apply a linear transformation to operators $\hat{a}_\mu^+$ and $\hat{a}_\mu$ as follows:

$$\hat{Q}_\mu \cdot \omega_\mu = \alpha_\mu \left(\hat{a}_\mu^+ + \hat{a}_\mu\right) \qquad (14.67)$$

$$\hat{P}_\mu = i \cdot \alpha_\mu \left(\hat{a}_\mu^+ - \hat{a}_\mu\right) \qquad (14.68)$$

Hereby the parameter α_μ is determined so that the commutation relation of coordinate and momentum in Eq. (14.65) implies the following commutation relation of ladder operators:

$$[\hat{a}_{\mu'}, \hat{a}_\mu^+] = \delta_{\mu,\mu'} \qquad (14.69)$$

In order to derive the commutation relation (Eq. 14.69), we insert Eqs. (14.67, 14.68) into Eq. (14.65):

$$[\hat{Q}_\mu, \hat{P}_{\mu'}] = \frac{2i\alpha_\mu^2}{\omega_\mu} \cdot [\hat{a}_\mu, \hat{a}_{\mu'}^+] = \frac{2i\alpha_\mu^2}{\omega_\mu} \cdot \delta_{\mu,\mu'} \qquad (14.70)$$

We compare this term with Eq. (14.65). So we get:

$$\frac{2i\alpha_\mu^2}{\omega_\mu} = i \cdot \hbar \;\text{ or }\; \alpha_\mu = \sqrt{\hbar\omega_\mu/2} \qquad (14.71)$$

Altogether, we derived the commutation relation in Eq. (14.69), and we obtain the following transformation:

$$\hat{Q}_\mu \cdot \omega_\mu = \sqrt{\hbar\omega_\mu/2}\left(\hat{a}_\mu^+ + \hat{a}_\mu\right) \qquad (14.72)$$

$$-i\hat{P}_\mu = \sqrt{\hbar\omega_\mu/2}\left(\hat{a}_\mu^+ - \hat{a}_\mu\right) \qquad (14.73)$$

(3) **Inverse transformation:** From the above Eqs., the inverse transformation is derived by solving for $\hat{a}_\mu$ and $\hat{a}_\mu^+$. Thus, we get:

$$\hat{a}_\mu^+ = (\hat{Q}_\mu \cdot \omega_\mu - i\hat{P}_\mu)/\sqrt{2\hbar\omega_\mu} \tag{14.74}$$

$$\hat{a}_\mu = (\hat{Q}_\mu \cdot \omega_\mu + i\hat{P}_\mu)/\sqrt{2\hbar\omega_\mu} \tag{14.75}$$

(4) **Energy operator:** We insert the operators of the coordinate $\hat{Q}_\mu$ and momentum $\hat{P}_\mu$ (Eqs. 14.72, 14.73) into Eq. (14.64). For it, we derive the products

$$\hat{Q}_\mu \hat{Q}^*{}_\mu \cdot \omega_\mu^2 = \frac{\hbar\omega_\mu}{2} \cdot \left(\hat{a}_\mu^+ \hat{a}_\mu^+ + \hat{a}_\mu \hat{a}_\mu^+ + \hat{a}_\mu^+ \hat{a}_\mu + \hat{a}_\mu \hat{a}_\mu\right) \tag{14.76}$$

$$\text{and } \hat{P}_\mu \hat{P}^*{}_\mu = \frac{\hbar\omega_\mu}{2} \cdot \left(\hat{a}_\mu^+ \hat{a}_\mu^+ - \hat{a}_\mu \hat{a}_\mu^+ - \hat{a}_\mu^+ \hat{a}_\mu + \hat{a}_\mu \hat{a}_\mu\right) \tag{14.77}$$

Thus, the energy operator is the difference of these products multiplied by one half:

$$\hat{H}_\mu = \frac{1}{2} \cdot \hbar\omega_\mu \cdot \left(\hat{a}_\mu \cdot \hat{a}_\mu^+ + \hat{a}_\mu^+ \cdot \hat{a}_\mu\right) \tag{14.78}$$

We apply the commutator. So we get:

$$\hat{H}_\mu = \hbar\omega_\mu \cdot \left(\hat{a}_\mu^+ \cdot \hat{a}_\mu + 1/2\right). \quad \text{We summarize :} \tag{14.79}$$

Theorem 28 Energy operator of mode of a RGW:

Each mode of a wave packet, see THM (27), has an energy operator or Hamilton operator as follows:

(1) The energy operator can be expressed as a function of the operators of generalized coordinate and momentum:

$$\hat{H}_\mu = \frac{1}{2} \cdot \left(\hat{Q}_\mu \hat{Q}^*{}_\mu \cdot \omega_\mu^2 - \hat{P}_\mu \hat{P}^*{}_\mu\right) \tag{14.80}$$

(2) The operators of generalized coordinate and momentum are transformed to ladder operators:

$$\hat{a}_\mu^+ = (\hat{Q}_\mu \cdot \omega_\mu - i\hat{P}_\mu)/\sqrt{2\hbar\omega_\mu} \tag{14.81}$$

$$\hat{a}_\mu = (\hat{Q}_\mu \cdot \omega_\mu + i\hat{P}_\mu)/\sqrt{2\hbar\omega_\mu} \tag{14.82}$$

(3) The energy operator can be expressed as a function of the ladder operators:

$$\boxed{\hat{H}_\mu = \hbar\omega_\mu \cdot \left(\hat{a}_\mu^+ \cdot \hat{a}_\mu + 1/2\right)} \tag{14.83}$$

14.5.3 Number states of a mode of a RGW

Idea: Each mode of a RGW has the Hamilton operator $\hat{H}_\mu$ in THM (28). With it, we derive the energy spectrum for each mode:

(1) **Essential operator in $\hat{H}_\mu$:** We analyze the operator $\hat{a}_\mu^+\hat{a}_\mu$ in $\hat{H}_\mu$, usually called **number operator**:

$$\hat{N}_\mu = \hat{a}_\mu^+\hat{a}_\mu \tag{14.84}$$

Moreover we call its normalized Eigenstates $|n_\mu\rangle$ and the eigenvalues n_μ:

$$\hat{N}_\mu \cdot |n_\mu\rangle = n_\mu \cdot |n_\mu\rangle \tag{14.85}$$

(2) **Eigenstates of the number operator:** We apply $\hat{N}_\mu$ to $\hat{a}_\mu \cdot |n_\mu\rangle$, and we use the commutator. So we get:

$$\hat{N}_\mu \cdot \hat{a}_\mu \cdot |n_\mu\rangle = \hat{a}_\mu \cdot (n_\mu - 1) \cdot |n_\mu\rangle = (n_\mu - 1) \cdot \hat{a}_\mu \cdot |n_\mu\rangle \tag{14.86}$$

This Eq. shows that $\hat{a}_\mu \cdot |n_\mu\rangle$ is an Eigenstate with the eigenvalue $n_\mu - 1$.

Similarly we apply $\hat{N}_\mu$ to $\hat{a}_\mu^+ \cdot |n_\mu\rangle$, and we utilize the commutator. So we obtain:

$$\hat{N}_\mu \cdot \hat{a}_\mu^+ \cdot |n_\mu\rangle = \hat{a}_\mu^+ \cdot (n_\mu + 1) \cdot |n_\mu\rangle = (n_\mu + 1) \cdot \hat{a}_\mu^+ \cdot |n_\mu\rangle \tag{14.87}$$

This Eq. shows that $\hat{a}_\mu^+ \cdot |n_\mu\rangle$ is an Eigenstate to the eigenvalue $n_\mu + 1$.

(3) **Effect of ladder operators:** Firstly, we analyze the matrix element $\langle n_\mu|\hat{a}_\mu\hat{a}_\mu^+|n_\mu\rangle$. Here we identify the number operator:

$$\langle n_\mu|\hat{a}_\mu\hat{a}_\mu^+|n_\mu\rangle = \langle n_\mu|\hat{N}_\mu + 1|n_\mu\rangle = (n_\mu + 1)\langle n_\mu|n_\mu\rangle = n_\mu + 1 \tag{14.88}$$

Secondly, we analyze the matrix element $\langle n_\mu|\hat{a}_\mu^+\hat{a}_\mu|n_\mu\rangle$. As above, we identify the number operator:

$$\langle n_\mu|\hat{a}_\mu^+\hat{a}_\mu|n_\mu\rangle = \langle n_\mu|\hat{N}_\mu|n_\mu\rangle = (n_\mu)\langle n_\mu|n_\mu\rangle = n_\mu \tag{14.89}$$

Both Eqs. (14.88, 14.89) are fulfilled by the following relations:

$$\hat{a}_\mu^+|n_\mu\rangle = \sqrt{n_\mu + 1}|n_\mu + 1\rangle \tag{14.90}$$

$$\hat{a}_\mu|n_\mu\rangle = \sqrt{n_\mu}|n_\mu - 1\rangle \tag{14.91}$$

We summarize the matrix elements of the ladder operator $\hat{a}_\mu^+$ as follows:

$$\boxed{\langle n'_\mu|\hat{a}_\mu^+|n_\mu\rangle = \sqrt{n_\mu + 1}\cdot\delta_{n'_\mu,n_\mu+1}} \tag{14.92}$$

Accordingly, the ladder operator $\hat{a}_\mu^+$ is called **raising operator**. Similarly, the matrix elements of $\hat{a}_\mu$ are represented as follows:

$$\boxed{\langle n'_\mu|\hat{a}_\mu|n_\mu\rangle = \sqrt{n_\mu}\cdot\delta_{n'_\mu,n_\mu-1} \text{ for } n_\mu > 0} \tag{14.93}$$

Correspondingly, the ladder operator $\hat{a}_\mu$ is called **lowering operator.**

(4) **Spectrum:** In order to derive the full spectrum of the number operator, we show that the lowering of states ends at the state $|n_\mu\rangle = 0$:

$$\hat{a}_\mu|1\rangle = \sqrt{1}|0\rangle \text{ and } \hat{a}_\mu|0\rangle = \sqrt{0}|-1\rangle = 0 \tag{14.94}$$

Starting at this state, the raising operator can successively create the states with all positive natural numbers:

$$\boxed{n_\mu \in \{0, 1, 2, 3, ...\}} \tag{14.95}$$

(5) **Zero-point energy of a mode μ:** The spectrum of the number operator has the smallest value zero at the state $|0\rangle$. However, the eigenvalue of the energy of the state $|0\rangle$ is $\hbar\omega_\mu/2$, it can be derived as follows:

$$\langle 0|\hat{H}_\mu|0\rangle = \hbar\omega_\mu \cdot (\langle 0|\hat{N}_\mu|0\rangle + \langle 0|1/2|0\rangle) = \hbar\omega_\mu \cdot (0+1/2) \quad (14.96)$$

This energy $\hbar\omega_\mu/2$ is the **zero - point energy, ZPE** of the mode μ of the RGW:

$$\boxed{ZPE_\mu = \hbar\omega_\mu \cdot 1/2} \quad (14.97)$$

We summarize our results:

Theorem 29 Quantization of modes of RGW:

Each mode in THMs (27, 28) of a wave packet of a RGW is quantized as follows:

(1) The generalized coordinate and momentum of each mode are quantized by application of the usual commutation rule:

$$[\hat{Q}_\mu, \hat{P}_{\mu'}] = i \cdot \hbar \cdot \delta_{\mu,\mu'} \quad (14.98)$$

(2) The generalized coordinate and momentum are transformed to ladder operators:

$$\hat{a}_\mu^+ = (\hat{Q}_\mu \cdot \omega_\mu - i\hat{P}_\mu)/\sqrt{2\hbar\omega_\mu} \quad (14.99)$$

$$\hat{a}_\mu = (\hat{Q}_\mu \cdot \omega_\mu + i\hat{P}_\mu)/\sqrt{2\hbar\omega_\mu} \quad (14.100)$$

(3) As a consequence, the ladder operators obey the following commutation rule of bosons:

$$[\hat{a}_{\mu'}, \hat{a}_\mu^+] = \delta_{\mu,\mu'} \quad (14.101)$$

(4) Hence there is the following number operator

$$\hat{N}_\mu = \hat{a}_\mu^+ \hat{a}_\mu \quad (14.102)$$

and its eigenstates are the number states $|n_\mu\rangle$ with the following eigenvalues:

$$n_\mu \in \{0, 1, 2, 3, ...\} \qquad (14.103)$$

(5) So the energy operator is expressed by the number operator:

$$\hat{H}_\mu = \hbar\omega_\mu \cdot \left(\hat{a}_\mu^+ \cdot \hat{a}_\mu + 1/2\right) = \hbar\omega_\mu \cdot \left(\hat{N}_\mu + 1/2\right) \qquad (14.104)$$

(6) Thus the ladder operators raise or lower the numbers:

$$\langle n'_\mu|\hat{a}_\mu^+|n_\mu\rangle = \sqrt{n_\mu + 1} \cdot \delta_{n'_\mu, n_\mu+1} \qquad (14.105)$$

$$\langle n'_\mu|\hat{a}_\mu|n_\mu\rangle = \sqrt{n_\mu} \cdot \delta_{n'_\mu, n_\mu-1} \;\; for \;\; n_\mu > 0 \qquad (14.106)$$

(7) The zero-point energy, ZPE, is as follows:

$$ZPE_\mu = \hbar\omega_\mu \cdot 1/2 \qquad (14.107)$$

(8) Inherent to the quantized RGWs, there is only one restriction of the wavelengths: the light horizon, R_{LH}, inherent to the modes of the RGWs. Thus, the quantized modes of a wave packet of a RGW exhibit a continuous spectrum at a very good approximation only limited by R_{LH}.

(9) Each mode of a wave packet of a RGW represents a generalized coordinate $\hat{Q}_\mu$, which represents the amplitude $\hat{\varepsilon}_\mu$ of volume ε_L.

(9a) According to the Higgs mechanism, volume can transform to matter, see e. g. Higgs (1964), Carmesin (2021a), Carmesin (2022c). Thereby, an excited state at $n_\mu \geq 1$ can occur.

(9b) Natural volume is not an excited state, as otherwise energy of natural volume could be transformed to another energy. Thus, natural volume is a zero-point oscillation, ZPO. It is at $n_\mu = 0$, and it has the ZPE. A portion of natural volume is a wave packet, it is formed by a superposition of modes ZPE_μ.

Thereby, the portion inherits a positive energy $ZPE_\mu > 0$. Furthermore, the modes of a portion inherit the Lorentz invariance from the Lorentz invariance of the generalized coordinate $\hat{Q}_\mu$.

(9c) A state at $n_\mu \geq 1$ can be achieved from a ZPO by an excitation, for details see Carmesin (2021a), Carmesin (2021e), Carmesin (2022e).

14.6 Probabilistic outcomes

In this section, we derive the following postulate about probabilistic outcomes of measurements (Kumar, 2018, p. 169, 170). Hereby, the used eigenfunctions form an orthonormal basis, (Kumar, 2018, p. 169):

Postulate 5 Probabilistic outcomes of measurements

If a measurement of an observable A is made in a state $|\Psi(t)\rangle$ of the quantum mechanical system, then the following holds:

(1) The probability of obtaining one of the non-degenerate discrete eigenvalues a_j of the corresponding operator $\hat{A}$ is given by

$$P(a_j) = \frac{|\langle\phi_j|\Psi\rangle|^2}{\langle\Psi|\Psi\rangle}, \tag{14.108}$$

where $|\phi_j\rangle$ is the eigenfunction of $\hat{A}$ with the eigenvalue a_j. If the state vector is normalized to unity, $P(a_j) = |\langle\phi_j|\Psi\rangle|^2$.

(2) If the eigenvalue a_j is m_j-fold degenerate, this probability is given by

$$P(a_j) = \frac{\Sigma_{i=1}^{m_j}|\langle\phi_{j,i}|\Psi\rangle|^2}{\langle\Psi|\Psi\rangle}, \tag{14.109}$$

(3) If the operator $\hat{A}$ possesses a continuous eigenspectrum $\{a\}$, the probability that the result of a measurement will yield a value

between a and $a + da$ is given by

$$P(a) = \frac{|\langle\phi(a)|\Psi\rangle|^2}{\langle\Psi|\Psi\rangle} da = \frac{|\langle\phi(a)|\Psi\rangle|^2}{\int_{-\infty}^{\infty} |\Psi(a')|^2 da'} da \qquad (14.110)$$

Derivation: In the following, we derive the probabilistic outcomes of measurements, and we derive the probabilities.

14.6.1 Necessity of probabilistic outcomes

In the present theory based on the SQ, randomness is a necessary consequence for the following reason:

We analyze an object emitted at $\vec{r} = \vec{0}$ in an isotropic manner. Its wave function Ψ spreads in an isotropic manner.

Hereby, Ψ is proportional to the rate $\dot{\varepsilon}_L$. As the wave function Ψ represents the object, Ψ is a wave packet with a positive energy $E_{packet} > 0$, see THM (29). Thus, the wave packet has a positive energy density $u(\Psi) > 0$.

As a result of the isotropic spreading, after some time, the amplitude of Ψ is small. Thereby, at a location $\vec{r}$ and at a volume dV, the energy

$$dE(\vec{r}, dV) = u(\Psi(\vec{r})) \cdot dV \qquad (14.111)$$

can be insufficient for the formation of the energy $E_{packet} > 0$ of the object.

As a consequence, the object forms in a probabilistic manner at the location $\vec{r}$ and at the volume dV.

14.6.2 Probability of observation of an object

In this section, we analyze the probability $p(\vec{r}, dV)$ to measure an object described by a wave packet within a volume dV at a location $\vec{r}$. Thereby, the wave packet has a positive energy $E_{packet} > 0$. Moreover, the corresponding energy density of the wave packet is described by the density $u_{kin}(\vec{r})$ of the kinetic energy, see C. (13).

In this section, we show that the probability $p(\vec{r}, dV)$ is proportional to the energy density $u_{kin}(\vec{r})$ of the wave packet at that volume:

$$\boxed{p(\vec{r}, dV) \propto u_{kin}(\vec{r})} \tag{14.112}$$

This relation is derived as follows:

(1) If N objects are emitted at $\vec{r} = \vec{0}$, and if N_{obs} objects are detected at the location $\vec{r}$ and within a volume dV, the **relative frequency** $\bar{N}_{obs}$ in statistics is as follows, see (Olofsson and Andersson, 2012, p. 2):

$$\bar{N}_{obs} = \frac{N_{obs}}{N} \tag{14.113}$$

(2) According to the (empirical) law of large numbers, see e. g. Kolmogorov (1956), in the limit N to infinity, the expectation value and the probability describe experiments in a precise manner. Correspondingly, the probability $p(\vec{r}, dV)$ is the limit N to infinity of the relative frequency $\bar{N}_{obs}$:

$$\lim_{N \to \infty} \bar{N}_{obs} = p(\vec{r}, dV) \tag{14.114}$$

(3) The expectation value of the energy at the location $\vec{r}$ and within a volume dV is the probability $p(\vec{r}, dV)$ to measure an object multiplied with its energy E_{packet}:

$$\langle dE(\vec{r}, dV) \rangle = p(\vec{r}, dV) \cdot E_{packet} \tag{14.115}$$

(4) The energy density $u_{kin}(\vec{r})$ of the wave packet is the ratio of the expectation value $\langle dE(\vec{r}, dV) \rangle$ and the volume dV:

$$u_{kin}(\vec{r}) = \frac{\langle dE(\vec{r}, dV) \rangle}{dV} = \frac{p(\vec{r}, dV) \cdot E_{packet}}{dV} \propto p(\vec{r}, dV) \tag{14.116}$$

This shows the relation in Eq. (14.112).

14.6.3 Probability $p(t, \vec{r})$ proportional to $|\Psi(t, \vec{r})|^2$

Question: How is the energy density $u_{kin}(\vec{r})$ related to the wave function?

(1) The energy density $u_{kin}(\vec{r})$ of the kinetic energy is proportional to the square of the rates, see part (II) and C. (13):

$$u_{kin}(\vec{r}) \propto \dot{\varepsilon}_L^2(\vec{r}) \tag{14.117}$$

As the rate is proportional to the wave function Ψ, the energy density is proportional to the absolute square of Ψ:

$$u_{kin}(\vec{r}) \propto \langle\Psi|\Psi\rangle(\vec{r}) \tag{14.118}$$

(2) The probability $p(t, \vec{r}, dV)$ to measure an object described by a wave packet within a volume dV at a location $\vec{r}$ and at a time t is equal to a probability density function $f_R(t, \vec{r})$ at $\vec{r}$ and at t multiplied by dV, Olofsson and Andersson (2012), Jahnke et al. (2005), Müller (1975), Ash (2008):

$$p(t, \vec{r}, dV) = f_R(t, \vec{r}) \cdot dV \tag{14.119}$$

Thereby, the probability density function is proportional to the energy density u_{kin} (Eq. 14.116), which is proportional to the absolute square of Ψ (Eq. 14.118):

$$f_R(\vec{r}) \propto |\Psi(\vec{r})|^2 \tag{14.120}$$

Next, we normalize the above probability density function:

$$f_R(\vec{r}) = \frac{|\Psi(\vec{r})|^2}{\langle\Psi|\Psi\rangle} \text{ with } \langle\Psi|\Psi\rangle = \int d\vec{r}\,'\Psi^{cc}(\vec{r}\,')\Psi(\vec{r}\,')$$
$$\Psi^{cc} = \text{ complex conjugated of } \Psi \tag{14.121}$$

14.6.4 Probability $P(a_j)$ in item (1)

In this section, we derive item (1) of the postulate.

Derivation of the probability: For it, we use the probability density function in Eq. (14.121), and we apply the Dirac notation (Kumar, 2018, section 4.2):

$$f_R(\vec{r}) = \frac{|\Psi(\vec{r})|^2}{\langle\Psi|\Psi\rangle} \quad \text{with} \quad |\Psi(\vec{r})|^2 = \Psi^{cc}(\vec{r}) \cdot \Psi(\vec{r})$$
$$\text{and} \quad \Psi(\vec{r}) = |\Psi(\vec{r})\rangle \quad \text{and} \quad \Psi^{cc}(\vec{r}) = \langle\Psi(\vec{r})|$$
$$\text{and} \quad \int d\vec{r}|\Psi(\vec{r})|^2 = \langle\Psi|\Psi\rangle \quad (14.122)$$

In order to obtain the traditional form of the postulate, we transform the probability density function to the probability. For it, we multiply by dV:

$$p(\vec{r}, dV) = f_R(\vec{r}) \cdot dV = \frac{|\Psi(\vec{r})|^2}{\langle\Psi|\Psi\rangle} \cdot dV \quad (14.123)$$

Next, we apply the integral $\int d\vec{r}$ to Eq. (14.123), and we divide by dV:

$$\int d\vec{r} p(\vec{r}, dV)/dV = \int d\vec{r} f_R(\vec{r}) = \frac{\int d\vec{r}|\Psi(\vec{r})|^2}{\langle\Psi|\Psi\rangle} \quad (14.124)$$

Transformation of the numerator: The numerator in the above Eq. (14.124) is expressed as a scalar product:

$$\int d\vec{r}|\Psi(\vec{r})|^2 = \langle\Psi|\Psi\rangle \quad (14.125)$$

Next, we transform the state $|\Psi\rangle$ with the orthonormal[3] eigenvectors $|\Phi_j\rangle$ in item (1). So, we expand the ket $|\Psi\rangle$ as follows (Kumar, 2018, Eq. 4.7.1):

$$|\Psi\rangle = \sum_j |\Phi_j\rangle\langle\Phi_j|\Psi\rangle \quad (14.126)$$

[3]The eigenvectors of a hermitian operator are orthogonal (Kumar, 2018, THM 4.6.2), and we normalize them.

Similarly, we transform the bra $\langle\Psi|$:

$$\langle\Psi| = \sum_k \langle\Psi|\Phi_k\rangle\langle\Phi_k|, \quad \text{thus,} \tag{14.127}$$

$$\int d\vec{r}|\Psi(\vec{r})|^2 = \langle\Psi|\Psi\rangle = \sum_k \sum_j \langle\Psi|\Phi_k\rangle\langle\Phi_k|\Phi_j\rangle\langle\Phi_j|\Psi\rangle \tag{14.128}$$

As the eigenfunctions are orthonormal, the above scalar product $\langle\Phi_k|\Phi_j\rangle$ is equal to the Kronecker delta δ_{kj} (Kumar, 2018, example 4.11.1):

$$\int d\vec{r}|\Psi(\vec{r})|^2 = \sum_k \sum_j \langle\Psi|\Phi_k\rangle\delta_{kj}\langle\Phi_j|\Psi\rangle \tag{14.129}$$

Using the Kronecker delta δ_{kj}, we evaluate one of the sums:

$$\int d\vec{r}|\Psi(\vec{r})|^2 = \sum_j \langle\Psi|\Phi_j\rangle \cdot \langle\Phi_j|\Psi\rangle \tag{14.130}$$

The product of the two scalar products in the above Eq. is equal to the absolute square of one scalar product:

$$\int d\vec{r}|\Psi(\vec{r})|^2 = \sum_j |\langle\Phi_j|\Psi\rangle|^2 \tag{14.131}$$

Transformed probability: Next, we apply the above integral to the integral of the probability in Eq. (14.124):

$$\int d\vec{r}p(\vec{r}, dV)/dV = \int d\vec{r} f_R(\vec{r}) = \sum_j \frac{|\langle\Phi_j|\Psi\rangle|^2}{\langle\Psi|\Psi\rangle} \tag{14.132}$$

The integral of the probability density function provides the complete probability one, $\int d\vec{r} f_R(\vec{r}) = 1$. Similarly, the integral $\int d\vec{r}p(\vec{r}, dV)/dV = 1$ provides the whole probability. Correspondingly, the sum $\sum_j$ is a sum of probabilities P_j as follows:

$$1 = \sum_j P_j \ \text{ with } \ P_j = \frac{|\langle\Phi_j|\Psi\rangle|^2}{\langle\Psi|\Psi\rangle} \tag{14.133}$$

Hereby, the scalar product $\langle\Phi_j|\Psi\rangle$ describes the projection of a wave function $|\Psi(t,\vec{r})\rangle$ to the new basis vector $|\Phi_j\rangle$ in Eq. (14.126). In the following, we do not mark the time, according to the postulate (5). Correspondingly, P_j is the probability to find the eigenvalue a_j of the new basis vector $|\Phi_j\rangle$ in the projection of $|\Psi(\vec{r})\rangle$. So, we mark that probability by $P_{|\Psi(\vec{r})\rangle}(a_j)$:

$$P_j = P_{|\Psi(\vec{r})\rangle}(a_j) = \frac{|\langle\Phi_j|\Psi\rangle|^2}{\langle\Psi|\Psi\rangle} \tag{14.134}$$

For comparison, the probability $P(a_j)$ in item (1) of the postulate describes the probability to find the eigenvalue a_j of the new basis vector $|\Phi_j\rangle$ in the projection of $|\Psi\rangle$. We mark the respective state, and we remind the term in that item (1):

$$P_{|\Psi\rangle}(a_j) = \frac{|\langle\Phi_j|\Psi\rangle|^2}{\langle\Psi|\Psi\rangle} \tag{14.135}$$

Thus, we derived the probability in item (1).

14.6.5 Probability $P(a_j)$ in item (2)

In this section, we derive item (2) of the postulate.

Transformation of the numerator in Eq. (14.124): In the numerator in Eq. (14.124), we transform the state $|\Psi\rangle$ to the orthonormal[4] eigenvectors $|\Phi_{j,i}\rangle$ in item (2). In order to transform the ket $|\Psi\rangle$ and bra $\langle\Psi|$, we expand in terms of the new basis[5] (Kumar, 2018, Eq. 4.7.1):

$$|\Psi\rangle = \sum_j \sum_{i=1}^{m_j} |\Phi_{j,i}\rangle\langle\Phi_{j,i}|\Psi\rangle$$

[4]The eigenvectors of a hermitian operator and of different eigenvalues are orthogonal (Kumar, 2018, theorem 4.6.2), those of equal eigenvalues can be chosen orthogonal, and all eigenvectors can be normalized in addition.

[5]In principle, the upper bounds of the sum can tend to infinity.

$$\langle\Psi| = \sum_k \sum_{n=1}^{m_k} \langle\Psi|\Phi_{k,n}\rangle\langle\Phi_{k,n}| \tag{14.136}$$

Next, we apply the above transformations to the numerator in Eqs. (14.123, 14.125):

$$\int d\vec{r}|\Psi(\vec{r})|^2 = \langle\Psi|\Psi\rangle =$$

$$\sum_k \sum_{n=1}^{m_k} \sum_j \sum_{i=1}^{m_j} \langle\Psi|\Phi_{k,n}\rangle\langle\Phi_{k,n}|\Phi_{j,i}\rangle\langle\Phi_{j,i}|\Psi\rangle \tag{14.137}$$

The scalar product $\langle\Phi_{k,n}|\Phi_{j,i}\rangle$ in the above Eq. is equal to the product of Kronecker deltas $\delta_{kj}\delta_{in}$:

$$\int d\vec{r}|\Psi(\vec{r})|^2 = \sum_k \sum_{n=1}^{m_k} \sum_j \sum_{i=1}^{m_j} \langle\Psi|\Phi_{k,n}\rangle\delta_{kj}\delta_{in}\langle\Phi_{j,i}|\Psi\rangle \tag{14.138}$$

Using the Kronecker deltas $\delta_{kj}\delta_{in}$, we evaluate two of the sums:

$$\int d\vec{r}|\Psi(\vec{r})|^2 = \sum_j \sum_{i=1}^{m_j} \langle\Psi|\Phi_{j,i}\rangle\langle\Phi_{j,i}|\Psi\rangle \tag{14.139}$$

The product of two scalar products in the above Eq. is equal to the absolute square of one scalar product:

$$\int d\vec{r}|\Psi(\vec{r})|^2 = \sum_j \sum_i^{m_j} |\langle\Phi_{j,i}|\Psi\rangle|^2 \tag{14.140}$$

Transformed probability: In the numerator of the probability in Eq. (14.124), we insert the transformed scalar product in Eq. (14.140):

$$\int d\vec{r}\frac{p(\vec{r}, dV)}{dV} = \int d\vec{r} f_R(\vec{r}) = \sum_j \frac{\sum_i^{m_j} |\langle\Phi_{j,i}|\Psi\rangle|^2}{\langle\Psi|\Psi\rangle} \tag{14.141}$$

In the above Eq., the lhs is a probability. Correspondingly, the rhs is a sum of probabilities P_j as follows:

$$\begin{aligned} 1 &= \int d\vec{r}\,\frac{p(\vec{r},dV)}{dV} = \sum_j P_j \text{ with} \\ P_j &= \frac{\sum_i^{m_j} |\langle\Phi_{j,i}|\Psi\rangle|^2}{\langle\Psi|\Psi\rangle} \end{aligned} \tag{14.142}$$

Similarly as in item (1), P_j is the probability to find the eigenvalue a_j of the new basis vector $|\Phi_{j,i}\rangle$ in the projection of $|\Psi\rangle$. Correspondingly, we name that state by $P_{|\Psi\rangle}(a_j)$:

$$P_j = P_{|\Psi\rangle}(a_j) = P(a_j) = \frac{\sum_i^{m_j} |\langle\Phi_{j,i}|\Psi\rangle|^2}{\langle\Psi|\Psi\rangle} \tag{14.143}$$

So, we derived the probability $P(a_j)$ in item (2) of the postulate.

14.6.6 Probability $P(a)$ in item (3)

In this section, we derive item (3) of the postulate.

Transformation of the numerator in Eq. (14.124): We transform the state $|\Psi\rangle$ to the orthonormal eigenvectors $|\Phi(a)\rangle$ in item (3). In order to transform the ket $|\Psi\rangle$ and bra $\langle\Psi|$, we expand in terms of the new basis (Kumar, 2018, Eq. 4.7.1):

$$\begin{aligned} |\Psi\rangle &= \int da |\Phi(a)\rangle\langle\Phi(a)|\Psi\rangle \\ \langle\Psi| &= \int db \langle\Psi|\Phi(b)\rangle\langle\Phi(b)| \end{aligned} \tag{14.144}$$

Next, we apply the above ket and bra to Eq. (14.124):

$$\begin{aligned} &\int d\vec{r}|\Psi(\vec{r})|^2 = \langle\Psi|\Psi\rangle \\ &= \int da \int db \langle\Psi|\Phi(b)\rangle\langle\Phi(b)| \cdot |\Phi(a)\rangle\langle\Phi(a)|\Psi\rangle \end{aligned} \tag{14.145}$$

As the eigenfunctions are chosen orthonormal, the scalar product $\langle\Phi(b)|\cdot|\Phi(a)\rangle$ in the above Eq. is equal to the delta function alias delta distribution $\delta(a-b)$:

$$\int d\vec{r}|\Psi(\vec{r})|^2 = \int da \int db \langle\Psi|\Phi(b)\rangle\delta(a-b)\langle\Phi(a)|\Psi\rangle \quad (14.146)$$

Using the delta function $\delta(a-b)$, we evaluate one integral:

$$\int d\vec{r}|\Psi(\vec{r})|^2 = \int da \langle\Psi|\Phi(a)\rangle \cdot \langle\Phi(a)|\Psi\rangle \qquad (14.147)$$

The product of two scalar products in the above Eq. is equal to the absolute square of one scalar product:

$$\int d\vec{r}|\Psi(\vec{r})|^2 = \int da |\langle\Phi(a)|\Psi\rangle|^2 \qquad (14.148)$$

Transformed probability: In the numerator in Eq. (14.124), we insert Eq. (14.148):

$$\int d\vec{r} p(\vec{r}, dV)/dV = \int d\vec{r} f_R(\vec{r}) = \frac{\int da |\langle\Phi(a)|\Psi\rangle|^2}{\langle\Psi|\Psi\rangle} \quad (14.149)$$

In the above Eq., the lhs is a probability. Correspondingly, the rhs is an integral of probability density functions $f_A(a)$ as follows:

$$\int d\vec{r} p(\vec{r}, dV)/dV = \int da f_A(a) \text{ with}$$
$$f_A(a) = \frac{|\langle\Phi(a)|\Psi\rangle|^2}{\langle\Psi|\Psi\rangle} \qquad (14.150)$$

Hereby, the scalar product $\langle\Phi(a)|\Psi\rangle$ describes the amplitude of the state $|\Psi\rangle$ with respect to the new basis vector $|\Phi(a)\rangle$ in the expansion in Eq. (14.144). Accordingly, $f_A(a)$ is the probability density function to find the eigenvalue a of the new basis vector $|\Phi(a)\rangle$ in the projection of the state $|\Psi\rangle$. Correspondingly, we multiply that probability density function by da in order to derive the probability to find the eigenvalue a of the new basis vector $|\Phi(a)\rangle$ in that projection of $|\Psi\rangle$ in the interval $[a, a+da]$, and we name that probability $P_{|\Psi\rangle}(a)$:

$$P_{|\Psi\rangle}(a) = \frac{|\langle\Phi(a)|\Psi\rangle\rangle|^2}{\langle\Psi|\Psi\rangle} \cdot da = P(a) \qquad (14.151)$$

So, we derived the probability $P(a)$ in item (3). We summarize:

Theorem 30 Probabilistic outcomes of measurements

The states of volume or of matter form a Hilbert space $\mathcal{H}$, whereby the following holds:

(I.1) At each location $\vec{r}$, there occur states, so that the corresponding rate $\dot{\varepsilon}_L(t,\vec{r})$ is proportional to a wave function $\Psi(t,\vec{r})$. Hereby, the corresponding energy density u_{kin} is proportional to the probability density function $f_R(t,\vec{r})$ of the wave function.

(I.2) The normalized probability density function is as follows:

$$f_R(t,\vec{r}) = \frac{|\Psi(t,\vec{r})|^2}{\langle\Psi(t,\vec{r})|\Psi(t,\vec{r})\rangle}$$
$$\text{with} \quad \langle\Psi(t,\vec{r})|\Psi(t,\vec{r})\rangle = \int dr^3 \Psi^{cc}(t,\vec{r}) \cdot \Psi(t,\vec{r})$$
$$\Psi^{cc} = \text{complex conjugated of } \Psi \quad (14.152)$$

The corresponding probability to find a quantum in a vicinity of $\vec{r}$ and with a volume dV is as follows:

$$p(t,\vec{r},dV) = f_R(t,\vec{r}) \cdot dV \qquad (14.153)$$

(I.3) The above probability represents a second order function (square) of the state vector $|\Psi(t,\vec{r})\rangle$ in $\mathcal{H}$, THM (26).

(I.4) Moreover, that probability is the basis of linear combinations, by which a square of the state vector $|\Psi(t,\vec{r})\rangle$ in Hilbert space is expanded with respect to eigenfunctions in Hilbert space. Thereby, in particular, the probabilities of the measurement of the eigenvalues are derived.

(II) If a measurement of an observable A with an operator $\hat{A}$ is made at a state $|\Psi\rangle$, then the probability in item (I.2) provides the probability to measure an eigenvalue of $\hat{A}$ as follows.

(II.1) The probability of obtaining one of the non-degenerate discrete eigenvalues a_j of the corresponding operator $\hat{A}$ is represented as follows:

$$P(a_j) = \frac{|\langle\phi_j|\Psi\rangle|^2}{\langle\Psi|\Psi\rangle} \tag{14.154}$$

Hereby, $|\phi_j\rangle$ represent orthonormal eigenfunctions of $\hat{A}$, corresponding to respective eigenvalues a_j. If the state vector is normalized to unity, the the probability for a discrete set of states is $P(a_j) = |\langle\phi_j|\Psi\rangle|^2$.

(II.2) If the eigenvalue a_j is m_j-fold degenerate, that probability to measure an eigenvalue a_j is as follows:

$$P(a_j) = \frac{\Sigma_{i=1}^{m_j}|\langle\phi_{j,i}|\Psi\rangle|^2}{\langle\Psi|\Psi\rangle} \tag{14.155}$$

(II.3) If the operator $\hat{A}$ possesses a continuous eigenspectrum $\{a\}$, then the probability that the result of a measurement will yield a value between a and $a + da$ is as follows:

$$\begin{aligned} P(a) &= \frac{|\langle\phi(a)|\Psi\rangle|^2}{\langle\Psi|\Psi\rangle}da \\ \text{with } \langle\Psi|\Psi\rangle &= \int_{-\infty}^{\infty}|\Psi(a')|^2 da' \end{aligned} \tag{14.156}$$

14.7 Mixed states

In this section, we derive the following postulate about the expectation value of an observable in the case of a mixed state.

What is a mixed state?

Firstly, a pure state is a vector in Hilbert space.

However, if we have insufficient knowledge about the objects of a system, then we can describe the system in the framework of statistical physics, see e. g. Landau and Lifschitz (1980). In the case of a quantum system, such a system is in a mixed state.

A mixed state can be characterized as follows, see e. g. (Ballentine, 1998, p. 46, 50):

Definition 13 Mixed state

(1a) In a mixed state, the orthonormal eigenfunctions ϕ_j of an operator $\hat{A}$ of an observable A and of a non-degenerate or degenerate eigenvalue a_j occur at corresponding probabilities p_j.

(1b) The probabilities are non-negative and their sum is one:

$$p_j \geq 0 \quad \sum_{j=1}^{N_A} p_j = 1 \tag{14.157}$$

Hereby, N_A denotes the number of eigenvectors of $\hat{A}$.

(2) A mixed state can be described by a density operator as follows (Sakurai and Napolitano, 1994, p. 180, 181):

$$\hat{\rho} = \sum_{j=1}^{N_A} |\phi_j\rangle p_j \langle\phi_j| \tag{14.158}$$

The density operator is also called state operator or statistical operator, and the above form of that operator $\hat{\rho}$ is called spectral representation (Ballentine, 1998, p. 46 and section 2.3).

Postulate 6 Expectation value of a mixed state

To each state there corresponds a unique state operator. The expectation (or average) value of a dynamic variable (or observable) A, represented by the operator $\hat{A}$, in the virtual ensemble of events that may result from a preparation procedure for the state, represented by an operator $\hat{\rho}$ is:

$$\langle A\rangle = \frac{Tr(\hat{\rho}\cdot\hat{A})}{Tr(\hat{\rho})} \quad \text{Hereby, Tr marks the trace.} \tag{14.159}$$

Derivation: According to the definition of an expectation value (Olofsson and Andersson, 2012, DEF 2.4.1), the expectation value $\langle A \rangle$ is the sum of the products of the probabilities and eigenvalues:

$$\langle A \rangle = \sum_{j=1}^{N_A} p_j \cdot a_j \tag{14.160}$$

As the DEQ of the RGWs is linear, and as the SEQ derived therefrom is linear too, we can use linear algebra. With it, we derive the postulate as follows:

The above sum is equal to the trace of a diagonal matrix, in which the products $p_j \cdot a_j$ are the diagonal elements. Such a matrix can be represented as follows:

$$\text{diagonal matrix} = \sum_{j=1}^{N_A} |\phi_j\rangle p_j \cdot a_j \langle \phi_j| \quad \text{with } \langle \phi_j|\phi_k\rangle = \delta_{jk} \tag{14.161}$$

So, the expectation value is the trace of that matrix:

$$\langle A \rangle = Tr\left(\sum_{j=1}^{N_A} |\phi_j\rangle p_j \cdot a_j \langle \phi_j|\right) \tag{14.162}$$

We add an additional sum of δ_{ij}, and we change two indices from j to i, so that the value remains the same:

$$\langle A \rangle = Tr\left(\sum_{j=1}^{N_A}\sum_{i=1}^{N_A} |\phi_i\rangle p_i \cdot \delta_{ij} \cdot a_j \langle \phi_j|\right) \tag{14.163}$$

Next, we replace δ_{ij} by the scalar product of orthonormal eigenfunctions $\langle \phi_i|\phi_j\rangle$:

$$\langle A \rangle = Tr\left(\sum_{j=1}^{N_A}\sum_{i=1}^{N_A} |\phi_i\rangle p_i \cdot \langle \phi_i|\phi_j\rangle \cdot a_j \langle \phi_j|\right) \tag{14.164}$$

Next, we move the sum $\sum_{j=1}^{N_A}$ to the place at which indices j occur the first time, so that the value remains the same:

$$\langle A\rangle = Tr\left(\sum_{i=1}^{N_A} |\phi_i\rangle \cdot p_i \cdot \langle\phi_i| \cdot \sum_{j=1}^{N_A} |\phi_j\rangle \cdot a_j \cdot \langle\phi_j|\right)$$

$$\text{we identify} \quad \hat{\rho} = \sum_{i=1}^{N_A} |\phi_i\rangle \cdot p_i \cdot \langle\phi_i|$$

$$\text{we identify} \quad \hat{A} = \sum_{j=1}^{N_A} |\phi_j\rangle \cdot a_j \cdot \langle\phi_j| \quad (14.165)$$

Here, we identified the first sum with the spectral representation of the density operator, and we identified the second sum with the spectral representation of $\hat{A}$. So, the expectation value is the trace of the following product of operators:

$$\langle A\rangle = Tr(\hat{\rho} \cdot \hat{A}) \quad (14.166)$$

As we use orthonormal eigenfunctions, the trace of the spectral representation of the density operator is one, $Tr\,(\hat{\rho}) = 1$, so we can divide by that trace[6]:

$$\langle A\rangle = \frac{Tr(\hat{\rho} \cdot \hat{A})}{Tr(\hat{\rho})} \quad \text{We summarize :} \quad (14.167)$$

Theorem 31 Expectation value in a mixed state

The DEQ of the RGWs is linear, and the SEQ derived therefrom is linear too. So, linear algebra can be applied to the states of quantum physics. With it, the above postulate has been derived:

In a mixed state, represented by a density operator $\hat{\rho}$, the expectation value $\langle A\rangle$ of an observable A, represented by the operator $\hat{A}$, is as follows:

$$\langle A\rangle = \frac{Tr(\hat{\rho} \cdot \hat{A})}{Tr(\hat{\rho})} \quad (14.168)$$

[6]Note that in another representation, that trace $Tr\,(\hat{\rho})$ might have a value different from one.

14.8 Angular momentum and spin

In this section, we summarize a result that is useful in the following section (14.10).

Based on the postulates of QP, the quantum physics of angular momentum and spin can be developed (Sakurai and Napolitano, 1994, chapter 3), (Scheck, 2013, chapter 4), (Ballentine, 1998, chapter 7). So, angular momentum and spin are consequences of the SQ.

14.9 Identical particles

In this section, we derive the physics of identical particles.

14.9.1 Indistinguishability

In a system of N particles, each particle j is described by a configuration ξ_j of physical quantities such as location, spin, charge, etc., (Landau and Lifschitz, 1965, § 61). Thus, the wave function and the Hamiltonian are functions of these variables:

$$\Psi = \Psi(\xi_1, \xi_2, ..., \xi_N) \tag{14.169}$$

$$H = H(\xi_1, \xi_2, ..., \xi_N) \tag{14.170}$$

Definition 14 Indistinguishable particles

(1) The **permutation operator** P_{ij} *exchanges particles* i *and* j. *E. g. , at a wave function,* P_{ij} *acts as follows:*

$$P_{ij}\Psi(\xi_1, \xi_2, ..., \xi_{i-1}, \xi_i, ..., \xi_{j-1}, \xi_j, ...\xi_N) \tag{14.171}$$

$$= \Psi(\xi_1, \xi_2, ..., \xi_{i-1}, \xi_j, ..., \xi_{j-1}, \xi_i, ...\xi_N) \tag{14.172}$$

(2) N *particles are called* **indistinguishable**, *if the Hamiltonian does not change as a result of the permutation operator* P_{ij}, *see e. g. (Ballentine, 1998, section 17.3).*

(3) If N *particles are indistinguishable, then they are called* **identical**, *see e. g. (Ballentine, 1998, section 17.3).*

14.9.2 Time evolution

The time evolution of a system of identical particles is provided by the SEQ, see e. g. (Scheck, 2013, section 4.3.3) or (Ballentine, 1998, section 17).

In the case of identical particles, the Hamiltonian is invariant with respect to the permutation operator. As a consequence of the above postulates (1, 2, 3, 4, 5), the Hamiltonian and the Permutation operator can be transformed to the diagonal form simultaneously, so they have eigenvectors and eigenvalues independently, see e. g. (Ballentine, 1998, section 17.1). Thereby, the only eigenvalues of P_{ij} are ± 1, as P_{ij}^2 has the eigenvalue one:

$$P_{ij}\Psi = \pm 1 \cdot \Psi \tag{14.173}$$

If a wave function Ψ of P_{ij} has the eigenvalue $+1$, then Ψ is called **symmetric**. If a wave function Ψ of P_{ij} has the eigenvalue -1, then Ψ is called **antisymmetric**.

Postulate 7 Symmetrization postulate

(1) The particles of a species are classified into two classes:

(1a) Either the particles of a species have symmetric wave functions. Such particles are called **Bosons**.

(1b) Or the particles of a species have antisymmetric wave functions. Such particles are called **Fermions**.

Derivation: As the permutation operator and the Hamiltonian can be transformed to the diagonal form simultaneously, the symmetry or antisymmetry of the wave function do not change during the time evolution. Thus, a type of particles has either symmetric wave functions at all times, or these particles have antisymmetric wave functions at all times. Hence, the types of particles are classified into Bosons and Fermions.

14.10 Entanglement

14.10.1 System with several degrees of freedom

In general, a system S can consist of several degrees of freedom ξ_i, with $i \in \{1, 2, 3, ..., N\}$. This includes the case that a system consists of several objects. So, most generally, the wave function of S is a function of all degrees of freedom:

$$\Psi = \Psi(t, \xi_1, \xi_2, ..., \xi_N) \tag{14.174}$$

As derived above, the wave function describes a pure state, whereby the case of mixed states is treated similarly as shown in section (14.7).

As a consequence, by application of Eq. (14.120) to the present case, we derive the **joint density function**, see e. g. (Ash, 2008, section 2.6), $f(t, \xi_1 \cap \xi_2 \cap ... \cap \xi_N)$ or $f(t, \xi_1, \xi_2, ..., \xi_N)$. Hereby, that joint density function is proportional to the probability for the simultaneous occurrence of the values ξ_1 and ξ_2 and ... and ξ_N. In particular, we derive that $f(t, \xi_1, , \xi_2, ..., \xi_N)$ is equal to the absolute square of the normalized wave function Ψ_{norm}:

$$f(t, \xi_1, \xi_2, ..., \xi_N) = |\Psi_{\text{norm}}(t, \xi_1, \xi_2, ..., \xi_N)|^2 \tag{14.175}$$

The corresponding joint probability $P(t, \xi_1 \cap \xi_2 ... \cap \xi_N)$ to find $\xi_i \in [\xi_i - \delta q/2, \xi_i + \delta q/2]$ with $i \in \{1, 2, 3, ..., N\}$ is equal to the probability density function multiplied by δq^N, see (Ash, 2008, section 2.6):

$$P(t, \xi_1 \cap \xi_2 ... \cap \xi_N) = |\Psi_{\text{norm}}(t, \xi_1, \xi_2, ..., \xi_N)|^2 \cdot (\delta q)^N \tag{14.176}$$

Such a probability for the simultaneous occurrence of several events is described in (Ash, 2008, section 2.6), (Olofsson and Andersson, 2012, sections 1.2, 1.3, 1.4), for instance.

14.10.1.1 System with independent degrees of freedom

In particular, a system S can consist of several independent degrees of freedom ξ_i, with $i \in \{1, 2, ..., N\}$, see e. g. (Kolmogorov, 1956, § 5 in chapter I or chapter VI), (Ash, 2008, section 2.6, 2.7, 2.8, 2.9).

As a consequence, the probability for the simultaneous occurrence of several events in Eq. (14.176) becomes a probability for the simultaneous occurrence of several **independent events**. According to probability theory, see (Olofsson and Andersson, 2012, DEF 1.5.2, 1.5.3, 1.5.4), the probability in Eq. (14.176) becomes a product of the probabilities:

$$P(t, \xi_1 \cap \xi_2 ... \cap \xi_N) = \prod_{i=1}^{N} P(t, \xi_i) \text{ or}$$
$$P(t, \xi_1 \cap \xi_2 ... \cap \xi_N) = \prod_{i=1}^{N} |\Psi_{\text{norm}}(t, \xi_i)|^2 \cdot \delta q \qquad (14.177)$$

As the above rule should hold for all possible wave functions, the wave function $\Psi_{\text{norm}}(t, \xi_1, \xi_2, ..., \xi_N)$ is a product of the wave functions of the single degrees of freedom:

$$\Psi_{\text{norm}}(t, \xi_1, \xi_2, ..., \xi_N) = \prod_{i=1}^{N} \Psi_{\text{norm}}(t, \xi_i) \qquad (14.178)$$

In the literature, that product has also been named **tensor product**, and the corresponding multiplication has been marked by $\otimes$, see e. g. Sanz et al. (2016):

$$\Psi_{\text{norm}}(t, \xi_1, \xi_2, ..., \xi_N) = \Psi_{\text{norm}}(t, \xi_1) \otimes \Psi_{\text{norm}}(t, \xi_1) \otimes ... \otimes \Psi_{\text{norm}}(t, \xi_N) \qquad (14.179)$$

This product rule for wave functions has been postulated in quantum physics, see e. g. (Kinzel, 2021, section 3.1) or (Ballentine, 1998, p. 470). In the literature, such a product state has also been named **separable**, see e. g. Sanz et al. (2016). As a result of the above derivation, this postulate is a consequence of the SQ.

14.10.1.2 System with dependent degrees of freedom

More generally, a system S can consist of several degrees of freedom ξ_i, with $i \in \{1, 2, ..., N\}$ that are not independent.

As a consequence, the probability for the simultaneous occurrence of several events in Eq. (14.176) does not represent a probability of independent events. According to probability theory, see (Olofsson and Andersson, 2012, DEF 1.5.2, 1.5.3, 1.5.4), the probability in Eq. (14.176) is not a product of the probabilities:

$$P(t, \xi_1 \cap \xi_2 ... \cap \xi_N) \neq \prod_{i=1}^{N} P(t, \xi_i) \quad \text{or}$$
$$P(t, \xi_1 \cap \xi_2 ... \cap \xi_N) \neq \prod_{i=1}^{N} |\Psi_{\text{norm}}(t, \xi_i)|^2 \cdot \delta q \qquad (14.180)$$

As a further consequence, the above wave function of several degrees of freedom in Eq. (14.180) $\Psi_{\text{norm}}(t, \xi_1, \xi_2, ..., \xi_N)$ is not a product of the wave functions of the single degrees of freedom:

$$\Psi_{\text{norm}}(t, \xi_1, \xi_2, ..., \xi_N) \neq \prod_{i=1}^{N} \Psi_{\text{norm}}(t, \xi_i) \qquad (14.181)$$

Thus, the state $\Psi_{\text{norm}}(t, \xi_1, \xi_2, ..., \xi_N)$ in Eq. (14.180) is not separable. By definition, a state is called **entangled** if and only if it is not separable, see e. g. Sanz et al. (2016) or Hordecki et al. (2009).

So, the state $\Psi_{\text{norm}}(t, \xi_1, \xi_2, ..., \xi_N)$ in Eq. (14.180) is entangled. Hence, we derived that entangled states are a consequence of the SQ[7].

[7]Correspondingly, entangled states occur in a variety of systems, see e. g. Aspect et al. (1982). Entangled states do even occur in macroscopic or semiclassical systems containing membranes, Rodrigo et al. (2021), or containing living bacteria, Marletto et al. (2017).

Moreover, properties of entangled states and measures of entanglement can be derived on the basis of the SQ. For instance, the **conditional variance** V_c is a measure of usual probability theory, see e. g. (Olofsson and Andersson, 2012, section 3.7.3), and V_c can be applied as an efficient indicator for entanglement, even in macroscopic systems, Rodrigo et al. (2021).

Theorem 32 Separability and entanglement

(1) In a system consisting of many degrees of freedom ξ_i, with $i \in \{1, 2, ..., N\}$, including many objects, the normalized wave function is a function of these variables ξ_i:

$$\Psi_{\text{norm}} = \Psi_{\text{norm}}(t, \xi_1, \xi_2, ..., \xi_N) \tag{14.182}$$

(1a) If these degrees of freedom ξ_i are independent, then the state is called separable and the wave function factorizes:

$$\Psi_{\text{norm}}(t, \xi_1, \xi_2, ..., \xi_N) = \prod_{i=1}^{N} \Psi_{\text{norm}}(t, \xi_i) \tag{14.183}$$

Then the product rule can be applied, see e. g. (Kinzel, 2021, section 3.1) or (Ballentine, 1998, p. 470). So, independent states are a possible consequence of the SQ.

(1b) If these degrees of freedom ξ_i are not independent, then the wave function does not factorize:

$$\Psi_{\text{norm}}(t, \xi_1, \xi_2, ..., \xi_N) \neq \prod_{i=1}^{N} \Psi_{\text{norm}}(t, \xi_i) \tag{14.184}$$

By DEF, a state is **entangled** *if and only if it is not separable. So, entangled states are a possible consequence of the SQ.*

Theorem 33 Derivation of quantum postulates

For the postulates of quantum physics
on the time evolution (postulate 1),

on Hilbert space (postulate 2),
on observables (postulate 3),
on possible outcomes of measurements (postulate 4),
on probabilities of these outcomes (postulate 5)
on expectation values of observables at mixed states (postulate 6),
on the symmetrization postulate (7),
on several degrees of freedom (section 14.10.1),
on several separable degrees of freedom (postulate on independent states in section 14.10.1.1),
on several entangled degrees of freedom (section 14.10.1.2),
the following holds:

(1) The volume dynamics implies these postulates of quantum physics. Thereby, objects at $v = c$ and at $v < c$ are included. So, the **postulates have become derived rules** *of quantum physics.*

(2) As matter forms from volume by a phase transition, see e. g. Higgs (1964), Carmesin (2021a), the volume dynamics applies to matter as well as to volume. So, the derived postulates apply to objects of matter additionally.

(3) The usual advanced theories of quantum physics are based on the postulates derived here, see chapter (15).

(4) So, **volume dynamics implies quantum physics.**

Chapter 15

Consequences of Quantum Postulates

Idea: Based on the SQ, we derived the usual postulates of quantum physics, QP, as a consequence (chapter 14). As a matter of fact, these postulates have been used in order to derive the essential advanced theories about QP. Thus, the essential advanced theories of QP are consequences of the SQ.

Moreover, we explained the usual postulates of QP by the dynamics of volume (part II). Accordingly, we explained the advanced theories of QP by the dynamics of volume. In this chapter, we summarize these consequences of the SQ:

15.1 Phenomena

Based on the postulates of quantum physics, QP, the Heisenberg uncertainty relation can be derived (Ballentine, 1998, section 8.4), (Kumar, 2018, section 3.10). Moreover, based on the postulates of QP, the states in atoms can be derived (Ballentine, 1998, chapter 10).

15.2 Theories

15.2.1 Path integrals and semiclassical limit

Based on the postulates of QP, Feynman's path integral can be developed (Sakurai and Napolitano, 1994, section 2.6, Eq. 2.6.49), (Ballentine, 1998, section 4.8).

15.2.2 Gauge invariance and interaction

Based on the postulates of QP, the principle of gauge invariance can be developed, and it can be applied in order to derive terms describing fundamental interactions, (Sakurai and Napolitano, 1994, section 2.7).

Relativistic quantum physics: Based on the postulates of QP, the relativistic quantum theory, including the Dirac equation, can be developed (Sakurai and Napolitano, 1994, C. 8).

Second quantization: We derived ladder operators in section (14.5). That method is usually called second quantization, see e. g. (Sakurai and Napolitano, 1994, p. 460). Here, we provide the dynamics of volume underlying the method of second quantization.

Quantum electrodynamics: Using the method of second quantization (section 14.5), the theory of quantum electrodynamics or the quantum theory of the electromagnetic field can be derived, see e. g. (Ballentine, 1998, chapter 19).

Quantum field theory: With an application of the method of path integrals (section 15.2.1), the theory of quantum electrodynamics or the quantum theory of the electromagnetic field can be derived, see e. g. Weinberg (1996). Alternatively, we can use the method of second quantization (section 14.5), in order to derive quantum field theory, see e. g. Bialynicki-Birula and Bialynicki-Birula (1975).

Chapter 16

On Bell's theorem

Idea: Einstein et al. (1935) proposed that a physical theory should be realistic and local. However, quantum physics appears to be nonlocal. Accordingly, Einstein et al. (1935) proposed that quantum physics is incomplete and should be supplemented by hypothetical hidden variables.

Bell (1964) provided a scheme in order to investigate such hypothetical hidden variables. Accordingly, we summarize that tool of investigation and the experimental results. Moreover, we present implications of the dynamics of volume concerning the issue of a realistic and local theory of nature.

16.1 On Bell's inequality

We consider a system consisting of two components or particles, see Fig. (16.1). Each component can be measured, whereby two results are possible, called ± 1. Each measurement device has a set of orientations or directions $\vec{a}$ and $\vec{b}$ of measured polarization or spin. Each measurement depends on the orientations $\vec{a}$ and $\vec{b}$ and possibly on hidden variables λ:

$$A(\vec{a}, \lambda) = \pm 1 \text{ for particle 1 and} \tag{16.1}$$

$$B(\vec{b}, \lambda) = \pm 1 \text{ for particle 2} \tag{16.2}$$

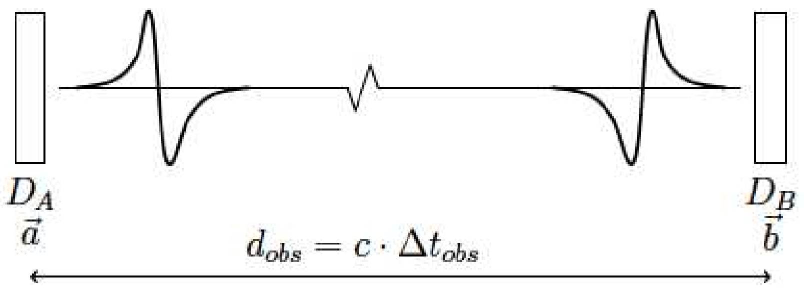

Figure 16.1: Experiment providing the Bell inequality: The particle at the left is measured with the detector D_A at a direction $\vec{a}$ of measured spin or polarization. The particle at the right is measured with the detector D_B at a direction $\vec{b}$. Hereby, the difference Δt_{obs} of the times at which the detectors D_A and D_B execute their observations multiplied by c is smaller than the distance d_{obs} between the detectors.

The hidden variables correspond to some probability distribution $\rho(\lambda)$. We introduce a correlation function as follows:

$$C(\vec{a},\vec{b}) = \int A(\vec{a},\lambda) \cdot B(\vec{b},\lambda) \cdot \rho(\lambda) d\lambda \text{ with} \tag{16.3}$$

$$\rho(\lambda) \geq 0 \text{ and } \int \rho(\lambda) d\lambda = 1 \tag{16.4}$$

Instead of $A(\vec{a},\lambda) = \pm 1$ and $B(\vec{b},\lambda) = \pm 1$, we use a weaker condition:

$$|A(\vec{a},\lambda)| \leq 1 \text{ and } |B(\vec{b},\lambda)| \leq 1 \tag{16.5}$$

We derive the absolute value of the following difference of correlations with various arbitrary directions $\vec{a}$, $\vec{a}'$, $\vec{b}$ and $\vec{b}'$ of the detectors and with arbitrary signs $\pm$:

$$|C(\vec{a},\vec{b}) - C(\vec{a},\vec{b}')| \tag{16.6}$$

$$= \left| \int [A(\vec{a},\lambda)B(\vec{b},\lambda) - A(\vec{a},\lambda)B(\vec{b}',\lambda)]\rho(\lambda)d\lambda \right| \tag{16.7}$$

$$= | \int [A(\vec{a},\lambda)B(\vec{b},\lambda)\{1 \pm A(\vec{a}',\lambda)B(\vec{b}',\lambda)\}]\rho(\lambda)d\lambda \tag{16.8}$$

$$- \int [A(\vec{a},\lambda)B(\vec{b}',\lambda)\{1 \pm A(\vec{a}',\lambda)B(\vec{b},\lambda)\}]\rho(\lambda)d\lambda \ | \tag{16.9}$$

In the above equation, the curly brackets are not negative. Thus the absolute value is not decreased, if the products $A(\vec{a},\lambda)\cdot B(\vec{b},\lambda)$ and $A(\vec{a},\lambda)B(\vec{b}',\lambda)$ are replaced by one and the difference is replaced by a sum (see Eq. (16.5)). So we derive:

$$|C(\vec{a},\vec{b})-C(\vec{a},\vec{b}')| \tag{16.10}$$
$$\leq \left| \int [1 \pm A(\vec{a}',\lambda)B(\vec{b}',\lambda)]\rho(\lambda)d\lambda \right. \tag{16.11}$$
$$\left. + \int [1 \pm A(\vec{a}',\lambda)B(\vec{b},\lambda)]\rho(\lambda)d\lambda \right| \tag{16.12}$$
$$= \left| 2 \pm [C(\vec{a}',\vec{b}')+C(\vec{a}',\vec{b})] \right| \tag{16.13}$$

In the above equation, the term $2 \pm [C(\vec{a}',\vec{b}')+C(\vec{a}',\vec{b})]$ does not become negative. Thus, it is not necessary to apply the absolute:

$$|C(\vec{a},\vec{b})-C(\vec{a},\vec{b}')| \leq 2 \pm [C(\vec{a}',\vec{b}')+C(\vec{a}',\vec{b})] \tag{16.14}$$

Next, in the above equation, the $\pm$ sign is chosen so that the term $\pm[C(\vec{a}',\vec{b}')+C(\vec{a}',\vec{b})] \leq 0$ or $\pm[C(\vec{a}',\vec{b}')+C(\vec{a}',\vec{b})] = -|C(\vec{a}',\vec{b}')+C(\vec{a}',\vec{b})|$. Thus, the Eq. (16.14) implies:

$$|C(\vec{a},\vec{b})-C(\vec{a},\vec{b}')| \leq 2 - |C(\vec{a}',\vec{b}')+C(\vec{a}',\vec{b})| \text{ or} \tag{16.15}$$
$$|C(\vec{a},\vec{b})-C(\vec{a},\vec{b}')| + |C(\vec{a}',\vec{b}')+C(\vec{a}',\vec{b})| \leq 2 \tag{16.16}$$

Hereby, we abbreviate the above sum by S:

$$S \leq 2 \quad \text{with} \tag{16.17}$$
$$S = |C(\vec{a},\vec{b})-C(\vec{a},\vec{b}')| + |C(\vec{a}',\vec{b}')+C(\vec{a}',\vec{b})| \tag{16.18}$$

This relation is called Bell's inequality, see e. g. Bell (1964), Ballentine (1998).

In order to investigate nonlocal phenomena (section 16.1.1), the distance d_{obs} between the detectors D_A and D_B in Fig. (16.1) is arranged sufficiently large: For it, the time difference Δt_{obs} of the times at which the detectors D_A and D_B in Fig.

(16.1) execute their observations multiplied by c is smaller than the distance d_{obs} between the detectors. Thus, no communication at $v \leq c$ between the particles can generate an additional correlation:

$$\text{no communication at } v \leq c \text{ increases } S \tag{16.19}$$

16.1.1 Einstein locality principle

Einstein (1948) described the Einstein locality principle as follows, see also (Ballentine, 1998, p. 585), (Sakurai and Napolitano, 1994, p. 241):

'Für die relative Unabhängigkeit räumlich distanter Dinge (A und B) ist die Idee charakteristisch: äußere Beeinflussung von A hat keinen unmittelbaren Einfluß auf B.'

'For the relative independence of spatially distant things (A and B), the following idea is characteristic: An external influence upon A has no unmediated influence upon B.'

Thereby, spatially distant things are spacelike, see e. g. (Hobson et al., 2006, p. 7), events with the negative difference, see e. g. (Sakurai and Napolitano, 1994, p. 241):

$$\Delta s^2 = c^2 \Delta t^2 - \Delta x^2 - \Delta y^2 - \Delta z^2 \leq 0 \text{ or} \tag{16.20}$$

$$\Delta s^2 = c^2 \Delta t_{obs}^2 - d_{obs}^2 \leq 0 \text{ is spacelike} \tag{16.21}$$

A phenomenon violating Einstein locality principle is usually named **nonlocal**, see e. g. Vaidman (2019), (Scheck, 2013, section 5.1).

16.2 Experimental test of Bell's inequality

Idea: The Bell inequality (Eq. 16.18) provides the maximal value of the sum S of correlations that can be explained by

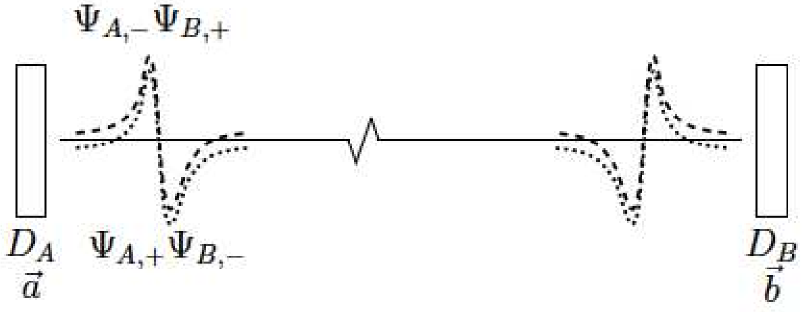

Figure 16.2: Wave function Ψ used for a test of Bell's inequality, see e. g. (Rosenfeld et al., 2017, Eq. 1), (Sakurai and Napolitano, 1994, 3.10.1) or (Ballentine, 1998, Eq. 20.20): The linear combination in Eq. (16.23) is used. Thereby, the product functions $\Psi_{A,+}\Psi_{B,-}$ (dotted) and $\Psi_{A,-}\Psi_{B,+}$ (dashed) are combined.

hidden variables. Thus, nonlocality can be tested by two observations with the following properties:

(1) Both observations are nonlocal according to Eq. (16.21).

(2) The results of both observations are evaluated so that the sum S of correlations is provided.

Here, we summarize the results of such an experiment with electrons, for more details see Rosenfeld et al. (2017).

Rosenfeld et al. (2017) execute observations at two electrons. These have been placed at locations A and B at the following distance:

$$d_{obs} = 398\,\mathrm{m} \tag{16.22}$$

The electrons have been prepared in a maximally entangled state, see Fig. (16.2).:

$$\Psi = \frac{\Psi_{A,+}\Psi_{B,-} - \Psi_{A,-}\Psi_{B,+}}{\sqrt{2}} \tag{16.23}$$

The observations start by the choice of the directions $\vec{a}$ of detector D_A and $\vec{b}$ of detector D_B in Fig. (16.2). The observations end when these detectors send the observed signals towards further devices. The time between the start and end of the observations is as follows:

$$\Delta t_{obs} = 120\,\text{ns} \tag{16.24}$$

Thus, the experiment is nonlocal according to Eq. (16.21):

$$c \cdot \Delta t_{obs} = 36\,\text{m} > d_{obs} = 398\,\text{m} \tag{16.25}$$

In order to test Bell's inequality, two orthogonal directions $\vec{a}$ and $\vec{a}'$ are chosen, two orthogonal directions $\vec{b}$ and $\vec{b}'$ are selected at the following angles (Rosenfeld et al., 2017, p. 2):

$$\text{e.g.} \quad \alpha = 90^o, \alpha' = 0^o, \beta = 45^o, \beta' = -45^o \tag{16.26}$$

Hereby, we use polar coordinates, so that $\alpha' = 0^o$ corresponds to the unit vector $\vec{e}_x$ in the direction of the x-axis. Accordingly, $\alpha = 90^o$ corresponds to the unit vector $\vec{e}_y$ in the direction of the y-axis.

According the hidden variables, Bell's inequality should hold, so that the sum S is limited from above by two:

$$S \leq 2 \quad \text{with} \tag{16.27}$$

$$S = |C(\vec{a}, \vec{b}) - C(\vec{a}, \vec{b}')| + |C(\vec{a}', \vec{b}') + C(\vec{a}', \vec{b})| \tag{16.28}$$

In this case, the corresponding quantum correlations can be evaluated with help of scalar products:

$$C(\vec{a}, \vec{b}) = \cos 45^\circ = \frac{1}{\sqrt{2}} = C(\vec{a}', \vec{b}) = C(\vec{a}', \vec{b}') \tag{16.29}$$

$$\text{and} \quad C(\vec{a}, \vec{b}') = \cos 135^\circ = \frac{-1}{\sqrt{2}} \tag{16.30}$$

Altogether, the above sum of quantum correlations is larger than two:

$$S = \left| \frac{1}{\sqrt{2}} - \frac{-1}{\sqrt{2}} \right| + \frac{2}{\sqrt{2}} = \frac{4}{\sqrt{2}} = 2\sqrt{2} > 2 \tag{16.31}$$

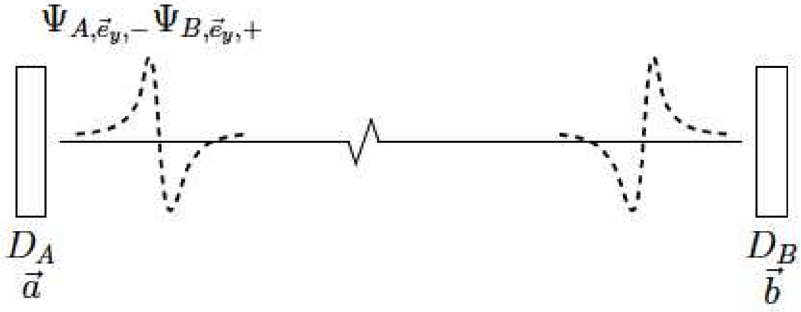

Figure 16.3: An observation at D_A with corresponding to the operator $\hat{A}_{\vec{e}_y}$ can provide the result $A,-$, see Fig. (16.2). As a result, the entangled wave function Ψ is projected to the $\hat{A}_{\vec{e}_y}\Psi = \frac{-\Psi_{A,\vec{e}_y,-}\Psi_{B,\vec{e}_y,+}}{\sqrt{2}}$. Thereby, the dotted summand in Fig. (16.2) vanishes.

The experiment provides the following value of the sum, see Rosenfeld et al. (2017):

$$S_{obs} = 2.221 \pm 0.033 \qquad (16.32)$$

Thus, Bell's inequality is violated by an amount of seven standard deviations.

Thus, the observed correlations are larger than the correlations that can be provided by hidden variables. Hereby, the additional correlations cannot be provided by a physical object that propagates slower than the velocity of light, as the two observations are nonlocal according to Eq. (16.21). Thus, a kind of communication at $v > c$ between the electrons took place. Thence, a kind of nonlocality has been observed, see section (16.1.1). Note that many experiments have been executed that violate Bell's inequality, see e. g. Aspect et al. (1982), Hensen et al. (2015). Especially interesting is a violation of Bell's inequality at cosmic scales, see e. g. Handsteiner et al. (2017).

16.3 Explanation by the dynamics of volume

The entangled electrons have the common wave function Ψ in Eq. (16.23). As the electrons are quantum objects, they fulfill the SEQ.

By chance, one of the detectors measures first. For instance, it is detector D_A. It observes in one of the two directions $\vec{e}_x$ or $\vec{e}_y$ (Eq. 16.26). In the experiment, the direction is chosen at random according to a number generator. For instance, the direction $\vec{e}_y$ is selected. Hereby, the result at D_A might be $-$.

Thereby, the corresponding operator $\hat{A}_{\vec{e}_y}$ acts upon the wave function Ψ. As a result, at D_A, the wave function is polarized according to $-\vec{e}_y$ (Eq. 16.23):

$$\hat{A}_{\vec{e}_y}\Psi = \frac{-\Psi_{A,\vec{e}_y,-}\Psi_{B,\vec{e}_y,+}}{\sqrt{2}} \tag{16.33}$$

Accordingly, the wave function in Eq. (16.23) becomes the projected wave function in Eq. (16.33), see Fig. (16.3).

The change of the solution Ψ of the SEQ towards the solution $\hat{A}_{\vec{e}_y}$ requires some duration $\Delta t_{transient}$ for the transient phenomenon, see e. g. Bergin and Collins (1951). The duration $\Delta t_{transient}$ is limited from below by the distance d_{obs} between two detectors observing the transient phenomenon, divided by the highest possible velocity v_{dyn} available by the dynamical equation, the SEQ:

$$\Delta t_{transient} \geq \frac{d_{obs}}{v_{dyn}} \tag{16.34}$$

However, the SEQ provides no restriction to the highest velocity v_{dyn}. As a consequence, the transient time tends to zero:

$$\lim_{v_{dyn}\to\infty} \Delta t_{transient} \geq \frac{d_{obs}}{v_{dyn}} = 0 \tag{16.35}$$

Consequently, the pair of entangled electrons change their solution Ψ of the SEQ towards the solution $\hat{A}_{\vec{a}}\Psi$ within a negligible duration of the transient phenomenon $\Delta t_{transient}$. This fully explains the kind of communication at $v > c$ that causes the value $S > 2$ of the indicator, see section (16.3.1).

16.3.1 Laplace transforms describe transients

Idea: A transient phenomenon starts to form at a time at which the system is changed by an observation or by any other external influence. If the system is described by a linear differential equation including phase velocities, then the transients are formed as a linear combination of solutions propagating at the phase velocity. That linear combination can be described by the Laplace transform, see e. g. Schiff (1991), Zamorano and Campos (2007), Kim et al. (2018) or Geers and Sobel (1971).

In general, the Laplace transform provides a transformation of a function $f(t)$ of time to a domain of possibly complex transient frequencies $s = x + i \cdot y$ as follows, see e. g. (Schiff, 1991, Eq. 1.1):

$$F(s) = \mathcal{L}(f(t)) = \int_0^\infty e^{-s \cdot t} \cdot f(t) dt \tag{16.36}$$

$$= \lim_{t' \to \infty} \int_0^{t'} e^{-s \cdot t} \cdot f(t) dt \tag{16.37}$$

If a function $f(t)$ is defined at the open interval $[0, \infty[$, then it can be described by the inverse transform $\mathcal{L}^{-1}(F(s))$, see e. g. (Schiff, 1991, Eq. 4.2):

$$f(t) = \frac{1}{2\pi} \cdot \int_{-\infty}^\infty e^{x \cdot t} \cdot e^{iy \cdot t} F(x, y) dy \;\text{ for }\; t > 0 \tag{16.38}$$

As y is an integration variable, it can be renamed by ω. Accordingly, y can be interpreted by the circular frequency of the RGW:

$$f(t) = \frac{1}{2\pi} \cdot \int_{-\infty}^\infty e^{x \cdot t} \cdot e^{i\omega \cdot t} F(x, \omega) d\omega \;\text{ for }\; t > 0 \tag{16.39}$$

Accordingly, the above representation can be interpreted or used as follows:

(1) The transient function $f(t)$ describes a transient effect or transient phenomenon of a solution of the SEQ.

(2) The circular frequencies ω describe the RGW.

(3) Hereby, each circular frequency ω corresponds to a wave number $|\vec{k}|$ with a phase velocity v_p as follows:

$$v_p = \frac{\omega}{|\vec{k}|} \text{ or } \omega = v_p \cdot |\vec{k}| \tag{16.40}$$

The wave number is nonzero, as the wavelength $\lambda = \frac{2\pi}{|\vec{k}|}$ is limited by the light horizon. As v_p is unlimited and $|\vec{k}|$ is nonzero, the circular frequency ω is unlimited. As a consequence, the transform $F(x,\omega)$ can be the function $F(x,\omega) = e^{-x\cdot t}$. Thus, the transient function $f(t)$ in Eq. (16.39) is as follows:

$$f(t) = \frac{1}{2\pi} \cdot \int_{-\infty}^{\infty} e^{x\cdot t} \cdot e^{i\omega\cdot t} e^{-x\cdot t} d\omega \text{ or} \tag{16.41}$$

$$f(t) = \frac{1}{2\pi} \cdot \int_{-\infty}^{\infty} e^{i\omega\cdot t} d\omega = \delta(t) \tag{16.42}$$

Hereby, $\delta(t)$ represents the δ distribution. Thus, the transient function $f(t)$ is nonzero only at $t = 0$. Hence, the transient phenomenon can take place instantly. Thereby, the potential ϕ_L drives the transient phenomenon, and as the circular frequencies are unlimited, the process takes place as fast as possible. Thus the transient phenomenon takes place instantly.

(4) Thereby, the velocity of the propagation of the transient phenomenon in spacetime is described by the unlimited phase velocity v_p, so that the distance represents no limitation. We summarize our results:

Proposition 6 Velocity of transient phenomenon

(1) If a first solution of the SEQ changes to a second solution of the SEQ, then this change takes place by a transient phenomenon.

(2) The time evolution of the transient phenomenon is described by a transient function $f(t)$. As a result of the unlimited phase velocity v_p, the transient function $f(t)$ can become a delta - distribution. Thus, the transient effect can take place instantly. As the transient phenomenon is driven by the potential, it rakes place in the fastest possible manner: instantly.

Using PROP (6) and THMs (5, 12), we derive the explanation of the observed nonlocality, see section (16.2).

Theorem 34 Explanation of nonlocality

If detectors D_A and D_B executes an observations according to the condition in part (1), then the results in parts (2-7) hold:

CONDITION:

(1) The detector D_A executes an observation with an observable A and an operator $\hat{A}$ at a wave function Ψ. The detector D_B at a distance d_{obs} executes an observation at a duration Δt_{obs} after the observation executed by D_A. Thereby, D_B executes its observation with an observable B and an operator $\hat{B}$ at a transformed version $\Psi_{transf} = \hat{A}\Psi$ of the same (or entangled) wave function Ψ.

CONSEQUENCES:

(2) Before the observation executed by D_A, the wave function Ψ was a first solution of the SEQ.

(3) The observation executed by D_A changes the wave function Ψ to a second solution Ψ_{transf} of the SEQ. This change takes place by a transient phenomenon.

(4) The time evolution of the transient phenomenon can be described by a function $f(t)$. That function can be expressed with help of the Laplace transform in terms of a linear combination of circular frequencies ω as follows:

$$f(t) \;=\; \frac{1}{2\pi}\cdot\int_{-\infty}^{\infty} e^{x\cdot t}\cdot e^{i\omega\cdot t}F(x,\omega)d\omega \;\text{ for }\; t>0 \quad (16.43)$$

(5) Hereby, each circular frequency ω corresponds to a wave number $|\vec{k}|$ with a phase velocity v_p as follows, see THM (5, part (12)) and THM (12):

$$v_p = \frac{\omega_0}{|\vec{k}|} + v_g \text{ is unlimited from above} \tag{16.44}$$

In this manner, the phase velocity v_p of the SEQ determines the evolution of the transient phenomenon in spacetime. As a consequence, the duration $\Delta t_{transient}$ of the transient phenomenon is unlimited from below:

$$\Delta t_{transient} = \frac{d_{obs}}{v_p} \text{ is unlimited from below} \tag{16.45}$$

(6) Consequently, the nonlocality observed in section (16.2) is explained by the rapid transient phenomenon in part (5). The rapid transient effect is enabled by the unlimited phase velocities in THMs (5, 12). The high phase velocities become possible in the dynamics of volume inherent to the RGW in chapters (7, 8), see THM (12, parts (3b,4b) and corollary (8).

Altogether, the duration $\Delta t_{transient}$ of the transient effect is shorter than the duration of both observations Δt_{obs}.

(7) As the definition of the Einstein locality principle is applicable to an unmediated dynamics only, see section (16.1.1), and since the observed nonlocality (section 16.2) is achieved or mediated by the dynamics of volume, the Einstein locality principle cannot be applied. Thus, the observed nonlocality does not violate the Einstein locality principle, as the premise of that principle (unmediated dynamics) is not fulfilled.

(8) The volume mediates nonlocality as follows: Two wave functions at a distance (see e. g. Figs. 16.1, 16.2, 16.3) are rates $\dot{\varepsilon}_L$ of volume. Between the two wave functions, there is volume. Within it, the transient phenomenon can take place.

Chapter 17

Mapping theorem

Ideas: Firstly, in relativity, a volume dV can be expressed in terms of the metric tensor g_{ij}, (Hobson et al., 2006, section 2.14). Thus, we derive the dynamics of the rate $\dot{\varepsilon}_L$ and of the proportional wave function Ψ as a function of the metric tensor.

Secondly, Einstein (1915) proposed the Einstein field equation, EFE, in order to describe the dynamics of spacetime. That dynamics has been expressed in terms of the Ricci flow, describing the dynamics of the metric tensor g_{ij}, Anderson (2004), Balmer (2021). Thus, we derive the dynamics of the rate $\dot{\varepsilon}_L$ and of the proportional wave function Ψ as a function of the Ricci flow.

Thirdly, we provide the relation between the dynamics of the EFE and of the Ricci flow on the one hand and the dynamics of the rate $\dot{\varepsilon}_L$ and of the proportional wave function Ψ on the other hand.

Theorem 35 Mapping of rates, tensors and Ricci flow

(1) In a D dimensional metric space with a metric tensor g_{ij} with a determinant $|g_{ij}|$, a volume element has the following volume, (Hobson et al., 2006, section 2.14):

$$dV_L = \sqrt{|g_{ij}|} \cdot \Pi_{k=1}^{k=D} dx_k \tag{17.1}$$

In a local coordinate system with a diagonal metric tensor, the volume is as follows:

$$dV_L = \sqrt{\Pi_{k=1}^{k=D}|g_{kk}|} \cdot \Pi_{k=1}^{k=D} dx_k \tag{17.2}$$

(2) The additional volume is the following function of the metric in curved space and the corresponding metric $g_{ij,flat}$ in flat space, see chapter (7):

$$\delta V = \sqrt{|g_{ij}|} \cdot \Pi_{k=1}^{k=D} dx_k - \sqrt{|g_{ij,flat}|} \cdot \Pi_{k=1}^{k=D} dx_k \quad \text{or} \tag{17.3}$$

$$\delta V = \left(\sqrt{|g_{ij}|} - \sqrt{|g_{ij,flat}|}\right) \cdot \Pi_{k=1}^{k=D} dx_k \tag{17.4}$$

(3) The relative additional volume is the following function of the metric in curved space and the corresponding metric $g_{ij,flat}$ in flat space, see chapter (7):

$$\varepsilon_L = \frac{\delta V}{dV_L} \quad \text{and} \tag{17.5}$$

$$\varepsilon_L = \frac{\sqrt{|g_{ij}|} - \sqrt{|g_{ij,flat}|}}{\sqrt{|g_{ij}|}} \quad \text{or} \tag{17.6}$$

$$\boxed{\varepsilon_L = 1 - \frac{\sqrt{|g_{ij,flat}|}}{\sqrt{|g_{ij}|}}} \tag{17.7}$$

(3a) If the metric tensors are represented in a diagonal form, and if the metric tensor of flat space and of curved space differ in one direction j only, then the relative additional volume is **unidirectional**, *see chapters (7,10):*

$$g_{ii} = g_{ii,flat} \quad \text{for} \quad i \neq j \tag{17.8}$$

$$\varepsilon_{L,jj} = 1 - \frac{\sqrt{|g_{jj,flat}|}}{\sqrt{|g_{jj}|}} \tag{17.9}$$

(3b) If the metric tensors are represented in a diagonal form, and if the nonzero elements of the metric tensor are equal, then the relative additional volume is **isotropic**, *see chapters (7,10):*

$$g_{ii} = g_{ii,flat} \text{ for all } 1 \leq i \leq D \quad (17.10)$$

$$\varepsilon_{L,iso} = 1 - \frac{\sqrt{|g_{jj,flat}|^D}}{\sqrt{|g_{jj}|^D}} \quad (17.11)$$

The isotropic rate $\varepsilon_{L,iso}$ can also be expressed in a less specific manner by ε_L.

(4) The rate of relative additional volume is the time derivative of the relative additional volume, see chapter (7):

$$\frac{\partial}{\partial \tau}\varepsilon_L = \dot{\varepsilon}_L \text{ and} \quad (17.12)$$

$$\frac{\partial}{\partial \tau}\varepsilon_{L,jj} = \dot{\varepsilon}_{L,jj} \quad (17.13)$$

(5) According to the chain rule, the rate of relative additional volume is the following function of the metric tensor, C. (7):

$$\dot{\varepsilon}_L = -\frac{\partial}{\partial \tau}\frac{\sqrt{|g_{ij,flat}|}}{\sqrt{|g_{ij}|}} \text{ and} \quad (17.14)$$

$$\dot{\varepsilon}_L = \frac{\sqrt{|g_{ij,flat}|}}{2\sqrt{|g_{ij}|}^3} \cdot \frac{\partial}{\partial \tau}|g_{ij}| \quad (17.15)$$

(5a) If the metric tensor is in a diagonal form, then the rate in Eq. (17.15) is as follows, see parts (1) and (5):

$$\dot{\varepsilon}_L = \frac{\sqrt{\Pi_{j=1}^{j=D}|g_{jj,flat}|}}{2\sqrt{\Pi_{j=1}^{j=D}|g_{jj}|}^3} \cdot \frac{\partial}{\partial \tau}\Pi_{j=1}^{j=D}|g_{jj}| \quad (17.16)$$

(5b) If the metric tensor is in a diagonal form with positive g_{jj}, then the rate in (5a) is as follows:

$$\dot{\varepsilon}_L = \frac{\sqrt{\Pi_{j=1}^{j=D} g_{jj,flat}}}{2\sqrt{\Pi_{j=1}^{j=D} g_{jj}}^3} \cdot \underbrace{\frac{\partial}{\partial \tau} \Pi_{j=1}^{j=D} g_{jj}}_{\text{poly-directional change}} \tag{17.17}$$

In general, the product $\Pi_{j=1}^{j=D} g_{jj}$ *represents a metric change in D directions. Accordingly, the product is* **poly-directional.** *The time derivative characterizes a change. Correspondingly,* $\frac{\partial}{\partial \tau} \Pi_{j=1}^{j=D} g_{jj}$ *describes a* **poly-directional change.**

(5c) In order to provide a mapping to the Ricci flow, the rate in (5b) is expanded by arbitrary fixed parts of line elements dx_j^2 *as follows:*

$$\dot{\varepsilon}_L = \frac{\sqrt{\Pi_{j=1}^{D} g_{jj,flat}}}{2\sqrt{\Pi_{j=1}^{D} g_{jj}}^3} \cdot \frac{1}{\Pi_{j=1}^{D} dx_j^2} \frac{\partial}{\partial \tau} \Pi_{j=1}^{D} g_{jj} dx_j^2 \tag{17.18}$$

The product rule provides the following rate:

$$\dot{\varepsilon}_L = \frac{\sqrt{\Pi_{j=1}^{D} g_{jj,flat}}}{2\sqrt{\Pi_{j=1}^{D} g_{jj}}^3} \frac{1}{\Pi_{j=1}^{D} dx_j^2} \sum_k^D S_k \frac{\partial}{\partial \tau} g_{kk} dx_k^2 \tag{17.19}$$

Hereby, for each direction k, the factor S_k *summarizes the factors of the respective subspace orthogonal to direction k:*

$$S_k = \Pi_{j=1, j\neq k}^{D} g_{jj} dx_j^2 \tag{17.20}$$

(5d) In the case of a unidirectional rate of relative additional volume in a direction i, the time derivative is nonzero for direction i only. So among the factors S_k*, only* S_i *is multiplied with a nonzero derivative. Thus, the factor* S_i *and the derivative can be extracted from the sum in Eq. (17.19):*

$$\dot{\varepsilon}_{L,ii} = \frac{\sqrt{\Pi_{j=1}^{D} g_{jj,flat}}}{2\sqrt{\Pi_{j=1}^{D} g_{jj}}^3} \frac{S_i}{\Pi_{j=1}^{D} dx_j^2} \frac{\partial}{\partial \tau} g_{ii} dx_i^2 \tag{17.21}$$

In the context of the Ricci flow, (Balmer, 2021, section 2), the line element ds^2 *is named* g*, (Hobson et al., 2006, section 2.11),* $ds^2 = \sum_{k,j}^{D} g_{kj} dx_k dx_j = g$*. In the case of unidirectional formation of volume, the time derivative of* g *reduces to the term* $g_{ii} dx_i^2$ *in the above equation:*

$$\dot{\varepsilon}_{L,ii} = \frac{\sqrt{\Pi_{j=1}^{D} g_{jj,flat}}}{2\sqrt{\Pi_{j=1}^{D} g_{jj}}^3} \frac{S_i}{\Pi_{j=1}^{D} dx_j^2} \frac{\partial}{\partial \tau} g_i \quad \text{with} \tag{17.22}$$

$$g = \sum_{k}^{D} g_{kk} dx_k^2 \quad \text{for diagonal } g_{kj} \tag{17.23}$$

$$g = \sum_{k,j}^{D} g_{kj} dx_k dx_j \tag{17.24}$$

$$g_i = g_{ii} dx_i^2 \quad \text{for unidirectional } g_{kj} \tag{17.25}$$

The derivative of the line element is identified with the Ricci flow as follows, (Anderson, 2004, Eqs. 4-6), (Balmer, 2021, section 2):

$$\frac{\partial}{\partial \tau} g = -2 \cdot Ric_g \quad \text{with} \tag{17.26}$$

$$Ric_g \quad \text{is} \quad \text{the Ricci tensor of } g \tag{17.27}$$

Thus, the rate in Eq. (17.22) is expressed as a function of the Ricci tensor:

$$\dot{\varepsilon}_{L,ii} = -\frac{\sqrt{\Pi_{j=1}^{D} g_{jj,flat}}}{\sqrt{\Pi_{j=1}^{D} g_{jj}}^3} \frac{S_i}{\Pi_{j=1}^{D} dx_j^2} \cdot Ric_{g_i} \tag{17.28}$$

(6) The dynamic volume and the Ricci flow are related as follows:

(6a) The rate of unidirectional relative additional volume can be expressed as a function of the Ricci flow at a unidirectional line element g_i*, see part (5d).*

(6b) The rate of a poly-directional flow, see part (5b), is characterized by a product of D tensor elements, $\frac{\partial}{\partial\tau}\Pi_{j=1}^{j=D} g_{jj}$*. In contrast, the Ricci flow and the line element g are characterized by tensor elements that are not multiplied with each other. Thus, the rate of relative additional volume is more complex than the Ricci flow. This complexity of the rate of relative additional volume is a consequence of the fact that the volume is characterized by a product of D tensor elements, see part (1).*

(6c) Altogether, the dynamics of the dynamical volume, DV, can be derived on the basis of the EFE, see the cognitive map in Fig. (12.3). Thereby, the DV is more complex than the Ricci flow or the curvature tensor underlying the EFE. That additional complexity is essential for the unification of gravity, spacetime and quantum physics.

(6d) The relation between DV and the Ricci flow can be calculated by using parts (1), (2) and (3).

(6e) The relation between DV and the EFE can be calculated by using parts (1), (2) and (3) and by expressing the EFE in terms of the metric tensor. For it, the Ricci tensor is expressed in terms of the metric tensor, (Landau and Lifschitz, 1971, § 101), the Ricci scalar is expressed as a product of Ricci tensor and metric tensor, (Landau and Lifschitz, 1971, Eq. 92.12), and the nonhomogeneous EFE is expressed in terms of the Ricci tensor, the Ricci scalar and the energy momentum tensor, (Landau and Lifschitz, 1971, Eq. 95.5), and the homogeneous EFE is expressed in terms of the Ricci tensor and the Ricci scalar.

Chapter 18

Interpretation

18.1 Role of paradoxes

A paradox is a statement that is in contrast to our everyday experience, and that tries to point at the complexity of phenomena, reflecting just a specific form of truth, Brockhaus (1998). In physics, a paradox is a phenomenon that seems or appears to be in contrast to laws of physics, Brockhaus (1998). In quantum physics, there are several paradoxes, Einstein et al. (1935), Aharonov and Rohrlich (2005) (Scheck, 2013, p. 720), Hobson (2017), (Kumar, 2018, p. 93, 181). We treat a double slit paradox that has been regarded as 'all of the mystery of QP', see (Feynman, 1965, p. 130).

18.2 Delayed choice experiment

18.2.1 Experiment

Wheeler (1984) proposed the delayed choice experiment: A source emits single photons. So there is at most one photon in the experiment. That photon can pass a double slit, Fig. (18.1). Then it can hit a screen. However, after the photon passed the double slit, the experimenter can make the **delayed choice** to remove the screen, before the photon reaches the screen. In that case, the photon can reach one of two detectors

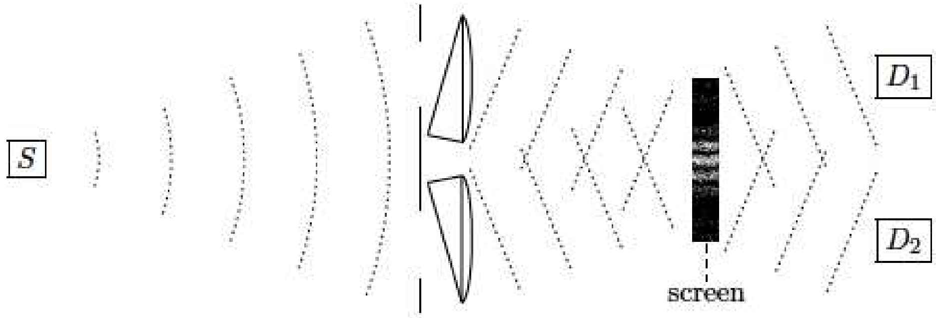

Figure 18.1: Scheme of delayed choice experiment: The source S emits single photons. Dotted lines indicate some wave fronts. While the photon is between double slit and screen, the screen can be removed. In that case, the detectors D_1 and D_2 can detect the photon.

D_1 or D_2. The experiment is repeated many times, and the pattern of photons hitting the screen is stored and displayed. For it, the screen can be a photographic plate or a camera sensor.

18.2.2 Observation

In the above experiment, the following should be observed:
(1) At the screen, many photons are detected and the diffraction pattern of the double slit forms, see Fig. (18.1).
(2) At each detector and at an instant of time, a photon can only be detected, if the screen is removed, and if no photon is detected at the other detector.
(3) At both detectors, the probability of detecting a photon is proportional to the absolute square of the wave function $|\Psi|^2$.

Paradox and solution:

If the detector D_1 detects a photon, then the following is assumed as a result of the basic concept of geometrical optics, see e. g. (Born and Wolf, 1980, C. III):

Basic concept of geometrical optics: *The photon passed the lower slit in Fig. (18.1), without passing the upper slit.*

However, if the screen would not have been removed, then that photon would have contributed to the diffraction pattern. This is explained with the improved concept of electromagnetic waves, , see e. g. (Born and Wolf, 1980, C. I):

Improved concept of electromagnetic waves: *The light passed both slits in Fig. (18.1).*

However, there is only one photon in the experiment at a time. This is verified by the fact that only one of the detectors can detect a photon at a time.

Advanced concept of the postulates of quantum physics: *The photon is observed at the screen or at one of the detectors in Fig. (18.1). Thereby, the postulates do not explain the propagation of the photon between double slit and screen or between screen and detector. This view corresponds to the Copenhagen interpretation, see e. g. Heisenberg (1958).*

According to the other advanced concept of relativity, the following is expected:

Advanced concept of relativity: *No physical effect should propagate faster than the velocity of light c in natural volume.*

However, if the wave function arrives at both detectors, and if D_1 detects the photon, then the wave function vanishes at D_2 immediately, so that D_2 does not detect a second photon at the same time. Such an immediate vanishing of the wave function is sometimes called **collapse of the wave function or state vector**, see e. g. (Isham, 1995, p. 240) or Weinberg (2017).

Altogether, there is an apparent paradox: The advanced concept of relativity cannot explain all observations. The advanced concept of quantum postulates can explain all results detected here - however, quantum postulates do not explain essential achievements of relativity, and quantum postulates do not explain how a physical object achieves an immediate change at a distance.

Advanced concept of dynamic volume, DV: DV explains the paradox: The wave function Ψ of an object represents the rate of relative additional volume. It propagates through both slits. If the screen is not removed, then the object is observed with the correct probability $|\Psi|^2(\vec{r})$, according to the diffraction pattern. If the screen is removed, and if the object is observed at one of the two detectors, then Ψ is transformed to that solution of the SEQ, that has the probability one at that detector. That transformation takes place according to the transient phenomenon at phase velocities that are above (in an unlimited manner) the velocity of light c in natural volume. As a consequence, the object is not detected at the other detector. So, DV explains the delayed choice experiment.

Moreover, DV causes the curvature of spacetime (C. 7, 8, 9). Furthermore, the DV causes the expansion of space since the Big Bang (C. 5, 12, 20, 21, 22). So, DV explains the results of GR and beyond (C. 12, 20, 21, 22).

18.2.3 Real experiment

Jaques et al. (2007) performed a slightly modified delayed choice experiment: Mach-Zehnder interferometer has two paths. An electro-optical modulator is rapidly controlled by a voltage and provides a delayed choice. The observations are as in section (18.2.2).

18.2.4 Truths learnt in a delayed choice experiment

As elaborated in section (18.1), one or more specific forms of truth can be learned from a paradox in physics. What are these truths in the delayed choice experiment?

Firstly, a wrong assumption is that the photon would pass one slit only. Instead, the wave function Ψ does always describe the deterministic and the probabilistic property of quantum physics: The wave function describes the deterministic propagation according to the SEQ. And the wave function describes the probabilistic occurrence of the whole object proportional to $|\Psi|^2$ and according to section (14.6.1).

Secondly, if a photon is detected by D_1, then no photon is detected by D_2 at the same time, see item (2) in section (18.2.2). Thus, the two possibly detected events 'detection in D_1' and 'detection in D_2' are not independent of each other. Thus, the wave function Ψ or state $|\Psi\rangle$ is not separable. Thence, the state $|\Psi\rangle$ is entangled, see Sanz et al. (2016).

Thirdly, in the delayed choice experiment, the mechanism by which nature provides entanglement is explained by the rapid transient phenomenon of the dynamics of volume. Hereby, it is essential that this rapid transient phenomenon is derived from first principles only. For it, no hypothesis or fit is used.

Fourthly, the observed nonlocality does not violate Einstein's principle of locality: The dynamics of volume is derived from fundamental principles of physics (C. 2), and it explains the observed nonlocality. Hereby, the dynamics of volume mediates physical processes as follows: A physical process takes place in volume, and the wave function of that process is the rate of relative additional volume. As Einstein formulated his locality principle only for unmediated processes, his locality principle is not applicable. Thus, his locality principle is not violated.

18.2.5 All of the mystery of QP

Feynman (1965) wrote (p. 130) that the double slit experiment contains 'all of the mystery of quantum mechanics'. This mystery essentially is the secret of the mechanism of **nonlocality**. In particular, the entanglement of distant objects or quantities provides nonlocality, Vaidman (2019). The dynamics of volume explains the double slit experiment and thereby solves Feynman's 'mystery of quantum mechanics'.

18.3 DV overcomes Copenhagen interpretation

Idea: The DV explains the essential paradoxes of QP. Thus, the DV should overcome interpretations of QP that have been used during the era at which there was no sufficient explanation of quantum paradoxes, see e. g. Einstein et al. (1935), Feynman (1965), Aharonov and Rohrlich (2005), Hobson (2017), Weinberg (2017).

The paradoxes of QP have been interpreted in various manners, see e. g. Hobson (2017). Thereby, the Copenhagen interpretation is regarded as the standard textbook interpretation, see (Hobson, 2017, p. 263). In that interpretation, a quantum state or wave function does not represent objective reality. Instead, it represents only our knowledge of reality. Hobson (2017) summarizes (p. 197): 'The Copenhagen interpretation is an effort to fix quantum physics by interpreting it non-realistically.'

The DV is derived form fundamental principles of physics only, without using any hypothesis, see part (II). As a consequence, the dynamics of volume explains the essential paradox of QP, see section (18.2). Moreover, the dynamics of volume explains nonlocality in nature, see C. (16). Furthermore, the dynamics of volume explains mediation in nature, see C. (14, 16). Thereby, the DV shows that Einstein's principle of locality is not violated, see C. (16). In this manner, the DV overcomes the non-realistic Copenhagen interpretation as follows: The DV provides a derived nonlocal explanation that does not violate Einstein's principle of locality.

Part IV

Basic Dynamics of Spacetime & Gravity

Chapter 19

Derivation of Dark Energy

Idea: We derived the dynamics of the locally formed volume, LFV, in THMs (15, 18). That dynamics should also provide the formation of a **present-day probe volume** dV_0 at an arbitrary location R_0. That process of formation took place since the Big Bang or during the Hubble time t_{H_0} (Fig. 19.1):

$$dV_0 \ \text{forms during}\ t_{H_0} \approx t_0 \tag{19.1}$$

As that dynamics is related to the field $G^* = GM/R^2$, it should provide the energy density $u_{vol} = \rho_{vol}c^2$ of volume. We analyze that process progressively in three steps:

(1) In an ideal process, we derive u_{vol} in a universe consisting of volume only, see chapter 19.

(2) We derive u_{vol} in a universe consisting of volume and a homogeneous density of matter as well as radiation.

(3) We derive u_{vol} in a universe consisting of volume and a homogeneous and heterogeneous density of matter as well as radiation, see chapter (21).

19.1 Nature of density of volume

During the expansion of space since the Big Bang, the amounts of volume increase. As volume propagates at $v = c$, it is quantized (chapter 4). A quantum of volume is at its lowest energy state, the zero-point energy, ZPE. The reason is as follows: Otherwise, a newly formed quantum of volume could reach a lower energy state and emit the energy difference, whereby that difference could violate the law of energy conservation, which is applicable here according to the Noether (1918) theorem. Thus, the energy of volume is the energy of zero-point oscillations, ZPOs[1].

19.2 u_{vol} in a universe of volume

Idea: As a first and ideal case, we analyze the process of formation of volume, and we derive the energy density u_{vol} in a universe that consists of volume only.

19.2.1 Homogeneous, isotropic and constant volume

In the present case, there is no radiation or matter. Thus, the system is homogeneous and isotropic. Accordingly, we derive the homogeneous density $\rho_{vol,h.}$ of the volume.

19.2.2 Separation of space and time

In the constant and homogeneous density $\rho_{vol,h.}$ of the volume modeled here, the time increases at a homogeneous and constant rate[2]. Accordingly, we investigate space and time separately.

19.2.3 Formation of volume by volume

An incremental volume dV_j has the dynamic mass dM_j:

$$dM_j = dV_j \cdot \rho_{vol,h.} \tag{19.2}$$

According to the law of **unidirectional** formation of volume, see THM (15), the dynamic mass dM_j exhibits a field at the

[1] Wavelengths of these ZPOs have been derived in more detail in Carmesin (2018c,b, 2019b, 2021b).

[2] Of course, in the vicinity of a local mass, the rate of increase of time is changed. But there is no special local mass in the considered system with homogeneous density.

probe volume dV_0 at a distance R. Thus, the rate of formed volume is proportional to the field:

$$d\dot{\underline{\varepsilon}}_L(R, dM_j) = \frac{|d\vec{G}_j^*|(R)}{c} = \frac{G \cdot dM_j}{R^2 \cdot c} \tag{19.3}$$

Hereby, we chose a minimal possible dM_j, so that we know that dM_j is quantized, see chapter (4). Thereby, the field $\vec{G}^*$ cannot be measured and remains uncertain, similar to the uncertainty relation, see Heisenberg (1927), PROP (4) in C. (10). Accordingly, we denote the above rate by $d\dot{\underline{\varepsilon}}_{L,G^* \text{ uncertain}}$. We summarize:

Proposition 7 Rates emitted by volume

(1) A dynamic mass of volume dM_j causes a rate at a distance R, that can be calculated as follows:

$$\boxed{d\dot{\underline{\varepsilon}}_{L,G^* \text{ uncertain}}(R, dM_j) = \frac{G \cdot dM_j}{R^2 \cdot c}} \tag{19.4}$$

(2) Photons and matter emit fields that can in principle be compensated by fields of other photons or particles of matter. Many photons or particles of matter can be described by a homogeneous density plus a heterogeneity. The homogeneous density does not cause a gravitational field, see chapter (20).

(3) Correspondingly, photons can be localized in an optical resonator, for instance. And matter can be localized in an electrical or gravitational field, for instance. In contrast, volume propagates at $v = c$ and cannot be localized in such devices.

In the above three cases, three-dimensional volume and its energy density are analyzed based on our very general four principles in chapter (2). Accordingly, our results hold for a large variety of cosmological models, see e. g. Hobson et al. (2006), Carmesin (2019b).

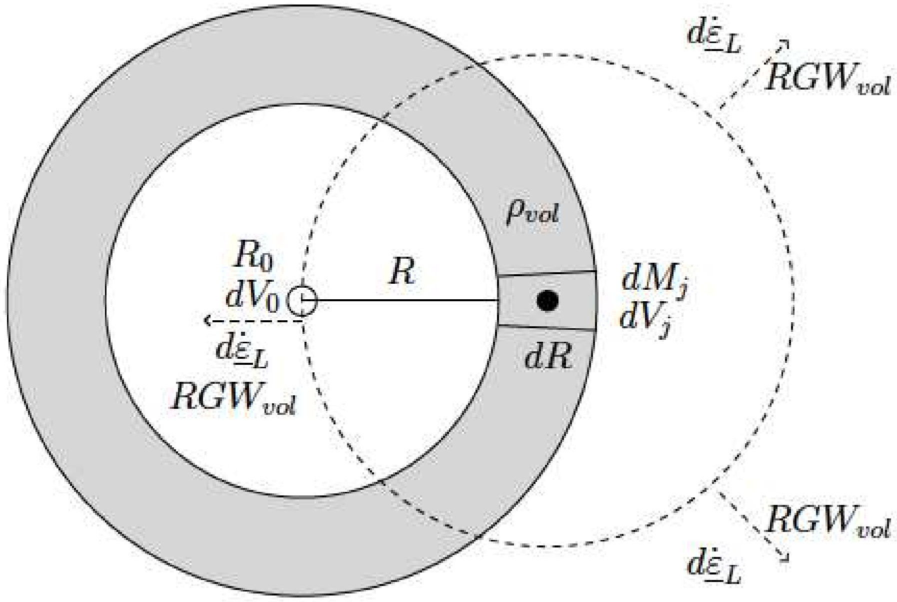

Figure 19.1: The density ρ_{vol} in an area at a distance R from R_0 has a $j-th$ dynamic mass dM_j. It generates rates $d\dot{\underline{\varepsilon}}_L = d\dot{\underline{\varepsilon}}_{L,G^* \text{ uncertain}}(R, dM_j)$ propagating towards all directions in the same manner.

19.2.4 RGWs propagating towards R_0

The rate gravity waves RGW_{vol} formed by a $j-th$ dynamic mass according to Eq. (19.3) steadily propagate towards all directions in an isotropic manner, see section (19.2.1). In this section, we integrate those RGW_{vol} that steadily propagate towards the volume dV_0 (Fig. 19.1, Eq. 19.1).

19.2.4.1 Rates arriving at R_0

Idea: We integrate all rates that steadily arrive at dV_0 (Fig. 19.1, Eq. 19.1).

Shell around R_0: The dynamic masses dM_j at a distance R from R_0 constitute a shell with center R_0 and with a distance R from R_0, and with a thickness dR, so that the mass of the shell is the sum of the masses dM_j in the shell, see Fig. (19.1):

$$dM(R) = \sum_{j,\, R_j \in \text{shell}} dM_j \tag{19.5}$$

In the present analysis of the formation of LFV in a universe consisting of volume only, the FDA becomes exact and the increments dL and dR are equal. Accordingly, also the squares of the rates of relative and normalized LFV are equal, see Eq. (9.41). Hereby, the sign of these rates describes the difference between a Big Bang and a conceivable Big Crunch, see Goodstein (1997).

At R_0, each of these masses causes the rate in Eq. (19.4). These rates represent the volume $\underline{\delta} V$ formed per volume dV and per time $\underline{\delta} t$. As volume is an additive quantity, the sum of these rates $d\dot{\underline{\varepsilon}}_{L,G^* \text{ uncertain}}(R, dM_j)$ arrives at R_0, see Fig. (19.3):

$$d\dot{\underline{\varepsilon}}_{L,G^* \text{ uncertain}}(R, dM(R)) = \sum_j d\dot{\underline{\varepsilon}}_{L,G^* \text{ uncertain}}(R, dM_j) \tag{19.6}$$

$$d\dot{\underline{\varepsilon}}_{L,G^* \text{ uncertain}}(R, dM(R)) = \frac{1}{c} \cdot \frac{G \cdot dM(R)}{R^2} \tag{19.7}$$

In the following, we abbreviate $d\dot{\underline{\varepsilon}}_{L,G^* \text{ uncertain}}$ by $d\dot{\underline{\varepsilon}}$:

$$d\dot{\underline{\varepsilon}}(R, dM(R)) = \frac{1}{c} \cdot \frac{G \cdot dM(R)}{R^2} \tag{19.8}$$

Mass of shell around R_0: That mass $dM(R)$ is equal to the product of the density $\rho_{vol,h.}$ and the volume $dV = 4\pi \cdot R^2 \cdot dR$ of the shell, see Fig. (19.1):

$$dM(R) = \rho_{vol,h.} \cdot 4\pi \cdot R^2 \cdot dR \tag{19.9}$$

Rate caused by shell and arriving at R_0: We insert the mass in Eq. (19.9) into Eq. (19.8):

$$d\dot{\underline{\varepsilon}}(R, dM(R)) = \frac{1}{c} \cdot \frac{G \cdot \rho_{vol,h.} \cdot 4\pi R^2 dR}{R^2} \tag{19.10}$$

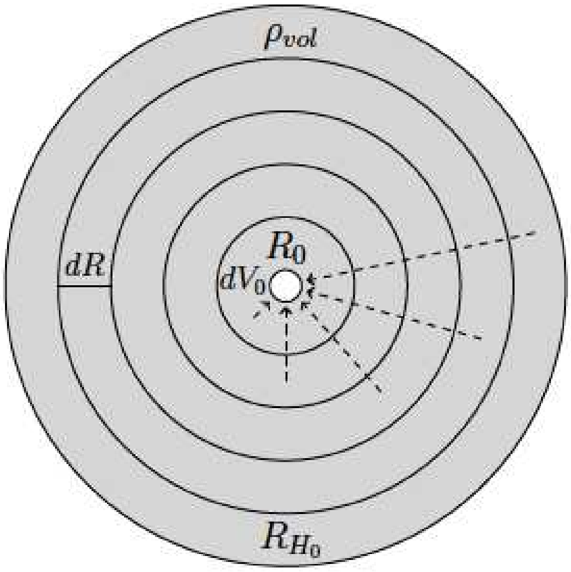

Figure 19.2: Ball with center R_0 and Hubble radius R_{H_0}: That ball is partitioned into shells with center R_0 and thickness dR. Each shell causes the same rate (dashed), $d\dot{\varepsilon}(R, dM(R))$, arriving at R_0.

We cancel R^2. So, we derive the rate that is caused by the shell at R, with a thickness dR, whereby the rate arrives at R_0:

$$d\underline{\dot{\varepsilon}}(R, dM(R)) = \frac{G \cdot \rho_{vol,h.} \cdot 4\pi}{c} \cdot dR \tag{19.11}$$

As the mass $dM(R)$ is a function of the density and dR, we write the above Eq. accordingly:

$$d\underline{\dot{\varepsilon}}(dR, \rho_{vol,h.}) = \frac{G \cdot \rho_{vol,h.} \cdot 4\pi}{c} \cdot dR \tag{19.12}$$

19.2.4.2 Invariance of rates $d\dot{\varepsilon}(dR, \rho_{vol,h.})$

The above rate in Eq. (19.11) exhibits the following property: Each shell around R_0 with thickness dR causes the same rate $d\dot{\varepsilon}(R)$ that arrives at R_0, irrespective of the radius R of the shell, see Fig. (19.2). Thus, the rate per dR of the rates $d\dot{\varepsilon}(R)$ is a constant K_0:

$$\frac{d\underline{\dot{\varepsilon}}(dR, \rho_{vol,h.})}{dR} = \frac{4\pi G \cdot \rho_{vol,h.}}{c} = K_0 \tag{19.13}$$

That rate per dR is a function of the dynamic density $\rho_{vol,h.}$ of volume and of the universal constants G and c only.

19.2.4.3 Integration of $d\dot{\varepsilon}(R)$

In order to integrate the rates $d\underline{\dot{\varepsilon}}(dR, \rho_{vol,h.})$ of the rate gravity waves RGW_{vol} arriving at R_0, we analyze the properties of these waves RGW_{vol}:

(1) The waves RGW_{vol} propagate at $v = c$, whereby they are not disturbed by any other object, see PROP (7) in chapter (19).

(2) The waves RGW_{vol} have formed since the Big Bang in the shells around R_0 described above, see Fig. (19.2).

(3) The largest light-travel time of the RGW_{vol} arriving at t_0 is the Hubble time[3] $t_{H_0} = 1/H_0$.

(4) Thus, the largest radius of the light-travel distance of the shells described above is $R_{H_0} = t_{H_0} \cdot c$, the Hubble radius.

(5) Accordingly, if we integrate the above shells, then the upper limit of the integration is R_{H_0}.

(6) If we integrate the above shells, then the lower limit of integration is a length near the Planck length L_P. Planck (1899) introduced $L_P = 1.616 \cdot 10^{-35}$ m. That length is negligible here at a very good approximation, and it is set to zero.

(7) The upper limit of the integration of rates provides the sum of all rates that steadily arrive at R_0. Accordingly, we mark it by $\underline{\dot{\varepsilon}}_{\text{at } R_0}$.

According to the above properties of the RGW_{vol}, the integration of the shells is as follows, see Eq. (19.11):

$$\int_0^{\underline{\dot{\varepsilon}}_{\text{at } R_0}} d\underline{\dot{\varepsilon}} = \frac{4\pi \cdot G}{c} \cdot \int_0^{R_H} \rho_{vol,h.} dR \qquad (19.14)$$

[3] The Hubble time describes the age of the universe at a relatively high precision, see e. g. Planck-Collaboration (2020), Carmesin (2019b).

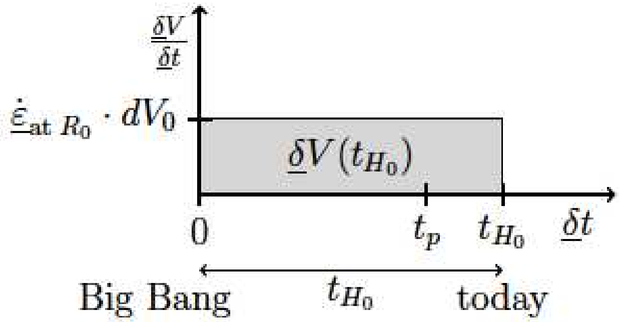

Figure 19.3: Amount of volume $\underline{\delta} V(t_{H_0})$ formed in the considered present-day volume dV_0 during the Hubble time t_{H_0}. At each time t_p, a corresponding partial volume $\underline{\delta} V_p = \dot{\underline{\varepsilon}}_{\text{at } R_0 \text{ of } t_p} \cdot dV_0 \cdot \underline{\delta} t$ is caused, see section (19.2.5).

We substitute $R = c \cdot t$:

$$\int_0^{\dot{\underline{\varepsilon}}_{\text{at } R_0}} d\dot{\underline{\varepsilon}} = 4\pi \cdot G \cdot \int_0^{t_{H_0}} \rho_{vol,h.} dt \tag{19.15}$$

We evaluate the integrals. So, we derive the rate of formation of volume that steadily arrives at R_0 and originates from radii $R \leq R_{H_0} = c \cdot t_{H_0}$:

$$\dot{\underline{\varepsilon}}_{\text{at } R_0}(R_{H_0}) = 4\pi G \cdot t_{H_0} \cdot \rho_{vol,h.} \tag{19.16}$$

19.2.5 LFV corresponding to a time

Question: Corresponding to a time $t_p \leq t_{H_0}$ (Fig. 19.3) and during an increment of time $\underline{\delta} t$, there forms the following increment of partial volume:

$$\underline{\delta} V_p(\underline{\delta} t) = \dot{\underline{\varepsilon}}_{\text{at } R_0 \text{ of } t_p} \cdot dV_0 \cdot \underline{\delta} t \tag{19.17}$$

This is a direct consequence of the definition of the rate $\dot{\underline{\varepsilon}} = \frac{\underline{\delta} V / \underline{\delta} t}{dV}$. What partial volume $\underline{\delta} V_p(t_{H_0})$ forms during the time ranging from $t = 0$ towards $t = t_{H_0}$? How large is the rate $\dot{\underline{\varepsilon}}_{\text{at } R_0 \text{ of } t_p}$ corresponding to $\underline{\delta} V_p(t_p)$?

At the volume $\underline{\delta}V_p(t_p)$ and during the time ranging from $t = 0$ towards $t = t_p$, there arrives the following accumulated rate, see Eq. (19.16):

$$\underline{\dot{\varepsilon}}_{\text{at } R_0 \text{ } until \text{ } t_p} = 4\pi G \cdot t_p \cdot \rho_{vol,h.} \tag{19.18}$$

Remind that the above rate is a result of the integration of incremental rates from $t = 0$ towards $t = t_p$, see Eq. (19.15).

During the remaining time ranging from t_p towards $t = t_{H_0}$, the remaining rate arrives:

$$\underline{\dot{\varepsilon}}_{\text{at } R_0 \text{ } since \text{ } t_p} = 4\pi G \cdot (t_{H_0} - t_p) \cdot \rho_{vol,h.} \tag{19.19}$$

Remind that the above rate is a result of the integration of incremental rates from $t = t_p$ towards $t = t_{H_0}$, see Eq. (19.15).

Thus, the full rate arriving at R_0 during the time ranging from $t = 0$ towards $t = t_{H_0}$ is the rate obtained by the full integral of incremental rates ranging from $t = 0$ towards $t = t_{H_0}$, determined by Eq. (19.16). It is the sum of the rates in Eqs. (19.18, 19.19):

$$\underline{\dot{\varepsilon}}_{\text{at } R_0 \text{ } of \text{ } t_p} = \underline{\dot{\varepsilon}}_{\text{at } R_0 \text{ } until \text{ } t_p} + \underline{\dot{\varepsilon}}_{\text{at } R_0 \text{ } since \text{ } t_p} \tag{19.20}$$

$$\underline{\dot{\varepsilon}}_{\text{at } R_0 \text{ } of \text{ } t_p} = \underline{\dot{\varepsilon}}_{\text{at } R_0}(R_{H_0}) = 4\pi G \cdot t_{H_0} \cdot \rho_{vol,h.} \text{ for each } \underline{\delta}V_p \tag{19.21}$$

Consequently, the following partial volume forms during the time ranging from $t = 0$ towards $t = t_{H_0}$

$$\underline{\delta}V_p(\underline{\delta}t = t_{H_0}) = \underline{\dot{\varepsilon}}_{\text{at } R_0}(R_{H_0}) \cdot dV_0 \cdot \underline{\delta}t \quad \text{We summarize :} \tag{19.22}$$

Proposition 8 Accumulated rate

In a universe consisting of homogeneous volume, at an arbitrary location R_0, there arrives an accumulated rate of volume as follows:

(1) At R_0, the rate per shell with thickness dR of the rates $d\dot{\varepsilon}(R)$ is a constant K_0:

$$\frac{d\underline{\dot{\varepsilon}}(dR, \rho_{vol,h.})}{dR} = \frac{4\pi G \cdot \rho_{vol,h.}}{c} = K_0(\rho_{vol,h.}) \tag{19.23}$$

That rate is a function of the constant dynamic density $\rho_{vol,h.}$ of volume and of the universal constants G and c only.

(2) At R_0, and at each partial volume $\underline{\delta} V_p(t_p)$ corresponding to an arbitrary partial time $t_p \in [0, t_{H_0}]$, there is the following accumulated rate of formation of volume originating from radii $R \leq R_{H_0} = c \cdot t_{H_0}$:

$$\boxed{\underline{\dot{\varepsilon}}_{\text{at } R_0}(R_{H_0}) = 4\pi G \cdot t_{H_0} \cdot \rho_{vol,h.}} \tag{19.24}$$

19.2.6 Rate of volume formed at dV_0

In this section, we derive the rate of volume $\frac{\delta V}{\underline{\delta} t}$ that steadily forms at the considered present-day volume dV_0 at R_0, see Figs. (19.1, 19.2).

For it, we express the rate $\underline{\dot{\varepsilon}}_{\text{at } R_0}$ in Eq. (19.24) in terms of its definition in terms of increments:

$$\underline{\dot{\varepsilon}}_{\text{at } R_0} = \frac{\delta V}{\underline{\delta} t \cdot dV_0} \tag{19.25}$$

In order to derive the rate of volume $\frac{\delta V}{\underline{\delta} t}$ that forms in the considered present-day volume dV_0 at R_0, we multiply the above Eq. (19.25) by that volume dV_0:

$$\underline{\dot{\varepsilon}}_{\text{at } R_0} \cdot dV_0 = \frac{\delta V}{\underline{\delta} t} \tag{19.26}$$

Result: The rate of volume $\frac{\delta V}{\underline{\delta} t}$ that forms in the considered present-day volume dV_0 at R_0 is equal to the product of the volume dV_0 and the rate $\underline{\dot{\varepsilon}}_{\text{at } R_0}$ that describes the normalized rate of formation of volume $\underline{\dot{\varepsilon}}_{\text{at } R_0} = \frac{\delta V / \underline{\delta} t}{dV}$. In the considered universe consisting of volume only, that rate is a constant.

19.2.7 Volume formed at dV_0

In this section, we derive the amount of volume $\underline{\delta} V(t_{H_0})$ that has formed at the considered present-day volume dV_0 at R_0 during the Hubble time t_{H_0}, see Figs. (19.1, 19.2, 19.3).

Derivation: For it, we multiply the constant rate of formation of volume in dV_0, see Eq. (19.26) and Fig. (19.3), by t_{H_0}:

$$\underline{\delta} V(t_{H_0}) = \dot{\underline{\varepsilon}}_{\text{at } R_0} \cdot t_{H_0} \cdot dV_0 \tag{19.27}$$

Proposition 9 Volume formed by the accumulated rate

In a universe consisting of volume only, at an arbitrary location R_0, in a present-day probe volume dV_0, during the Hubble time t_{H_0}, at the arriving accumulated rate of formation of volume (PROP 8), the formed volume $\underline{\delta} V(t_{H_0})$ is equal to the probe volume dV_0:

$$\underline{\delta} V(t_{H_0}) = dV_0 \tag{19.28}$$

19.2.8 Derivation of the density of volume

In this section, we derive the density of volume. For it, we insert the formed volume $\underline{\delta} V(t_{H_0})$ in Eq. (19.27) in the above equality of volumes (Eq. 19.28):

$$\dot{\underline{\varepsilon}}_{\text{at } R_0} \cdot t_{H_0} \cdot dV_0 = dV_0 \tag{19.29}$$

We insert the rate $\dot{\underline{\varepsilon}}_{\text{at } R_0}$ (Eq. 19.24), and we divide by dV_0:

$$4\pi \cdot G \cdot t_{H_0} \cdot \rho_{vol,h.} \cdot t_{H_0} = 1 \tag{19.30}$$

We solve for $\rho_{vol,h.}$, and we mark that theoretically derived density by $\rho_{vol,theo}$:

$$\boxed{\rho_{vol,h.} = \frac{1}{4\pi \cdot G \cdot t_{H_0}^2} = \rho_{vol,theo}} \tag{19.31}$$

The corresponding energy density of volume is as follows:

$$\boxed{u_{vol,h.} = \rho_{vol,h.} \cdot c^2 = \frac{c^2}{4\pi \cdot G \cdot t_{H_0}^2} = u_{vol,theo}} \tag{19.32}$$

We summarize our findings:

Proposition 10 Rate arriving at a probe volume

If a rate $\dot{\underline{\varepsilon}}_{\text{at } R_0}$ of LFV arrives at an arbitrary probe volume dV_0 at an arbitrary location R_0, then the following holds:

(1) During the Hubble time t_{H_0} and at dV_0, the rate forms the volume dV_0:

$$\dot{\underline{\varepsilon}}_{\text{at } R_0} \cdot t_{H_0} \cdot dV_0 = dV_0 \tag{19.33}$$

(2) If the rate is caused by a density $\rho_{vol,h.}$, then the rate fulfills the following relation (Eq. 19.24 applies here, as the corresponding summation and integration can be used here.):

$$\dot{\underline{\varepsilon}}_{\text{at } R_0} = 4\pi G \cdot t_{H_0} \cdot \rho_{vol,h.} \tag{19.34}$$

19.2.9 Comparison with observed density $\rho_{vol,obs}$

In this section, we compare the theoretical value $\rho_{vol,theo}$ of the density of volume with an observed value $\rho_{vol,obs}$.

Hereby, each observation of $\rho_{vol,obs}$ uses a physical object that was emitted at some time t_{em}. As a matter of fact, the observation depends slightly on that time t_{em}, see e. g. Carmesin (2018b), Carmesin (2021a), Carmesin (2021c). Accordingly, we choose a time t_{em} that represents a relatively homogeneous universe. Such a time corresponds to the early universe[4].

Accordingly, we compare with an observation at high redshift z. Correspondingly, we compare with an observation based on the CMB. In particular, the observations of the CMB by the Planck satellite provide observations based on temperature power spectra as follows, see Planck-Collaboration (2020):

$$H_{0,obs,CMB} = 66.88\,(\pm 0.92)\,\frac{\text{km}}{\text{s} \cdot \text{Mpc}} \tag{19.35}$$

$$\Omega_{\Lambda,obs} = 0.679 \pm 0.013 \tag{19.36}$$

[4]Note that a homogeneous density of radiation does hardly affect the observation, see e. g. (Carmesin, 2021d, section 7.5), Carmesin (2021a), Carmesin (2021c)

Hereby, the density parameter Ω_Λ is defined as the ratio of ρ_Λ and the critical density ρ_{cr,t_0}. The critical density ρ_{cr,t_0} is defined as the present-day density, at which the curvature parameter k in the FLE is zero, see e. g. Hobson et al. (2006) or Carmesin (2019b). Hereby, $k = 0$ is the realistic value, see Planck-Collaboration (2020), (Carmesin, 2021d, theorem 32(6)) and Eq. (5.10):

$$H_0^2 = \frac{8\pi G \cdot \rho_{cr,t_0}}{3} - k \cdot \frac{c^2}{r^2} \qquad \text{with } k = 0, \text{ so} \tag{19.37}$$

$$\rho_{cr,t_0} = \frac{3H_0^2}{8\pi G} \tag{19.38}$$

We derive the density parameter $\Omega_{vol,theo}$:

$$\Omega_{vol,theo} = \frac{\rho_{vol,theo}}{\rho_{cr,t_0}} = \frac{1}{4\pi \cdot G \cdot t_{H_0}^2} \cdot \frac{8\pi G}{3H_0^2} = \frac{2}{3} \tag{19.39}$$

Thus, the theoretical density parameter $\Omega_{vol,theo} = \frac{2}{3}$ is in precise accordance with the observed value $\Omega_{\Lambda,obs} = 0.679 \pm 0.013$.

Theorem 36 Formation of volume by volume

In a universe consisting of volume only, the following holds:

(1) The density parameter of volume is equal to 2/3:

$$\Omega_{vol,theo} = \frac{2}{3} \tag{19.40}$$

That result is in precise accordance with observation of early dark energy with help of the CMB:

$$\Omega_{\Lambda,obs} = 0.679 \pm 0.013 \tag{19.41}$$

(2) The dynamic density of volume is as follows:

$$\rho_{vol,h.} = \frac{1}{4\pi \cdot G \cdot t_{H_0}^2} = \rho_{vol,theo} \tag{19.42}$$

Thereby, the rate arriving at R_0 and caused by volume is equal to the inverse Hubble time:

$$\underline{\dot{\varepsilon}}_{\text{at } R_0} = \frac{1}{t_{H_0}} \tag{19.43}$$

Accordingly, the dynamic density of volume is as follows, see PROP (10):

$$\frac{\underline{\dot{\varepsilon}}^2_{\text{at } R_0}}{4\pi \cdot G} = \rho_{vol,theo} = \frac{\underline{\dot{\varepsilon}}_{\text{at } R_0}}{4\pi \cdot G \cdot t_{H_0}} \tag{19.44}$$

$$\frac{c}{4\pi \cdot G} \cdot K_0(\rho_{vol,h.}) = \rho_{vol,theo} \tag{19.45}$$

(3) There is a constant and homogeneous density $\rho_{vol,h.}$, see Eq. (19.45).

(4) At a present-day probe volume dV_0 at an arbitrary location $\vec{R}_0$, there occurs the accumulated rate of formation of volume:

$$\underline{\dot{\varepsilon}}_{\text{at } R_0} = 4\pi G \cdot t_{H_0} \cdot \rho_{vol,h.} \tag{19.46}$$

At that rate, the present-day probe volume dV_0 forms during the Hubble time t_{H_0}.

19.3 u_{vol} at another time

Question: What is the value of the energy density u_{vol} of volume at another value t_{H_1} of the Hubble time?

For it, we use the accumulated rate of formation of volume originating from radii $R \leq R_{H_0} = c \cdot t_{H_0}$, see PROP (8):

$$\underline{\dot{\varepsilon}}_{\text{at } R_0}(R_{H_0}) = 4\pi G \cdot t_{H_0} \cdot \rho_{vol,h.} \tag{19.47}$$

In the case of another value t_{H_1} of the Hubble time, the accumulated rate originates from radii $R \leq R_{H_1} = t_{H_1}$:

$$\underline{\dot{\varepsilon}}_{\text{at } R_0}(R_{H_1}) = 4\pi G \cdot t_{H_1} \cdot \rho_{vol,h.} \tag{19.48}$$

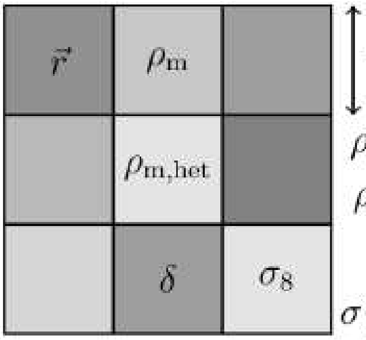

$$L_{\mathrm{box}} = 8\,\frac{\mathrm{Mpc}}{h} \quad \text{with } h = \frac{H}{100\,\frac{\mathrm{km/s}}{\mathrm{Mpc}}}$$

$$\rho_{\mathrm{m}}(t,\vec{r}) = \rho_{\mathrm{m,hom}}(t) + \rho_{\mathrm{m,het}}(t,\vec{r})$$

$$\rho_{\mathrm{m,het}}(t,\vec{r}) = \rho_{\mathrm{m,hom}}(t) \cdot \underbrace{\delta(t,\vec{r})}_{\text{overdensity}}$$

$$\sigma(t) = \sqrt{\langle \delta^2(t,\vec{r})\rangle_{\vec{r}}} \quad \text{and } \sigma(t_0) = \sigma_8$$

Figure 19.4: In order to measure the density as a function of location, space is partitioned into boxes. A box has a location $\vec{r}$, and the density $\rho_{\mathrm{m}}(t,\vec{r})$ is measured for each box.

This relation holds for the following reason: In the derivation of PROP (8), we did not use the particular value t_{H_0} of the Hubble constant. Consequently, PROP (8) holds for each value t_{H_1} of the Hubble constant. Thus, PROP (8) provides the above Eq.

We emphasize that the homogeneous density $\rho_{vol,h.}$ is the same in both rates in Eqs. (19.47, 19.48). As these terms result from the integration with respect to R or t with the same homogeneous integrand $\rho_{vol,h.}$, see Eq. (19.15). The ratio of these Eqs. (19.47, 19.48) provides the relation of rates and times as follows:

$$\frac{\dot{\underline{\varepsilon}}_{\text{at } R_0}(R_{H_1})}{\dot{\underline{\varepsilon}}_{\text{at } R_0}(R_{H_0})} = \frac{t_{H_1}}{t_{H_0}} \quad \text{or} \quad \frac{\dot{\underline{\varepsilon}}_{\text{at } R_0}(R_{H_1})}{t_{H_1}} = \frac{\dot{\underline{\varepsilon}}_{\text{at } R_0}(R_{H_0})}{t_{H_0}} \tag{19.49}$$

We analyze the possibility of a density $\rho_{vol,h.}(t_{H_1})$ at the time t_{H_1}. An observer at t_{H_1} could determine $\rho_{vol,h.}(t_{H_1})$ with the rate in Eq. (19.48):

$$\dot{\underline{\varepsilon}}_{\text{at } R_0}(R_{H_1}) = 4\pi G \cdot t_{H_1} \cdot \rho_{vol,h.}(t_{H_1}) \tag{19.50}$$

In order to determine $\rho_{vol,h.}(t_{H_1})$, the observer could solve the above Eq. for $\rho_{vol,h.}(t_{H_1})$:

$$\rho_{vol,h.}(t_{H_1}) = \frac{\dot{\underline{\varepsilon}}_{\text{at } R_0}(R_{H_1})}{t_{H_1}} \frac{1}{4\pi G} \tag{19.51}$$

In order to compare the analyzed density $\rho_{vol,h.}(t_{H_1})$ with the homogeneous density $\rho_{vol,h.}$ in Eq. (19.47), we apply the relation of rates in Eq. (19.49):

$$\rho_{vol,h.}(t_{H_1}) = \frac{\dot{\underline{\varepsilon}}_{\text{at } R_0}(R_{H_0})}{t_{H_0}} \frac{1}{4\pi G} \tag{19.52}$$

Using the rate in Eq. (19.47), we identify the right hand side in the above Eq. with the homogeneous density in Eq. (19.47):

$$\rho_{vol,h.}(t_{H_1}) = \rho_{vol,h.}, \quad \text{so we get :} \tag{19.53}$$

Theorem 37 Homogeneity implies constant $\rho_{vol,h.}$

In a universe consisting of homogeneous volume only, the following holds:

(1) The energy density u_{vol} of volume that forms at the present-day Hubble time t_{H_0} is equal to the energy density that forms at an arbitrary value t_{H_1} of the Hubble time:

$$\rho_{vol,h.}(t_{H_1}) = \rho_{vol,h.} = \rho_{vol,theo} = \frac{1}{4\pi G \cdot t_{H_0}^2} \quad \text{and} \tag{19.54}$$

$$u_{vol,h.}(t_{H_1}) = u_{vol,h.} = \rho_{vol,theo} \cdot c^2 = \frac{c^2}{4\pi G \cdot t_{H_0}^2} \tag{19.55}$$

(2) The rate of LFV at the present-day Hubble time t_{H_0} and the rate of LFV at another value t_{H_1} of the Hubble time are related as follows:

$$\frac{\dot{\underline{\varepsilon}}_{\text{at } R_0}(R_{H_1})}{\dot{\underline{\varepsilon}}_{\text{at } R_0}(R_{H_0})} = \frac{t_{H_1}}{t_{H_0}} \quad \text{or} \quad \frac{\dot{\underline{\varepsilon}}_{\text{at } R_0}(R_{H_1})}{t_{H_1}} = \frac{\dot{\underline{\varepsilon}}_{\text{at } R_0}(R_{H_0})}{t_{H_0}} \tag{19.56}$$

(3) Thus, the density of volume is transformed as follows: As a consequence of the relation of rates in Eq. (19.56), the density $\rho_{vol,h.}(t_{H_1})$ cannot be determined by replacing the value of the Hubble time only in equation $\rho_{vol,theo} = \frac{1}{4\pi G \cdot t_{H_0}^2}$. Instead, the value of the Hubble time AND the value of the rate are transformed. This implies the constant energy density in Eq. (19.54).

Chapter 20

Dark Energy in a Homogeneous Universe

Question: If a homogeneous density ρ_{hom} is added to the universe consisting of volume only (section 19.2), then there occurs a homogeneous universe, and then there are additional masses or dynamic masses m_i. Do these m_i cause an extra rate $\dot{\underline{\varepsilon}}_{\text{at } R_0}$ at the present-day probe volume dV_0? As the essential example, we analyze the density of matter ρ_m.

20.1 Spatial averages in cosmology

Idea: In order to measure a homogeneous density ρ_{hom}, it is necessary to execute an average in a volume L_{box}^3. In this section, we summarize methods of such averaging in cosmology, see Fig. (19.4) and see e. g. Peebles (1973), Kravtsov and Borgani (2012), Carmesin (2021d), Haude et al. (2022).

Boxes: As a convention, the spatial average is performed within a cubic volume $V_{win} = L_{box}^3$, related to 8 Mpc as follows, see e. g. Kravtsov and Borgani (2012), Carmesin (2021d)[1]:

[1]Note that this scaling of the size L_{box} is a convention. In general, the scaling of L_{box} is not identical to the scale factor describing the expansion of space since the Big Bang. Sometimes, averages are performed in spheres, White et al. (1993).

$$L_{box} = 8h^{-1}\,\text{Mpc} \ \ \text{with} \ \ h = H_0 \cdot \frac{1}{100}\frac{\text{km}}{\text{s} \cdot \text{Mpc}} \tag{20.1}$$

Local density: A box has a location $\vec{r}$. A local density at a time t is measured for each box:

$$\text{local density} \ \ \rho_m(t, \vec{r}) \tag{20.2}$$

Global density: The globally averaged density is introduced:

$$\text{global density} \ \ \rho_{m,hom}(t) \tag{20.3}$$

Overdensity: The overdensity is introduced as follows:

$$\text{overdensity} \ \ \delta(t, \vec{r}) = \frac{\rho_m(t, \vec{r}) - \rho_{m,hom}(t)}{\rho_{m,hom}(t)} \tag{20.4}$$

The density $\rho_{m,het}(t, \vec{r})$ of the heterogeneity is the product of $\rho_{m,hom}(t)$ and the overdensity:

$$\rho_{m,het}(t, \vec{r}) = \rho_{m,hom}(t) \cdot \delta(t, \vec{r}) \tag{20.5}$$

We summarize the densities in the surroundings of the volume:

$$\rho = \rho_{m,hom}(t) + \rho_{m,het}(t, \vec{r}) + \rho_r + \rho_\Lambda \tag{20.6}$$

20.1.1 Averages of fluctuations

In this section, we summarize spatial averaging of fluctuations in cosmology, see for instance Peebles (1973), Kravtsov and Borgani (2012), Carmesin (2021d).

A spatial average of a function $f(\vec{r})$ is applied within a volume V_{window} or V_{win} of a considered region (window) of averaging:

$$\langle f(\vec{r}) \rangle_{V_{win}} = \frac{\int_{V_{win}} f(\vec{r})\, dr^3}{\int_{V_{win}} 1\, dr^3} \tag{20.7}$$

Fluctuations of a function $f(\vec{r})$ are usually described by the standard deviation $\sigma_{V_{win}}$:

$$\sigma^2_{V_{win}} = \langle [f(\vec{r}) - \langle f(\vec{r})\rangle_{V_{win}}]^2\rangle_{V_{win}} = \langle f^2(\vec{r})\rangle_{V_{win}} - \langle f(\vec{r})\rangle^2_{V_{win}} \tag{20.8}$$

As a convention, the spatial average is performed within a cubic volume $V_{win} = L^3_{box}$, related to 8 Mpc as follows, see Eq. (20.1) or e. g. Kravtsov and Borgani (2012), Carmesin (2021d)[2]. In that case, the standard deviation is named $\sigma_8(t)$ or $\delta(t)$:

$$\sigma_8(t) = \delta(t) = \sigma_{\delta,V_{win}}(t) \;\; \text{with} \;\; \sigma_{8,0} = \sigma_8(t_0) \tag{20.9}$$

20.2 Formation and propagation of volume

Idea: The dynamics of additional volume and of volume in general is described by the formation and propagation of volume (chapter 11). After averaging, a homogeneous density $\rho_{m,hom}(t)$ does not cause an extra rate $\dot{\underline{\varepsilon}}_{\text{at } R_0}$ at the present-day probe volume dV_0. The formation of volume in dV_0 is based on a solution of the nonhomogeneous DEQ, so it could be caused by a local heterogeneity $\rho_{m,het}(t,\vec{r})$ only. In contrast, the propagation of volume is described by a solution of the homogeneous DEQ. Here, we elaborate local and averaged results.

Theorem 38 Formation & propagation at homogeneity
(1) In a universe with a homogeneous density $\rho_{m,hom}$, the following holds:

(1a) Each mass or dynamic mass m_i causes unidirectional formation of volume $\dot{\underline{\varepsilon}}_L$ in its **near vicinity**. *It is described by a* **nonhomogenous solution** *of the DEQ (11.7). Each such solution is characterized by a nonzero gravitational field $\vec{G}^*_i$.*

(1b) At a **larger vicinity**, *heterogeneity cancels out, so that the density is homogeneous. Correspondingly, the fields $\vec{G}^*_i$ of*

[2]Note that this scaling of the size L_{box} is a convention. In general, the scaling of L_{box} is not identical to the scale factor describing the expansion of space since the Big Bang.

different masses m_i compensate each other, so that the field $\vec{G}^*$ is zero. As a consequence, the **homogeneous solution** *of the DEQ describes the dynamics. Consequently, the density $\rho_{\mathrm{m,\,hom}}$ does not cause any extra rate $\dot{\underline{\varepsilon}}_{\mathrm{at}\ R_0}$ at the present-day probe volume dV_0.*

(1c) The homogeneous density, $\rho_{\mathrm{m,\,hom}}$ causes the squared normalized rate of globally formed volume $\left(\frac{\dot{V}}{V}\right)^2 = 24\pi G\rho_{\mathrm{m,\,hom}}$. If such GFV arrives at the present-day probe volume dV_0, it passes dV_0 without forming volume at dV_0, as it propagates according to the **homogeneous solution.**

(2) A possible homogeneous density $\rho_{\mathrm{r,\,hom}}$ of radiation exhibits the same properties with respect to dV_0, see part (1).

(3) For each averaged density ρ_1, the LFV or GFV exhibit a solution of the DEQ (11.7). That solution includes a solution of the corresponding homogeneous DEQ. Accordingly, that solution also describes a squared normalized rate of globally formed volume $\left(\frac{\dot{V}}{V}\right)^2 = 24\pi G\rho_1$.

(4) In the universe consisting of volume only, the density parameter of volume is equal to two thirds, $\Omega_{vol} = \frac{2}{3}$.

(5) In the homogeneous universe, the density parameter of volume is equal to two thirds, $\Omega_{vol} = \frac{2}{3}$. A homogeneous density $\rho_{\mathrm{m,\,hom}}$ causes GFV, but $\rho_{\mathrm{m,\,hom}}$ does not cause a change of the density of volume ρ_{vol}.

(6) In a universe with heterogeneous matter with a corresponding density $\rho_{m,hom} + \rho_{m,het}$, the following holds:

(6a) Each local heterogeneity $\rho_{m,het}(\vec{r})$ causes unidirectional formation of volume $\dot{\underline{\varepsilon}}_L$. It is described by a nonhomogenous solution of the DEQ (11.7). Each such solution is characterized by a nonzero gravitational field $\vec{G}_i^*$.

(6b) Consequently, a local heterogeneity $\rho_{m,het}(\vec{r})$ causes an extra rate $\dot{\underline{\varepsilon}}_{\mathrm{at}\ R_0}$ at the present-day probe volume dV_0.

Chapter 21

Dark Energy by Heterogeneity

Essential question: The formation of LFV according to unidirectional formation of volume (THM 15) at a homogeneous density $\rho_{\mathrm{m,hom}}$ provides a value $u_{vol,\mathrm{theo,hom}}$ of the energy density of volume (THM 36, 37, 38). For comparison, the value $u_{\Lambda,obs,CMB}$ of the energy density of Λ has been observed with help of the cosmic microwave background, CMB. That value is in precise accordance with our derived value $u_{vol,\mathrm{theo,hom}}$ (C. 19). However, Riess et al. (2022) discovered a highly significant discrepancy among different observations of the Hubble constant H_0. What is the physical reason of that difference?

21.1 Physics of the observed discrepancy

Idea: In usual cosmological models, a homogeneous universe is used, Friedmann (1922), Lemaitre (1927), Hobson et al. (2006). With it, the rate of expansion is described by the Hubble parameter, Eq. (5.27):

$$H(z) = H_0\sqrt{\Omega_\Lambda + \Omega_{m,0}(1+z)^3 + \Omega_{r,0}(1+z)^4} \qquad (21.1)$$

Thereby, the redshift z describes a calendar date, we apply $\Omega_{k,0} = 0$, and the Hubble constant H_0 is a constant. In our heterogeneous universe, the factor H_0 in Eq. (21.1) might be a function of z. We provide a first test of that possibility:

21.1.1 Observed discrepancy

Based on the CMB, emitted at $z_{\mathrm{em}} = 1090.3$, the observed value of H_0 is as follows, Planck-Collaboration (2020):

$$H_{0,obs,CMB} = 66.88(\pm 0.92)\,\frac{\mathrm{km}}{\mathrm{s}\cdot\mathrm{Mpc}} \tag{21.2}$$

Riess et al. (2022) used radiation emitted from supernovae of type Ia in near galaxies and obtained the following H_0-value:

$$H_{0,obs,near,Ia} = 73.04(\pm 1.01)\,\frac{\mathrm{km}}{\mathrm{s}\cdot\mathrm{Mpc}} \tag{21.3}$$

Thereby, the averaged redshift is $\langle z \rangle = 0.055$, see (Riess et al., 2022, sections 5.1 and 5.2). So, observers discovered an interesting discrepancy at the five σ confidence level, and it might be related to the redshift z_{em}.

21.1.2 How are different values of H_0 observed?

Idea: The values of the Hubble parameter $H(z)$ and the root in Eq. (21.1) can be observed. That Eq. can be solved for H_0:

$$H_0 = \frac{H(z)}{\sqrt{\Omega_\Lambda + \Omega_{m,0}(1+z)^3 + \Omega_{r,0}(1+z)^4}} \tag{21.4}$$

If an observer uses radiation emitted at a redshift z_{em}, then the state and the value of H_0 at $z = z_{\mathrm{em}}$ are observed:

$$H_0(z_{\mathrm{em}}) = \frac{H(z_{\mathrm{em}})}{\sqrt{\Omega_\Lambda + \Omega_{m,0}(1+z_{\mathrm{em}})^3 + \Omega_{r,0}(1+z_{\mathrm{em}})^4}} \tag{21.5}$$

21.1.3 Plan and results

In the following, we will explain the discrepancy in section (21.1.1) by fundamental physics: Firstly, we show how H_0 becomes a function of time or of $z = z_{\mathrm{em}}$ (section 21.2). Secondly, we will derive a reference value of H_0, corresponding to the homogeneous universe (section 21.3). Thirdly, we will derive the observed discrepancy. Fourthly, we will precisely predict possible future observations of such discrepancies (section 21.4).

21.2 Time dependence of H_0

Fact of time dependence: Of course, the usual or ideal value $H_{0,ideal}$ of the Hubble constant does not depend on time, see e. g. Hobson et al. (2006); Planck-Collaboration (2020); Workman et al. (2022). However, each observation of the Hubble constant uses a probe, the CMB or light emitted by near galaxies, for instance. As a matter of fact, each probe has been emitted at a time t_{em} of emission. Thus, each observed value $H_{0,obs}$ of the Hubble constant is a function of the time of emission:

$$H_{0,obs} = H_{0,obs}(t_{\mathrm{em}}) \tag{21.6}$$

In principle, $H_{0,obs}$ could depend on even more peculiar details of observation. However, we will show that the largest part of the observed variation of $H_{0,obs}$ can be explained by the time evolution of the universe[1].

21.3 Derivation of the ideal value of H_0

Idea: We introduce an ideal reference value $H_{0,hom}$ corresponding to the homogeneous universe. For it, we derive $H_{0,hom}$ from our theoretical value of the energy density in the homogeneous universe (THMs 36 and 38):

$$\rho_{vol,theo}(t_{\mathrm{em}} = t_{\mathrm{hom}}) = \frac{1}{4\pi G \cdot t^2_{H_{0,hom}}} \tag{21.7}$$

Remind that a homogeneous density of matter causes more volume, but no increased density of volume. This reference value is an ideal value for the following reasons:

[1]See e. g. Carmesin (2018c), Carmesin (2018b), Carmesin (2019b), Carmesin (2021d), Carmesin (2021a), Carmesin (2021b), Carmesin (2021c).

(1) The homogeneous case is ideal, as the corresponding density $\rho_{vol,theo}(t_{\text{em}} = t_{\text{hom}})$ is equal to the density of the universe consisting of volume only:

$$\rho_{vol,theo}(t_{\text{em}} = t_{\text{hom}}) = \rho_{vol,c.h.} \tag{21.8}$$

(2) Only this homogeneous case is ideal, as heterogeneity is peculiar. Hereby, t_{hom} describes the time at which the universe was homogeneous. Accordingly, $t_{H_{0,hom}} = 1/H_{0,hom}$ describes the time corresponding to the ideal Hubble constant $H_{0,hom}$.
(3) As the universe was most homogeneous in the early universe, a probe emitted at t_{hom} can sample a very huge volume. Thus, possible peculiar local deviations can be averaged out.
Methods: We derive the ideal value $H_{0,hom}$ by several methods, in order to show the robustness of the concept:

21.3.1 First derivation of $H_{0,hom}$

The ideal value $H_{0,hom}$ corresponds to the time t_{hom} at which the universe was homogeneous. Correspondingly, $H_{0,hom}$ is the value of $H_{0,obs}$ at t_{hom}:

$$H_{0,hom} = H_{0,obs}(t_{\text{em}} = t_{\text{hom}}) \tag{21.9}$$

Estimation of $H_{0,hom}$: As the universe has been nearly homogeneous at the emission of the CMB, the ideal value is that of the CMB, in a good approximation:

$$H_{0,hom} \approx H_0(t_{\text{em}} = t_{\text{CMB}}) = 66.88\,(\pm 0.92)\,\frac{\text{km}}{\text{s} \cdot \text{Mpc}} \tag{21.10}$$

As that value essentially represents the present-day age of the universe, $t_{H_0} = 1/H_0$, it cannot be derived, it is measured.

21.3.2 Second derivation of $H_{0,hom}$

Idea: We derive $H_{0,hom}$ on the basis of the local dynamics of LFV. For it, we use the density $\rho_{vol,theo}(t_{\text{em}} = t_{\text{hom}})$ in Eq.

(21.7), that we derived on the basis of that local dynamics, C. (19).

Firstly, we apply $t_{H_{0,hom}} = 1/H_{0,hom}$ to the density in Eq. (21.7), and we solve for $H^2_{0,hom}$:

$$H^2_{0,hom} = \rho_{vol,theo}(t_{\rm em} = t_{\rm hom}) \cdot 4\pi G \tag{21.11}$$

Hereby, the density is the product of the density parameter and the critical density,

$$\rho_{vol,theo}(t_{\rm em} = t_{\rm hom}) = \Omega_{vol,0}(t_{\rm em} = t_{\rm hom}) \cdot \rho_{cr,0}(t_{\rm em} = t_{\rm hom}) \tag{21.12}$$

$$\text{or} \quad \rho_{vol,theo}(t_{\rm em} = t_{\rm hom}) = \frac{2}{3}\rho_{cr,0}(t_{\rm em} = t_{\rm hom}) \tag{21.13}$$

and the critical density is as follows (Eq. 19.38):

$$\rho_{cr,0}(t_{\rm em} = t_{\rm hom}) = \frac{3H_0^2(t_{\rm em} = t_{\rm hom})}{8\pi G} \tag{21.14}$$

Secondly, we insert the above relations of densities in Eqs. (21.12, 21.13) into the term of $H^2_{0,hom}$ in Eq. (21.11):

$$H^2_{0,hom} = \frac{2}{3}\frac{3H_0^2(t_{\rm em} = t_{\rm hom})}{8\pi G} \cdot 4\pi G = H_0^2(t_{\rm em} = t_{\rm hom}) \tag{21.15}$$

Thus, the ideal value of H_0 is the value of the Hubble constant at the time when the universe was homogeneous:

$$H_{0,hom} = H_0(t_{\rm em} = t_{\rm hom}) \tag{21.16}$$

This result is in accordance with Eqs. (21.9, 21.10).

21.4 Parameter measured with a probe

Idea: If the value of H_0 is measured, then a probe is used that has been emitted at a time $t_{\rm em}$ (Fig. 21.1). In that probe, heterogeneity that formed at times $t_{\rm form}$ before $t_{\rm em}$ is included. In this section, we derive rates of LFV caused by heterogeneity at such times $t_{\rm form}$, see Eq. (21.2).

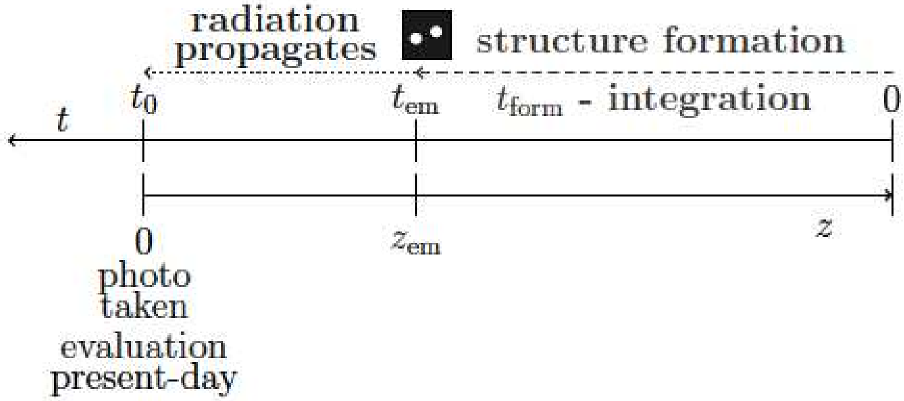

Figure 21.1: Measurement of a cosmological parameter: The structure formed during the time between $t = 0$ and $t_{\rm em}$ (dashed). The structure, e. g. the above two stars, emits radiation at a time $t_{\rm em}$. That radiation propagates to the observer during the time between $t_{\rm em}$ and t_0 (dotted).

21.4.1 Field caused at a time $t_{\rm form}$

At a time $t_{\rm form}$, a mass $dM_{\rm j,het}(t_{\rm form})$ causes the field at R:

$$|d\vec{G}_j^*|(R) = \frac{G \cdot dM_{\rm j,het}(t_{\rm form})}{R^2} \tag{21.17}$$

If the mass is at a location $\vec{r}$, then the mass is expressed by the density and overdensity, see Eq. (20.5):

$$dM_{\rm j,het}(t_{\rm form}) = \rho_{\rm m,hom}(t_{\rm form}) \cdot \delta(t_{\rm form}, \vec{r}) \cdot dV_j(t_{\rm form}) \tag{21.18}$$

In the expanding universe, the scale radius can change from a value $a(t_{\rm form})$ to a value $a(t_0)$. Thereby, the volume dV_j changes as follows:

$$dV_j(t_0) = dV_j(t_{\rm form}) \left(\frac{a(t_0)}{a(t_{\rm form})}\right)^3 \tag{21.19}$$

Consequently, the density changes as follows:

$$\rho_{\rm m}(t_0) = \rho_{\rm m}(t_{\rm form}) \left(\frac{a(t_{\rm form})}{a(t_0)}\right)^3 \tag{21.20}$$

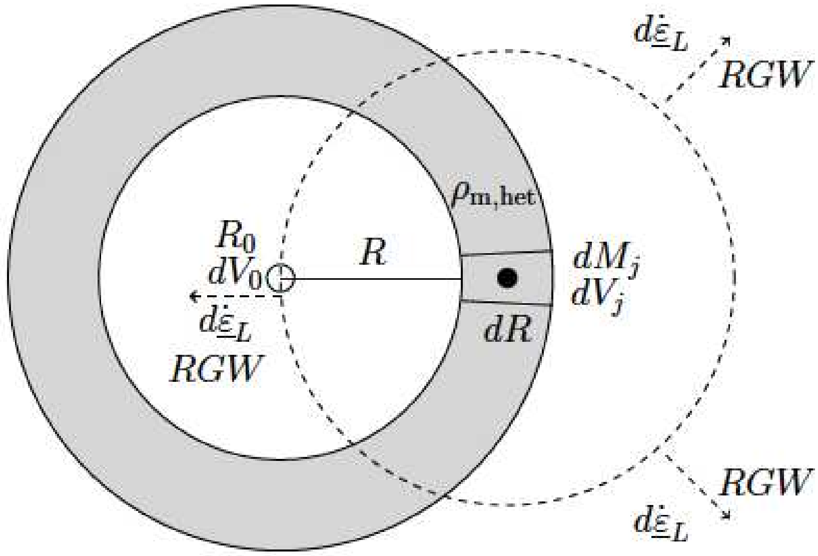

Figure 21.2: The density $\rho_{\mathrm{m,het}}$ in an area at a distance R from R_0 has a $j-th$ mass dM_j. It generates rates $d\dot{\underline{\varepsilon}}_L$ propagating towards all directions in the same manner.

The mass in Eq. (21.18) is transformed to the mass term in Eq. (21.21) by inserting the changes in Eqs: (21.19, 21.20):

$$dM_{\mathrm{j,het}}(t_{\mathrm{form}}) = \rho_{\mathrm{m,hom}}(t_0) \cdot \delta(t_{\mathrm{form}}, \vec{r}) \cdot dV_j(t_0) \qquad (21.21)$$

21.4.2 Fluctuations caused at a time t_{form}

Idea: In order to analyze fluctuations of fields, we investigate squares and their averages.

At a time t_{form}, masses $dM_{\mathrm{j,het}}(t_{\mathrm{form}})$ cause the field in Eq. (21.17) and its square at R. Hereby, we express the mass in terms of the density in Eq. (21.21):

$$\langle d\vec{G}^{*2}_{\vec{r},\,\mathrm{from}\ t_{\mathrm{form}}}(t_0, R)\rangle = \frac{G^2 \cdot \rho^2_{\mathrm{m,hom}}(t_0) \cdot \langle \delta^2(t_{\mathrm{form}}, \vec{r})\rangle \cdot dV_L^2}{R^4} \qquad (21.22)$$

Thereby, we replace the subscript j of a mass by the subscript $\vec{r}$ of the location, and we use the volume of the shell $dV_L = 4\pi R^2 dL$. In the present global analysis, we can replace dL by

dR is a very good approximation. Additionally, we apply the average with respect to the fluctuations of heterogeneity.

Next, we use the law of unidirectional formation of volume (THM 15), and we apply the standard deviation $\langle \delta^2 \rangle = \sigma^2$:

$$\langle d\dot{\underline{\varepsilon}}^2_{\text{het}}(t_0, t_{\text{form}}, R) \rangle = \frac{G^2 \cdot \rho^2_{\text{m,hom}}(t_0) \cdot \sigma^2(t_{\text{form}}) \cdot 16\pi^2 dR^2}{c^2} \tag{21.23}$$

21.4.3 Linear growth theory

Idea: The time evolution of the heterogeneity is described by the time evolution of the standard deviation $\sigma^2(t_{\text{form}})$ in Eq. (21.23). For it, we apply the linear growth theory.

Based on the FLE, the linear growth theory describes the time evolution of density fluctuations. As a result, the standard deviation is a linear function of time as follows[2]:

$$\sigma(t) = \sigma_{8,0} \cdot \frac{t}{t_{H_0}} \tag{21.24}$$

21.4.4 Integration and equivalent rate

Ideas: Firstly, for each time of emission t_{em}, we integrate the fluctuations that formed in the universe since the Big Bang at $t_{\text{form}} = 0$ until t_{em}.

Secondly, the squared rates $\langle d\dot{\underline{\varepsilon}}^2_{\text{het}}(t_0, t_{\text{form}}, R) \rangle$ in Eq. (21.23) correspond to RGWs with a kinetic energy (THM 19). The presence of that nonzero kinetic energy shows that there are nonzero RGWs with a corresponding equivalent rate $d\dot{\underline{\varepsilon}}_{\text{het,equi}}$.

Accordingly, we express $\langle d\dot{\underline{\varepsilon}}^2_{\text{het}}(t_0, t_{\text{form}}, R) \rangle$ by the kinetic energy of corresponding RGWs, see THM (19):

$$\langle d\dot{\underline{\varepsilon}}^2_{\text{het}}(t_0, t_{\text{form}}, R) \rangle = \langle du_{kin} \rangle \cdot \frac{8\pi G}{c^2} \tag{21.25}$$

[2] Kravtsov and Borgani (2012), (Carmesin, 2021d, Eq. (7.123)), with normalization to $\sigma(t_{H_0}) = \sigma_{8,0}$. Eq. (21.24) is a good approximation, Mandal and Nadkarni-Ghosh (2020).

According to THM (19), the kinetic energy corresponds to a square of equivalent rates:

$$\langle du_{kin}\rangle = \frac{c^2}{8\pi G}\cdot d\dot{\underline{\varepsilon}}^2_{\text{equi,het}}, \quad \text{consequently,} \tag{21.26}$$

$$d\dot{\underline{\varepsilon}}_{\text{het,equi}} = \sqrt{\langle d\dot{\underline{\varepsilon}}^2_{\text{het}}(t_0, t_{\text{form}}, R)\rangle}, \tag{21.27}$$

We identify the increment dR with the time of formation multiplied by c or $|dR| = c\cdot|dt_{\text{form}}|$. So the rate is transformed to the following term, see Eq. (21.23):

$$d\dot{\underline{\varepsilon}}_{\text{het,equi}} = \frac{G\cdot\rho_{\text{m,hom}}(t_0)\cdot\sigma_{8,0}\cdot t_{\text{form}}\cdot 4\pi\cdot dt_{\text{form}}}{t_{H_0}} \tag{21.28}$$

The ratios of densities and density parameters are equal:

$$\frac{\rho_{\text{m,hom}}(t_0)}{\Omega_{m,0}} = \frac{\rho_{\Lambda,\text{hom}}(t_0)}{\Omega_{\Lambda,0}} \text{ or} \tag{21.29}$$

$$\rho_{\text{m,hom}}(t_0) = \rho_{\Lambda,\text{hom}}(t_0)\cdot\frac{\Omega_{m,0}}{\Omega_{\Lambda,0}} \tag{21.30}$$

We apply Eq. (21.30) to the rate in Eq. (21.28):

$$d\dot{\underline{\varepsilon}}_{\text{het,equi}} = \frac{t_{\text{form}}}{t_{H_0}}\frac{dt_{\text{form}}}{t_{H_0}}[4\pi G\rho_{\Lambda,\text{hom}}(t_0)t_{H_0}]\frac{\sigma_{8,0}\cdot\Omega_{m,0}}{\Omega_{\Lambda,0}} \tag{21.31}$$

$$\text{We use scaled time}: \tilde{t} := \frac{t_{\text{form}}}{t_{H_0}}, \quad \text{with it,} \tag{21.32}$$

$$d\dot{\underline{\varepsilon}}_{\text{het,equi}} = \tilde{t}d\tilde{t}\cdot[4\pi G\cdot\rho_{\Lambda,\text{hom}}(t_0)\cdot t_{H_0}]\cdot\frac{\sigma_{8,0}\cdot\Omega_{m,0}}{\Omega_{\Lambda,0}} \tag{21.33}$$

We apply the integral. Moreover, we identify the rectangular bracket with the rate in the homogeneous universe (part (4) in THM 36):

$$\dot{\underline{\varepsilon}}_{\text{hom}} = 4\pi G\cdot\rho_{\Lambda,\text{hom}}(t_0)\cdot t_{H_0} \text{ and} \tag{21.34}$$

$$\int_0^{\dot{\underline{\varepsilon}}_{\text{het,equi,0}}} d\dot{\underline{\varepsilon}}_{\text{het,equi}} = \int_0^{\tilde{t}_{\text{em}}} \tilde{t}d\tilde{t}\cdot\dot{\underline{\varepsilon}}_{\text{hom}}\cdot\frac{\sigma_{8,0}\cdot\Omega_{m,0}}{\Omega_{\Lambda,0}} \text{ or} \tag{21.35}$$

$$\underline{\dot{\varepsilon}}_{\text{het,equi,0}}(\tilde{t}_{\text{em}}) = \underline{\dot{\varepsilon}}_{\text{hom}} \cdot \frac{\tilde{t}_{\text{em}}^2 \sigma_{8,0} \cdot \Omega_{m,0}}{2\Omega_{\Lambda,0}} \tag{21.36}$$

We abbreviate the ratios of the rate $\underline{\dot{\varepsilon}}_{\text{het,equi,0}}$ caused by heterogeneity and the rate $\underline{\dot{\varepsilon}}_{\text{hom}}$ of the homogeneous universe:

$$\kappa(\tilde{t}_{\text{em}}) = \frac{\underline{\dot{\varepsilon}}_{\text{het,equi,0}}(\tilde{t}_{\text{em}})}{\underline{\dot{\varepsilon}}_{\text{hom}}} = \frac{\tilde{t}_{\text{em}}^2 \sigma_{8,0} \cdot \Omega_{m,0}}{2\Omega_{\Lambda,0}} \quad \text{or} \tag{21.37}$$

$$\kappa(z_{\text{em}}) = \frac{\sigma_{8,0} \cdot \Omega_{m,0}}{2\Omega_{\Lambda,0} \cdot (1 + z_{\text{em}})^2} \quad \text{or} \tag{21.38}$$

$$\underline{\dot{\varepsilon}}_{\text{het,equi,0}}(\tilde{t}_{\text{em}}) = \kappa(\tilde{t}_{\text{em}}) \cdot \underline{\dot{\varepsilon}}_{\text{hom}} \quad \text{or} \tag{21.39}$$

$$\underline{\dot{\varepsilon}}_{\text{het,equi,0}}(\tilde{t}_{\text{em}}) = \kappa(z_{\text{em}}) \cdot \underline{\dot{\varepsilon}}_{\text{hom}} \tag{21.40}$$

21.4.5 Equivalent density

Idea: The density of heterogeneity is zero. However, the heterogeneity causes an additional rate. This can be represented by an equivalent density $\rho_{het,equi}$

In order to derive the equivalent density, we apply the abbreviation in Eq. (21.37) and the rate $\underline{\dot{\varepsilon}}_{\text{hom}}$ in Eq. (21.34) to the rate $\underline{\dot{\varepsilon}}_{\text{het,equi,0}}$ in Eq. (21.36):

$$\underline{\dot{\varepsilon}}_{\text{het,equi,0}}(\tilde{t}_{\text{em}}) = 4\pi G \cdot \rho_{\Lambda,\text{hom}}(t_0) \cdot t_{H_0} \cdot \kappa(\tilde{t}_{\text{em}}) \tag{21.41}$$

The product $\rho_{\Lambda,\text{hom}}(t_0) \cdot \kappa(\tilde{t}_{\text{em}})$ in the above Eq. is caused by heterogeneity. Accordingly, we call the product **equivalent density of heterogeneity**:

$$\rho_{het,equi} = \rho_{\Lambda,\text{hom}}(t_0) \cdot \kappa(\tilde{t}_{\text{em}}) \tag{21.42}$$

With it, the rate $\underline{\dot{\varepsilon}}_{\text{het,equi,0}}$ in Eq. (21.41) is as follows:

$$\underline{\dot{\varepsilon}}_{\text{het,equi,0}}(\tilde{t}_{\text{em}}) = 4\pi G \cdot \rho_{het,equi} \cdot t_{H_0} \tag{21.43}$$

In order to obtain the complete rate $\underline{\dot{\varepsilon}}_{\text{sum}}$, we add the two rates in Eqs. (21.41) and (21.34):

$$\underline{\dot{\varepsilon}}_{\text{sum}}(\tilde{t}_{\text{em}}) = \underline{\dot{\varepsilon}}_{\text{hom}} + \underline{\dot{\varepsilon}}_{\text{het,equi,0}}(\tilde{t}_{\text{em}}) = 4\pi G[\rho_{\Lambda,\text{hom}}(t_0) + \rho_{het,equi}]t_{H_0} \tag{21.44}$$

We apply the abbreviation in Eq. (21.39) to the above rate:

$$\underline{\dot{\varepsilon}}_{\text{sum}}(\tilde{t}_{\text{em}}) = \underline{\dot{\varepsilon}}_{\text{hom}} \cdot [1 + \kappa(\tilde{t}_{\text{em}})] \tag{21.45}$$

We abbreviate the sum of densities in Eq. (21.44), and we use $\rho_{\Lambda,\text{hom}}(t_0) = \rho_{vol}$, C. (20):

$$\rho_{\Lambda,\text{hom}}(t_0) + \rho_{het,equi} = \rho_{vol+equi} = \rho_{vol} + \rho_{het,equi} \tag{21.46}$$

We insert the density and the rate in Eqs. (21.45, 21.46) into the rate in Eq. (21.44). Additionally, we divide by $4\pi G \cdot t_{H_0}$:

$$\underline{\dot{\varepsilon}}_{\text{hom}} \cdot [1 + \kappa(\tilde{t}_{\text{em}})] \cdot \frac{1}{4\pi G \cdot t_{H_0}} = \rho_{vol+equi} \tag{21.47}$$

We describe the ratio of the densities $\rho_{vol+\text{equi}}$ and $\rho_{\Lambda,\text{hom}}(t_0)$ with help of an exponent ξ that we derive in the following:

$$\rho_{vol+equi} = \rho_{\Lambda,\text{hom}}(t_0)[1+\kappa(\tilde{t}_{\text{em}})]^{\xi} = \rho_{vol,\text{theo}}[1+\kappa(\tilde{t}_{\text{em}})]^{\xi} \tag{21.48}$$

Hereby, we use the equality of $\rho_{\Lambda,\text{hom}}(t_0)$ and $\rho_{vol,\text{theo}}$. With it, the density in Eq. (21.47) is as follows:

$$\underline{\dot{\varepsilon}}_{\text{hom}} \cdot [1+\kappa(\tilde{t}_{\text{em}})] \cdot \frac{1}{4\pi G} \cdot \frac{1}{t_{H_0}} = \rho_{\Lambda,\text{hom}}(t_0) \cdot [1+\kappa(\tilde{t}_{\text{em}})]^{\xi} \quad \text{or} \tag{21.49}$$

$$\underline{\dot{\varepsilon}}_{\text{hom}} \cdot [1 + \kappa(z_{\text{em}})] \cdot \frac{1}{4\pi G} \cdot \frac{1}{t_{H_0}} = \rho_{\Lambda,\text{hom}}(t_0) \cdot [1 + \kappa(z_{\text{em}})]^{\xi} \tag{21.50}$$

21.4.6 Hubble constant measured with a probe

Idea: If the Hubble constant $H_{0,obs}$ is measured with a probe emitted at a time t_{em}, then the rate $\underline{\dot{\varepsilon}}_{\text{sum}}(\tilde{t}_{\text{em}})$ in Eq. (21.44) arrives at the probe volume dV_0. Accordingly, the observed Hubble constant $H_{0,obs}$ includes the sum of densities $\rho_{vol+\text{equi}}$. The resulting Hubble constant $H_{0,obs}$ is elaborated in this section.

For it, we use the fact that the Hubble constant is a function of the density. The radiation era is characterized by redshifts above $z_{eq} = 3411 \pm 48$, (Planck-Collaboration, 2020, table 2).

Heterogeneity was still very small at the redshift $z_{\mathrm{CMB}} = 1090$ of the emission of the CMB, Smoot et al. (1992) or (Carmesin, 2021d, Eq. 7.104):

$$\sigma_8(z_{\mathrm{CMB}} = 1090) = 44 \cdot 10^{-6} \tag{21.51}$$

Accordingly, in our present analysis of heterogeneity, we can neglect the density of radiation in a good approximation. Thus, H_0 is as follows:

$$H_0^2 = \frac{8\pi G}{3} \cdot (\rho_{\mathrm{m,hom}} + \rho_\Lambda) \tag{21.52}$$

In the observed Hubble constant $H_{0,obs}$, the rate caused by heterogeneity is included. This rate corresponds to the density $\rho_{\mathrm{het,equi}}$. Thus, this rate can be included in the Hubble constant in Eq. (21.52) by using the sum of the densities $\rho_{vol+\mathrm{equi}}$ instead of the density of volume ρ_Λ. So we derive the squared observed Hubble constant:

$$H_{0,obs}^2(z_{\mathrm{em}}) = \frac{8\pi G}{3} \cdot (\rho_{\mathrm{m,hom}} + \rho_{vol+\mathrm{equi}}) \tag{21.53}$$

In the above Eq., we insert $\rho_{vol+\mathrm{equi}}$ in Eq. (21.48):

$$H_{0,obs}^2 = \frac{8\pi G}{3} \cdot (\rho_{\mathrm{m,hom}} + \rho_{vol,theo} \cdot [1 + \kappa(z_{\mathrm{em}})]^\xi) \tag{21.54}$$

In the above Hubble constant Eq. (21.54), we apply the density parameters. As $H_{0,obs}$ describes the present-day rate of expansion of the universe, the present-day density parameter of matter is used:

$$\Omega_{m,0} = \frac{\rho_{\mathrm{m,hom}}}{\rho_{cr.,0}} \text{ and} \Omega_{vol,0,theo} = \frac{\rho_{vol,theo}}{\rho_{cr.,0}} = \frac{2}{3} \tag{21.55}$$

So we derive:

$$H_{0,obs}^2 = \frac{8\pi G \cdot \rho_{cr.,0}}{3} \cdot (\Omega_{m,0} + \Omega_{vol,0,theo} \cdot [1 + \kappa(z_{\mathrm{em}})]^\xi) \tag{21.56}$$

We identify the fraction in the above Eq. with the squared Hubble constant $H^2_{0,\text{without het}}$ without heterogeneity:

$$H^2_{0,obs}(z_{\text{em}}) = H^2_{0,\text{without het}} \cdot (\Omega_{m,0} + \Omega_{vol,0,theo} \cdot [1 + \kappa(z_{\text{em}})]^{\xi}) \tag{21.57}$$

We apply the root.

$$H_{0,obs}(z_{\text{em}}) = H_{0,\text{without het}} \cdot \sqrt{\Omega_{m,0} + \Omega_{vol,0,theo} \cdot [1 + \kappa(z_{\text{em}})]^{\xi}} \tag{21.58}$$

We apply the Hubble times $t_{H_0,obs} = 1/H_{0,obs}(z_{\text{em}})$ and $t_{H_0,hom} = 1/H_{0,\text{without het}}$ to the above equation:

$$1/t_{H_0,obs} = 1/t_{H_0,hom} \cdot \sqrt{\Omega_{m,0} + \Omega_{vol,0,theo} \cdot [1 + \kappa(z_{\text{em}})]^{\xi}} \tag{21.59}$$

We apply the inverse Hubble time $1/t_{H_0,obs}$ to the density in Eq. (21.50). As the heterogeneity is included in Eq. (21.50), the observed Hubble time is used:

$$\begin{aligned} \underline{\dot{\varepsilon}}_{\text{hom}} \cdot [1 + \kappa(z_{\text{em}})] \cdot \frac{1}{4\pi G} \cdot \frac{1}{t_{H_0,obs}} &= \rho_{\Lambda,\text{hom}}(t_0) \cdot [1 + \kappa(z_{\text{em}})]^{\xi} \quad \text{or} \\ \underline{\dot{\varepsilon}}_{\text{hom}} [1 + \kappa(z_{\text{em}})] \sqrt{\Omega_{m,0} + \Omega_{vol,0,theo} \cdot [1 + \kappa(z_{\text{em}})]^{\xi}} \cdot \frac{1}{4\pi G} \frac{1}{t_{H_0,hom}} & \\ = \rho_{\Lambda,\text{hom}}(t_0) \cdot [1 + \kappa(z_{\text{em}})]^{\xi} & \end{aligned} \tag{21.60}$$

We apply $\underline{\dot{\varepsilon}}_{\text{hom}} = \frac{1}{t_{H_0,hom}}$ (Eq. 19.29) to the above Eq.:

$$\begin{aligned} [1 + \kappa(z_{\text{em}})] \quad \cdot \quad & \sqrt{\Omega_{m,0} + \Omega_{vol,0,theo} \cdot [1 + \kappa(z_{\text{em}})]^{\xi}} \\ \cdot \frac{1}{4\pi G \cdot t^2_{H_0,hom}} \quad = \quad & \rho_{\Lambda,\text{hom}}(t_0) \cdot [1 + \kappa(z_{\text{em}})]^{\xi} \end{aligned} \tag{21.61}$$

We apply $\frac{1}{4\pi G \cdot t^2_{H_0,hom}} = \rho_{\Lambda,\text{hom}}(t_0)$ (Eq. 19.31) to the above Eq.. Additionally, we divide the Eq. by $\rho_{\Lambda,\text{hom}}(t_0)$:

$$\boxed{[1+\kappa(z_{\rm em})]\sqrt{\Omega_{m,0}+\Omega_{vol,0,theo}\cdot[1+\kappa(z_{\rm em})]^{\xi}}=[1+\kappa(z_{\rm em})]^{\xi}} \tag{21.62}$$

The exponent ξ is determined by this equation.

21.4.7 Derivation of the exponent ξ

In order to solve Eq. (21.62), we apply the square. Additionally, we abbreviate $1+\kappa(z_{\rm em})$ by y, and we abbreviate y^{ξ} by w:

$$y^2(\Omega_{m,0}+\Omega_{vol,0,theo}\cdot w)=w^2 \text{ or} \tag{21.63}$$

$$0=w^2-w\cdot\Omega_{vol,0,theo}\cdot y^2-\Omega_{m,0}\cdot y^2 \text{ with} \tag{21.64}$$

$$y=1+\kappa(z_{\rm em}) \text{ and } w=y^{\xi} \tag{21.65}$$

The above quadratic equation has the following two solutions:

$$w_{\pm}=\frac{\Omega_{vol,0,theo}\cdot y^2}{2}\cdot\left(1\pm\sqrt{1+\frac{4\Omega_{m,0}}{\Omega^2_{vol,0,theo}\cdot y^2}}\right) \tag{21.66}$$

The solution w_- is negative. Thus, it does not provide a real exponent, see Eq. (21.65). Accordingly, we solve the above equation for the exponent ξ by using the solution w_+ (see Eq. 21.65):

$$\xi=\frac{\ln(w_+)}{\ln(y)} \text{ and } y=1+\kappa(z_{\rm em}) \text{ with} \tag{21.67}$$

$$w_{+}=\frac{\Omega_{vol,0,theo}\cdot y^2}{2}\cdot\left(1+\sqrt{1+\frac{4\Omega_{m,0}}{\Omega^2_{vol,0,theo}\cdot y^2}}\right) \tag{21.68}$$

21.4.8 H_0 measured with the CMB

Idea: If the Hubble constant $H_{0,obs}$ is measured with a probe emitted at a time $t_{\rm em}$, then it is described by the term in Eq. (21.57). With it, we derive the theoretical value of the observed Hubble constant for the case of observation based on the CMB, $H_{0,obs}(z_{\rm em})$ with $z_{\rm em} = z_{\rm CMB}$.

In the above Eq., we insert the following values:
$\Omega_{vol,0,theo} = \frac{2}{3}$, $\Omega_{m,0} = 1 - \Omega_{vol,0,theo} = \frac{1}{3}$,
$\sigma_{8,0} = 0.8118 \pm 0.0089$, (Planck-Collaboration, 2020, table 2),
$z_{\rm CMB} = 1090.3 \pm 0.41$, (Planck-Collaboration, 2020, table 2),
$H_{0,obs,CMB} = 66.88\,(\pm 0.92)\,\frac{\rm km}{\rm s\cdot Mpc}$, (Planck-Collaboration, 2020, table 2).

Thus, the ratio of rates $\kappa(z_{\rm em})$ in Eqs. (21.39, 21.40) has the following value:

$$\kappa(z_{\rm CMB}) = \frac{0.8118 \cdot 1/3}{2 \cdot 2/3 \cdot (1 + 1090.3)^2} = 1.7 \cdot 10^{-7} \qquad (21.69)$$

With it, we solve Eq. (21.62), see section (21.4.7):

$$\xi_{\rm CMB} = 1.5 \qquad (21.70)$$

Consequently, the observable Hubble constant without heterogeneity has the same value as plus a relative correction of the order of $\kappa(z_{\rm CMB}) \approx 10^{-7}$, see Eq. (21.57):

$$H_{0,\text{without het}} = H_{0,obs,CMB} \cdot (1 + \mathcal{O}(10^{-7})) \qquad (21.71)$$

21.4.9 H_0 measured with near galaxies

Idea: If the Hubble constant $H_{0,obs}$ is measured with a probe emitted at a time $t_{\rm em}$, then it is described by the term in Eq. (21.57). With it, we derive the theoretical value of the observed Hubble constant for the case of observation based on the emitted radiation of near galaxies at $z_{\rm em} = z_{\rm near} = 0.055$, see (Riess et al., 2022, sections 5.1 and 5.2).

In Eq. (21.57), we insert the following values:
$\Omega_{vol,0,theo} = \frac{2}{3}$, $\Omega_{m,0} = 1 - \Omega_{vol,0,theo} = \frac{1}{3}$,
$\sigma_{8,0} = 0.8118 \pm 0.0089$, (Planck-Collaboration, 2020, table 2),
$z_{\text{near}} = 0.055$, (Riess et al., 2022, sections 5.1 and 5.2),
$H_{0,\text{without het}} = 66.88\,(\pm 0.92)\,\frac{\text{km}}{\text{s}\cdot\text{Mpc}}$, Eq. (21.71).

Thus, the ratio of rates $\kappa(z_{\text{near}})$ in Eqs. (21.39, 21.40) has the following value:

$$\kappa(z_{\text{near}}) = \frac{0.8118 \cdot 1/3}{2 \cdot 2/3 \cdot (1+0.055)^2} = 0.182 \pm 0.002 \qquad (21.72)$$

With it, we solve Eq. (21.62), see section (21.4.7):

$$\xi_{\text{near}} = 1.5317 \qquad (21.73)$$

Consequently, the theoretical value of the observable Hubble constant is as follows:

$$H_{0,theo}(z_{\text{near}}) = H_{0,\text{without het}}\sqrt{\frac{1}{3} + \frac{2}{3} \cdot 1.182^{1.5317}} \qquad (21.74)$$

$$= 73.11 \pm 1.08\,\frac{\text{km}}{\text{s}\cdot\text{Mpc}} \qquad (21.75)$$

Thus, our theoretical result is in precise accordance (within errors of measurement) with the currently most precise observation in Eq. (21.3):

$$H_{0,obs,near} = 73.04\,(\pm 1.01)\,\frac{\text{km}}{\text{s}\cdot\text{Mpc}} \ \text{ at } \langle z\rangle = 0.055 \qquad (21.76)$$

This is the baseline result in (Riess et al., 2022, sections 5.1 and 5.2), obtained at the "near field" or 'low redshift' $\langle z\rangle = 0.055$.

The relative difference between theory and measurement is very low at 0.096 %:

$$\Delta_{obs,theo} = \frac{H_{0,obs,near} - H_{0,theo}(z_{\text{near}})}{H_{0,obs,near}} = \frac{73.11 - 73.04}{73.04} = 0.096\% \qquad (21.77)$$

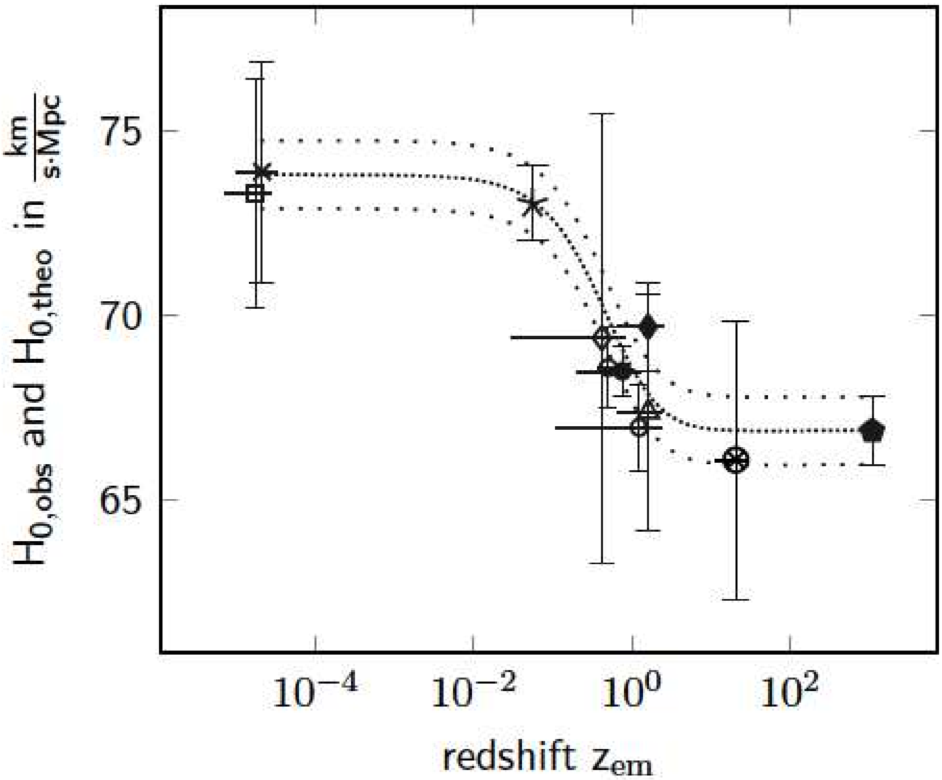

Figure 21.3: Observed values of Hubble constant $H_{0,obs}$ as a function of the redshift z_{em} of the emission of the respective probe. **Probes:** $\times$, megamaser, Pesce et al. (2020). $\star$, distance ladder with SN type I, Riess et al. (2022). full full $\diamond$, starburst galaxies, Cao et al. (2021). o, baryonic acoustic oscillations, BAO, Philcox et al. (2020), Addison et al. (2018)). $\bullet$, weak gravitational lensing and galaxy clustering, Abbott et al. (2020)). Δ, strong gravitational lensing, Birrer et al. (2020). $\diamond$, gravitational wave, Escamilla-Rivera and Najera (2022). $\otimes$, old galaxies or stars, Cimatti and Moresco (2023), (Tab. 1). Square, surface brightness, Blakeslee et al. (2021). Pentagon, CMB, Planck-Collaboration (2020).
Theory: densely dotted (loosely dotted: range of theoretical values, resulting from error of measurement of the CMB value).
Comparison: Measured values and theoretical values are in precise accordance within the errors of measurement.

Theorem 39 Time evolution of the Hubble constant
(1) The Hubble constant H_0 is an essential parameter of space-time and of cosmology. However, observations show that H_0 is not constant Planck-Collaboration (2020); Riess et al. (2022). Thus, the physical nature of that discrepancy is essential for the foundations of physics.
(2) At a good approximation, $\Omega_{r,0} = 0$, $\Omega_{K,0} = 0$. With it, we derived, explained and calculated the discrepancy as follows:
(2a) For the case of a homogeneous universe, corresponding to the universe at the redshift $z = 1090$, we derived the dynamic density of volume $\rho_{vol,theo}$ and the Hubble constant, both in precise accordance with observation:

$$\rho_{vol,theo} = \frac{1}{4\pi \cdot G \cdot t_H^2} \text{ and } \Omega_{vol,0,theo} = \frac{2}{3} \tag{21.78}$$

(2b) For the case of a heterogeneous universe, corresponding to the present-day universe at the redshift $z \approx 0$, we derived the same dynamic density of volume $\rho_{vol,theo}$, but an increased Hubble constant, both in precise accordance with observation.
(2c) The theoretical value $H_{0,theo}(z_{\rm em})$ of the observable Hubble constant is the following function of the redshift $z_{\rm em}$ (of the emission of the probe used in the observation):

$$H_{0,theo}(z_{\rm em}) = H_{0,\text{without het}} \cdot \sqrt{\Omega_{m,0} + \Omega_{vol,0,theo} \cdot [1 + \kappa(z_{\rm em})]^{\xi}} \tag{21.79}$$

$$\text{with } \kappa(z_{\rm em}) = \frac{\sigma_{8,0} \cdot \Omega_{m,0}}{2\Omega_{\Lambda,0} \cdot (1 + z_{\rm em})^2} = \frac{\dot{\underline{\varepsilon}}_{\text{het},0}(\tilde{t}_{\rm em})}{\dot{\underline{\varepsilon}}_{\text{hom}}} \text{ and} \tag{21.80}$$

$$H^2_{0,\text{without het}} = \frac{8\pi G}{3} \cdot \rho_{cr.,0} \tag{21.81}$$

Hereby, the exponent ξ is the solution of the following equation:

$$[1 + \kappa(z_{\rm em})]\sqrt{\Omega_{m,0} + \Omega_{vol,0,theo} \cdot [1 + \kappa(z_{\rm em})]^{\xi}} = [1 + \kappa(z_{\rm em})]^{\xi} \tag{21.82}$$

With it, the exponent ξ is as follows:

$$\xi = \frac{\ln(w_+)}{\ln(y)} \text{ and } y = 1 + \kappa(z_{\text{em}}) \text{ with} \tag{21.83}$$

$$w_+ = \frac{\Omega_{vol,0,theo} \cdot y^2}{2} \cdot \left(1 + \sqrt{1 + \frac{4\Omega_{m,0}}{\Omega^2_{vol,0,theo} \cdot y^2}}\right) \tag{21.84}$$

(2d) Our results are in precise accordance with observation. The difference between the measured and the theoretical value is 0.096 % only:

$$H_{0,theo}(z_{\text{near}}) = 73.11 \pm 1.08 \, \frac{\text{km}}{\text{s} \cdot \text{Mpc}} \tag{21.85}$$

$$H_{0,obs,near} = 73.04 \, (\pm 1.01) \, \frac{\text{km}}{\text{s} \cdot \text{Mpc}} \text{ at } \langle z \rangle = 0.055 \tag{21.86}$$

$$\Delta_{obs,theo} = \frac{H_{0,obs,near} - H_{0,theo}(z_{\text{near}})}{H_{0,obs,near}} = 0.096\% \tag{21.87}$$

Thereby, we do not execute any fit or introduce any hypothesis.
(2d1) We solve the observed discrepancy, the so-called Hubble tension.
(2d2) We provide the physical basis for the energy density of volume:

$$u_{vol,theo} = \rho_{vol,theo} \cdot c^2 \tag{21.88}$$

Thus, we solve the dark energy problem, see e. g. Cugnon (2012). Thereby, we overcome the hypothetical character of the cosmological constant Λ.
(2d3) We extend the isotropic GFV described by the FLE, so that the Hubble constant in part (2c) additionally includes the unidirectional LFV. Thereby, we show that the expansion of space is based on the formation of volume, whereby that formation is explained with our theory of the dynamics of volume, see part (II).

(2d4) The energy of the volume is a zero-point energy, ZPE, C. (22).
(2d5) The energy of the volume represents a zero-point oscilation. It represents a wave packet, C. (22) and section (14.5). In contrast, the energy of a harmonic wave of the volume is zero, C. (11).
(2d6) Our results predict the observed values $H_{0,obs}(z_{\rm em})$ of the Hubble constant as a function of the redshift of the emission of the used probe, see part (2c). For the case of various observed $H_{0,obs}(z_{\rm em})$, our prediction is in precise accordance with observation, see Fig. (21.3).
(3) In a homogeneous universe, a constant energy density of volume u_{vol} can be derived, see THM (37) and (Carmesin, 2021d, THM 22, part (3b)). On that basis, a steady state universe could be conceivable. However, the time evolution of heterogeneity clearly excludes that possibility, as a result of theory and in precise accordance with observation, Fig. (21.3).
(4) As $H_{0,obs}(z)$ is a function of time or z, it modifies the age of the homogeneous universe $t_{0,hom}$ to the age of the heterogeneous universe $t_{0,het}$, according to (Carmesin, 2019b, Eq. (2.29) and part (2c) in this THM.
(4a) The parameters $\Omega_{vol,0,theo} = \frac{2}{3}$, $\Omega_{m,0} = 1 - \Omega_{vol,0,theo}$, $\sigma_{8,0} = 0.8118 \pm 0.0089$ and $H_{0,\rm without\ het} = 66.88\,(\pm 0.92)\,\frac{\rm km}{\rm s\cdot Mpc}$, (Planck-Collaboration, 2020, table 2, TT-mode) provide $t_{0,het} = 13.17 \cdot (1 \pm 0.19) \cdot 10^9$ years. This is in precise accordance with various observations, Valcin et al. (2021), Robertson et al. (2023). For comparison, $t_{0,hom} = 13.68 \cdot (1 \pm 0.19) \cdot 10^9$ years.
(4b) The parameters $\Omega_\Lambda = 0.6847 \pm 0.0073$, $\Omega_{m,0} = 1 - \Omega_\Lambda$, $\sigma_{8,0} = 0.8111 \pm 0.0060$, $H_{0,\rm without\ het} = 67.36\,(\pm 0.54)\,\frac{\rm km}{\rm s\cdot Mpc}$, see (Planck-Collaboration, 2020, table 2, col. 6), provide $t_{0,het} = 13.31 \cdot (1 \pm 0.21) \cdot 10^9$ years. This is in precise accordance with observations, Valcin et al. (2021), Robertson et al. (2023). For comparison, $t_{0,hom} = 13.8 \cdot (1 \pm 0.2) \cdot 10^9$ years.

Chapter 22

Dark Energy at 'Cosmic Inflation'

22.1 Incompleteness of GR

Question: The scale factor can be analyzed as a function of time, see Fig. (22.1). The graph shows: At early times, the scale factor was small.

At small scale factors, the density is large. However, the density cannot be larger than the Planck density ρ_P, see glossary or Carmesin (2019b). At what scale factor x_1 does the density of the universe $\rho(t_1)$ reach the value ρ_P? Is that scale factor x_1 larger than the Planck length L_P?

The present-day light horizon R_{lh} has been analyzed as a function of time, see Fig. (22.2). For it, the values of $R_{lh}(t)$ at earlier times have been derived in the framework of GR, see e.g. Carmesin (2019b, 2020b,a, 2021d,a); Heeren et al. (2020).

According to the laws of physics, the density cannot be larger than the Planck density $\rho_P = 5.155 \cdot 10^{96}\,\frac{\text{kg}}{\text{m}^3}$, and lengths as small as the Planck length $L_P = 1.616 \cdot 10^{-35}$ m can be observed, see e.g. Carmesin (2017), Carmesin (2019b), Carmesin (2021a). Moreover, corresponding to the laws of physics, the length can be as small as the Planck length, see e.g. Carmesin (2017), Carmesin (2019b), Carmesin (2021a).

Next, we compare the time evolution of the density $\rho(t)$ and

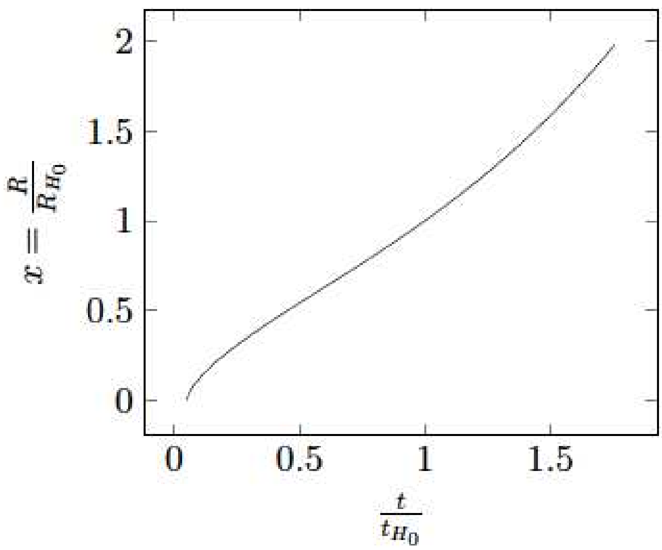

Figure 22.1: Time evolution of the scale factor. The time is presented in units of the Hubble time t_{H_0}, while the scale factor is shown in units of the Hubble length R_{H_0}.

of the value of $R_{lh}(t)$ of the light horizon in the universe. In the framework of GR, the Planck density $\rho_P = 5.155 \cdot 10^{96}\,\frac{\mathrm{kg}}{\mathrm{m}^3}$ is already achieved, when $R_{lh}(t)$ is approximately equal to 0.003 mm, see Fig. (22.2). As a consequence, GR is not complete, as GR does not describe the full physically possible time evolution of $R_{lh}(t)$, ranging from the Planck length $L_P = 1.616 \cdot 10^{-35}\,\mathrm{m}$ to the present-day light horizon $R_{lh} \approx 4.1 \cdot 10^{26}\,\mathrm{m}$.

Proposition 11 Incompleteness of GR

(1) The theory of general relativity, GR, describes the time evolution of the light horizon $R_{lh}(t)$ *ranging from* $R_{lh} \approx 0.003\,\mathrm{mm}$ *towards the present-day light horizon* $R_{lh} \approx 4.1 \cdot 10^{26}\,\mathrm{m}$.

(2) However, the physically observable lengths range from the Planck length $L_P = 1.616 \cdot 10^{-35}\,\mathrm{m}$ *towards the present-day light horizon* $R_{lh} \approx 4.1 \cdot 10^{26}\,\mathrm{m}$.

(3) So GR is incomplete.

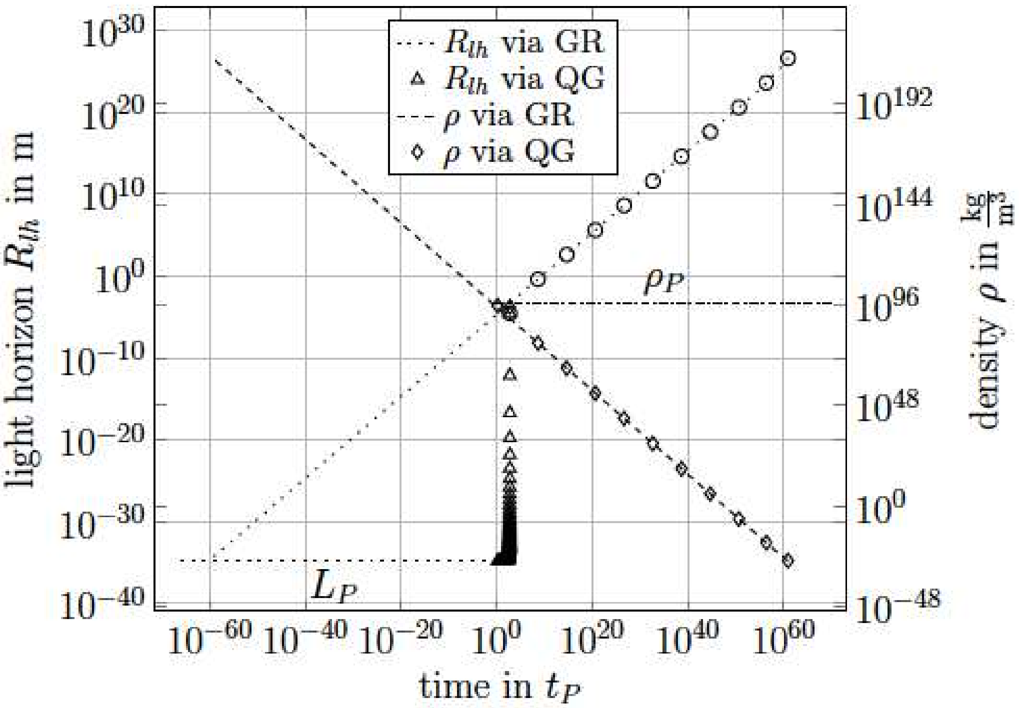

Figure 22.2: Density limit of expansion of space: The time evolution of R_{lh} according to general relativity, GR, ($\circ$) ranges from the present-day value $4.14 \cdot 10^{26}$ m backwards to 0.003 mm, as at this point the density ($\diamond$) achieves the Planck density $\rho_P = 5.155 \cdot 10^{96} \frac{\text{kg}}{\text{m}^3}$ (dashdotted), and no higher density is physically possible.
However, the physically possible lengths can be as short as the Planck length L_P (loosely dotted). Hence the time evolution of the GR is **incomplete**.
In contrast, we derive the **complete time evolution** of $R_{lh}(t)$, ranging from the current value $4.14 \cdot 10^{26}$ m backwards to L_P. For it, we apply dimensional phase transitions ($\triangle$) derived by quantum gravity. Thereby, the phase transitions cause the 'cosmic inflation'. We explain it by the **extremely rapid distance enlargement in the early universe**.

22.2 Gravity at higher dimension

Idea: The law of Gaussian gravity (chapter 2) is based on the isotropic emission of gravity by a mass or dynamical mass. That law can be applied to dimensions $D \geq 3$. In this section, we derive the law of gravity at dimensions $D \geq 3$. For it, we emphasize that physics in dimensions $D > 3$ has been observed in experiments with photons as well as in experiments with electrons, see Lohse et al. (2018), Zilberberg et al. (2018).

22.2.1 Kinetic energy in D dimensions

In this section, we make transparent how the kinetic energy of a mass m is naturally defined in D dimensions:

$$E_{kin} = \frac{1}{2m} \Sigma_{j=1}^{j=D} p_j^2 \tag{22.1}$$

22.2.2 Gravity in $D \geq 3$ dimensions

In this section, we show that the gravitational energy is naturally defined in $D \geq 3$ dimensions. For it, we remind that GRT can be derived from Gaussian gravity, see (Carmesin, 2021d, theorem 1). And Gaussian gravity can naturally be defined in $D \geq 3$ dimensions, see e. g. Fig. (22.3).

22.2.2.1 Gravity term for $D \geq 3$

According to Gaussian gravitation, the gravitational field $G^*(R)$ at a distance R from a mass is proportional to $1/R^{D-1}$ (Fig. 22.3, and Gauss (1840)):

$$G^* \propto \frac{1}{R^{D-1}} \tag{22.2}$$

The same proportionality applies to the gravitational force F which a mass M exerts on a mass m at the distance R. More-

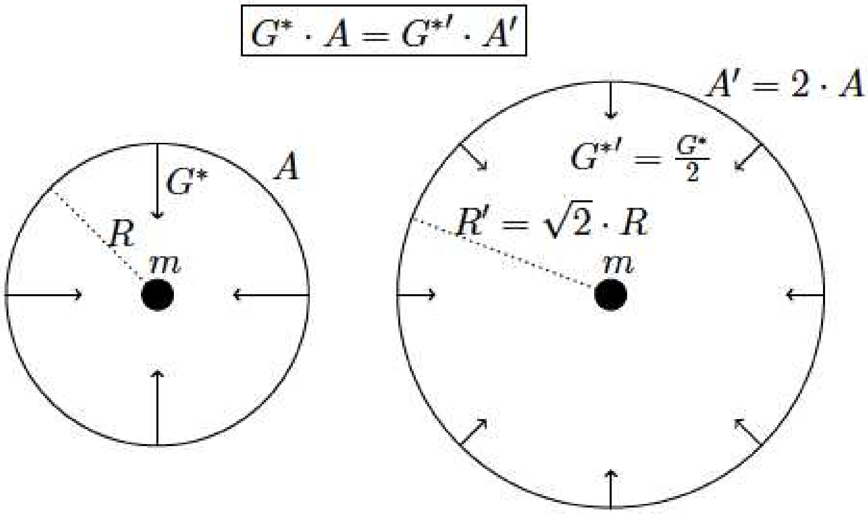

Figure 22.3: Gaussian gravity of a mass or dynamic mass m: All balls around m have the same flux $G^*(R) \cdot A(R)$. This means the same product of the gravitational field $G^*(R)$ and area $A(R)$. Consequently, we derive in D dimensions: $G^*(R) \propto \frac{1}{A(R)} \propto \frac{1}{R^{D-1}}$.

over, the force is proportional to each of the masses:

$$F \propto \frac{M \cdot m}{R^{D-1}} \tag{22.3}$$

The proportionality factor is a gravitational constant for dimension D, G_D:

$$F = -G_D \cdot \frac{M \cdot m}{R^{D-1}} \tag{22.4}$$

The potential energy or gravitational energy is the integral of the force. By DEF., the energy is zero in the limit R to infinity:

$$E_G = -G_D \cdot \frac{M \cdot m}{(D-2) \cdot R^{D-2}} \tag{22.5}$$

The gravitational constant can be derived (see e.g. Carmesin (2017), Carmesin (2019b)). The following holds:

$$G_D = G \cdot (D-2) \cdot L_P^{D-3} \text{ We summarize :} \tag{22.6}$$

Proposition 12 Gravitation in D dimensions

(1) Two objects at a distance R, with masses or dynamic masses M and m, exert the gravitational force $F = -G_D \cdot \frac{M \cdot m}{R^{D-1}}$ on each other in $D \geq 3$ dimensions with $G_D = G \cdot (D-2) \cdot L_P^{D-3}$.

(2) The corresponding energy is: $E_G = -G_D \cdot \frac{M \cdot m}{(D-2) \cdot R^{D-2}}$

(3) As kinetic and gravitational energy are naturally defined in $D \geq 3$ dimensions, the conditions must be analyzed, at which space at dimensions $D > 3$ is more stable than the present-day space at $D = 3$, see e. g. Carmesin (2017), Carmesin (2018a), Carmesin (2021d).

(4) When the space changes from a dimension $D + s$ to a dimension D, then s directions of translation symmetry are lost. Thus, such a transition is a symmetry breaking phase transition, see Landau and Lifschitz (1979), we call it **dimensional phase transition**.

22.2.2.2 Special radii at scaled densities $\tilde{\rho}_D$

Question: At high density, radiation is an essential content in the volume, see e. g. Hobson et al. (2006), Carmesin (2019b). Moreover, at sufficiently high density, small black holes form spontaneously, see (Carmesin, 2020b, section 4.4.7). What are the radius b of a black hole and the radius a_M that radiation with dynamic mass M requires, as a function of the density $\tilde{\rho}_D$.

Radius a_M depending on the scaled density: We derive how the radius a_M depends on the scaled density ρ_D. We use natural units (see table 25.3).

According to the redshift, the dynamic mass is proportional to the inverse wavelength $M_{dyn} \propto \frac{1}{a_M}$. For example, for $a_M = L_P$, there is $M_{dyn} = \frac{M_P}{2}$. Both relations result in:

$$\frac{1}{2\tilde{a}_M} = \tilde{M}_{dyn} \tag{22.7}$$

Here we use the term for the density, where V_D denotes the volume of a hyper ball with radius 1:

$$\rho_D = \frac{M_{dyn}}{V_D \cdot a^D} \tag{22.8}$$

Hereby the volume of a unit ball is as follows:

$$V_D = \frac{\pi^{D/2}}{\Gamma(1 + D/2)}; \, \Gamma(x+1) = \Gamma(x) \cdot x; \Gamma(1) = 1; \Gamma\left(\frac{1}{2}\right) = \sqrt{\pi} \tag{22.9}$$

We use the Planck density related to a ball $\bar{\rho}_{D,P} = \frac{M_P}{V_D \cdot L_P^D}$ (table 25.3). So we get:

$$\tilde{\rho}_D = \frac{\rho_D}{\bar{\rho}_{D,P}} = \frac{\tilde{M}_{dyn}}{\tilde{a}_M^D} \tag{22.10}$$

In total we get:

$$\frac{1}{2\tilde{a}_M} = \tilde{M}_{dyn} = \tilde{\rho}_D \cdot \tilde{a}_M^D \tag{22.11}$$

Resolved we get:

$$\boxed{\tilde{a}_M = (2\tilde{\rho}_D)^{-1/(D+1)}} \tag{22.12}$$

Schwarzschild radius: We determine the Schwarzschild radius b depending on the density. We proceed like Michell (Michell (1784)). We equate the kinetic energy $\frac{1}{2}M \cdot v^2$ with the potential energy and choose the velocity of light c. So we get:

$$\frac{1}{2} \cdot c^2 = \frac{G_D \cdot m}{(D-2) \cdot b^{D-2}} \tag{22.13}$$

We use $G_D = G \cdot (D-2) \cdot L_P^{D-3}$ and we use natural units. So we get (table 25.3):

$$\boxed{\tilde{b} = (2\tilde{\rho}_D)^{-1/2}} \tag{22.14}$$

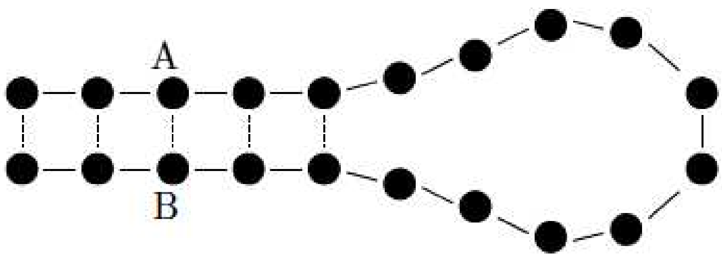

Figure 22.4: At high density near the Planck scale, $\rho \approx \rho_P$, the space exhibits a grainy structure (dots) at the scale of the Planck length, $L \approx L_P$. At such a density, a layer of **shortcuts** (dotted) can form spontaneously. The corresponding critical density is derived in S. (22.3.1).

22.3 Phase transitions in the early universe

Question: If the density is increased in a system of masses, then the distances between masses decrease, so that the attractive forces between the masses increase. Are these forces sufficiently large to fold the space to a higher dimension, see Fig. (22.4)?

22.3.1 Critical density $\rho_{cr.sc.}$ for shortcuts

In this section, we derive an example of a dimensional phase transition: At a critical density $\rho_{cr.conn.}$, connections of a length $dL \approx L_P$ and with the volume $dV \approx L_P^3$ form spontaneously, for an illustration of several formed connections see Fig. (22.4). Thereby the dimension is increased and a dimensional phase transition takes place.

Condition for the transition: If the rate of change of the volume inside the connection $\dot{\varepsilon}_{inside} = \frac{\delta V}{\delta t \cdot dV}|_{inside}$ is negative, then the shortcut permanently looses volume, so it vanishes. If the rate of change of the volume inside the connection $\dot{\varepsilon}_{inside}$ would be larger than zero, then the shortcut would permanently get new volume, so that can happen for a short time only. If the rate of change of the volume inside the connection $\dot{\varepsilon}_{inside}$ is equal to zero, then the shortcut contains a constant amount of volume, correspondingly, the shortcut is stable. This shows that the shortcut becomes stable at the condition $\dot{\varepsilon}_{inside} = 0$. Hence, at the critical density $\rho_{cr.conn.}$, the rate of change of the volume inside the connection $\frac{\underline{\delta} V}{\underline{\delta} t \cdot dV}|_{inside}$ is zero.

Contributions to the rate $\dot{\varepsilon}_{inside}$: Some volume flows from the connection to neighboring regions A and B, see Fig. (22.5), at a rate $\dot{\varepsilon}_{out}$. Similarly, some volume flows from neighboring regions A and B to the connection at another rate $\dot{\varepsilon}_{in}$. Thirdly, some volume forms in the connection at a rate $\dot{\varepsilon}_{formation}$. Next, we analyze these rates in detail.

Rate of outward flow: The relative volume propagates within the **available** space, see THM (18). So the volume dV of the connection in Fig. (22.5) can escape towards the volumes A and B in that figure. The volume dV of the connection can escape at the velocity of light in these two directions, see Fig. (22.5). At the Planck scale, that volume corresponds to one quantum. An escape towards the volume A in Fig. (22.5) takes the time $dt = L_P/c = t_P$ and has the probability 50 %, whereby t_P is the Planck time. The same holds for an escape towards the volume B in Fig. (22.5). Thus, during the time t_P, the volume dV of the connection leaves that volume. So the rate of outward flow is as follows:

$$\frac{\underline{\delta} V}{\underline{\delta} t}|_{out} = -\frac{dV}{t_P} \tag{22.15}$$

We solve for the rate per volume:

$$\dot{\varepsilon}_{out} = \frac{\underline{\delta} V}{\underline{\delta} t \cdot dV}|_{out} = -\frac{1}{t_P} \tag{22.16}$$

Rate of inward flow: As the cube of length L_P at a region A has six equal surfaces, one of which is directed to the connection, the

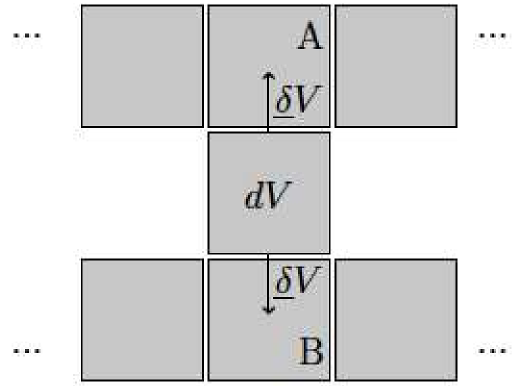

Figure 22.5: Flow of volume $\underline{\delta}V$ from dV: We assume that the volume essentially flows to existing volume. In order to get an estimation we analyze cubes with length $L \approx L_P$.

sixth part of its rate $\frac{\delta V}{\underline{\delta} t \cdot dV}|_{from\ A}$ propagates to the connection:

$$\dot{\varepsilon}|_{from\ A} = -\frac{1}{6 \cdot t_P} \tag{22.17}$$

So the rate propagating from A to the connection is positive and has the absolute value of the above term:

$$\dot{\varepsilon}_{in, from\ A} = +\frac{1}{6 \cdot t_P} \tag{22.18}$$

The same rate propagates to the connection coming from B. So we derive:

$$\dot{\varepsilon}_{in} = \frac{2}{6 \cdot t_P} \tag{22.19}$$

Rate of formation of volume: Additionally, the density ρ of the connection forms volume. The exact rate depends on the symmetry. We model and analyze the rate for the unidirectional formation of volume, as it may propagate orthogonal to the surface of the cube. So we get, see THMs (17 and 8):

$$\dot{\varepsilon}_{formation} = \sqrt{8\pi \cdot G \cdot \rho} \tag{22.20}$$

Sum of rates: We add the above three rates. So the total rate is as follows:

$$\dot{\varepsilon}_{inside} = \dot{\varepsilon}_{out} + \dot{\varepsilon}_{in} + \dot{\varepsilon}_{formation} \tag{22.21}$$

We insert the corresponding terms and set the rate to zero:

$$\dot{\varepsilon}_{inside} = \frac{-1}{t_P} + \frac{2}{6 \cdot t_P} + \sqrt{8\pi \cdot G \cdot \rho} = 0 \tag{22.22}$$

We solve for the root in the above Eq.:

$$\sqrt{8\pi \cdot G \cdot \rho} = \frac{2}{3 \cdot t_P} \tag{22.23}$$

We solve for the density:

$$\rho = \frac{1}{18\pi} \cdot \frac{1}{t_P^2 \cdot G} \tag{22.24}$$

The second fraction in the above Eq. (22.24) is equal to the Planck density. So we derive the following for the **critical density of spontaneous connection formation**, $\rho_{cr.conn.}$:

$$\boxed{\rho_{cr.conn.} = \frac{1}{18\pi} \cdot \rho_P = 0.018 \cdot \rho_P} \tag{22.25}$$

In terms of the Planck density for a ball $\bar{\rho}_P = \rho_P \cdot 3/(4\pi)$ (see appendix), we get:

$$\boxed{\rho_{cr.conn.} = \frac{2}{27} \cdot \bar{\rho}_P = 0.074 \cdot \bar{\rho}_P} \tag{22.26}$$

Theorem 40 New volume can form new connections.

In a D-dimensional space, new connections can form as follows:

(1) Space has at least three dimensions. The reason is as follows: Quanta of volume propagate in one direction. Additionally, in an appropriate coordinate system, these quanta exhibit

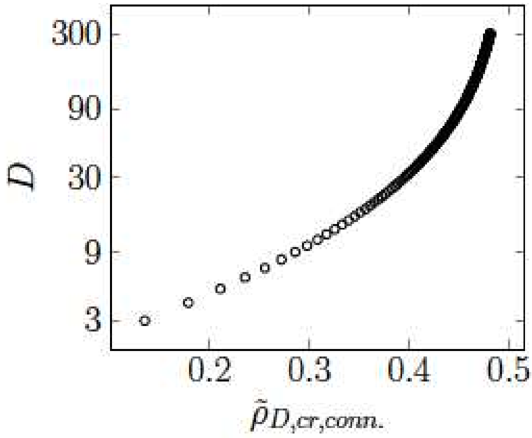

Figure 22.6: Dimension D as a function of the critical densities.

diagonal elements of the volume - tensor in the $D-1$ transverse directions, as the volume requires an extension in each direction. Thereby, the trace of the $D-1$ transverse directions is zero, as there forms no volume in these directions. For it, there are at least two elements of the volume - tensor in the transverse directions, so these exhibit trace zero. Consequently, space has at least three dimensions.

(2) In order to analyze the dynamics of new connections in Fig. (22.5), we analyze a conceivable two-dimensional space. In it, new connections forming three-dimensional space can form spontaneously at densities above the critical density $\tilde{\rho}_{cr.conn.} = \frac{2}{27}$.

(3) If the density in a system is sufficiently increased, then the system experiences a sequence of critical densities $\tilde{\rho}_{D,cr,conn.}$, at which a phase transition from D to $D+1$ takes place, see (Carmesin, 2021a, Eq. 3.93) and Fig. 22.6):

$$\boxed{\tilde{\rho}_{D,cr,conn.} = \frac{1}{2} \cdot \left(\frac{D}{(D+1)^{3/2}} \right)^{\frac{4}{D}}} \qquad (22.27)$$

Thus, for the case $D = 2$ in part (2), Eq. (22.27) provides

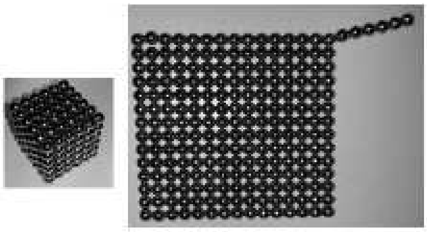

Figure 22.7: 216 magnetic balls model local objects or observable regions at high density and illustrate the relation between the distance and the dimension D: If the dimension increases from two (right) to three (left), then the largest distance decreases. More generally and conversely, a decrease of the dimension D implies an increase of the largest distance.

$\tilde{\rho}_{2,cr,conn.} = \frac{1}{2} \cdot \left(\frac{2}{3^{3/2}}\right)^{\frac{4}{2}} = \frac{2}{27}$.

(4) In particular, three-dimensional space emerges from four-dimensional space at the following critical density:

$$\tilde{\rho}_{3,cr,conn.} = \frac{1}{2} \cdot \left(\frac{3}{4^{3/2}}\right)^{\frac{4}{3}} = 0.1352 \qquad (22.28)$$

22.3.2 Dimensional horizon $D_{horizon}$

In the time evolution of the universe, the density was high initially, and it decreased as a function of the time. So the dimension D was high originally near or at the Planck scale. Then the density decreased according to the FLE[1], and whenever a critical density was reached, a dimensional phase transition reduced the **dimension of space**. So D decreased until $D = 3$ was achieved. That process is called **dimensional unfolding** or **cosmic unfolding**, Carmesin (2021d), Carmesin (2017).

During the process of dimensional unfolding, the dimension D decreased, and thereby the distances were enlarged, see Fig. (22.7). At a transition from a dimension $D + s$ to a dimension

[1]For it, a version of the FLE applicable in dimension D has been derived, Carmesin (2021a)).

D, the distances enlarge by a so-called **dimensional distance enlargement factor** $Z_{D+s\to D}$, (Carmesin, 2021d, 8.2.9). The space that is enclosed in the actual light horizon achieved a largest dimension, the so-called **dimensional horizon**, $D_{horizon}$ or shortly D_{hori}, (Carmesin, 2021d, 8.2.10). Thereby the following relation holds:

$$Z_{D_{hori}\to D=3} = 2^{(D_{hori}-3)/3} \tag{22.29}$$

In order to determine the dimensional horizon, we use the complete scale factor $k_{D_{hori}\to t_0}$ ranging from the dimensional horizon until today. If three-dimensional space expands according to a scale factor $k_{\tilde{\rho}_{r,1}\to\tilde{\rho}_{r,2}}$ ranging from a state at a density of radiation $\tilde{\rho}_{r,1}$ towards a state at a density of radiation $\tilde{\rho}_{r,2}$, then the volume increases by the factor $k^3_{\tilde{\rho}_{r,1}\to\tilde{\rho}_{r,2}}$, and the energy of radiation decreases by the factor $1/k_{\tilde{\rho}_{r,1}\to\tilde{\rho}_{r,2}}$, according to the redshift. Thus, the density of radiation $\tilde{\rho}_{r,1}$ decreases by the factor $1/k^4_{\tilde{\rho}_{r,1}\to\tilde{\rho}_{r,2}}$:

$$\tilde{\rho}_{r,2} = \tilde{\rho}_{r,1}/k^4_{\tilde{\rho}_{r,1}\to\tilde{\rho}_{r,2}} \text{ or } k_{\tilde{\rho}_{r,1}\to\tilde{\rho}_{r,2}} = \left(\frac{\tilde{\rho}_{r,1}}{\tilde{\rho}_{r,2}}\right)^{1/4} \tag{22.30}$$

At the onset of dimensional transitions, the density of radiation is already near the Planck density. Thence, the density of radiation does only slightly change in the era of dimensional phase transitions. Thus, at a good approximation, Eq. (22.30) can be applied to the full expansion ranging from the dimensional horizon towards the present-day state, (Carmesin, 2021d, Eq. 8.79):

$$k_{D_{hori}\to t_0} \approx \left(\frac{\tilde{\rho}_{r,D_{hori}}}{\tilde{\rho}_{r,t_0}}\right)^{1/4} \approx 2.96\cdot 10^{31} \tag{22.31}$$

Accordingly, the scale factor $k_{\rho_{D=3,c}\to t_0}$ ranging from the state at the dimensional phase transition at three-dimensional space towards the present-day state is almost the same as $k_{D_{hori}\to t_0}$:

$$k_{D_{hori}\to t_0} \approx k_{\rho_{D=3,c}\to t_0} \tag{22.32}$$

Additionally, we apply the complete enlargement factor $q_{D_{hori}\to t_0}$ ranging from the dimensional horizon until today, and we form the fraction:

$$Z_{D_{hori}\to D=3} = \frac{q_{D_{hori}\to t_0}}{k_{D_{hori}\to t_0}} \tag{22.33}$$

Hereby, the complete enlargement ranges from the Planck length L_P towards the light horizon R_{LH}. The corresponding complete enlargement factor is as follows, (Carmesin, 2021d, Eq. 8.80):

$$q_{D_{hori}\to t_0} = \frac{R_{LH}(t_0)}{L_P} \approx 2.56 \cdot 10^{61} \tag{22.34}$$

The exact value of the dimensional horizon depends on the details of the dimensional phase transitions, and these depend on the details of the fluid in the early universe. However, all realistic cases show that the actual value of the dimensional horizon is as follows, (Carmesin, 2021d, 8.2.10):

$$D_{hori} \in [301, 302] \tag{22.35}$$

The dimensional distance enlargement factor is shown as a function of the dimension in Fig. (22.8).

For the case of the Bose gas, the critical density at the dimensional horizon is practically equal to the maximal possible value 0.5:

$$\boxed{\tilde{\rho}_{D_{hori},c} \approx 0.5} \tag{22.36}$$

For the more realistic case of the binary fluid in the early universe, the dimensional horizon is as follows, see (Carmesin, 2021d, Eq. 8.82):

$$\boxed{D_{hori} \approx 301.3} \tag{22.37}$$

22.4 Quanta of dark energy

Questions: The volume did already exist at the dimensional horizon. What is the energy of quanta of volume at the Planck

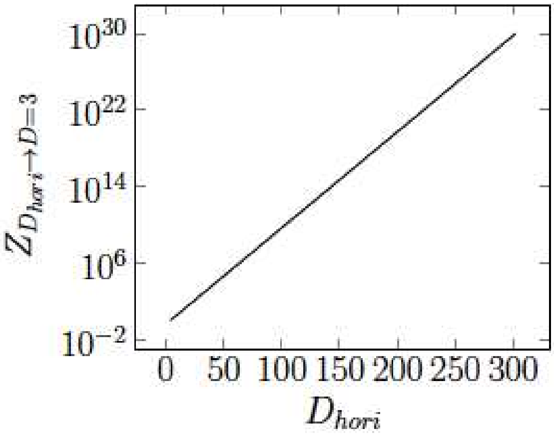

Figure 22.8: Dimensional distance enlargement factor $Z_{D_{hori}\to D=3}$ as a function of the dimensional horizon D_{hori}.

scale? How did that energy of quanta of volume evolve during cosmic unfolding? What are the directions of polarization of these quanta? What is the density of volume of these quanta of volume?

22.4.1 Causal limitation provides ZPE

As the volume propagates at $v = c$, it is quantized, and the energy is related to the wavelength as follows (chapter 4):

$$E_{vol,D_{hori}} = \frac{\hbar \cdot c}{\lambda_{vol,D_{hori}}} \tag{22.38}$$

The available space is limited by the causal horizon L_P. So, the lowest energy is at $\lambda_{vol,D_{hori}} = 2L_P$:

$$E_{vol,D_{hori}} = \frac{\hbar \cdot c}{2L_P} = \frac{E_P}{2} \tag{22.39}$$

22.4.2 Increase by dimensional unfolding

During the dimensional phase transitions ranging from the dimensional horizon D_{hori} towards three-dimensional space $D = 3$, the space is enlarged by the dimensional distance enlargement factor $Z_{D_{hori}\to 3}$. As space is formed by the quanta of volume, their wavelength is enlarged by that factor. Consequently, their energy is divided by that factor.

At each dimension, there are $D-1$ transverse directions, each representing a direction of polarization, see THM (40, part (1)). Thus, 300 transverse directions of polarization at the dimensional horizon $D_{hori} = 301$ reduce to two directions of polarization at the present-day three-dimensional space, $D = 3$. Thence, the energy is reduced by the polarization factor:

$$\frac{D_{hori}-1}{2} = 150 \tag{22.40}$$

Altogether, at the emergence of three-dimensional space at the critical density $\rho_{D=3,c}$, the energy of a quantum of volume is as follows:

$$E_{vol,\rho_{D=3,c}} = E_{vol,D_{hori}} \cdot \frac{1}{150 \cdot Z_{D_{hori}\to 3}} = \frac{E_P}{300 \cdot Z_{D_{hori}\to 3}} \tag{22.41}$$

22.4.3 Dimensional distance enlargement factor

The dimensional distance enlargement factor is as follows, see Eqs. (22.33, 22.34):

$$Z_{D_{hori}\to 3} = \frac{R_{LH}}{L_P \cdot k_{\rho_{D=3,c}\to t_0}} \tag{22.42}$$

Thereby, the light horizon is as follows:

$$R_{LH} = \frac{K_{LH}\cdot c}{H_0} \quad \text{with} \quad K_{LH} = \frac{R_{LH}}{R_{H_0}} = 2.9926 \tag{22.43}$$

Hereby, the value of H_0 of the homogeneous universe is appropriate, as the early universe has been very homogeneous, see chapter (21). Additionally, the expansion of space can be described with help of the density of radiation. As radiation exhibits redshift, the expansion factor is as follows, Carmesin

(2019b), Hobson et al. (2006), Eqs. (22.30, 22.31, 22.32):

$$k_{\rho_c \to t_0} = \left(\frac{\rho_{D=3,c}}{\rho_{r,0}} \right)^{1/4} = \left(\frac{\tilde{\rho}_{D=3,c}}{\tilde{\rho}_{r,0}} \right)^{1/4} \tag{22.44}$$

Hereby, the present-day density can be described with help of the density parameter, Carmesin (2019b), Hobson et al. (2006):

$$\rho_{r,0} = \Omega_{r,0} \cdot H_0^2 \cdot \frac{3}{8\pi G} \text{ with } \Omega_{r,0} = 9.265 \cdot 10^{-5}; \ \tilde{\rho}_{r,0} = \frac{\rho_{r,0}}{\bar{\rho}_P} \tag{22.45}$$

22.4.4 Enlargement of wavelength of quanta of volume

If the dimension changes from the dimensional horizon D_{hori} to a dimension D, then the following dimensional distance enlargement factor occurs, see (Carmesin, 2021d, THM 26):

$$Z_{D_{hori} \to D} = 2^{\frac{D_{hori} - D}{D}} \tag{22.46}$$

Consequently, if the dimension changes from a dimension D_1 to a dimension D_2, then the following dimensional distance enlargement factor occurs:

$$Z_{D_1 \to D_2} = Z_{D_{hori} \to D_2} / Z_{D_{hori} \to D_1} \tag{22.47}$$

Thereby, the wavelength of a quantum of volume changes as follows:

$$\lambda_{vol,D_2} = \lambda_{vol,D_1} \cdot Z_{D_1 \to D_2} \tag{22.48}$$

22.4.5 Density of volume

At the dimensional horizon, the available space is a hyperball with radius L_P. During the dimensional phase transitions towards three-dimensional space, the radius is enlarged by the dimensional distance enlargement factor $Z_{D_{hori} \to 3}$. Thus, the enlarged radius is the following product:

$$R_{enlarged} = L_P \cdot Z_{D_{hori} \to 3}, \tag{22.49}$$

Thence, the enlarged volume is as follows:

$$V_{enlarged} = R^3_{enlarged} \cdot \frac{4\pi}{3} = L_P^3 \cdot Z^3_{D_{hori}\to 3} \cdot \frac{4\pi}{3} \tag{22.50}$$

Thence, the density at three-dimensional volume at ρ_c is the dynamical mass $\frac{E_{vol,\rho_{D=3,c}}}{c^2}$ divided by the enlarged volume:

$$\rho_{vol,\rho_{D=3,c}} = \frac{E_{vol,\rho_{D=3,c}}}{c^2} \frac{1}{L_P^3 \cdot Z^3_{D_{hori}\to 3}\frac{4\pi}{3}} \tag{22.51}$$

We use the energy in Eq. (22.41):

$$\rho_{vol,\rho_{D=3,c}} = \frac{E_P/c^2}{300 Z_{D_{hori}\to 3}} \frac{1}{L_P^3 \cdot Z^3_{D_{hori}\to 3}\frac{4\pi}{3}} \tag{22.52}$$

The Planck density of a ball is as follows, see appendix:

$$\bar{\rho}_P = \frac{E_P/c^2}{\frac{4\pi}{3} L_P^3} \tag{22.53}$$

Thus, the density of volume is as follows:

$$\rho_{vol,\rho_{D=3,c}} = \bar{\rho}_P \cdot \frac{1}{300 \cdot Z^4_{D_{hori}\to 3}}. \quad \text{We summarize :} \tag{22.54}$$

Theorem 41 $\rho_{vol,\rho_{D=3,c}}$ emerging at phase transition

(1a) The quanta of volume have one direction of propagation and $D-1$ directions of transverse **polarization.**

(1b) As a consequence of part (1a), space has at least three dimensions, $D \geq 3$.

(2a) At the end of 'cosmic inflation', there occurs a dimensional phase transition **towards three-dimensional space,** *$D = 3$. That transition takes place at a critical density $\rho_{D=3,c}$.*

(2b) At the dimensional phase transition at the density $\rho_{D=3,c}$, there emerge quanta of volume with the following energy:

$$E_{vol,\rho_{D=3,c}} = \frac{E_P}{300 \cdot Z_{D_{hori}\to 3}} \tag{22.55}$$

(3a) At the dimensional phase transition at the density $\rho_{D=3,c}$, the emerging quanta of volume have the following **density of volume***:*

$$\rho_{vol,\rho_{D=3,c}} = \frac{H_0^2}{4\pi G} \cdot \tilde{\rho}_{D=3,c} \cdot 2.6915 \qquad (22.56)$$

This result is obtained by combining the above relations.

(3b) Thereby, the fraction in the above equation is equal to the density of volume $\rho_{vol,theo}$ occurring in the process of permanent formation of volume in three-dimensional space, see THM (36):

$$\rho_{vol,\rho_{D=3,c}} = \rho_{vol,theo} \cdot \tilde{\rho}_{D=3,c} \cdot 2.6915 \qquad (22.57)$$

(3c) If the critical density is

$$\tilde{\rho}_{D=3,c} = \frac{1}{2.6915} = 0.3715, \qquad (22.58)$$

Then the two densities are equal:

the density of volume $\rho_{vol,\rho_{D=3,c}}$ emerging in the process of cosmic unfolding (Eq. 22.57)

and the density of volume $\rho_{vol,theo}$ occurring in the process of permanent formation of volume in three-dimensional space (THM 36).

(3d) As the density is a classical quantity, it depends on the universal constants G and c only, whereas the density does not depend on the Planck constant, see Eq. (22.57).

(4) The **dimensional phase transition** *at $\rho_{vol,\rho_{D=3,c}}$ has been modeled by four independent models:*

(4a) In a Bose gas, the critical density has the following value $\rho_{vol,\rho_{D=3,c}} = 0.435$, Carmesin (2021d), Sawitzki and Carmesin (2021).

(4b) In a model using two representative objects, similarly as in the van der Waals model, the critical density has the following value $\rho_{vol,\rho_{D=3,c}} = 0.11569$, (Carmesin, 2021a, section 3.4.5).

(4c) In a model describing volume connecting volume, the critical density has the following value $\rho_{vol,\rho_{D=3,c}} = 0.1352$*, see for instance (Carmesin, 2021a, THM 1).*

(4d) In a model using two droplets, the critical density has the following value $\rho_{vol,\rho_{D=3,c}} = 0.37$*, see (Carmesin and Schöneberg, 2022, Fig. 4).*

Altogether, the models of that phase transition provide the following interval for the critical density:

$$\tilde{\rho}_{D=3,c} \in [0.11569, 0.435] \tag{22.59}$$

The value $\rho_{vol,\rho_{D=3,c}} = 0.3715$ *of the critical density provides equality of dark energy at* $D > 3$ *and at* $D = 3$.

That value $\rho_{vol,\rho_{D=3,c}} = 0.3715$ *is in the interval of modeled values.*

Moreover, that value $\rho_{vol,\rho_{D=3,c}} = 0.3715$ *is practically equal to the value obtained in the droplet model* $\rho_{vol,\rho_{D=3,c},droplet} = 0.37$.

(5) The energy of volume is **quantized**:

(5a) The total classical value of the energy of volume is zero, as kinetic and potential energy densities cancel each other.

(5b) The quanta of volume exhibit a zero-point energy, ZPE. At the critical density $\rho_{D=3,c}$*, each quantum of energy has the following value:*

$$E_{vol,\rho_{D=3,c}} = \frac{E_P}{300 \cdot Z_{D_{hori} \to 3}} = 43.9\ \mu\ \mathrm{eV} \tag{22.60}$$

(5c) In general, a quantum of volume with a wavelength λ *exhibit a zero-point energy fulfilling the following relation:*

$$E_{vol} = \frac{h \cdot c}{\lambda} \tag{22.61}$$

(5d) Quanta of volume can take part in phase transitions. Such phase transitions can provide higher dimensional space, matter,

Carmesin (2021a), Carmesin (2022c), and fundamental interactions, Carmesin (2021e), Carmesin (2022e).

(6) The **volume extends** *as follows:*

(6a) In D-dimensional space, each quantum of volume has $D-1$ transverse directions of polarization and one direction of propagation. In this manner, each quantum fills D-dimensional volume.

(6b) A quantum of energy δE_{vol} has the following $3D$-volume:

$$\delta V = \frac{\delta E_{vol}}{u_{vol}} = 2\pi R_{H_0}^2 \frac{2G \cdot \delta E_{vol}/c^2}{c^2} = 2 \cdot \pi R_{H_0}^2 \cdot R_S \quad (22.62)$$

$$R_S = \frac{2G \cdot \delta E_{vol}/c^2}{c^2} \quad (22.63)$$

(6c) A quantum of energy $E_{vol,\rho_{D=3,c}}$ has the following wavelength:

$$\lambda = L_P \cdot 300 \cdot Z_{D_{hori} \to 3} = 6.616 \cdot 10^{-35}\,\mathrm{m} \cdot 300 \cdot 9.26 \cdot 10^{29} = 4,5\,\mathrm{mm} \quad (22.64)$$

(6d) A quantum of energy $E_{vol,\rho_{D=3,c}}$ has the following volume:

$$\delta V = 2 \cdot \pi R_{H_0}^2 \cdot R_S = 1.4 \cdot 10^{-14}\,\mathrm{m}^3 = 1.4 \cdot 10^{-5}\,\mathrm{mm}^3 \quad (22.65)$$

(7) As quanta of volume are zero-point oscillations, ZPOs, with ZPE, their energy is not available for transformation to other objects. Thus, the universality of the position factor does not apply, see THM (4). Hence, the quanta of volume do NOT exhibit a redshift in the vicinity of a mass or dynamical mass.

In contrast, the quanta of volume exhibit a change of the wavelength at each dimensional phase transition. An increase of the wavelength of a quantum of volume at a dimensional phase transition is called **redchange**, *glossary. Similarly, radiation does not exhibit a redshift or a redchange at a dimensional phase transition.*

(8) If quanta of volume form a mass by a phase transition, then the transformed quanta are no longer ZPOs, they are at transformed or excited states. Thus, the transformed quanta have energy that is available for transformation to other objects. Thence, the universality of the position factor does apply, see THM (4).

(9) Altogether, the dark energy in three-dimensional space and the dark energy at 'cosmic inflation' are derived in a **unified manner**. *Hereby, the derived results are in precise accordance with observation. Thereby, no hypothesis has been introduced at all. Moreover, no fit is executed. For it, the parameters of the volCDM-model have been derived from first principles in Carmesin (2021a).*

Proof: The proof is provided within the theorem.

In order to provide additional support, the derivation of Eq. (22.57) is elaborated here in detail: According to Eq. (22.54), the density of volume is as follows:

$$\rho_{vol,\rho_{D=3,c}} = \bar{\rho}_P \cdot Z^{-4}_{D_{hori}\to 3} \cdot \frac{1}{300} \tag{22.66}$$

In the above density (Eq. 22.66), we express the dimensional distance enlargement factor $Z_{D_{hori}\to 3}$ with Eq. (22.42):

$$\rho_{vol,\rho_{D=3,c}} = \bar{\rho}_P \cdot \frac{L_P^4 \cdot k^4_{\rho_{D=3,c}\to t_0}}{R^4_{LH}} \cdot \frac{1}{300} \tag{22.67}$$

In the above density (Eq. 22.67), we include the terms for the light horizon (Eq. 22.43) and for the scale factor (Eq. 22.44):

$$\rho_{vol,\rho_{D=3,c}} = \bar{\rho}_P \cdot \frac{L_P^4 H_0^4}{c^4 K^4_{LH}} \cdot \frac{\tilde{\rho}_{D=3,c}}{\tilde{\rho}_{r,0}} \cdot \frac{1}{300} \tag{22.68}$$

In the above density (Eq. 22.68), we include the terms for the density of radiation (Eq. 22.45)[2]:

$$\rho_{vol,\rho_{D=3,c}} = \bar{\rho}_P^2 \cdot \frac{L_P^4 H_0^4}{c^4 K_{LH}^4} \cdot \frac{G}{H_0^2} \frac{\tilde{\rho}_{D=3,c}}{\Omega_{r,0}} \frac{8\pi}{3} \cdot \frac{1}{300} \tag{22.69}$$

We simplify the above term:

$$\rho_{vol,\rho_{D=3,c}} = (\bar{\rho}_P^2 L_P^4) \cdot \frac{H_0^2}{c^4} \cdot G \frac{\tilde{\rho}_{D=3,c}}{300\Omega_{r,0} K_{LH}^4} \frac{8\pi}{3} \tag{22.70}$$

According to the Planck units, see appendix, the above bracket is equal to $\left(\frac{3}{4\pi}\right)^2 \frac{c^4}{G^2}$. Thus, the density (Eq. 22.70) is as follows:

$$\rho_{vol,\rho_{D=3,c}} = \frac{H_0^2}{4\pi G} \cdot \frac{\tilde{\rho}_{D=3,c}}{300\Omega_{r,0} K_{LH}^4} \frac{8\pi}{3} \frac{9}{4\pi} \quad \text{or} \tag{22.71}$$

$$\rho_{vol,\rho_{D=3,c}} = \frac{H_0^2}{4\pi G} \cdot \frac{\tilde{\rho}_{D=3,c}}{50\Omega_{r,0} K_{LH}^4} = \frac{H_0^2}{4\pi G} \cdot \tilde{\rho}_{D=3,c} \cdot 2.6915, \quad \text{q.e.d.} \tag{22.72}$$

[2]We remind that $\Omega_{r,0}$ has been used to quantify the redshift experienced by radiation. More generally, an analysis of all energy transformations, including redshifts and redchanges, ranging from the early universe at the Planck scale towards the present-day universe, see Carmesin (2020b) or Carmesin (2021f).

Chapter 23

Derivation of GR

In this chapter, we show that the Einstein field equation, EFE, is a consequence of the spacetime quadruple, SQ, in a semi-classical limit. The EFE describes the curvature of spacetime. Objects exhibit geodesic motion. That motion is obtained from the principle of extremal action derived from the SQ in a semi-classical limit.

23.1 Curvature of spacetime is included in the SQ

The spacetime quadruple, SQ, includes both essential distances, the gravitational parallax distance, d_{GP} and the light-travel distance d_{LT}.

The light-travel distance d_{LT} includes the curvature of spacetime. So, the SQ includes theories that describe the curvature of spacetime. There are several such theories. Early theories about the curvature of spacetime have been proposed by Einstein (1911a) or Nordstrom (1913). The presently used and very successful theory of general relativity, GR, has been proposed by Einstein (1915) and Hilbert (1915). That theory can be represented by the Einstein field equations, see Einstein (1915) or e. g. (Hobson et al., 2006, section 19.12).

So, the question arises, whether GR and the EFE can be derived from the SQ. By construction, GR is a non-quantized (classical or semiclassical) theory, Lee (1997), Einstein (1915), Hilbert (1915). In contrast, the SQ includes the quantization in chapters (4, 14). So, GR and the EFE can only be derived in a semiclassical limit within the SQ.

23.2 Semiclassical limit via path integrals

Such a semiclassical limit can be obtained by the path integral method Feynman (1948), (Ballentine, 1998, section 4.8). Hereby, the concept of a path is a semiclassical concept, as classical paths do not exist according to the Heisenberg uncertainty principle, which is a consequence of the postulates of QP, (Ballentine, 1998, section 8.4), (Kumar, 2018, section 3.10).

In the path integral method, all paths $x(\tau)$ connecting an initial point (t_0, x_0) and a final point (t, x) are considered. For each path, an action $S[x(\tau)]$ is developed. If the quantum system is initially at (t_0, x_0), then the SEQ implies that the probability to find the system at the final point (t, x) is proportional to $|f(t_0, x_0, t, x)|^2$ with (Ballentine, 1998, Eq. 4.55):

$$f(t_0, x_0, t, x) = \int \exp(i \cdot S[x(\tau)]/\hbar) dx(\tau) \tag{23.1}$$

Hereby, the integral is the functional integral over all paths $x(\tau)$.

23.3 Semiclassical limit at stationary action

In the path integral method, the semiclassical limit is obtained as follows (Ballentine, 1998, p. 120): The semiclassical limit holds, roughly speaking, when the classical action $S[x(\tau)]$ is much larger than the quantum action $\hbar$. In that case, small changes of a path may result in a change of the phase in Eq. (23.1) by π, so that the sign of the integrand changes and a cancellation occurs. So, most paths cancel out, and only a path $x(\tau)$ with an extremal action $S[x(\tau)]$ remains. The extremal action is also called stationary action, including least action. If there are several paths with the same extremal phase or action, then these paths remain. Such a path can be determined searching the extremal action. That method is also called the principle of stationary (or least) action, PLA, e. g. Fermat (1657), Landau and Lifschitz (1971), Feynman (1985), Weinberg (1996), Grebe-Ellis (2011), Carmesin (2022e). In this manner, the PLA is a consequence of quantum physics. Accordingly, the PLA is a consequence of the SQ. Moreover, the PLA provides a semiclassical limit of the SQ.

23.4 Most simple action

Curved spacetime can be described by a most simple action. That most simple possible action is the Einstein-Hilbert action, see e. g. Hilbert (1915), Landau and Lifschitz (1971), (Hobson et al., 2006, sections 19.8-19.11).

In physics, it is a usual concept to describe a system by an action that is complicated enough to describe the system under investigation, and that is the most simple action that can describe the system under investigation. That principle of a most simple action is not excluded by the SQ, so it is included in the SQ.

The analysis shows that the Einstein-Hilbert action provides the EFE, see e. g. Hilbert (1915), Landau and Lifschitz (1971), (Hobson et al., 2006, sections 19.8-19.11). In this sense, the EFE is a consequence of the SQ. We summarize our result:

Theorem 42 The SQ implies the EFE

(1) The SQ includes the light-travel distance d_{LT}. So, the SQ includes curved spacetime and theories of GR.

(2) The SQ implies the postulates of QP. So, the SQ implies the PLA in the semiclassical limit.

(3) The SQ includes the principle to describe a system with the simplest possible action that covers the phenomena of the system. So, the SQ includes the Einstein-Hilbert action as a possible description of curved spacetime according to the usual GR.

(4a) As a consequence, the SQ includes the Einstein-Hilbert action for the description of the usual GR.

(4b) The SQ implies the quantization of volume and QP. Thus, the SQ implies the PLA as a semiclassical consequence.

(4c) The SQ includes the Einstein-Hilbert action in (4a), and the PLA in (4b), the application of which provides the EFE. In this manner, the SQ implies the EFE in the semiclassical limit.

(5) And in this manner, the SQ provides the foundation of the applicability of the PLA to the Einstein-Hilbert action, whereas in usual GR, that applicability is assumed without foundation, see e. g. Hobson et al. (2006).

(6) Moreover, the SQ includes essential phenomena beyond the usual GR, see for instance chapters (21, 4, 14).

Chapter 24

Discussion

24.1 Achieved key results

Based on fundamental principles of physics, we derive the **theory of the dynamics of volume in nature**, including the formation of volume, see part (II). For it, we use relativity and gravity, see C. (2), in order to derive the dynamics of the volume. We will see that volume is an essential quantity of its own, providing curvature, gravity, transformations, phase transitions and quanta. Using that theory, we derive the following results and answers in a unifying manner:

(1) We derive the **curvature and expansion** of spacetime proposed in a semiclassical manner in general relativity, GR, see part (II) and C. (3, 5, 6, 23). In this manner, we overcome the semiclassical character of present-day GR. Moreover, in present-day GR, the density of Λ ρ_Λ has one observational value $\rho_{\Lambda,obs}$. Planck-Collaboration (2020) observed $\rho_{\Lambda,obs} = 0.679 \cdot (1 \pm 0.013) \cdot \frac{3H_0^2}{8\pi G}$, see THM (36). However, present-day GR cannot test that observed value by theory. Thus, the concept of the density ρ_Λ in present-day GR cannot be falsified, Popper (1974). Thus, the concept of the density ρ_Λ in present-day GR has a hypothetical character. This hypothetical character of dark energy in present-day GR is overcome by our theory, as we derive the value $\rho_{vol,theo} = 2/3$ in THM (36).

(2) Similarly, proposed alternative theories of the density ρ_Λ use fit parameters, or they use a hypothesis, see (Kamionkowski and Riess, 2023, section 4), or they use a 'scale parameter that must ultimately be determined with input from measurements', (Schulz, 2020, p. 22 and p. 67). These results cannot be falsified, as they explain one observable quantity only, ρ_Λ, whereby they use fit parameters or hypotheses or fitted scale parameters. Accordingly, these alternative theories remain hypothetical. In contrast, our dynamics of the volume provides ρ_Λ, ρ_{vol} and $\rho_{het,rqui}$ without any fit, without any hypothesis, without any scale parameter, with a full derivation from fundamental principles of physics and based on volume, which can be measured and which is an element of physical reality, see DEF (15).

(3) Using the dynamics of volume, we derive the **postulates of quantum physics**, see chapters (4, 14). Thereby, we overcome the hypothetical character of quantum physics.

(4) Using the dynamics of volume, we show that the relative additional volume, together with volume, is the **entity in which electromagnetic waves propagate**, see C. (7, 8, 11).

(5) Using the dynamics of volume, we derive the Schrödinger equation, C. (14). Furthermore, we derive generalizations of the SEQ, see part (II) and C. (22).

(6) Using the dynamics of volume, we show that the rate of relative additional volume has the properties of the wave function of volume and of matter, C. (14). Accordingly, the **wave function in quantum physics in postulate (1)** is a normalized rate of relative additional volume. In this manner, we overcome the hypothetical character of the wave function in QP.

(7) Using the DV, we show that the relative additional volume exhibits a transient phenomenon that explains the **nonlocal character of wave functions** in QP, C. (16):

A harmonic RGW fulfills $0 = \frac{\dot{\varepsilon}_L^2 c^2}{8\pi G} - \frac{(\vec{G}^*)^2}{8\pi G} = u_{kin} - u_{\text{grav.}} = u = 0$, or $E = 0$, THMs (13, 14, 19). Thus, a harmonic RGW has no inertia and can achieve an unlimited phase velocity v_p, THM (12). These RGWs provide an infinitely rapid transient phenomenon, which changes from one solution of the SEQ to another solution of the SEQ, THM (34). Hence, **transient phenomena are nonlocal** as v_p is not limited, neither by inertia nor by the DEQ (12). In contrast, a wave packet of volume exhibits a nonzero ZPE, $E > 0$, THMs (22, 29). Thus, such a wave packet has inertia and zero rest mass. So, the wave packet propagates at the group velocity $v_g = c$, according to SR. Hence, **wave packets propagate at** $v_g \leq c$.

(8) Einstein proposed a principle of locality for unmediated processes. So, the principle does not apply to the observed nonlocality of quanta, as that nonlocality is mediated by volume, as volume represents the wave function, C. (16). Thus, **Einstein's principle of locality is not violated** by the nonlocality of quanta. Presumably, Einstein was aware of the fact that his locality in relativity relies on unmediated processes. But he did not know that processes in nature are mediated by volume.

(9) Using the dynamics of volume in a homogeneous and in a heterogeneous universe, we derive and explain the various observed values of the Hubble constant, C. (19, 20, 21, 22). In this manner, we overcome the present-day insufficient understanding of the **Hubble tension** and of the related rate of expansion of space. Moreover, thereby, we predict the Hubble constant $H_{0,obs}(z)$ as a function of the redshift z, C. (21). With it, we derive the **dynamics of our heterogeneous universe**:

(9a) Usual cosmological models use the cosmological principle: a homogeneous and isotropic universe, Hobson et al. (2006). In such a model, the rate of expansion is described by the following Hubble parameter as a function of the redshift z, see Eq. (5.27):

$$H(z) = H_0\sqrt{\Omega_\Lambda + \Omega_{m,0}(1+z)^3 + \Omega_{r,0}(1+z)^4} \qquad (24.1)$$

Hereby, we apply $\Omega_{k,0} = 0$. In such models, the Hubble parameter H_0 is a constant.

(9b) However, our universe is heterogeneous. Thus, in general, the factor H_0 in Eq. (24.1) is the following function of z:

$$H_0(z) = \frac{H(z)}{\sqrt{\Omega_\Lambda + \Omega_{m,0}(1+z)^3 + \Omega_{r,0}(1+z)^4}} \tag{24.2}$$

If an observer attempts to measure the factor H_0 in Eq. (24.1) in our heterogeneous universe, then the observer will measure the value of $H_0(z)$ in Eq. (24.2). For it, the observer uses radiation that has been emitted at a calendar date $z = z_{\mathrm{em}}$. That radiation shows the state of the universe at $z = z_{\mathrm{em}}$. Thus, that radiation shows $H_0(z)$ at $z = z_{\mathrm{em}}$: $H_0(z_{\mathrm{em}})$. We derived that value in C. (21). Hence, the measured value $H_0(z_{\mathrm{em}})$ and Eq. (24.1) provide the rate of expansion, see THM (39):

$$H(z) = H_0(z)\sqrt{\Omega_\Lambda + \Omega_{m,0}(1+z)^3 + \Omega_{r,0}(1+z)^4}, \text{ with} \tag{24.3}$$

$$H_0(z) = H_{0,\text{without het}} \cdot \sqrt{\Omega_{m,0} + \Omega_\Lambda \cdot [1+\kappa(z)]^\xi}, \text{ with} \tag{24.4}$$

the ratio of rates, THM (39)

$$\kappa(z) = \frac{\sigma_{8,0} \cdot \Omega_{m,0}}{2\Omega_{\Lambda,0} \cdot (1+z)^2} = \frac{\dot{\underline{\varepsilon}}_{\text{het},0}(z)}{\dot{\underline{\varepsilon}}_{\text{hom}}}, \text{ with} \tag{24.5}$$

the standard deviation of matter fluctuations, section (21.4.3):

$$\text{with } \sigma(t) = \sigma_{8,0} \cdot \frac{t}{t_{H_0}} = \frac{\sigma_{8,0}}{1+z} \tag{24.6}$$

Hereby, as heterogeneity is essential in the matter era or later, we use $\Omega_{r,0} = 0$ in a good approximation. Additionally, $\xi \approx 1.5$ in Eq. (24.4), see THM (39).

(9c) Altogether, heterogeneity at a calendar date described by a redshift z changes the rate $H(z)$ of expansion according to Eq. (24.3). Correspondingly, the factor $H_0(z)$ in the rate in Eq. (24.3) can be observed with radiation emitted at $z = z_{\mathrm{em}}$.

The three objects redshift z, rate $H(z)$ and the factor $H_0(z)$ can be observed and are elements of **physical reality**, DEF (15). Observed and theoretical values $H_0(z)$ or $H_0(z_{\rm em})$ are in precise accordance, see Fig. (21.3), front cover and THM (39).
(10) Using the dynamics of volume in the late and in the early universe, we derive and explain the era of **'cosmic inflation'**, see chapter (22). In this manner, we overcome the hypothetical character and insufficient understanding of 'cosmic inflation'. Moreover, we confirm that there was a rapid increase of distances in the early universe, Carmesin (2017, 2019b, 2021b).
(11) Using DV, we overcome the non - realistic (DEF 15, Hobson (2017), Isham (1995)) Copenhagen interpretation of QP by deriving dynamical and nonlocal explanations of the essential paradoxes in QP, C. (16) and section (18.3). In the Copenhagen interpretation, the wave function Ψ is interpreted in an abstract manner. The DV overcomes that abstract interpretation, as the wave function Ψ is proportional to the rate $\dot{\varepsilon}_L$, which describes the local and global formation of volume since the Big Bang. Similarly, all postulates of QP achieve an interpretation in terms of the volume, which is an element of physical reality, DEF (15).
(12) Using DV, we overcome the interpretation of the measurement process by a so-called 'collapse' of the wave function, (Isham, 1995, p. 240): Before the measurement, there is a wave function Ψ_{before}. It is a solution of the SEQ. At a measurement, the operator $\hat{A}$ corresponding to the measured observable transforms the solution Ψ_{before} to the solution $\Psi_{after} = \hat{A}\Psi_{before}$ of the SEQ. The change is achieved by the transient phenomenon provided by the dynamics of the harmonic waves inherent to the wave function Ψ_{before}. According to the DV, that transient phenomenon has an unlimited phase velocity v_p, see C. 16. Thus, the transient phenomenon takes place at an unlimited velocity. Altogether, based on the DV, the so-called 'collapse' of the wave function is overcome and replaced by a transformation of Ψ[1].

[1] For instance, if a quantum object is emitted at the origin of a coordinate system, then

(13) Using the derived energy conservation and the derivation of the global dynamics on the basis of the local dynamics, we **solve the flatness problem**, C. (5). Hereby, we also analyze consequences of the energy density ρ_Λ. Thereby, we use the cosmological principle of homogeneity. Note that within the semiclassical theory of GR, homogeneity is founded by the fact 'that Ricci flow can not quickly turn an almost euclidean region into a very curved one, no matter what happens far away,' (Perelman, 2002, p. 4). Altogether, we overcome the insufficient understanding of global and local dynamics, of energy conservation and of the cosmological principle in the FLE.
(14) Using DV, we provide a mechanism that explains the gravitational interaction, part (II), in a manner corresponding to the graviton hypothesis, Blokhintsev and Galperin (1934).
(15) Using DV, we predict dimensional phase transitions of volume at critical densities $\tilde{\rho}_{D,c}$, C. (22). Hereby, we derive the values of these critical densities $\tilde{\rho}_{D,c}$. These phase transitions can in principle be observed and falsified, Popper (1974).

Moreover, these phase transitions provide the observed density of volume, C. (22). This finding provides additional evidence for these predicted phase transitions.

24.2 Fulfilled criteria

Our theory fulfills the following criteria:
(1a) We derive the theory in an **exact manner from fundamental principles of physics**, C. (2). In particular, we do not introduce any hypothesis or execute any fit. Our only numerical input is as follows: the gravitational constant G, the velocity of light c, the Planck constant h and the present-day time after the Big Bang $t_0 \approx 1/H_0$ (sections 25.3, 21.4.8, 21.4.9).

the wave function can be described by a spherical wave. When the object is measured at a location with a position vector $\vec{R}$, then the wave function transforms to a delta distribution proportional to $\delta(\vec{R})$.

(1b) The present-day time t_0 is a calendar date. In cosmology, a calendar date can be expressed in terms of the redshift z. The calendar date is no fit parameter: The calendar date of an event can be measured with appropriate clocks.

For instance, the density of the volume ρ_{vol} does not depend on the calendar date, see THM (37). In contrast, the observed Hubble constant $H_{0,obs}$ depends on the calendar date $z_{\rm em}$ of the emission of the radiation used for the observation, see THM (39) or Fig. (21.3).

If we use cosmological parameters, we derive these from fundamental principles, see Carmesin (2022e). Of course, we confirm our results with measured parameters, Riess et al. (2022), Planck-Collaboration (2020). Accordingly, **we use no hypothesis and we execute no fit.**

(2) Our theory **can in principle be falsified**, Popper (1974), as we derive observable values. For instance, we derive a value of the density of volume ρ_{vol} in C. (19, 22). Another example is the Hubble parameter $H_0(z_{\rm em})$ as a function of the redshift $z_{\rm em}$ of observed radiation in C. (21). An additional example is provided by the critical densities in C. (22). Further examples are the cosmological parameters, Carmesin (2021a). More examples are the coupling constants and charges in the electromagnetic and electroweak interactions, Carmesin (2021e, 2022e).

(3) We show that the volume can be measured (section 2.6, C. 7). So the volume **is an element of reality**, DEF (15).

(4) Our derivations **achieve precise accordance with observation**, within the accuracy of measurement.

(5) We **trace back quantum physics to geometry**. For it, we derive the dynamics of volume, including the tensor structure and dimensional phase transitions. Then we derive quantum physics from the dynamics of volume. This result is similar to the derivation of gravity from geometry in general relativity.

(6) We **derive the observed type of nonlocality.**

(7) We **achieve causality combined with the observed**

type of nonlocality, as our derived nonlocality is in full accordance with SR, since the nonlocal phenomenon does not transport any energy or wave packet.
(8) We **achieve the observed type of nonlocality without violating the Einstein locality principle.**

24.3 Relations among theories

Question: How is the theory of the dynamical volume related to other theories? For an overview, see Fig. (12.3).
Gravity: Kepler (1619) discovered his third law of planetary motion, based on observations by Brahe before 1601, see Brahe and Kepler (1627). Galileo (1638) discovered the **equivalence principle, EP**. Huygens (1673) discovered the law of the radial force of circular motion. Newton (1687) discovered the universal law of gravitation, which can be derived within a single page from the three above discoveries provided by Kepler (1619), Galileo (1638) and Huygens (1673), see e. g. Carmesin et al. (2023). Cavendish (1798) used a torsional balance proposed by Michell many years before. With it, Cavendish measured the universal constant G of gravity. In his theory, Newton (1687) proposed a flat space and a constant and homogeneous rate of increase of time. Both proposals do not describe nature correctly, as shown by tests of special relativity, SR, and by general relativity, GR, see Einstein (1905, 1915), Will (2014). Gauss (1809) provides a geometrical explanation of the $1/R^2$ law: At a distance R from a mass M, lines of the gravitational interaction spread in a uniform manner in space, this implies the $1/R^2$ law. Altogether, Newton (1687) discovered the universal law of gravitation. However, he proposed properties of space and time that are **too isolated** from motion and gravity. **Gaussian gravity, GG**, provides a geometrical explanation of the $1/R^2$ law.
Electrodynamics: Coulomb (1785) used the torsional balance

proposed by Michell in the field of gravity. With it, Coulomb discovered the $1/R^2$ law of the electric force. Faraday (1852) proposed the concept of magnetic fields. Maxwell (1865) used these results, and he proposed a hypothetical aether. On that basis, he developed the Maxwell equations of the dynamics of electromagnetic fields. Thereby, the Maxwell equations explain the universal propagation of electromagnetic waves at the universal velocity c. Furthermore, the dynamics of electromagnetic fields is universal according to the principle of gauge invariance, see e. g. Noether (1918), Pauli (1941), Landau and Lifschitz (1971), Carmesin (2021e, 2022e). Moreover, Einstein (1905) used the Maxwell equations and their properties in order to develop SR. However, SR implies that the proposed static aether does not exist. Altogether, Maxwell (1865) discovered the universal dynamics of electromagnetic fields, which provide a **bridge to SR**, but the proposed aether is **too static**.

Relativity: Einstein (1905) made use of the universal Maxwell equations and their properties in order to develop **SR**. Thereby, Einstein realized that the combination of space and time to a combined **spacetime** provides a coherent and simple explanation of the dynamics in electromagnetic fields. For it, two conditions are essential: [1] No object with nonzero energy should move or propagate faster than light. [2] No aether should exist.

The EP and GG provide the Schwarzschild metric and the **curvature of spacetime**, C. (3). Similarly, Einstein (1911a, 1915), Hilbert (1915) proposed general relativity, GR. Einstein et al. (1935) realized that quantum physics, QP, (developed since Planck (1899)), is nonlocal (it has processes faster than light). In that context, Einstein (1948) proposed a principle of locality, see [1], for unmediated, see [2], physical processes. However, the DV shows that the considered unmediated physical processes are **too isolated** from existing DV.

Dynamic volume, DV: The above three theories are successful, as they are in accordance with fundamental principles of physics: EP, GG, SR. However, each of the above theories has an aspect that is either too isolated or too static. Accordingly, the dynamics of volume should fulfill these principles: EP, GG, SR. Thus, the DV is derived from EP, GG and SR. Altogether, the DV implies and explains QP, including nonlocality. So, the Copenhagen interpretation of QP is overcome (section 18.3). Furthermore, the DV overcomes the shortcomings of the three above theories: The dynamics of volume explain curved spacetime as well as QP. Electromagnetic waves propagate in DV, not in a static aether. The geometrical and exactly derived DV provides DEQs that explain curvature of spacetime, gravity, nonlocality and a volume-based mediation of processes.

Dynamic volume provides a basis for path methods: In present-day quantum field theory or theoretical physics, physical processes are often described by paths, Hilbert (1915) or Schwartz (2014), Schulz (2020). However, at a double slit, a quantum object does not use a path through one slit with a probability, see the delayed choice experiment in C. (18). Thus, a path is not observable, so it is not an element of physical reality. However, dynamic volume can clarify the type of reality that can be assigned to a path: A quantum object causes a rate $t_n \cdot \dot{\varepsilon}_L$. It is proportional to a wave function $\Psi \propto t_n \cdot \dot{\varepsilon}_L$ (C. 14). Each path $x(\tau)$ has a classical action $S[x(\tau)]$. In a semiclassical limit, the wave function has the form $\Psi \propto \exp(i \cdot S[x(\tau)]/\hbar)$, (Landau and Lifschitz, 1965, Eq. 6.1). Thus, the rate has the same form $t_n \cdot \dot{\varepsilon}_L \propto \exp(i \cdot S[x(\tau)]/\hbar)$. In general, a path is a curved line in spacetime, at which the rate of propagating and forming volume is analyzed.

In an ideal case, there is a path with the least action, with the lowest oscillation, with the lowest cancellation and with the highest amplitude. In the principle of least action, PLA, such paths are selected. In principle, the rate-function $t_n \cdot \dot{\varepsilon}_L \propto$

$\exp(i \cdot S[x(\tau)]/\hbar)$ of a path can be measured with a sufficient number of interference experiments. In this manner, the dynamics of volume assign an element of reality to a path and to its rate-function in spacetime. Additionally, such paths may be transformed to paths in Hilbert space.

In particular, the Einstein (1915) field equation, EFE, in GR is usually derived from the Einstein-Hilbert action, Hilbert (1915), Hobson et al. (2006). For it, the PLA is applied: A path is chosen at which that action takes an extremal value. This procedure shows that the EFE and the present-day GR are semiclassical theories. Moreover, the DV provides a derivation of the semiclassical GR, if the simplest reasonable action is used, the Einstein-Hilbert action, and if the PLA is applied (C. 23).

Dynamic volume overcomes hypothetical character of quantum postulates: The DV implies and explains the quantum postulates. Accordingly, it is not necessary to propose hypothetical quantum postulates, Hilbert et al. (1928), Neumann (1932), Ballentine (1998), Kumar (2018). Instead, rules of quantum physics are derived from the DV.

Further essential relations of DV: DV provides the process underlying the elementary charge e and the electromagnetic interaction as well as the couplings and charges underlying the electroweak interaction, see Carmesin (2021e, 2022e). Thus the DV provides the charge that remains unexplained by the universal theory of electrodynamics.

Moreover, Einstein (1919) and Einstein and Rosen (1935) attempted to explain elementary particles on the basis of geometry or gravity of spacetime. However, these attempts have not been successful. The DV is a geometrical theory providing a wide range of results in a unifying manner: gravity, curvature of spacetime, quantum physics as well as the formation of elementary particles, see Carmesin (2021a, 2022c), and their fundamental interactions, Carmesin (2021e, 2022e).

Thus, the DV provides additional results underlying the electrodynamics and the elementary particles.

On non-linearity of DV: The DEQ of GR, the EFE, is nonlinear. In contrast, the DEQ of DV is linear, see C. (11). However, the DEQ of DV includes the local formation of volume, which changes the space in which the RGWs propagate. Thus, the DEQ of DV describes a non-linear process.

On entanglement of DV: In general, the wave function can describe conserved quantities such as the energy density. If two objects fulfill a conservation law in a combined manner, then they are not independent. Thus, they are entangled. So, entanglement is an ubiquitous phenomenon.

On the measurement process: In nature, as well as in quantum physics and in the more general DV, deterministic and probabilistic phenomena are combined in a precisely determined manner: The deterministic time evolution is represented by the Schrödinger (1926a) equation. Probabilistic outcomes can occur at the measurement process. Hereby, in general, rapid transient phenomena take place so that conservation laws are fulfilled and consequences of entanglement are fulfilled, see C. (16).

Ricci flow: Einstein (1915) proposed the Einstein field equation, EFE, in order to describe the dynamics of spacetime.

In the case without nonhomogeneity, the EFE describes the time evolution of spacetime in terms of a flow, the Ricci flow, Anderson (2004), Balmer (2021).

THM (35) shows that the dynamics of DV is more complex than the dynamics of the Ricci flow or of the EFE, as a product of tensors is inherent to the volume. That additional complexity is essential for the unification of gravity, spacetime and quantum physics, as poly-directional formation of volume is essential in the expansion of space (C. 12). Unidirectional relative additional volume can be transformed to the corresponding Ricci flow, C. (17).

Some improvements in the present book:

(1) In the present book, the unification of spacetime, gravity and quanta is *exact*. For comparison, I used the FDA in the derivation of the unification in Carmesin (2022d,f).

(2) In the present book, in the analysis of the H_0 *tension* in C. (21), I realized that the heterogeneity can be described in terms of an equivalent density $\rho_{\text{het,equi}}$ (section 21.4.5). With it, the density of volume ρ_{vol} and the equivalent density $\rho_{\text{het,equi}}$ can be treated separately. In Carmesin (2022d,f), I analyzed the density of volume ρ_{vol} and of the equivalent volume $\rho_{\text{het,equi}}$ in a summarizing manner in a so-called 'vacuum'. In this book, I isolate the dynamics and density of volume by the geometric properties of volume. As a result, the heterogeneity does not cause a time evolution of the density of volume ρ_{vol}.

Moreover, the separation of the equivalent density $\rho_{\text{het,equi}}$ and the density of volume ρ_{vol} provides a more differentiated analysis with help of a simultaneous change of H_0 and t_{H_0}, solved via an exponent ξ (section 21.4.5). With it, the derived density of volume ρ_{vol} is especially precise. A possible consideration of the effect of a local negative overdensity of the local universe is less precise. Moreover, it is not essential at the considered redshift $z = 0.055$. Accordingly, it is neglected.

(3) In the homogeneous universe, the density ρ_Λ of the cosmological constant Λ is equal to the density of three-dimensional volume ρ_{vol}, see sections (2.9, 25.2.4). In nature, that case occurs at a good approximation in the early universe. For instance, at the redshift $z_{CMB} = 1090.3$ of the emission of the cosmic microwave background, the universe has been very homogeneous, Smoot et al. (1992), Carmesin (2021d), C. (21). For that case, our derived values of the density ρ_{vol} and of the Hubble constant H_0 are in precise accordance with observation. However, in the heterogeneous universe, the density ρ_Λ is equal to a function f_Λ of the sum of the density of $3D$ volume ρ_{vol}

and the equivalent density of heterogeneity $\rho_{het,equi}$, Eq. (25.2), C. (2, 21): $\rho_\Lambda = f_\Lambda(\rho_{vol} + \rho_{het,equi})$. We derive that function $f_\Lambda(\rho_{vol} + \rho_{het,equi})$. With it, we derive, explain and solve the H_0 tension, discovered by Riess et al. (2022) at the 5σ confidence level. Thereby, we achieve precise accordance with observation at a relative difference of theory and observation of 0.096 %, C. (21). Hereby, we use no hypothesis and execute no fit.

In earlier publications, I did not always distinguish between the densities ρ_{vol} and $\rho_{het,equi}$. Accordingly, I often described the density ρ_Λ of the ΛCDM model. In this context, I describe three densities here: the density ρ_Λ of the ΛCDM model, the newly evaluated density ρ_{vol} of the $3D$ volume in nature, and the new equivalent density $\rho_{het,equi}$ of the heterogeneity in nature.

(4) In the present book, the analysis of the *transient effect* has been elaborated, see C. (16).

(5) In the present book, the *investigations* of the flatness (C. 5), of the LFV (C. 9), of the propagation and formation of volume (C. 11), of the GFV (C. 12), of the ZPE (C. 14) and of the wave packet (C. 14) are improved.

(6) In the present book, the following items are also *elaborated*: the mapping theorem (C. 17), additional interpretations (C. 18), the process of formation of stable quanta (C. 13), the analytic and comparative treatment of the time evolution of dark energy during 'cosmic inflation' (C. 22), the **age of the universe** is $13.3 \cdot 10^9$ years, instead of $13.8 \cdot 10^9$ years (THM 39).

Using the dynamics of volume, an element of physical reality, we unify spacetime, gravity and quantum physics.

Chapter 25

Appendix

In this book, the results are derived successively from first principles or fundamental principles of physics, see Fig. (12.3).

25.1 Mathematical methods

25.1.1 Analysis and Leibniz calculus

We apply the standard analysis, see e. g. Strang (2017). Hereby, we use the Leibniz calculus providing differences Δx and differentials or increments dx, δx or $\underline{\delta} x$, see e. g. Leibniz (1684). Moreover, we apply the Taylor (1715) expansion to these differentials, and we denote a term of order n or larger in dz by $\mathcal{O}(dz^n)$, Flanders (1989).

25.1.2 Vectors and tensors

In this book, we use vectors and tensors, see e. g. Riemann (1868) or also Landau and Lifschitz (1971), Carmesin (1996), Lee (1997), Hobson et al. (2006), Straumann (2013).

25.1.3 Probability theory

In this book, we use probability theory, see e. g. Kolmogorov (1956) or also Landau and Binder (2005) or Ash (2008) or Olofsson and Andersson (2012). Probability theory has a deep link to physics, especially to quantum physics.

In nature, in quantum physics and in the more general DV, deterministic and probabilistic phenomena are combined in a precisely determined manner, see chapters (16, 24). Accordingly, probability theory is applied in a manner that fulfills the laws of physics.

25.1.4 Geometry

The volume represents the substantial basis of geometry. Incidence structures and relations among points, lines and planes are provided by geometry, Hilbert (1903), Hart (1912). Curved spaces are described by differential geometry, including tensors Lee (1997) or Landau and Lifschitz (1971), Hobson et al. (2006). Higher dimensional spaces are derived on the basis phase transitions providing a conservation of volume, Carmesin (2017, 2018b, 2019b, 2020b, 2021d), Carmesin and Schöneberg (2022). Compound geometrical objects as well as polarization at phase transitions are analyzed according to the minimization of energy, Carmesin (2021a,e, 2022e).

25.2 Methods of physics

25.2.1 Frames

In relativity, frames are used as a tool, see e. g. (Hobson et al., 2006, section 1.1). Accordingly, we use frames as well[1].

25.2.2 Probe mass and probe volume

In physics, probe masses are used as tools for experiments or analysis, see e. g. Braginsky (2007). Accordingly, we use probe masses and corresponding field generating masses.

[1]Note that frames are already essential in classical mechanics. For instance, if you ride on your bicycle on a road, then the kinetic energy is zero in the frame of your bicycle. In contrast, your kinetic energy is nonzero in the frame of the road.

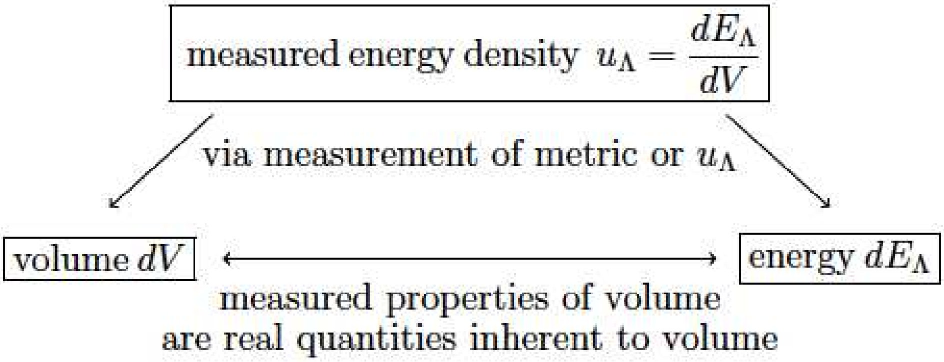

Figure 25.1: In physics, a volume dV contains a measurable energy density $u_\Lambda = \frac{dE_\Lambda}{dV}$ and the corresponding energy dE_Λ.

Additionally, we use the concept of a probe volume, similarly as in the theory of deformations, see e. g. (Sommerfeld, 1978, Eqs. 18, 19, Fig. 1) or (Landau and Lifschitz, 1975, § 1).

25.2.3 Physical reality

In this section, we propose a founded sufficient condition for physical reality, see e. g. Carmesin (2021d).

For it, we use a simple criterion proposed by (Einstein et al., 1935, p. 777): 'The elements of physical reality cannot be determined by a priori philosophical considerations, but must be found by an appeal to results of experiments and measurements.' Accordingly, we use the following definition:

Definition 15 Physical reality

If a physical quantity can be measured, then that quantity represents a part of the physical reality.

25.2.4 Dynamic volume

Einstein (1917) proposed a *cosmological constant* Λ. Zeldovich (1968) suggested a *density of the cosmological constant* ρ_Λ with $\Omega_\Lambda = \frac{\rho_\Lambda}{\rho_{cr.}} = \frac{\Lambda c^2}{3H^2}$ (Eq. VII.2). Accordingly, ρ_Λ is the density that remains, if you subtract the density of matter ρ_m and the density of radiation ρ_r from the whole density ρ (Hobson et al., 2006, Eqs. 15.1, 15.5):

$$\rho_\Lambda := \rho_0 - \rho_{m,0} - \rho_{r,0} = \frac{3H_0^2}{8\pi G} \text{ or } \Omega_\Lambda = 1 - \Omega_m - \Omega_r \quad (25.1)$$

The density ρ_Λ has also been named *density of vacuum* $\rho_{vac} = \frac{\Lambda c^2}{8\pi G}$ (Hobson et al., 2006, Eq. 8.22). However, very different 'densities of vacuum' have been proposed: For instance, Agency (2010) suggested a 'density of a quantum vacuum' $\rho_{\text{quantum vacuum}} \approx 10^{96}\,\frac{\text{kg}}{\text{m}^3}$. E. g. Zeldovich (1968) proposed another value of a 'density of a quantum vacuum' of elementary particles, with a estimate $\rho_{\text{quantum vacuum, Zeldovich}} = 10^{20}\,\frac{\text{kg}}{\text{m}^3}$ [Eq. IX.1]. Additionally, Zeldovich (1968) proposed a 'density of a classical vacuum' $\rho_{\text{classical vacuum, Zeldovich}} = 2 \cdot 10^{-26}\,\frac{\text{kg}}{\text{m}^3}$ [Eq. VII.1]. For instance, Zyla et al. (2020) used a 'vacuum expectation value' $vev = 246\,\text{GeV}$ [section 11].

Perlmutter et al. (1998), Riess et al. (2000) and Smoot (2007) observed a density ρ or energy density $u = \rho c^2$ of space. The corresponding energy $\delta E = u \cdot \delta V$ has been named *dark energy*, Huterer and Turner (1998). We mark it by the subscript DE. The observed value is $\rho_{DE} = u_{DE}/c^2 \approx 5 \cdot 10^{-27}\,\frac{\text{kg}}{\text{m}^3}$, see e. g. Planck-Collaboration (2020). In the framework of the ΛCDM model of cosmology, the density ρ_Λ could be determined from the observed value H_0, according to Eq. (2.65). However, the observed values of H_0 exhibit differences at the 5σ confidence level, Riess et al. (2022). So, the following question arises: **How can the concept of dark energy be improved by fundamental of physics?**

There is only one volume in nature, and it has only one **density of volume** $\rho_{vol} = \Omega_{vol} \cdot \rho_{cr.0}$.
(1) Volume is usually measured on the basis of the light travel distance d_{LT}, C. (2, 7, 17).

(2) The density of three-dimensional volume ρ_{vol} is determined by the quanta of volume[2] in C. (22, 20): $\Omega_{vol} = 2/3$.
(3) Heterogeneity causes an equivalent density $\rho_{het,equi}$. Hereby, $\rho_\Lambda = f_\Lambda(\rho_{vol+equi})$ is the following function f_Λ of the sum $\rho_{vol} + \rho_{het,equi} = \rho_{vol+equi}$: f_Λ is derived by inserting Eqs. (21.53, 21.46) and $\Omega_{r,0} \approx 0$ into Eq. (21.5), and by solving for ρ_Λ, whereby $H^2(z) = 8\pi G(\rho_{\rm m}(z) + \rho_\Lambda)/3$ and $\rho_{\Lambda,hom,0} = \rho_{vol}$:

$$\frac{H^2(z)}{\Omega_{\Lambda,hom,0} + \Omega_{m,0}(1+z)^3} = \frac{8\pi G}{3}[\rho_{\rm m,hom,0} + \rho_{vol+equi}] \text{ or}$$
$$\frac{\rho_{\rm m,hom,0} + \rho_{vol+equi}}{\rho_{\rm cr.,0}}(\rho_{vol} + \rho_{\rm m}(z)) - \rho_{\rm m}(z) = f_\Lambda(\rho_{vol+equi}) \quad (25.2)$$

Using the approximations $\frac{\rho_{\rm m,hom,0}+\rho_{vol}}{\rho_{\rm cr.,0}} \approx 1$ and $\frac{\rho_{equi}}{\rho_{\rm cr.,0}} \approx \rho_{equi}(z)$, we derive:

$$\rho_\Lambda = f_\Lambda(\rho_{vol} + \rho_{equi}) \approx \rho_{vol} + \rho_{equi} \quad (25.3)$$

25.3 Universal constants

quantity	observed value	reference
G	$6.674\,08(31) \cdot 10^{-11}\,\frac{\rm m^3}{\rm kg \cdot s^2}$	Zyla et al. (2020)
c	$299\,792\,458\,\frac{\rm m}{\rm s}$, exact	Zyla et al. (2020)
h	$6.626\,070\,15 \cdot 10^{-34}$ Js, exact	Newell et al. (2018)
k_B	$1.380\,649 \cdot 10^{-23}\,\frac{\rm J}{\rm K}$, exact	Newell et al. (2018)
ε_0	$8.854\,187\,817 \cdot 10^{-12}\,\frac{\rm F}{\rm m}$	Zyla et al. (2020)

Table 25.1: Universal constants, ((Newell et al., 2018, table 3), (Zyla et al., 2020, tables 1.1, 2.1)).

[2]In principle, there could be the hen egg problem: In order to derive the DEQ of dynamic volume, there must already be volume. However, this problem does not occur, as our theory includes the time evolution of volume since the Big Bang, C. (5, 12, 22).

25.4 Glossary on volume

increment: dr_i

changed increment: dr'_i

complete vol.: dV_L, e. g. $4\pi R^2 dL$ or $dA_z \cdot dz'$

reference vol.: $dV_R = \lim_{M\to 0} dV_L$

additional vol.: $\delta V = dV_L - dV_R$

formed vol.: $\underline{\delta} V = \delta V(\tau + \underline{\delta}\tau) - \delta V(\tau)$

relative additional vol.: $\varepsilon_L = \frac{\delta V}{dV_L}$

rate of locally formed vol., LFV: $rate_{LFV} = \frac{\underline{\delta} V}{\underline{\delta}\tau}$

normalized rate of LFV: $\dot{\underline{\varepsilon}}_L = \frac{rate_{LFV}}{dV_L}$

rate of relative additional vol.: $\partial_\tau \varepsilon_L$

rate of globally formed vol., GFV: $\frac{\dot{V}}{V}$

volume - tensor: $\varepsilon_{ij} = \frac{\partial dr_i}{\partial dr'_j}$

relative volume - tensor: $\varepsilon_{ij,L} = \frac{\varepsilon_{ij}}{dV_L}$

relative rate tensor: $\dot{\varepsilon}_{ij,L} = \frac{\dot{\varepsilon}_{ij}}{dV_{L,d\Omega}}$

u_{kin} - tensor: $\varepsilon_{ij,L,sq} = \frac{c^2}{8\pi G} \cdot \sum_k \varepsilon_{ik,L} \cdot \varepsilon_{kj,L}$

unidirectional additional vol.: $\delta V_j = \delta r_j \cdot dA_j$

Trace: either poly-directional relative additional vol., $\varepsilon_V = \Sigma_{j=1}^3 \frac{\delta V_j}{dV_L}$, or

isotropic relative additional vol.: $\varepsilon_V = \Sigma_{j=1}^3 \frac{\delta V_j}{dV_L}$ (with equal summands), also marked by $\varepsilon_{L,iso}$

present-day probe volume: dV_0

The **mapping theorem** (35) provides relative additional volume and corresponding rates as functions of the metric tensor. In particular, a unidirectional rate is expressed as a function of the corresponding Ricci flow.

25.5 Natural units

Planck (1899) introduced natural units. We mark quantities in natural units by a tilde. Natural units can be expressed by G, c and $\hbar$. Even the electric field constant ε_0, the elementary charge e and q_P are derived from SQ, G, c, $\hbar$ and via DV, Carmesin (2021e, 2022e). k_B relates statistics to physics.

physical entity	Symbol	Term	in SI-Units
Planck length	L_P	$\sqrt{\frac{\hbar G}{c^3}}$	$1.616 \cdot 10^{-35}\,\mathrm{m}$
Planck time	t_P	$\frac{L_P}{c}$	$5.391 \cdot 10^{-44}\,\mathrm{s}$
Planck energy	E_P	$\sqrt{\frac{\hbar \cdot c^5}{G}}$	$1.956 \cdot 10^{9}\,\mathrm{J}$
Planck mass	M_P	$\sqrt{\frac{\hbar \cdot c}{G}}$	$2.176 \cdot 10^{-8}\,\mathrm{kg}$
Planck volume	$V_{D,P}$	L_P^D	
Planck volume, ball	$\bar{V}_{D,P}$	$V_D \cdot L_P^D$	
Planck density	ρ_P	$\frac{c^5}{G^2\hbar}$	$5.155 \cdot 10^{96}\,\frac{\mathrm{kg}}{\mathrm{m}^3}$
Planck density, ball	$\bar{\rho}_P$	$\frac{3c^5}{4\pi G^2\hbar}$	$1.2307 \cdot 10^{96}\,\frac{\mathrm{kg}}{\mathrm{m}^3}$
Planck density, ball	$\bar{\rho}_{D,P}$	$\frac{M_P}{\bar{V}_{D,P}}$	
Planck temperature	T_P	$T_P = \frac{E_P}{k_B}$	$1.417 \cdot 10^{32}\,\mathrm{K}$
scaled volume	$\tilde{V}_D$	$\frac{V_D}{\bar{V}_{D,P}}$	
scaled energy	$\tilde{E}$		$E = \tilde{E} \cdot E_P$
scaled density	$\tilde{\rho}_D$	$\frac{\tilde{M}}{\tilde{r}^D} = \frac{\tilde{E}}{\tilde{r}^D}$	$\rho_D = \tilde{\rho}_D \cdot \bar{\rho}_{D,P}$
scaled length	$\tilde{x}$		$x = \tilde{x} \cdot L_P$
Planck charge	q_P	$M_P\sqrt{G4\pi\varepsilon_0}$	$11{,}71\, e$

Table 25.3: Planck - units.

25.6 Glossary

amplitude of matter fluctuations, σ_8: The amplitude of matter fluctuations describes the heterogeneity in the universe in a statistical manner, see e. g. Kravtsov and Borgani (2012) or C. (21).

Big Bang: The Big Bang represents the start of time evolution of visible space, see e. g. Karttunen et al. (1996).

Big Crunch: A global gravitational instability could in principle cause a global contraction, it is called a Big Crunch, see e. g. Goodstein (1997).

'cosmic inflation': Guth (1981) discovered a rapid enlargement of distances in the early universe. For it, he proposed an era of 'inflation' or expansion. However, the rapid enlargement was caused by dimensional phase transitions, by a cosmic unfolding, Carmesin (2017, 2019b, 2022b) or C. (22).

CMB, Cosmic Microwave Background: The radiation of the CMB has been emitted at $z \approx 1090$, see e. g. Penzias and Wilson (1965), Karttunen et al. (1996), Planck-Collaboration (2020).

cosmological constant: Einstein (1917) proposed a cosmological constant Λ. It corresponds to the dark energy with its energy density $u_\Lambda = \rho_\Lambda \cdot c^2$, see dark energy in the glossary and C. (19).

curvature parameter: The curvature parameter k describes the global curvature of space, see for instance Karttunen et al. (1996), Carmesin (2019b), Carmesin (2021d).

dark energy: Perlmutter Perlmutter et al. (1998), Riess Riess et al. (2000) and Smoot Smoot (2007) discovered the accelerated expansion of the universe. Einstein (1917) explained such an accelerated expansion with an additional constant, which he named cosmological constant Λ. That constant Λ can be transformed to an energy density u_Λ (Hobson et al., 2006, Eq. 8.22 or 15.4 with p. 389) (C. 19, 20, 21, 22):

$$u_\Lambda = \frac{\Lambda \cdot c^4}{8\pi \cdot G} \tag{25.4}$$

density, critical: The critical density ρ_{cr,t_0} or ρ_{cr} describe the density of the universe corresponding to the curvature parameter $k = 0$, see e. g. Karttunen et al. (1996), Carmesin (2019b), Carmesin (2021d).

density parameter: The ratio of a density ρ_j and the critical density ρ_{cr,t_0} has been named density parameter $\Omega_j = \rho_j/\rho_{cr,t_0}$, see e. g. Karttunen et al. (1996), Carmesin (2019b), Carmesin (2021d).

dynamic mass or relativistic mass: The concept of the relativistic mass has been described by Tolman (1934), for instance. For it, the energy mass relation of special relativity is used, $E = M \cdot c^2$, or equivalently, $M = \frac{E}{c^2}$. In particular, if the object propagates at $v = c$, then this relativistic mass can be named dynamic mass, in order to remind that the object has no rest mass.

dynamic volume, DV: Each portion of volume δV has a dark energy $\delta E_\Lambda = \delta V \cdot u_\Lambda$ and an energy density of volume u_{vol}, C. (2). Correspondingly, volume has a dynamics. If you want to emphasize that dynamics, you may say dynamic volume, DV (C. 2). But remind, there is only one volume. In earlier books, I did not always distinguish u_{vol} and u_Λ. correspondingly, I used the name vacuum, C. (2).

entanglement: If physical quantities or objects are not **separable**, then the respective wave functions cannot be factorized, and then these variables or objects are called entangled. As a consequence, the corresponding events are not statistically independent, C. (14).

EPR paradox: Einstein et al. (1935) realized that QP is nonlocal. For it, they proposed the apparent paradox, Bell (1964), Aspect et al. (1982), C. (16).

expansion of space: Hubble (1929) observed the expansion of the universe since the Big Bang, Karttunen et al. (1996), Carmesin (2021a), C. (5, 12, 22).

frame: Each observation apparatus is localized in spacetime. That localization establishes a frame, Einstein (1905)[3].

gravitational field: In an appropriate frame, the gravitational field G^* can be defined and measured, see C. (2), THMs (15, 38), and e.g. Carmesin (2021d)).

Hubble constant: When Hubble (1929) observed the rate of expansion of space, it was called Hubble constant H_0, Karttunen et al. (1996).

Friedmann (1922) analyzed the rate of expansion of space with a scaling factor $R(t)$.

That rate is called Hubble parameter $H(t) = \dot{R}/R(t)$, Karttunen et al. (1996). The value at the present-

[3] For instance, see also Einstein (1915), Landau and Lifschitz (1971), Hobson et al. (2006).

day time t_0 is an improved concept of the Hubble constant $H(t_0) = H_0$, Karttunen et al. (1996). Moreover, the Hubble constant is an important parameter in cosmological models, Hobson et al. (2006), Carmesin (2019b). Thus it is measured by various observers, achieve different results at the 5σ confidence level, Planck-Collaboration (2020), Riess et al. (2022), Carmesin (2021d,a), C. (21).

metric tensor g_{ij}: A metric tensor describes distances in curved or flat spaces, Einstein (1915), Schwarzschild (1916), Hobson et al. (2006), THM (3).

nonlocality: Some quantum correlations become effective at velocity $v \leq c$. Such quantum correlations are called nonlocal, (Scheck, 2013, section 5.1.1), (Ballentine, 1998, C. 20), C. (16).

observable physical length: If there is a measurement procedure for a physical length, then that physical length is observable (C. 2).

physical reality: According to Einstein et al. (1935), the elements of physical reality 'must be found by an appeal to results of experiments and measurements', see section (25.2.3).

position factor: The position factor characterizes the energy as a function of a position (C. 3).

principle of least or extremal action: In many systems, the dynamics can be obtained by using the principle of least or extremal action, Noether (1918), Pauli (1941), Landau and Lifschitz (1971), Carmesin (2022e).

principle in physics: A principle in physics is an essential and broadly useful concept in physics, Popper (1974), Ruben (1990), Styrman (2019), Hilbert (1915); Hilbert et al. (1928).

probe mass: A probe mass can be used in order to analyze a motion or an interaction in physics (C. 25).

rate gravity four-vector, RGV: It is a four-vector characterizing the RGW, see C. (9).

rate gravity scalar, RGS: It is a scalar characterizing the RGW, see C. (9).

RGW, rate gravity wave: It is a wave characterizing the volume, see Carmesin (2021d).

rate of the formation of volume: It is a rate characterizing the formation of volume, Carmesin (2022d), part (II).

redshift and redchange: The redshift is a relative increase of the wavelength of radiation $z = \frac{\Delta\lambda}{\lambda}$, Karttunen et al. (1996), Carmesin (2021d). A relative increase of the wavelength of quanta of volume is called redchange, as the process of that increase is very different from the processes yielding redshift, C. (22).

Schwarzschild radius R_S: At this radius, the escape velocity is equal to c.

Schwarzschild metric, SM: (THM 3)

spacetime: Combination of space and time, Einstein (1905), Carmesin (2021d).

successive derivation: In quantum physics, QP, the results are derived successively from quantum postulates, see e. g. Grawert (1977), Ballentine (1998), Kumar (2018). In this book, the results are derived successively from the four basic principles, the spacetime quadruple, SQ, see (C. 2). Thus, the SQ implies the quantum postulates, and these imply QP, Fig. (12.3).

uniform scaling: A uniform scaling is a transformation that enlarges or shrinks a vector $\vec{v}$ by a scale factor $k_{1\rightarrow 2}$, $\vec{v}' = k_{1\rightarrow 2}\vec{v}$ (C. 5).

vacuum: The word vacuum is derived from the latin adjective 'vacuus', essentially meaning empty. In physics, very different types of 'density of vacuum' have been proposed, see sections (2.9, 24.3, 25.2.4). The observed density of the cosmological constant $\rho_\Lambda = u_\Lambda/c^2$ has two components, the density of three-dimensional volume ρ_{vol} and the equivalent density of heterogeneity $\rho_{het,equi}$, Eq. (2.67).

zero-point energy, ZPE: The energy of a ZPO is called zero-point energy, Ballentine (1998), Sakurai and Napolitano (1994), C. (14).

zero-point oscillation, ZPO: A ZPO represents the usual ground state in quantum physics. It can be derived from the DV, C. (14).

Acknowledgement

I thank Matthias Carmesin for many helpful and physically interesting discussions as well as for proofreading the manuscript. I thank Philipp Schöneberg, Paul Sawitzki, Jannes Ruder and Lina Jarck for interesting discussions. I am especially grateful to I. Carmesin for many helpful and scientifically interesting discussions as well as for proofreading the manuscript.

abbreviation	meaning
C.	chapter
COR	corollary
DE	dark energy
DEF	definition
DEQ	differential equation
DV	dynamic volume
EP	equivalence principle
GFV	globally formed volume
GG	generalized Gaussian gravity
GR	general relativity
LFV	locally formed volume
PLA	principle of least action
PROP	proposition
QP	quantum physics
SEQ	Schrödinger equation
SM	Schwarzschild metric
SQ	spacetime quadruple
SR	special relativity
THM	theorem
VD	volume dynamics

Table 25.2: Abbreviations.

Bibliography

Aad, G. et al. (2012). Observation of a new particle in the search for the Standard Model Higgs boson with the ATLAS detector at the LHC. *Phys. Lett. B*, 716:1.

Abbott, B. P. e. a. (2016). Observation of gravitational waves from a binary black hole merger. *Phys. Rev. Lett.*, 116:1–16.

Abbott, T. M. C. et al. (2020). Dark energy survey year 1 results: Cosmological contraints from galaxy clustering and weak lensing. *Phys. Rev. D*, 102:1–34.

Addison, G. E., Watts, D. J., Bennett, C. L., Halperin, M., Hinshaw, G., and Weiland, J. L. (2018). Elucidating ΛCDM: Impact of Baryon Acoustic Oscillation Measurements on the Hubble Constant Discrepancy. *ApJ*, 853:1–12.

Agency, D. I. (2010). Concepts for extracting energy from the quantum vacuum. *Report*, DIA 08-1004-007:1–51.

Aharonov, Y. and Rohrlich, D. (2005). *Quantum Paradoxes - Quantum Theory for the Perplexed*. Wiley-VCH Verlag, Weinheim.

Anderson, Carl, D. (1933). Cosmic-ray positive and negative electrons. *Physical Revies*, 44:406–416.

Anderson, M. T. (2004). Geometrization of 3-manifolds via the ricci flow. *Notices of the AMS*, 51:184–193.

Ash, R. B. (2008). *Basic Probability Theory.* Dover, Mineola N Y.

Ashby, N. (2002). Relativity and the global positioning system. *Phys. Today*, 55:41–47.

Aspect, A., Grangier, P., and Roger, G. (1982). Experimental Realization of the Einstein-Podolski-Rosen-Bohm Gedankenexperiment: A new Violation of Bell's Inequalities. *Phys. Rev. Lett.*, 49:91–94.

Ballentine, L. E. (1998). *Quantum Mechanics.* World Scientific Publishing, London and Singapore.

Balmer, Richard, H. (2021). Recent developments in ricci flows. *Notices of the AMS*, 68:1486–1498.

Bartelmann, M. (2019). *General Relativity.* Heidelberg University Publishing, Heidelberg.

Bell, J. S. (1964). On the Einstein-Podolski-Rosen paradox. *Physics*, 1(3:195–200.

Bennett, C. L. et al. (2013). Nine-year Wilkinson microwave anisotropy probe (WMAP) Observations: final maps and results. *The Astrophysical Journal Supplement Series*, 208:1–54.

Bergin, W. E. and Collins, J. L. (1951). Transients and waveforms. *United States Government Printing Office*, pages 1–90.

Bialynicki-Birula, I. and Bialynicki-Birula, Z. (1975). *Quantum Electrodynamics.* Pergamon Press, Oxford, 1 edition.

Birrer, S. et al. (2020). TDCOSMO: IV. Hierarchical time-delay cosmography - joint inference of the Hubble constant and galaxy density profiles. *Astr. and Astroph.*, 643:1–40.

Blakeslee, J. P. et al. (2021). The Hubble Constant from Infrared Surface Brightness Fluctuation Distances. *The Astrophysical Journal*, 911(65):1–12.

Blokhintsev, D. I. and Galperin, F. M. (1934). Neutrino hypothesis and conservation of energy. *Pod Znamenem Marxisma*, 6:147–157.

Bohr, N. (1920). Über die Serienspektra der Elemente. *Z. f. Physik*, 2(5):423–469.

Born, M. and Wolf, E. (1980). *Principles of Optics*, volume 1. Pergamon Press, Oxford New York, 6 edition.

Braginsky, V. B. (2007). Experiments with probe masses. *PNAS*, 104(10):3677–3680.

Brahe, T. and Kepler, J. (1627). *Tabulae Rudolphinae*. Auftraggeber Rudolph und Ferdinand, Ulm.

Brockhaus, T. (1998). *Brockhaus, die Enzyklopädie*. Brockhaus GmbH, Leipzig - Mannheim, 20 edition.

Bucherer, A. H. (1908). Messungen an Becquerelstrahlen. Die experimentelle Bestätigung der Lorentz-Einsteinschen Theorie. *Physikalische Zeitschrift*, 9:755–762.

Cao, S., Ryan, J., and Ratra, B. (2021). Cosmological constraints from H II starburst galaxy, quasar angular size, and other measurements. *MNRAS*, 000:1–13.

Carmesin, H.-O. (1995). Self-Organization of Pinwheels in the Visual Cortex by Stochastic Hebb Dynamics: Equivalence to Kosterlitz-Thouless Model. *Acta Physica Slovaca*, 45(2):93–102.

Carmesin, H.-O. (1996). *Grundideen der Relativitätstheorie*. Verlag Dr. Köster, Berlin.

Carmesin, H.-O. (2006). Entdeckungen im Physikunterricht durch Beobachtungen des Himmels. In Nordmeier, V. and Oberländer, A., editors, *Tagungs-CD Fachdidaktik*

Physik, ISBN 978-386541-190-7, Berlin. Deutsche Physikalische Gesellschaft, Deutsche Physikalische Gesellschaft.

Carmesin, H.-O. (2017). *Vom Big Bang bis heute mit Gravitation: Model for the Dynamics of Space*. Verlag Dr. Köster, Berlin.

Carmesin, H.-O. (2018a). A Model for the Dynamics of Space - Expedition to the Early Universe. *PhyDid B, FU Berlin, hal-02077596*, pages 1–9.

Carmesin, H.-O. (2018b). *Entstehung der Raumzeit durch Quantengravitation - Theory for the Emergence of Space, Dark Matter, Dark Energy and Space-Time*. Verlag Dr. Köster, Berlin.

Carmesin, H.-O. (2018c). *Entstehung dunkler Energie durch Quantengravitation - Universal Model for the Dynamics of Space, Dark Matter and Dark Energy*. Verlag Dr. Köster, Berlin.

Carmesin, H.-O. (2019a). A Novel Equivalence Principle for Quantum Gravity. *PhyDid B - Didaktik der Physik - Beiträge zur DPG - Frühjahrstagung - Aachen - Germany - hal-02511998*, pages 1–9.

Carmesin, H.-O. (2019b). Die Grundschwingungen des Universums - The Cosmic Unification - With 8 Fundamental Solutions based on G, c and h. In Carmesin, H.-O., editor, *Universe: Unified from Microcosm to Macrocosm - Volume 1*, pages 1–226. Verlag Dr. Köster, Berlin.

Carmesin, H.-O. (2020a). Explanation of the Rapid Enlargement of Distances in the Early Universe. *PhyDid B*, pages 9–17.

Carmesin, H.-O. (2020b). The Universe Developing from Zero-Point Energy: Discovered by Making Photos, Experiments and Calculations. In Carmesin, H.-O., editor, *Universe: Unified from Microcosm to Macrocosm - Volume 3*, pages 1–279. Verlag Dr. Köster, Berlin.

Carmesin, H.-O. (2021a). Cosmological and Elementary Particles Explained by Quantum Gravity. In Carmesin, H.-O., editor, *Universe: Unified from Microcosm to Macrocosm - Volume 5*, pages 1–198. Verlag Dr. Köster, Berlin.

Carmesin, H.-O. (2021b). Lernende erkunden die Raumzeit. *Der Mathematik Unterricht*, 67(2):47–56.

Carmesin, H.-O. (2021c). Physical Explanation of the H_0-Tension. *International Journal of Engineering and Science Invention*, 10(8)II:34–38.

Carmesin, H.-O. (2021d). Quanta of Spacetime Explain Observations, Dark Energy, Graviton and Nonlocality. In Carmesin, H.-O., editor, *Universe: Unified from Microcosm to Macrocosm - Volume 4*, pages 1–273. Verlag Dr. Köster, Berlin.

Carmesin, H.-O. (2021e). The Elementary Charge Explained by Quantum Gravity. In Carmesin, H.-O., editor, *Universe: Unified from Microcosm to Macrocosm - Volume 6*, pages 1–149. Verlag Dr. Köster, Berlin.

Carmesin, H.-O. (2021f). The Origin of the Energy. *PhyDid B, FU Berlin*, pages 29–34.

Carmesin, H.-O. (2022a). Explanation of Quantum Physics by Gravity and Relativity. *PhyDid B Internet Journal*.

Carmesin, H.-O. (2022b). Geometric Derivation of the Spectrum of Vacuum. *International Journal of Engineering and Science Invention*, 11(4)I:1–11.

Carmesin, H.-O. (2022c). How Excitations of Vacuum Form Matter. *PhyDid B Internet Journal*.

Carmesin, H.-O. (2022d). Quantum Physics Explained by Gravity and Relativity. In Carmesin, H.-O., editor, *Universe: Unified from Microcosm to Macrocosm - Volume 7*, pages 1–148. Verlag Dr. Köster, Berlin.

Carmesin, H.-O. (2022e). The Electroweak Interaction Explained by and Derived from Gravity and Relativity. In Carmesin, H.-O., editor, *Universe: Unified from Microcosm to Macrocosm - Volume 8*, pages 1–168. Verlag Dr. Köster, Berlin.

Carmesin, H.-O. (2022f). Unification of Spacetime, Gravity and Quanta. In Carmesin, H.-O., editor, *Universe: Unified from Microcosm to Macrocosm - Volume 9*, pages 1–258. Verlag Dr. Köster, Berlin.

Carmesin, H.-O. (2023a). A Unifying Derivation of Dark Energy. *SciPost Physics*, preprint.

Carmesin, H.-O. (2023b). Geometric and Exact Unification of Spacetime, Gravity and Quanta. In Carmesin, H.-O., editor, *Universe: Unified from Microcosm to Macrocosm - Volume 10*, pages 1–320. Verlag Dr. Köster, Berlin.

Carmesin, H.-O., Emse, A., Konrad, U., and Pröhl, I. K. (2023). *Universum Physik Einführungsphase nordrhein-Westfalen*. Cornelsen Verlag, Berlin.

Carmesin, H.-O., Emse, A., Piehler, M., Pröhl, I. K., Salzmann, W., and Witte, L. (2020). *Universum Physik Sekundarstufe II Niedersachsen Qualifikationsphase*. Cornelsen Verlag, Berlin.

Carmesin, H.-O., Heermann, D., and Binder, K. (1986). Influence of a Continuous Quenching Procedure on the Initial Stages of Spinodal Decomposition. *Z. Phys. B - Condensed Matter 65, 89-102*, 65:89–102.

Carmesin, H.-O., Percus, J. K., and Frisch, H. L. (1989). Liquid crystals at high dimensionality. *Phys. Rev. B*, 40:9416–9418.

Carmesin, H.-O. and Schöneberg, P. (2022). Droplet Model Used to Analyze the Early Universe. *International Journal of Engineering and Science Invention*, 11(2)I:58–66.

Cavendish, H. (1798). Experiments to determine the density of the earth. *Phil. Trans. R. Soc. Lond.*, 88:469–516.

Cimatti, A. and Moresco, M. (2023). Revisiting oldest stars as cosmological probes: new constraints on the Hubble constant. *arXiv*, 2302.07899v1:1–10.

Collaboration, P. (2020). Planck 2018 results. VI. Cosmological parameters. *Astronomy and Astrophysics*, pages 1–73.

Condon, J. J. and Mathews, A. M. (2018). ΛCDM Cosmology for Astronomers. *Publications of the Astronomical Soc. of the Pacific*, 130:1–17.

Coulomb, C.-A. (1785). Construction et usage d'une balance electrique etc. *Histoire de l'Academie des sciences avec les memoires de mathematique et de physique*, 1788:569–577.

Cugnon, J. (2012). The Casimir Effect and the Vacuum Energy: Duality in the Physical Interpretation. *Few-Body Systems*, 53:181–188.

de Broglie, L.-V. (1925). On the theory of quanta - translated by kracklauer. *Ann. de Phys.*, 10.

de Sitter, W. (1913). Ein astronomischer Beweis für die Konstanz der Lichgeschwindigkeit. *Pysik. Zeitschr.*, 14:429.

Debs, T. A. and Redhead, M. L. G. (1996). The twin 'paradox' and the conventionality of simultaneity. *American Journal of Physics*, 64:384–392.

Einstein, A. (1905). Zur Elektrodynamik bewegter Körper. *Annalen der Physik*, 17:891–921.

Einstein, A. (1907). Über das Relativitätsprinzip und die aus demselben gezogenen Folgerungen. *Jahrbuch der Radioaktivität und Elektronik*, 4:411–462.

Einstein, A. (1911a). Über den Einfluss der Schwerkraft auf die Ausbreitung des Lichts. *Annalen der Physik*, 35:898–908.

Einstein, A. (1911b). Zum Ehrenfestschen Paradoxon. Eine Bemerkung zu V. Varicaks Aufsatz. *Phys. Z.*, 12:509–510.

Einstein, A. (1915). Die Feldgleichungen der Gravitation. *Sitzungsberichte der Königlich Preußischen Akademie der Wissenschaften*, pages 844–847.

Einstein, A. (1916). Näherungsweise Integration der Feldgleichungen der Gravitation. *Sitzungsberichte der Königlich Preußischen Akademie der Wissenschaften*, pages 688–696.

Einstein, A. (1917). Kosmologische Betrachtungen zur allgemeinen Relativitätstheorie. *Sitzungsberichte der Königlich Preußischen Akademie der Wissenschaften*, pages 142–152.

Einstein, A. (1919). Spielen Gravitationsfelder im Aufbau der materiellen Elementarteilchen eine wesentliche Rolle? *Sitzungsberichte der Königlich Preußischen Akademie der Wissenschaften*, pages 349–356.

Einstein, A. (1948). Quanten-Mechanik und Wirklichkeit - Quantum Mechanics and Reality. *Dialectica*, 2(3-4):320–324.

Einstein, A., Podolski, B., and Rosen, N. (1935). Can the quantum-mechanical description of physical reality be considered complete? *Phys. Rev.*, 47:777–780.

Einstein, A. and Rosen, N. (1935). The particle problem in the general theory of relativity. *Phys. Rev.*, 48:73–77.

Escamilla-Rivera, C. and Najera, A. (2022). Dynamical Dark Energy Models in the Light of Gravitational-Wave Transient Catalogues. *JCAP*, 2022(3):60–85.

Faraday, M. (1852). On the physical character of the lines of magnetic force. *The London, Edinburgh and Dublin Philosophical Magazine and Journal of Science, Taylor and Francis*, 4(3):401–428.

Fermat, P. (1657). *OEuvres, translated by Tannery.* Gauthier-Villars, Paris.

Feynman, R. P. (1948). Space-Time Approach to Non-relativistic Quantum Mechanics. *Rev. Mod. Phys.*, 20:367–387.

Feynman, R. P. (1965). *The Character of Physical Law.* MIT Press, Boston.

Feynman, R. P. (1985). *QED - The Strange Theory of Light and Matter.* Princeton University Press, Princton.

Flanders, H. (1989). *Differential Forms.* Dover, New York.

Fornasini, P. and Grisenti, R. (2015). On EXAFS Debye - Waller factor and recent advances. *Journal of Sychrotron Radiation*, 22:1242–1257.

Friedmann, A. (1922). Über die Krümmung des Raumes. *Z. f. Physik*, 10:377–386.

Galileo, G. (1638). *Dialogues concerning two new sciences (translated).* Elfevirii, Leida.

Gauss, C. F. (1809). *Theoria motus corporum coelestium in sectionibus conicis solem ambientium.* Perthes und Besser, Hamburg.

Gauss, C. F. (1840). Recursion der Untersuchungen über die Eigenschaften der positiven ternären quadratischen Formen von Ludwig August Seeber. *J. reine angew. Math.*, 20:312–320.

Geers, T. L. and Sobel, L. H. (1971). Analysis of transient linear wave propagation in shells by the finite difference method. *NASA*, pages 1–186.

Goodstein, D. (1997). The Big Crunch. *EOS, Transactions, American Geophysical Union*, 78:329–334.

Grawert, G. (1977). *Quantenmechanik*. Akademische Verlagsgesellschaft, Wiesbaden.

Grebe-Ellis, J. (2011). Von der Optik im Tastraum zu einer Optik des Sehens. *Humboldt Universität Berlin*.

Griffiths, D. (2008). *Introduction to Elementary Particles*. Wiley-VCH, Weinheim, 2 edition.

Griffiths, D. J. (1994). *Introduction to Quantum Mechanics*. Prentice Hall, Upper Saddle River.

Guth, A. H. (1981). Inflationary universe: A possible solution to the horizon and flatness problems. *Physical Review D*, 23:347–356.

Hamilton, R. S. (1982). Three manifolds with positive ricci curvature. *Differential Geometry*, 17:255–306.

Handsteiner, J. et al. (2017). Cosmic bell test: Measurement settings from milky way stars. *PRL*, 118):1–6.

Hart, C. A. (1912). *Plane and Solid Geometry*. American Book Company, New York - Cincinatti - Chicago.

Haude, S., Salehi, S., Vidal, S., Maturi, M., and Bartelmann, M. (2022). Model-independent determination of the cosmic growth factor. *SciPost Astronomy*, 2:1–22.

Heeren, L., Sawitzki, P., and Carmesin, H.-O. (2020). Comprehensive Derivation of a Density Limit of the Evolution of Space. *PhyDid B, FU Berlin*, pages 39–42.

Heisenberg, W. (1927). Über den anschaulichen Inhalt der quantentheoretischen Kinematik und Mechanik. *Z. f. Phys.*, 43:172–198.

Heisenberg, W. (1958). *Physics and Philosophy.* Harper and Brothers, New York.

Hensen, B., Bernien, H., Dreau, A., et al. (2015). Loophole-free Bell inequality violation using electron spins separated by 1.3 kilometres. *nature*, 526:682–686.

Higgs, P. W. (1964). Broken Symmetries, Massless Particles and Gauge Fields. *Phys. Lett.*, pages 132–133.

Hilbert, D. (1903). *Grundlagen der Geometrie.* Teubner, Leipzig.

Hilbert, D. (1915). Die Grundlagen der Physik. *Nachrichten von der Königlichen Gesellschaft der Wissenschaften zu Göttingen, Math-Physik. Klasse, November.*, pages 1–30.

Hilbert, D., Nordheim, L., and Neumann, J. v. (1928). Über die Grundlagen der Quantenmechanik. *Mathematische Annalen*, pages 395–407.

Hobson, M. P. (2017). *Tales of the Quantum.* Oxford University Press, Oxford.

Hobson, M. P., Efstathiou, G. P., and Lasenby, A. N. (2006). *General Relativity.* Cambridge University Press, Cambridge.

Hordecki, R., Hordecki, P., Hordecki, M., and Hordecki, K. (2009). Quantum Entanglement. *Rev. Mod. Phys.*, 81:865.

Hoskin, M. (1997). *The Cambridge Concise History of Astronomy*. Cambridge University Press, Cambridge.

Hubble, E. (1929). A relation between distance and radial velocity among extra-galactic nebulae. *Proc. of National Acad. of Sciences*, 15:168–173.

Huterer, D. and Turner, Michael, S. (1998). Prospects for probing the dark energy via supernova distance measurements. *FERMILAB-Pub-98*, 247A:1–10.

Huygens, C. (1673). De vi centrifuga. *Ouvres completes*, XVI:255–301.

Isham, C. J. (1995). *Quantum Theory*. Imperial College Press, London.

Jahnke, T. et al. (2005). *Mathematik - Stochastik*. Cornelsen, Berlin.

Jaques, V. et al. (2007). Experimental Realization of Wheeler's Delayed Choice Gedanken Experiment. *Science*, 315(5814):966.

Kamionkowski, M. and Riess, A. G. (2023). The hubble tension and early dark energy. *Ann. Rev. Nucl. Part. Sci.*, pages 1–34.

Karttunen, H., Kröger, P., Oja, H., Poutanen, M., and Donner, K. (1996). *Fundamental Astronomy*. Springer, Berlin, 3 edition.

Kaufmann, W. (1901). Die magnetische und elektrische Ablenkbarkeit der Bequerelstrahlen und die scheinbare Masse der Elektronen. *Göttinger Nachrichten*, 2:143–168.

Kaufmann, W. (1906). Über die konstitution des elektrons. *Annalen der Physik*, 19:487–553.

Kepler, J. (1619). Harmonice Mundi - Linz - Libri Verlag. In Caspar, M., editor, *Gesammelte Werke - 1940*, volume 6, pages 1–563. Clarendon Press, Oxford.

Kerr, R. (1963). Gravitational field of a spinning mass as an example of algebraically special metrics. *PRL*, 11:237–238.

Kiefer, C. (2003). Quantum gravity - a general introduction. In Giulini, D., Lämmerzahl, C., and Kiefer, C., editors, *Quantum Gravity*, pages 3–13. Springer, Berlin, 1 edition.

Kiefer, C. and Sandhöfer, B. (2008). Quantum cosmology. In Vaas, R., editor, *Beyond the Big Bang*, pages 1–29. Springer, Berlin, 1 edition.

Kim, K.-T., Lingbo, Z., and Bathe, K.-J. (2018). Transient implicit wave propagation dynamics with overlapping finite elements. *Computers and Structures*, 199:18–33.

Kinzel, W. (2021). *Klassische Mechanik und Quantenmechanik*. University Würzburg, Würzburg.

Klee, H., Carmesin, H.-O., and Knorr, K. (1988). Quadrupolar glass state of Ar1-x (N2)x. *Phys. Rev. Lett.*, 61:1855–1858.

Kolmogorov, A. N. (1956). *Foundations of the Theory of Probability - translation edited by Nathan Morrison*. Chelsea Publishing Company, New York, 2 edition.

Kosowsky, A., Milosavljevic, M., and Jimenez, R. (2002). Efficient cosmological parameter estimation from microwave background anisotropies. *Phys. Rev. D*, 66:063007.

Kravtsov, A. V. and Borgani, S. (2012). Formation of galaxy clusters. *Annual Rev. of Astr. and Astrophys.*, 50:353–409.

Kumar, A. (2018). *Fundamentals of Quantum Mechanics*. Cambridge University Press, Cambridge.

Lamb, W. E. and Retherford, R. C. (1947). Fine structure of the hydrogen atom by a microwave method. *Phys. Rev.*, 72:241–243.

Landau, D. and Binder, K. (2005). *A Guide to Monte Carlo Simulations in Statistical Physics*. Cambridge University Press, Cambridge, 2 edition.

Landau, L. (1937). On the Theory of Phase Transitions. *Zh. Eksp. Toer. Fiz.*, 7:19–32.

Landau, L. and Lifschitz, J. (1963). *Course of Theoretical Physics VIII - Electrodynamics of Continuous Media*. Pergamon Press, Oxford, 2. edition.

Landau, L. and Lifschitz, J. (1965). *Course of Theoretical Physics III - Quantum Mechanics*. Pergamon Press, Oxford, 2. revised edition.

Landau, L. and Lifschitz, J. (1971). *Course of Theoretical Physics II - The Classical Theory of Fields*. Pergamon Press, Oxford, 3. edition.

Landau, L. and Lifschitz, J. (1973). *Course of Theoretical Physics I - Mechanics*. Elsevier, Oxford, 3. edition.

Landau, L. and Lifschitz, J. (1975). *Course of Theoretical Physics VII - Theory of Elasticity*. Pergamon Press, Oxford, 2. edition.

Landau, L. and Lifschitz, J. (1979). *Lehrbuch der theoretischen Physik - Statistische Physik*. Akademie-Verlag, Berlin.

Landau, L. and Lifschitz, J. (1980). *Course of Theoretical Physics V - Statistical Physics*. Pergamon Press, Oxford, 3. edition.

Landau, L. and Lifschitz, J. (1981). *Lehrbuch der theoretischen Physik - Klassische Feldtheorie*. Akademie-Verlag, Berlin.

Landau, L. and Lifschitz, J. (1982). *Course of Theoretical Physics IV - Quantum Electrodynamics*. Pergamon Press, Oxford, 2. edition.

Laue, M. (1912). Zwei Einwände gegen die Relativitätstheorie und ihre Widerlegung. *Pysik. Zeitschr.*, pages 118–120.

Lee, J. M. (1997). *Riemannian Manifolds: An Introduction to Curvature*. Springer Verlag, New York.

Leibniz, G. W. (1684). Nova methodus pro maximis et minimis. *Acta Eruditorum*, pages 467–473.

Lemaitre, G. (1927). Un univers homogene de masse constante et de rayon croissant rendant compte de la vitesse radiale des nebuleuses extra-galactiques. *Annales de la Societe Scientifique de Bruxelles*, A47:49–59.

Lohse, M. et al. (2018). Exploring 4D Quantum Hall Physics with a 2D Topological Charge Pump. *Nature*, 553:55–58.

Mandal, A. and Nadkarni-Ghosh, S. (2020). One-point probability distribution function from spherical collapse: early dark energy versus ΛCDM. *MNRAS*, 498:355–372.

Marletto, C. et al. (2017). Entanglement between living bacteria and quantized light witnessed by rabi splitting. *arXiv*, 1702.08075v1:1–3.

Maxwell, J. C. (1865). A dynamical theory of the electromagnetic field. *Phil. Trans. of the R.l Soc. London*, 155:459–512.

Mayer, J. R. (1842). Remarks on the forces of inorganic nature. *Annalen der Chemie und Pharmacie*, 43:233.

Mehra, J. and Rechenberg, H. (1999). Planck's half quanta: A history of the concept of zero-point energy. *Foundations of Physics*, 29:91–132.

Michell, J. (1784). On the means of discovering the distance... *Phil. Trans. R. Soc. Lond.*, 74:35–57.

Moore, T. A. (2013). *A General Relativity Workbook*. University Science Books, Mill Valley, CA.

Müller, P. H. (1975). *Lexikon der Stochastik*. Akademie - Verlag, Berlin.

Neumann, J. v. (1932). *Mathematische Grundlagen der Quantenmechanik*. Springer, Berlin.

Newell, D. B. et al. (2018). The CODATA 2017 values of h, e, k, and N_A for the revision of the SI. *Metrologia*, 55:L13–L16.

Newton, I. (1687). *Philosophiae Naturalis Principia Mathematica*. Jussu Societatis Regiae ac typis Josephi Streater, London.

Noether, E. (1918). Invariante Variationsprobleme. *Nachrichten der Königlichen Gesellschaft der Wissenschaften zu Göttingen, Math-phys. Klasse*, pages 235–257.

Nordstrom, G. (1913). Zur Theorie der Gravitation vom Standpunkt des Relativitätsprinzips. *Ann. d. Physik*, 347:533–554.

Olofsson, P. and Andersson, M. (2012). *Probability, Statistics, and Stochastic Processes*. Wiley, New York.

Pauli, W. (1941). Relativistic field theories of elementary particles. *Rev. Mod. Phys.*, 13:203–232.

Peebles, P. J. E. (1973). Statistical analysis of catalogs of extragalactic objects. i. theory. *ApJ*, 185:413–440.

Penzias, A. and Wilson, R. W. (1965). A measurement of excess antenna temperature at 4080 mc/s. *Astrophysical Journal Letters*, 142:419–421.

Perelman, G. (2002). The entropy formula for the ricci flow and its geometric applications. *arXiv*, math0211159v1.

Perlmutter, S. et al. (1998). Discovery of a supernova explosion at half the age of the universe. *Nature*, 391:51–54.

Pesce, D. W. et al. (2020). The Megamaser Cosmology Project: XIII. Combined Hubble Constant Constraints. *Astrophysical Journal Letters*, 891:L1.

Philcox, O. H. E., Ivanov, Mikhail, M., Simonovic, M., and Zaldarriaga, M. (2020). Combining Full-Shape and BAO Analyses of Galaxy Power Spectra: A 1.6% CMB-Independent Constraint on H_0. *JCAP*, 2020:1–42.

Pich, A. (2007). The Standard Model of Electroweak Interactions. In Fleischer, R., editor, *European School of High-Energy Physics*, volume Report CERN-2007-005. CERN, Geneva.

Planck, M. (1899). Über irreversible Strahlungsvorgänge. *Verlag der Königlich Preußischen Akademie der Wissenschaften*, pages 440–480.

Planck-Collaboration (2020). Planck 2018 results. VI. Cosmological parameters. *Astronomy and Astrophysics*, pages 1–73.

Popper, K. (1974). *Objektive Erkenntnis.* Hoffmann und Campe, Hamburg, 2. edition.

Pound, R. V. and Rebka, G. A. (1960). Apparent weight of photons. *PRL*, 4:337–341.

Prinz, D. N. (2022). *Renormalization of Gauge Theories and Gravity.* PhD thesis, Humboldt-Universität Berlin.

Riemann, B. (1868). Über die Hypothesen, welche der Geometrie zu Grunde liegen. *Abhandlungen der Königlichen Gesellschaft der Wissenschaften zu Göttingen*, 13:133–150.

Riess, A. G. et al. (2000). Tests of the Accelerating Universe with Near-Infrared Observations of a High-Redshift Type Ia Supernova. *The Astrophysical Journal*, 536:62–67.

Riess, A. G. et al. (2022). A Comprehensive Measurement of the Local Value of the Hubble Constant with 1 km s^{-1} Mpc^{-1} Uncertainty from the Hubble Space Telescope and the SHOES Team. *The Astrophys. J. Lett.*, 934:L7:1 – 52.

Robertson, B. E. et al. (2023). Identification and properties of intense star-forming galaxies at redshifts $z > 10$. *nature astronomy*, 7:611–621.

Rodrigo, A. et al. (2021). Entanglement between distant macroscopic mechanical and spin systems. *Nature Physics*, 17:228–233.

Rosenfeld, W. et al. (2017). Event-Ready Bell Test Using Entangled Atoms Simultaneously Closing Detection and Locality Loopholes. *PRL*, 119:1–6.

Ross, Shepley, L. (2004). *Differential Equation.* Wiley India, New Delhi.

Ruben, D.-H. (1990). *Explaining Explanation.* Routledge, London.

Sakurai, J. J. and Napolitano, J. (1994). *Modern Quantum Mechanics.* Addison-Wesley, New York - London - Delhi.

Sanz, M., Egusquiza, I, L., Di Candia, R., Saberi, H., Lamata, L., and Solano, E. (2016). Entanglement classification with matrix product states. *Scientific Reports*, 6(30188):1–5.

Sawitzki, P. and Carmesin, H.-O. (2021). Dimensional transitions in a Bose gas. *PhyDid B, FU Berlin*, pages 53–59.

Scheck, F. (2013). *Quantum Physics.* Springer, Heidelberg - New York - Dordrecht - London, 2 edition.

Schiff, J. L. (1991). *The Laplace Transform: Theory and Applications.* Springer, New York.

Schrödinger, E. (1926a). Quantisierung als Eigenwertproblem I. *Annalen der Physik*, 79:361–376.

Schrödinger, E. (1926b). Quantisierung als Eigenwertproblem IV. *Annalen der Physik*, 81:109–139.

Schulz, B. (2020). *Quantum gravity and space - time foam*. PhD thesis, Ludwig - Maximilians - University, Munich.

Schwartz, M. D. (2014). *Quantum Field Theory and the Standard Model*. Cambridge University Press, Cambridge.

Schwarzschild, K. (1916). Über das Gravitationsfeld eines Massenpunktes nach der Einstein'schen Theorie. *Sitzungsberichte der Deutschen Akad. d. Wiss.*, pages 186–196.

Slipher, V. (1915). Spectrographic observations of nebulae. *Report of the American Astron. Soc.*, Meeteing 17:21–24.

Smoot, G. F. (2007). Nobel Lecture: Cosmic microwave background radiation anisotropies: Their discovery and utilization. *Review of Modern Physics*, 79:1347–1379.

Smoot, G. F. et al. (1992). Structure in the COBE differential microwave radiometer first-year maps. *Astr. J.*, 396:L1–L5.

Sommerfeld, A. (1978). *Mechanik der deformierbaren Medien*. Verlag Harri Deutsch, Frankfurt, 6. edition.

Stephani, H. (1980). *Allgemeine Relativitätstheorie*. VEB Deutscher Verlag der Wissenschaften, Berlin, 2. edition.

Strang, G. (2017). *Calculus*. Wellesley-Cambridge Press, Wellesley MA.

Straumann, N. (2013). *General Relativity* . Springer, Dordrecht - Heidelberg - New York - London, 2. edition.

Styrman, A. (2019). Economical Unification in Philosophy of Science Before and After Ernst Mach. In Stadler, F., editor, *Ernst Mach – Life, Work, Influence.* Springer Nature, Switzerland.

Taylor, B. (1715). *Methodus Incrementorum.* Typis Pearsonianis prostant apud Gul. Innys ad Insignia Principis in Coemeterio Paulino, London.

Teschl, G. (2014). *Mathematical Methods in Quantum Mechanics.* American Mathematical Society, Providence, 2. edition.

Tolman, R. C. (1934). *Relativity, Thermodynamics and Cosmology.* Clarendon Press, Oxford.

Tryon, Edward, P. (1973). Is the universe a vacuum fluctuation? *Nature*, 246:396–397.

Vaidman, L. (2019). Quantum nonlocality. *entropy*, 21(447):1–5.

Valcin, D. et al. (2021). Inferring the Age of the Universe with Globular Clusters. *JCAP*, 08:017.

van der Waals, J. D. (1873). *Over de Continuiteit van den gas-en vloeistoftoestand.* Sijthoff, Leiden.

Weinberg, S. (1996). *The Quantum Theory of Fields.* John Wiley and Sons, New York - London - Sydney - Toronto.

Weinberg, S. (2017). The Trouble with Quantum Mechanics. *The New York Review of Books.*

Wheeler, J. A. (1984). Law without law. In *Quantum Theory and Measurement*, pages 182–213. Princeton University Press, Princton.

White, S. D. M., Efstathiou, G., and Frenk, C. S. (1993). The amplitude ofmass fluctuations in the Universe. *MNRAS*, 262:1023–1028.

Will, C. M. (2014). The Confrontation between General Relativity and Experiment. *Living Revies in Relativity*, 17/4:1–117.

Wirtz, C. (1922). Radialbewegung der Gasnebel. *Astronomische Nachrichten*, 215:281–286.

Workman, R. L. et al. (2022). Review of Particle Physics (by Particle Data Group). *Progr. Theor. Exp. Phys.*, 083C01:1–2270.

Zamorano, P. G. and Campos, F. A. U. (2007). On the Application of the numerical Laplace transform for accurate electromagnetic transient analysis. *Revista Mexicana de Fisica*, 53(3):198–204.

Zeldovich, Y. B. (1968). The cosmological constant and the theory of elementary particles. *Sov. Astron. A. J.*, 11:381–393.

Zilberberg, O. et al. (2018). Photonic topological pumping through the edges of a dynamical four-dimensional quantum Hall system. *Nature*, 553:59–63.

Zyla, P. A. et al. (2020). Review of Particle Physics (by Particle Data Group). *Progr. Theor. Exp. Phys.*, 083C01:1–2092.